THE EFFECT OF NITRO GROUP ON THE COORDINATION OF CYCLIC LIGANDS

by

SOSSI DICHAKJIAN

A thesis submitted to the University of London

for the degree of Doctor of Pilosophy

January 1984

BEDFORD COLLEGE

UNIVERSITY OF LONDON

LONDON

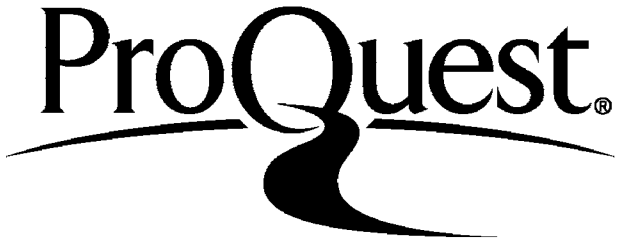

A B S T R A C T

The coordination chemistry of a number of nitro-substituted thiazoles and nitro-substituted pyridine N-oxides with a variety of acceptors has been investigated. The stoichiometry and stereochemistry of the transition metal complexes of these ligands depend on the metal, the anion and the substituents on the ligands. The influence of the nitro-group on the bonding abilities of these ligands is the most significant.

In part I, the preparation and characterisation of complexes of 2-amino-5-nitrothiazole (ANT) with Co(II), Ni(II), Cu(II), Cd(II), Cu(I), and Ag(I) are reported. From spectral data it is inferred that the complexes fall into two groups; those in which ANT is bound through the ring nitrogen, and those in which the exocyclic amine group is bound to the metal ion. In the former group are complexes ot the type $MCl_2.L_2$ (M = Co, Ni, Cu, Cd); compounds containing methanol, and $[Cu(AcO)_2.L]_2$, $CuCl.L_2$, $AgNO_3.L_2$ complexes. In the latter group are complexes prepared from and containing dimethylformamide. A protonated copper(II) chloride complex of ANT is also characterised. 2-Bromo-5-nitrothiazole and 2-chloro 5-nitrothiazole did not form complexes with the same metal salts.

In part II, the coordinating properties of nitro-substituted pyridine N-oxides toward copper(II) and cadmium(II) have been investigated. The ligands studied were 4-nitro 2-picoline N-oxide, 4-nitro 3-picoline N-oxide, 4-nitro 2,6-lutidine N-oxide, and 3-nitro 2,6-lutidine N-oxide. Several types of copper(II) halide complexes were isolated and characterised. These include (a) low magnetic moment 1:1 complexes, (b) a normal magnetic moment 1:1 complex, (c) distorted trans- and cis- 1:2 monomeric complexes with normal magnetic moment, (d) a polymeric halide-bridged 1:2 complex with normal magnetic moment, and (e) a grossly distorted trans-planar 1:2 complex with low magnetic moment. Among all the nitro-substituted pyridine N-oxides studied only 4-nitro 3-picoline N-oxide formed a complex with copper(II) acetate. Cadmium(II) chloride formed two series of complexes with these ligands; one with the general

formula $CdCl_2.L$ and the second with the formula $CdCl_2.L_2$. It was concluded that in the presence of a nitro substituent, steric factors near the donor site play a very important role in determining the structure of the complexes.

ACKNOWLEDGMENTS

I am sincerely grateful to my supervisor, Dr. M. E. Farago for her encouragement, valued guidance and constructive suggestions which made the completion of this work possible.

Despite the impossibility of thanking everyone who has been of help in completing this work, I would like to single out Dr. K. E. Howlett for his most helpful criticism and for proof-reading the thesis. I am also grateful to Mr. G. A. Leonard (University of Surrey) whose work on X-ray single crystal structure determination was exceedingly helpful to interpret the various spectroscopic data of many compounds. I am also indepted to Dr. A. Oduwole of Queen Mary College for the measurement of e.s.r. spectra and to Mr. D. Parkinson for n.m.r. spectra.

I would also like to thank the Lebanese University for a studentship. Finally, to my parents goes my deepest appreciation and thanks for their financial assistance and unlimited moral support during my stay in England.

CONTENTS

PART ONE

LIST OF TABLES (PART I)

LIST OF TABLES (PART II)

PART I

CHAPTER 1

THE COORDINATION CHEMISTRY OF THIAZOLES

1.1. Introduction

The activities of many enzymes depend upon the interaction of an imidazole or thiazole group with a transition-metal. These ligands are analogous to thiamine whose enzymatic action depends on the metal ion.[1,2]

Thiamine pyrophosphate is the coenzyme for a number of biochemical reactions including the nonoxidative decarboxylation of α-keto acids, oxidative decarboxylation of α-keto acids, and formation of α-ketols (acyloins). A number of theories have been put forward to explain the catalytic role of thiamine pyrophosphate in these reactions. Breslow[3] has proposed a mechanism involving the loss of the aromatic proton at position 2 of the thiazolium ring (I), with consecutive formation of a zwitterion (ylide structure).

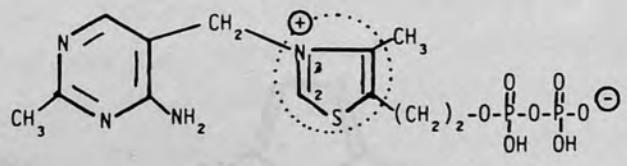

(I)

Magnesium has been shown to be an activator for enzymes which decarboxylate α-keto acids and which require thiamine pyrophosphate as a coenzyme. One of these enzymes, yeast carboxylase, is of particular interest, since it is one of the few of these isolated as homogeneous protein and containing a stoichiometric amount of the metal. The purified enzyme contains one gram atom of magnesium

and one mole of thiamine pyrophosphate per mole of protein. The removal of magnesium and the coenzyme by dialysis, resulted in loss of activity; their readdition resulting in its restoration.[4] The same enzyme was purified by others but reported to contain five gram atoms of magnesium instead of one. Addition of magnesium as well as manganese, iron, copper, cadmium, zinc, and cobalt reactivated the enzyme, but trivalent metals did not. The thiamine pyrophosphate-dependent carboxylase from heart muscle is activated by magnesium and manganese,[5] and the pyruvic acid oxidase system of brain by magnesium.[6]

Numerous analogues of thiamine pyrophosphate are tested in enzyme experiments and then used for the interpretation of the enzyme reaction.[2] As part of our study on model compounds for the interaction of metal ions and the thiazole ring systems in biological processes, we extended the work to the following thiazoles containing a nitro group at position 5: 2-amino-5-nitrothiazole (ANT), 2-chloro-5-nitrothiazole (CNT), and 2-bromo-5-nitrothiazole (BNT) which have several centres of coordination, the cyclic nitrogen, the nitro group,

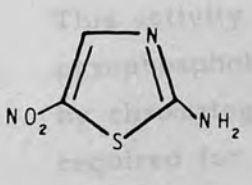

(ANT)
(II)

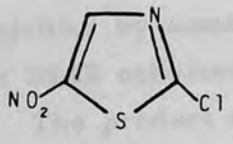

(CNT)
(III)

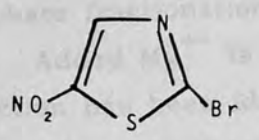

(BNT)
(IV)

cyclic sulphur, π electrons of the ring and the exocyclic nitrogen in case of 2-amino-5-nitrothiazole.

1.2. Thiazoles

1.2.1. Natural Occurrence and Biological Activity

Although unsubstituted thiazole is not found in nature, naturally occurring thiazoles are numerous. Their origin has been related to the cyclization of a peptide chain at a cysteine residue with formation of a thiazoline ring and thence by dehydrogenation of a thiazole ring.

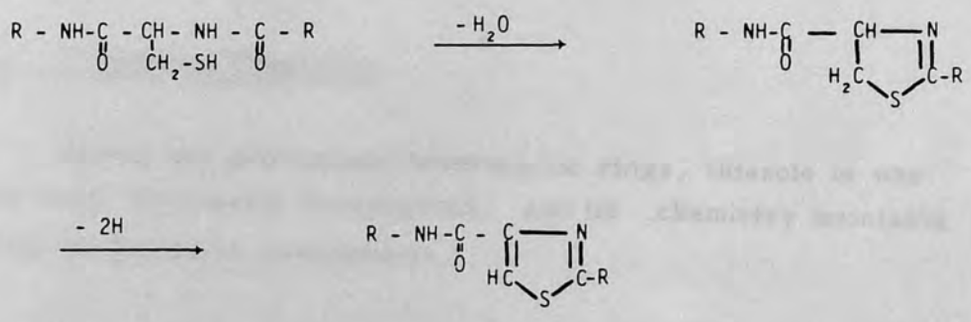

The presence of kinase phosphorylating 4-methyl-5-(β - hydroxyethyl)thiazole has been demonstrated in brewer's yeast.[7] This activity has been separated from pyrimidine kinase and thiamine pyrophosphokinase activities by ammonium sulphate fractionation followed by chromatography on DEAE cellulose columns. Added Mg^{++} is required for activity. The product of the reaction has been identified and shown to be an intermediate in thiamine phosphate synthesis.

Several antibiotics, such as althiomycine[8] and micrococcin,[9,10] contain a thiazole ring, as do many metabolic products of living organisms;[11] tomato,[13] coffee,[14, 15] roasted peanuts,[16] the basic fraction of Scotch whisky and Jamaica rum[17] and so on. Thiazoles have also been separated from nitrogen bases of some petroleums.[18]

The pharmaceutical properties of 2-amino-5-nitrothiazole and

the related compounds have been tested.[19-27] Thus 2-amino-5-nitrothiazole 0.07% in drinking water and 0.05% in feed, given to domestic cockerels at the appearance of teratomas induced by intratesticular injections of $ZnCl_2$, retarded tumor growth. Several Pt^{++} complexes of thiazole derivatives are found to be potential antitumour drugs,[28-30] The herbicidal and growth-regulating activity of some metal complex compounds of thiazole derivatives have been tested. The aminothiazole complexes CdL_4X_2 (X = Br, Cl), NiL_4Cl_2 and $Cd\ L_2X_2$ (X = Br, I, SCN) showed herbicidal activity.[31]

1.2.2. Theoretical Treatment

Among the pentaatomic heterocyclic rings, thiazole is one of the most intensively investigated, and its chemistry maintains steadily its intensive development.

Various theoretical treatments published on the thiazole molecule have shown some common trends in the electronic properties of this molecule.

1. In all cases the π net charge of sulphur is positive, whereas its σ net charge is sometimes positive[32,33] and sometimes negative.[34,35] The all-electrons methods, like ab initio, give a positive total net charge with the exception of CNDO/2 method for which it is negative.[36]

2. In all cases the total net charge of nitrogen is negative. In only one PPP calculation it is slightly positive.[37]

3. From the σ net charge the three hydrogen atoms have decreasing acidity in the order H-2 $\geq$ H-5 > H-4.

4. The discussion of the π-bond order is interesting because it gives a picture of the distribution of the π-electrons along the σ frame of the ring and, therefore, of its aromaticity, which can be accounted for by n.m.r. and ultraviolet spectroscopy. The HMO results can be divided into two groups, the ones giving thiazole a slightly aromatic character,[13,15,38] whereas the others are indicative of a more dienic structure.[39,40]

M.O. Huckel's calculations done for the thiazoles studied in this work, are given in the following table. No relation is established between the basicities of the donor groups and the π electronic charges.[30]

Table 1

Results of M.O. Huckel's calculations for the thiazoles

Substance	QN(≥ N)	QN($-NH_2$)	QS(> S)
2-bromo-5-nitrothiazole	1.1864		1.8421
2-amino-5-nitrothiazole	1.2402	1.9312	1.8498
2-aminothiazole	1.2860	1.9319	1.9371

Recently Lalitha et al.[34] calculated charge density distributions in a number of 2- and 5-substituted thiazoles (including, 2-amino-thiazole, 2-bromothiazole, and 2-chlorothiazole) by using the Huckel LCAO MO method for the calculation of π charges and its counter-part Del Re method for the calculation of σ charges. The total charge density on an atom was obtained by adding π and σ- charges on the atom. The charge density distributions obtained for the 2- and 5-substituted thiazoles are correlated with the pKa values of these compounds, and indicate that in all cases the ($\pi + \sigma$) charge

density at N-3 of the thiazole ring is the highest (Table 2). The results obtained seem to be in very good agreement with other experimental results,[46-50] and are contradictory to the results obtained by Doadrio et al.[30] for 2-aminothiazole which predict a higher electron density at $-NH_2$ nitrogen than at the ring nitrogen.

Table 2

π-Charges, σ-Charges and Total Charge Densities at Various Positions of 2-Aminothiazole, 2-Bromothiazole, and 2-Chlorothiazole with their pK_a Values

Position	Charge Density			
	π-charge	σ-charge	Total	pK_a
	2-Aminothiazole			
S_1	+0.693	-0.035	+0.658	
C_2	-0.055	+0.176	+0.121	
N_3	-0.375	-0.296	-0.671	
C_4	-0.147	+0.109	-0.038	+5.32
C_5	-0.188	-0.035	-0.223	
N_6	+0.072	-0.591	-0.519	
	2-Chlorothiazole			
S_1	+0.749	-0.029	+0.720	
C_2	-0.114	+0.179	+0.065	
N_3	-0.335	-0.259	-0.594	
C_4	-0.135	+0.104	-0.031	-0.75
C_5	-0.178	+0.066	-0.112	
Cl_6	+0.013	-0.125	-0.122	
	2-Bromothiazole			
S_1	+0.753	-0.026	+0.727	
C_2	-0.120	+0.171	+0.051	
N_3	-0.332	-0.262	-0.594	
C_4	-0.134	+0.116	-0.018	-0.86
C_5	-0.177	+0.027	-0.150	
Br_6	+0.010	-0.105	-0.095	

1.2.3. Correlations and Generalisations

The electrical effects of substituents bonded to heterocyclic systems which contain an aza-group (pyridine,[41,42] imidazole,[43] and related derivatives) have been extensively investigated. Considerable interest has been shown in substituents bonded in the α position with respect to the 'aza-group' and attempts to derive an 'ortho' polar effect from the pK_a values of these substrates have been carried out. Forlani et al.[44] have determined the pK_a values of a number of 2- and 5-substituted thiazoles and have found that pK_a is very sensitive to changes of substituent, and that for 2- and 5-substituted thiazoles (as well as for 2-substituted pyridines or imidazoles) the best correlation between pK_a and σ values is that obtained by using σ_m values, σ_I, σ°_m, σ_p and σ_p^+ giving unacceptable correlations. The same group has found that the only deviations from linearity observed in the plot of pK_a values of 2-substituted thiazoles versus σ_m values are those for NO_2, NH_2, NMe_2 substituents (see Figure), and

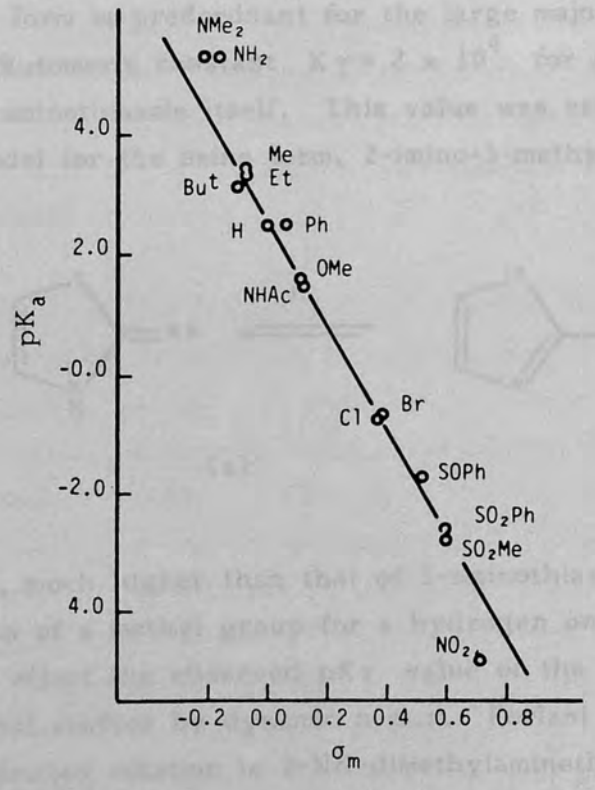

Fig. 1. Plot of pK_a values of 2-substituted thiazoles versus σ_m values.

concluded that only in the case of these three substituents strong mesomeric effects are important, and that the use of σ_m values for other groups indicates that the system considered is more sensitive to inductive than mesomeric effects. Steric effects appear to be absent.

The strong electron withdrawing ability of NO_2 when it is bonded to thiazole ring is manifested in the reaction of 5-substituted 2-halogenothiazoles with sodium thiophenoxide.[45] It is observed that, in contrast with 6-membered cyclic aromatic derivatives, nitro-activation in the five-membered ring is much more efficient than aza-activation for nucleophilic aromatic substitution of 2-chlorothiazoles, because the nitro-substituent, if present in a conjugated position, effectively removes negative charge from the ring.

The existence of tautomeric amino and imino forms in aminothiazoles is investigated by many workers.[46-50] It has been shown[46] that the aromatic amino form is predominant for the large majority of 2-amino-thiazoles. A tautomeric constant $K_T = 2 \times 10^4$ for process (a) is calculated for aminothiazole itself. This value was estimated by taking as a model for the imino form, 2-imino-3-methylthiazole which

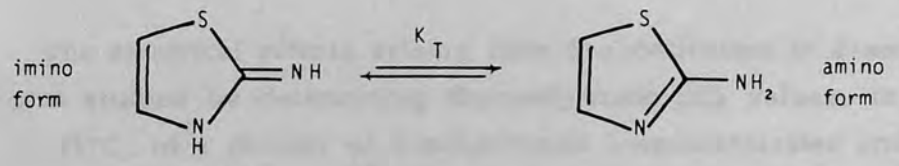

(a)

has a pK_a 9.6, much higher than that of 2-aminothiazole. However the introduction of a methyl group for a hydrogen on the endocyclic nitrogen could effect the observed pK_a value of the model compound. In conformational studies by dynamic n.m.r. Forlani et al.[47] have detected a restricted rotation in 2-NN-dimethylaminothiazole, 5-bromo- and 5-nitro-2-NN-dimethylaminothiazole. The n.m.r. signal (singlet), corresponding to the pairs of methyls in 2-NN-dimethyl-

aminothiazole, 5-bromo- and 5-nitro-2-NN-dimethylthiazole that are isochronous at room temperature is reversibly split into two equivalent lines resulting from the restricted rotation around the Ar - N bond and is ascribed to the relatively large contribution to the double bond character from resonance contributors, such as (V) and (VI) to structure (VII). Based upon measured free energies of activation (ΔG^*) at the coalescence temperature the authors suggest that the electron withdrawing capability of a nitro group in the para-like position-5 greatly enhances the Ar - N double bond character (more than 50%).

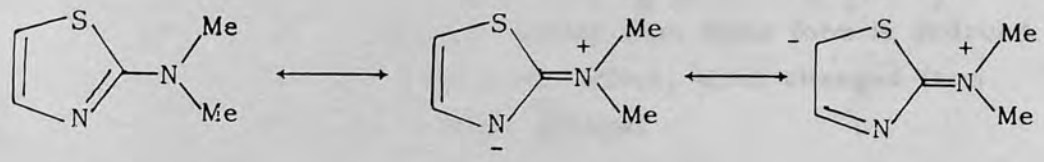

(V) (VI) (VII)

X-ray crystallographic data published recently[51] delineate a relatively short C-(2) - N(amino) bond length (1.330 Å) in 2-aminothiazole, indicating that the exocyclic nitrogen has sp^2 hybridization and there is significant delocalisation of the π system to include the amino nitrogen.

The electrical effects arising from 5-substitution in 2-aminothiazole is studied by determining thermodynamic pK_a values, in water at 25°C, of a number of 5-substituted 2-aminothiazoles and 2-NN-dimethylaminothiazoles.[44] Comparison of the pK_a values of 5-X-aminothiazoles (X = H, Me, OMe, Ph, SPh, Cl, Br, SO_2Ph, NO_2) with the pK_a values of the corresponding 5-X-2-NN-dimethylaminothiazoles has allowed the authors to assign the aromatic amino form to all 2-aminothiazole derivatives. The Hammett plot of pK_a values against σ_{meta} substituent constant is linear as required if the protonation centre is the endocyclic nitrogen in all cases. It is observed that cross-conjugation between the amino group in position-2 and the substituent in position-5 is present only when the nitro group is the substituent. The combined effects of the substituent in position-5 and the amino group are additive in all other compounds.

The conclusions arrived at by using thermodynamic data are further supported by ^{1}H n.m.r. studies on the electronic effects of substituents bonded to position 4- and 5- of 2-aminothiazole.[50] It is noticed that the δ_{NH_2} values could be related to σ_m and σ (as appropriate) values by Hammett plots and the best fit is obtained when the σ^- values are used. The conjugative interaction between the electron-withdrawing groups in position 5 and the amino group in position 2, is deduced from the fact that an acceptable correlation exists between σ_p^- values and chemical shift values of the protons bonded in position 4 for 5-substituted 2-aminothiazoles (5-substituent: H, CH_3, C_6H_5, Cl, $S\text{-}C_6H_5$, $SO_2\text{-}C_6H_5$, $COOC_2H_5$, NO_2). The prevalence of the amino form rather than imino form is deduced from the regularity of the substituent effect, when changed from electron-donor to electron-acceptor groups.

The I.R., U.V., and ^{13}C n.m.r. spectra of many thiazoles are studied in detail.[52-54] Depeshko et al.[52] have studied the U.V. spectra of a number of 2-substituted 5-nitrothiazoles, including 2-amino-5-nitrothiazole, and observed that all the 2-substituted 5-nitrothiazoles retained the U.V. peaks of unsubstituted thiazole and exhibited others resulting from interaction of the substituents with the π system of the ring. In concentrated H_2SO_4 The conjugate acids are formed, and in NaOH solution they exist as the aci-nitro salts.

Comparison of the X-ray crystallographic data published up to date for (2) thiazole, (3) 2-aminothiazole, (4) 2-amino-4-phenylthiazole hydrobromide monohydrate, (5) 2-methylaminobenzothiazole, (6) 2-amino 4,5-dihydro 7,8-dimethoxy [1.2-d] naphtholthiazole,[51,55-58] indicates that the thiazole ring is very little modified due to the effect of substitution. Only when, substitution is on the endocyclic nitrogen is there a systematic variation in the bond lengths and bond angles in the thiazole ring.[59-64]

1.2.4. Coordination Complexes

Several studies have been carried out involving metal(II) complexes of simple and substituted thiazoles.[65-75] It has been found that[69,75-80] substituents in 2-, 4- and 5-positions modify the stoichiometries and stereochemistries of the complexes of cobalt(II), nickel(II), and copper(II). X-ray crystallographic data indicate that the structure of dichlorobis(thiazole)copper(II)[81] consists of infinite chains of doubly chloride-bridged copper(II) ions, while bis[dibromobis(4-methylthiazole)copper(II)][82] is dimeric, with tetragonal-pyramidal geometry at each copper centre, and trans-dichlorobis(2,4-dimethylthiazole)copper(II)[83] is square planar and monomeric.

Thiazole has both nitrogen and sulphur as possible donor sites, and whereas the majority of complexes have been found to be nitrogen bonded, a case of sulphur coordination has been reported.[80] Thiazole forms complexes of the form $[M(t)_6](ClO_4)_2$ where M = Ni, Co or Zn;[65] $MX_2.(t)_4$ complexes where M = Co, X = Br, I or NCS; M = Ni, X = Cl, Br, I, NCS or ClO_4; M = Cu or Zn, X = NO_3 or ClO_4[65] and complexes of the form $MX_2.(t)_2$ where M = Co, X = Br, I, or NCS; M = Ni X = Cl Br, I, NCS or ClO_4; M = Cu, X = Cl or Br; M = Zn, X = Cl, Br or I and $MX_2.(t)$ where M = Co, X =Cl or Br and M = Cu, X = Cl. With the exception of $CoI_2.(t)$ and $CuCl_2.(t)_2$ and possibly $Zn(ClO_4)(t)_4$, all the other complexes are six coordinate in the solid state, bridging taking place when necessary. Polymeric octahedral structures have been assigned to all $MX_2.(t)_2$ complexes . The structure, which consists of infinite chains of doubly halogen-bridged metal(II) ions, is reminiscent of those of the pyridine analogues, and is confirmed by three-dimensional x-ray structure analysis of the dichlorobis(thiazole)copper(II) complex.[81]

It is worthwhile to consider the coordination chemistry of 2-aminothiazole and 2-bromothiazole in some detail, as they are the substituted thiazoles which are best related to 2-amino-5-nitro-thiazole, and 2-bromo-5-nitrothiazole, which are the subject of study in the present work.

It is noticed that 2-aminothiazole forms ($-NH_2$) group coordination for metal ions like Sn(IV) and Ti(IV).[71,73] The situation is not as clear-cut for nickel(II), Co(II), and Cu(II) where both ring nitrogen and amino nitrogen coordination is suggested by various authors.[72-76] Recent x-ray study on dichlorobis(2-aminothiazole)cobalt(II)[84] indicated that coordination is through ring nitrogen. The cobalt atom lies on a twofold axis and is tetrahedrally coordinated to the Cl atoms (Co - Cl 2.261Å) and to the heterocyclic N atoms in the thiazole rings (Co - N 2.010Å) The amino groups of the ligands form both intra- and intermolecular hydrogen bonds to the Cl atoms.

Some of the stoichiometries reported for various first row transition metal ions with 2-aminothiazole are as follows: $CoX_2.(AMT)_4$ (X = Cl, Br); $CoX_2.(AMT)_2$, (X = Cl, Br, I);[76] $NiX_2.(AMT)_4$ (X = Cl, Br, I, NCS, ClO_4, OAc);[72,76] $[(AMT)_2][Ni(AMT)_4(CLO_4)_2]$;[72] $NiCl_2.(AMT)$;[76] $CuX_2.(AMT)_2$, (X = Cl, Br, OAc)[68,75] and $CuX_2.(AMT)_2$, (X = Cl, Br).[76] It has been reported that the complexes of Co(II) having stoichiometry $CoX_2.L_2$ (X = Cl, Br, I) have distorted tetrahedral structures, while the corresponding copper(II) complexes have polymeric tetragonal structures.[72,76] Bridging AMT is reported only in $NiCl_2.(AMT)$, which is assigned an octahedral structure.[76]

Complexes of 2-aminobenzothiazole (abt) of the type $M(abt)_2X_2$ (M = Co, X = Cl, Br, I or NCS; M = Ni, X = Br) are pseudotetrahedral. In complexes $M(abt)_2X_2$ (M = Co or Ni, X = OAc or NO_3) the metal ion is in a six coordinated environment as it is in $Ni(abt)Cl_2.2H_2O$. $Ni(abt)_2X_2$ exists as both blue pseudotetrahedral and yellow tetragonal isomers when X = Cl and as a planar complex when X = I. Except for the yellow form of $Ni(abt)_2Cl_2$ in which the donor centre appears to be the amino-group, coordination takes place through the ring nitrogen atom.[85]

2-Bromothiazole forms complexes with Co(II) and Cu(II), and has low affinity for nickel(II). The only stoichiometry reported for these complexes is ML_2X_2 (X = Cl, Br), and they exhibit similar behaviour to AMT complexes of the same stoichiometry.[76]

The only transition metal complexes reported for 2-bromo-

5-nitrothiazole and 2-amino-5-nitrothiazole are with Pt(II). In $Pt(L_2)X_2$ where X = Cl, Br and L = 2-bromo-5-nitrothiazoloe, it is suggested that coordination is through the ring nitrogen, and that coordination is through the amino-nitrogen in the case of 2-amino-5-nitrothiazole.[30]

The ligand, 2-amino-5-nitrothiazole (ANT) is extensively used in the preparation of azo dyes. The azo dye (VIII) dyes nickel-containing polypropylene fibers light fast orange shades (R = C_{1-4} alkyls, $PhCh_2$, Ph) while, azo dye (IX) could be used in

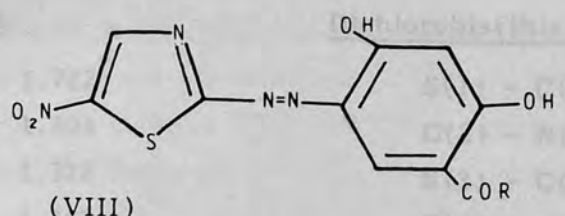

(VIII)

(R = C_{1-4} alkyl, $PhCH_2$, Ph)

photometric detection of Cu(II) ion without interference from many other ions.[87]

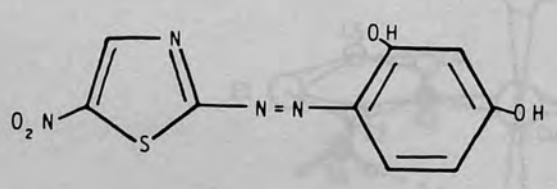

(IX)

Coordination of thiazoles to transition metals has little effect on the geometry of the ring. Comparison of the bond distances listed in tables 3 and 4 for thiazole,[55] dichlorobis(thiazole)copper(II),[81] and 2-aminothiazole,[51] dichlorobis(2-aminothiazole)copper(II)[84] respectively, suggests that while the effect of coordination on the geometry of thiazole is very insignificant (except for the S(1) - C(2) bond distance) there is a slight decrease in the S(1) - C(2), C(5) - S(1), and a slight increase in C(4) - C(5), C(2) - N(3), C(2) - N(6), and N(3) - C(4) bond distances in dichlorobis(2-amino-thiazole)copper(II) when compared with the corresponding values in 2-aminothiazole.

Table 3. Bond distances (Å) in (a) thiazole and (b) dichlorobis(thiazole)copper(II).

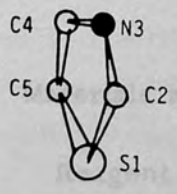

(X)

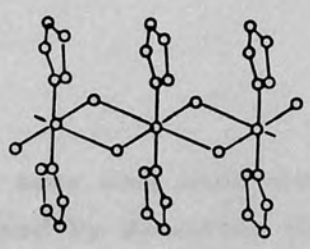

(XI)

Thiazole		Dichlorobis(thiazole)copper(II)	
S(1) - C(2)	1.722*	S(1) - C(2)	1.694
C(2) - N(3)	1.304	C(2) - N(3)	1.301
N(3) - C(4)	1.372	N(3) - C(4)	1.365
C(4) - C(5)	1.367	C(4) - C(5)	1.358
C(5) - S(1)	1.713	C(5) - S(1)	1.700

Table 4. Bond distances (Å) in (c) 2-aminothiazole and (d) dichlorobis(2-aminothiazole)copper(II).

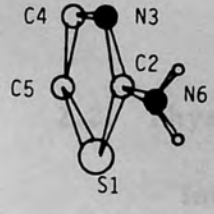

(XII)

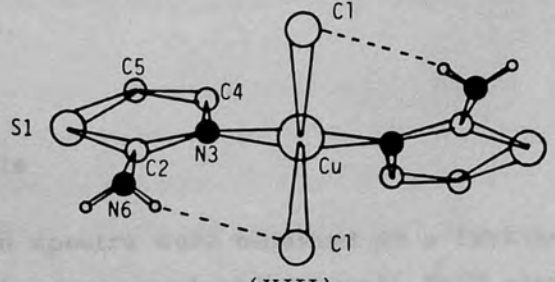

(XIII)

2-Aminothiazole		Dichlorobis(2-aminothiazole)copper(II)	
S(1) - C(2)	1.74*	S(1) - C(2)	1.713
C(2) - N(3)	1.31*	C(2) - N(3)	1.324
N(3) - C(4)	1.39*	N(3) - C(4)	1.400
C(4) - C(5)	1.3]	C(4) - C(5)	1.328
C(5) - S(1)	1.73*	C(5) - S(1)	1.713
C(2) - N(6)	1.330	C(2) - N(6)	1.341

* Means average bond distance.

CHAPTER 2

EXPERIMENTAL PROCEDURES

2.1. Materials and Manipulation

Reagent grade solvents and metal salts were used without further purification. $Ni(NCS)_2$ was obtained by dissolving nickel(II) carbonate in thiocyanic acid. CuCl(I) was prepared by the addition of $CuCl_2$ to a solution of anhydrous sodium sulphite, as described in ref. 88. 2-chloro-5-nitrothiazole was prepared by a Sandmeyer reaction from 2-amino-5-nitrothiazole.[89,90] 2-amino-5-nitrothiazole, and 2-bromo-5-nitrothiazole (Aldrich Chemicals), were used after crystallization from methanol

With the exception of $CuCl_4.(HANT)_2$ and $[Cu(AcO)_2.(ANT)]_2$ all the other complexes were very sensitive to air and moisture. Accordingly, experiments were carried out in all-glass apparatus under an atmosphere of high purity nitrogen. Before use, all apparatus was evacuated and filled with nitrogen, and the procedure was repeated several times.

2.2. Physical Measurements

Infrared absorption spectra were obtained on a Perkin-Elmer 457 instrument using samples in a nujol mull between NaCl plates or as KBr pellets. Electronic spectra in acetone, DMF, MeOH, were recorded on a PE 124 instrument. Reflectance spectra in the range 4000 - 45000 cm^{-1} were obtained with an S.P. 700 instrument. Magnetic measurements were made over the temperature range 90K - 363K on a Newport Instrument Gouy balance. Replicate determinations were made in most cases on separately prepared samples. The Gouy tube was calibrated with $HgCo(NCS)_4$ (taking χ_g as 16.44×10^{-6} c.g.s.u. at 20°C). The calibration was checked by measuring the susceptibility of $Ni(en)_3S_2O_3$ for which a value of χ_g equal to 11.02×10^{-6} c.g.s.u. was obtained. Corrections for the diamagnetic

portions of the molecule were obtained from Pascal's constants or by modifying the diamagnetic contributions of simpler molecules given in the literature as follows: To calculate the susceptibility per mole for ANT the contribution of the nitro group was estimated by comparing aniline and m-nitroaniline, the number found was added to the value of the susceptibility per mole for 2-amino-thiazole given in the literature. The value of μ_{eff} at each temperature was calculated using the equation

$$\mu_{eff} = 2.84(\chi_{m'} \times T)^{\frac{1}{2}}$$

where T is the absolute temperature, and $\chi_{m'}$ is the molar susceptibility corrected for diamagnetic effects and for temperature independent paramagnetism (TIP). The values of μ_{eff} are believed to be precise to within ± 0.05B.M. The reciprocals of χ_m values ((where χ_m is the molar susceptibility corrected for diamagnetic effects)) were plotted against temperature, and the best lines drawn. Whenever the straight lines so drawn intercepted the T axis at non-zero values, the T intercept, θ, was measured. Whenever appropriate μ_{eff} was calculated using the relationship

$$\mu_{eff} = 2.84[\chi_{m'}(T - \theta)]^{\frac{1}{2}}$$

where θ is the Weiss constant. At each temperature, measurements were performed at two different field strengths. The tube containing the samples was first heated and then gradually cooled.

The X-band e.s.r. spectra of the powdered samples were obtained on a Decca X3 spectrometer. The magnetic field range available is from 0 to 13,000 Gauss produced by a Newport Instrument eleven inch magnet type M4x. Carbon-13 n.m.r. spectra were recorded using a JEOL FX 90Q Fourier Transform n.m.r. spectrometer. X-ray diffraction powder photographs were recorded on a Philips diffractometer PW 1049 attached to a PW 1010 generator. An excitation voltage of 40 kV was used for copper Kα radiation.

2.2. Preparation of ANT.HCl

ANT was slowly added to magnetically stirred concentrated hydrochloric acid until a white precipitate formed. Stirring was continued for another hour and the precipitate filtered and dried in a desiccator.

2.4. Preparation of Complexes

$NiCl_2.(ANT)_2$; $NiBr_2.(ANT)_3(MeOH)_2$; $Ni(NCS)_2.(ANT)_2(MeOH)_2$; $CuCl_2.(ANT)_2$; $CdCl_2.(ANT)_2$.

These complexes were prepared by treating a concentrated solution of 2-amino-5-nitrothiazole (0.01 mole) in methanol with methanolic solutions of the metal salts (0.01 mole). The resultant complexes were filtered off warm, washed twice with methanol and dried in vacuo at 60°C. Changing metal to ligand ratio did not affect the composition of these complexes.

$CoCl_2.(ANT)_2$: A concentrated solution of $CoCl_2.6H_2O$ (0.01 mole) in methanol at 60°C was treated with a methanolic solution of ANT (0.01 mole). The resultant green solution was evaporated at 40°C to ca. one third, the yellow precipitate filtered off when warm, washed with methanol (ca. 20ml) and dried in vacuo at 50°C. When the solution containing the complex was cooled to 0°C to enhance precipitation, the free ligand was obtained.

$CoCl_2.(ANT)_2(MeOH)_2$: A solution of $CoCl_2$ (0.01 mole in 20 ml methanol) was slowly added to a stirred solution of 2-amino-5-nitrothiazole (0.03 mole in 100 ml methanol) at 60°C. A pink precipitate formed which was filtered off, washed in methanol and dried in vacuo at 60°C.

$CuSO_4(ANT)(DMF)$; $CuCl_2.(ANT)(DMF)$; $NiSO_4.(ANT)_2(DMF)_2$; $CoSO_4.(ANT)_2(DMF)_2$; $NiCl_2.(ANT)_2(DMF)_2$.

Warm concentrated solutions of metal salts in DMF were added to stirred concentrated solutions of ANT in DMF at 40°C. The precipitates were filtered off, washed with 2 portions of methanol, and dried in vacuo at 80°C. Metal to ligand ratio was always 1:1. Increasing the ligand to metal ratio to four times in the preparation of copper complexes, gave always the same product.

$Ni(NCS)_2.(ANT)_2(MeOH)$: This complex was obtained in the tube used for magnetic measurement during the course of the experiment.

The tube was filled with $Ni(NCS)_2(ANT)_2(MeOH)_2$, heated to 363 K subjected to two different magnetic fields, as previously mentioned, the temperature was lowered at 20 K intervals to 100 K At the end of the experiment a change in colour from brown to green was observed. The I.R., visible spectra and analytical analysis indicated that the complex is $Ni(NCS)_2.(ANT)_2(MeOH)$. Attempts to prepare this complex by prolonged heating at 363 K or cooling at liquid nitrogen temperature were not sucessful, Prolonged exposure to different magnetic fields at 363 K or at 100 K did not affect the composition of $Ni(NCS)_2.(ANT)_2(MeOH)_2$. The loss of one molecule of Methanol took place only under the experimental conditions described above.

$Cu(AcO)_2.(ANT)$: $Cu(AcO)_2.H_2O$ was prepared by adding copper powder to a solution consisting of 50% glacial acetic acid and 50% H_2O_2 at 100°C. When the solution was dark blue, it was filtered to get rid of any unreacted copper powder and the volume was reduced until crystallization started. Elemental analysis for C, H, N, and I.R. spectra indicated that the dark blue crystals are $Cu(AcO)_2.H_2O$. When ANT was added to the dark blue solution, stirred at 60°C, the solution turned green. The green crystals of $Cu(AcO)_2.(ANT)$ precipitated after cooling.

$CuCl.(ANT)_2$: 0.01 mole of CuCl(I) and 0.01 mole of ANT in ether were stirred until all the ANT reacted. The red precipitate was filtered and dried.

$Ag\ NO_3.(ANT)_2$: To a stirred solution of ANT (0.01 mole) in 50 ml. acetone at 0°C $AgNO_3$ crystals were added (0.0025 mole). The precipitate formed was filtered after the solution was stirred for about 5 hours, washed with acetone and dried in vacuo.

$CuCl_4.(HANT)_2$: When concentrated HCl was slowly added to a DMF solution of $Cu\ SO_4.(ANT)(DMF)$ or $CuCl_2.(ANT)(DMF)$ small shining green crystals precipitated. The crystals were washed with a small amount of acetone and petroleum ether, and dried in vacuo.

2.5. Attempted Preparation of 2-Bromo-5-nitrothiazole and 2-Chloro-5-nitrothiazole Complexes

No complexes could be prepared using 2-bromo-5-nitrothiazole or 2-chloro-5-nitrothiazole and the metal salts used in the preparation of 2-amino-5-nitrothiazole complexes. Other salts of the same metals including nitrates, bromides, iodides, sulphates, were also tested in several solvents e.g. acetone, methanol, DMF, nitromethane with no positive results.

CHAPTER 3

RESULTS AND DISCUSSION

3.1. C-13. N.M.R. Results

The carbon-13 n.m.r. spectra of substituted thiazoles were studied in order to probe the ground state electron distribution in this molecular framework, and to assess the relative contribution of the nitro substituent in determining this electron distribution.

The carbon-13 chemical shifts for 2-amino-5-nitrothiazole (ANT), 2-bromo-5-nitrothiazole (BNT), and 2-chlorothiazole (CNT), are given in table 5. Chemical shifts were obtained by using Me_4Si as an internal chemical shift standard. Proton coupled spectra were recorded as an aid in signal assignment. Comparison of reported chemical shifts of thiazole, 2-chlorothiazole, 2-bromothiazole also facilitated signal assignment.[54]

Table 5. Carbon-13 Chemical Shifts for Thiazole and Substituted Thiazoles**

Compound	Solvent	C(2)	C(4)	C(5)
Thiazole*	DMSO	153.6	143.3	119.6
2-chlorothiazole*	DMSO	150.6	141.4	122.9
CNT	MeOH	156.6	141.6	149.1
	DMSO	157.9	142.9	150.8
	Acetone	164.1	150.3	157.2
2-bromothiazole*	DMSO	136.8	144.0	125.2
BNT	Acetone	113.2	176.4	114.1
2-aminothiazole*	DMSO	170.3	139.0	107.7
ANT	MeOH	175.1	146.4	138.0
	DMSO	173.5	147.2	135.4

* means, data taken from ref. 54.

** chemical shifts are in ppm and were obtained by using Me_4Si as an internal chemical shift standard.

In order to gain more insight into the effect of the nitro group on the perturbation of electron density at each carbon, the carbon-13 chemical shifts of CNT, BNT, and ANT were compared with the chemical shifts of 2-chlorothiazole, 2-bromothiazole, and 2-aminothiazole, respectively. Table 6 contains the the carbon-13 chemical shift difference, $\Delta\delta$, caused by the effect of substitution of a nitro group at position 5 of the thiazole ring.

Table 6. Effect of Nitro Substitution on the Carbon-13 Chemical Shifts

Compound	$\Delta\delta$ *		
	C(2)	C(4)	C(5)
2-amino-5-nitrothiazole	+3.2	+8.2	+27.7
2-chloro-5-nitrothiazole	+7.3	+1.5	+27.9

* Means, chemical shifts are in ppm. The positive sign indicates that chemical shifts are towards the high-field region.

The chemical shift difference in 2-bromo-5-nitrothiazole is not included in table 6 because the spectrum of the latter could not be recorded in DMSO and comparison of the shifts in two different solvents would not be meaningful, especially since the carbon-13 chemical shifts of the compounds concerned show some dependence on the solvents used. However it seems that the perturbation induced by the nitro group in 2-bromo-5-nitrothiazole is quite different from the perturbation induced in 2-chloro-5-nitrothiazole and 2-amino-5-nitrothiazole.

As seen in table 6, the chemical shift difference $\Delta\delta$ induced by the nitro group at carbon-5 of the ring is nearly the

same for 2-chloro-5-nitrothiazole, and 2-amino-5-nitrothiazole, whereas, it is quite different at positions 4- and 2- of the ring.

3.2. Analyses

All compounds were analyzed for C, H, N. The results of analysis are listed in table 7. The compound $CuSO_4.(ANT)(DMF)$ was also analyzed for sulphur (Found: S, 16.13, repeat 15.89, calc. for $CuSO_4.(ANT)(DMF)$: S, 16.97). The compound $NiCl_2.(ANT)_2(DMF)_2$ was analyzed for sulphur and chlorine (found: S, 11.26, repeat 10.06; re-repeat 8.49, Cl, 12.11. Calc. for $NiCl_2.(ANT)_2(DMF)_2$ S,11.33, Cl, 12.53). The results of sulphur analyes indicated sample decomposition when exposed to the atmosphere.

3.3. Infrared Spectra

The infrared spectra of all the complexes showed a number of differences from the spectra of the free ligands (Table 8) principally in regions associated with the NH_2 group, the nitro group, and the ring vibrations. The solution spectrum of ANT in chloroform, could not be recorded for comparison, due to the insolubility of the ligand in that solvent. Accordingly, the spectra of the complexes in nujol or as KBr pellets had to be compared with the spectrum of ANT in solid state. The infrared spectrum of ANT revealed four bands in the $\nu(N - H)$ stretching frequency region (Fig. 2). The presence of four bands in this region instead of the usual two bands associated with amine $\nu_{asy}NH$ and $\nu_{sym}NH$ stretching frequencies implies the existence of two different types of -N-H bonds, which would result from intermolecular or intramolecular donor-acceptor interactions among the various coordination sites present in ANT. The infrared spectra of all the complexes, with the exception of mixed DMF ones, retained the four bands associated with $\nu_{asy}NH$ and $\nu_{sym}NH$, but the bands were shifted to lower frequencies.

In the spectra of mixed DMF complexes, the band associated

Table 7. Analytical Data

Compound		Analysis %		
		C	H	N
$CoCl_2.(ANT)_2$	Found	17.5	1.5	20.3
	Calcd.	17.2	1.4	20.1
$CoCl_2.(ANT)_2(MeOH)_2$	Found	19.7	2.8	17.9
	Calcd.	19.9	2.9	17.4
$CoSO_4.(ANT)_2(DMF)_2$	Found	19.7	3.0	15.5
	Calcd.	19.3	2.7	15.0
$NiCl_2.(ANT)_2$	Found	17.5	1.5	20.3
	Calcd.	17.2	1.5	20.0
$NiBr_2.(ANT)_3(MeOH)$	Found	16.9	1.9	18.0
	Calcd.	17.5	1.9	18.3
$Ni(NCS)_2.(ANT)_2(MeOH)_2$	Found	22.5	2.5	21.5
	Calcd.	22.1	2.6	21.2
$Ni(NCS)_2.(ANT)_2(MeOH)$	Found	21.6	2.0	22.4
	Calcd.	21.7	2.0	22.5
$NiSO_4.(ANT)_2(DMF)_2$	Found	24.1	3.4	18.4
	Calcd.	24.3	3.4	18.9
$NiCl_2.(ANT)_2(DMF)_2$	Found	25.3	3.5	20.2
	Calcd.	25.3	3.5	19.8
$CuCl_2.(ANT)_2$	Found	17.2	1.4	19.7
	Calcd.	17.0	1.4	19.8
$CuSO_4.(ANT)(DMF)$	Found	19.5	2.7	14.9
	Calcd.	19.1	2.7	14.8
$CuCl_2.(ANT)(DMF)$	Found	20.5	2.7	15.9
	Calcd.	20.4	2.8	15.9
$Cu(AcO)_2.(ANT)$	Found	25.6	2.8	13.0
	Calcd.	25.7	2.8	12 8
$CuCl_4.(HANT)_2$	Found	14.5	1.4	17.0
	Calcd.	14.5	1.4	16.9
$CuCl.(ANT)_2$	Found	18.6	1.4	21.2
	Calcd.	18.5	1.5	21.6
$CdCl_2.(ANT)_2$	Found	14.9	1.3	17.4
	Calcd.	15.2	1.3	17.7
$AgNO_3.(ANT)_2$	Found	15.5	1.2	21.1
	Calcd.	15.7	1.3	21.3

Table 8

I. R. Band Assignments (cm^{-1}.) for ANT and its Complexes

Ligand / Complex	ν N-H	δNH_2 or N-H def.	$\nu C\text{-}NO_2$	Ring stretching vibration	ν C=S
ANT	3430, 3395 3250, 3100	1623	1493	1507	738
$CoCl_2.(ANT)_2$	3405, 3305 3200, 3105	1617	1527	1480	735
$CoCl_2.(ANT)_2(MeOH)_2$	3390, 3230 3155, 3090	1605	1520	1500	738
$Co\ SO_4.(ANT)_2(DMF)_2$	3280, 3080	1623	1536	1520	738
$NiCl_2.(ANT)_2$	3405, 3305 3200, 3110	1617	1525	1475	735
$NiBr_2.(ANT)_3(MeOH)$	3300, 3155 3100	1613	1530	1505	740
$Ni\ NCS_2(ANT)_2(MeOH)_2$	3465, 3400 3295, 3215	1605	1535	1510	738

Infrared Band Assignments (cm^{-1}) for ANT Complexes (continuation)

$Ni(NCS)_2.(ANT)_2(MeOH)$	3400, 3260 3173, 3120	1598	1532	1492	738
$NiCl_2.(ANT)_2(DMF)_2$	3240, 3100	1623	1535	1507	738
$Ni\ SO_4.(ANT)_2(DMF)_2$	3280, 3080	1623	1535	1520	738
$CuCl_2.(ANT)_2$	3415, 3300 3200, 3115	1620	1532	1485	734
$CuCl_2.(ANT)(DMF)$	3305, 3160 3120	1623	1540	1512	737
$Cu\ SO_4.(ANT)(DMF)$	3300, 3120	1623	1560	1525	738
$Cu(AcO)_2.(ANT)$	3370, 3285 3193, 3117	1617	1527	1512	742
CuCl.(ANT)	3440, 3340 3240, 3100	1598	1520	1490	734
$CdCl_2.(ANT)_2$	3415, 3315 3200, 3100	1620	1525	1490	734
$Ag\ NO_3.(ANT)_2$	3390, 3280	1623	1530	1472	738

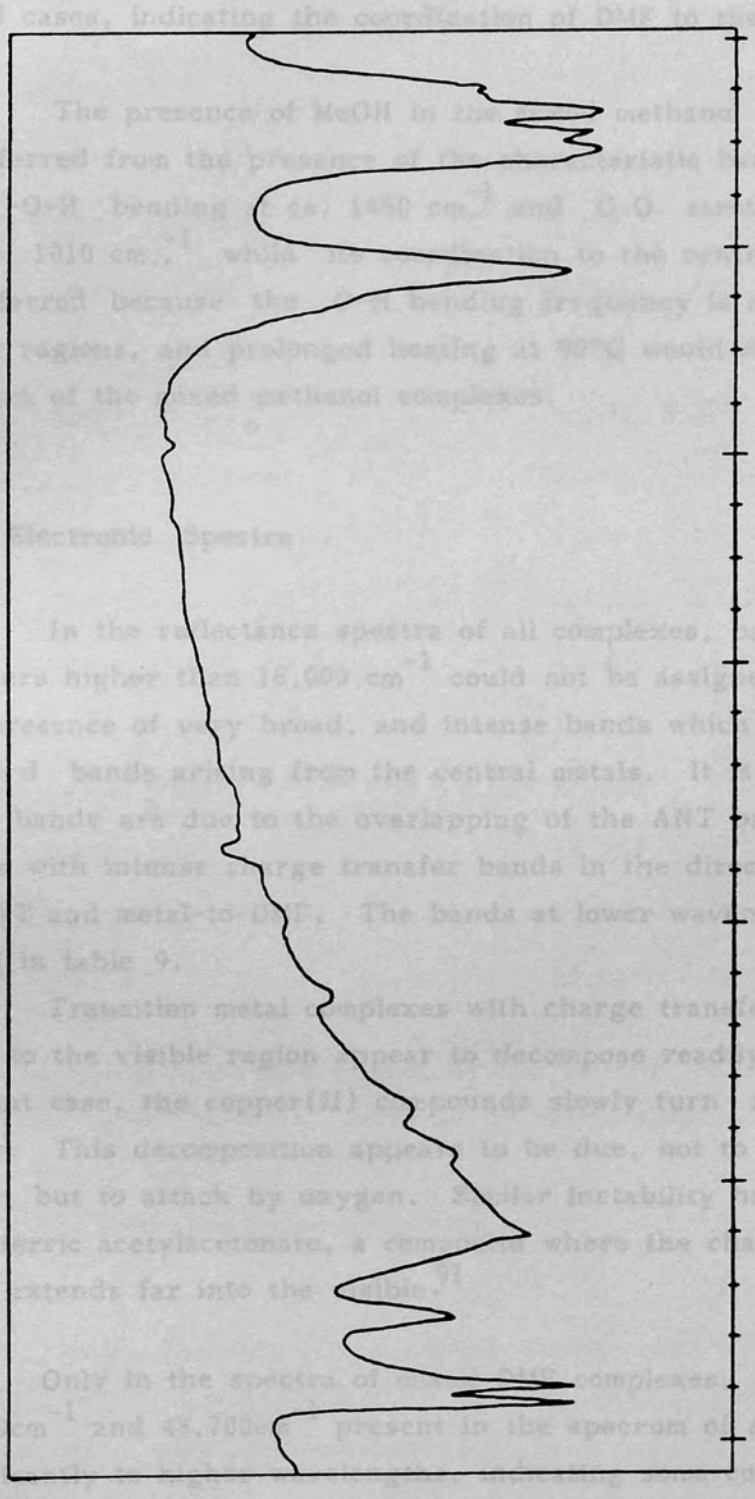

Fig. 2. Infrared spectrum of 2-amino-5-nitrothiazole as KBr pellet.

with the carbonyl absorption $\nu_{C=O}$ which is at 1675 $cm.^{-1}$ in the spectrum of DMF is shifted to lower frequencies by 20 - 40 $cm.^{-1}$ in all cases, indicating the coordination of DMF to the central metal ion.

The presence of MeOH in the mixed methanol complexes is inferred from the presence of the characteristic bands associated with -O-H bending at ca. 1460 $cm.^{-1}$ and C-O stretching vibration at ca. 1010 $cm.,^{-1}$ while its coordination to the central metal ion is inferred because the O-H bending frequency is shifted to lower regions, and prolonged heating at 90°C would not effect the spectra of the mixed methanol complexes.

3.4. Electronic Spectra

In the reflectance spectra of all complexes, bands of wavenumbers higher than 18,000 cm^{-1} could not be assigned due to the presence of very broad, and intense bands which were obscuring the d-d bands arising from the central metals. It is thought that these bands are due to the overlapping of the ANT bands and d-d bands with intense charge transfer bands in the direction metal-to-ANT and metal-to-DMF. The bands at lower wavenumbers are listed in table 9.

Transition metal complexes with charge transfer bands very close to the visible region appear to decompose readily. In the present case, the copper(II) compounds slowly turn reddish-black in air. This decomposition appears to be due, not to attack by water, but to attack by oxygen. Similar instability has been noted with ferric acetylacetonate, a compound where the charge transfer band extends far into the visible.[91]

Only in the spectra of mixed DMF complexes, the bands at 38,000cm^{-1} and 43,700cm^{-1} present in the specrum of ANT, shifted significantly to higher wavelengths, indicating some covalent character for M - N bond.

The solution electronic spectra of all the complexes indicated dissociation, which probably resulted from the low basicity of ANT

Table 9. Electronic Spectra (cm^{-1})

Compound	Band Maxima
$CoCl_2.(ANT)_2$	6,300, 14,700 18,000
$CoCl_2.(ANT)_2(MeOH)_2$	7,300, 14,500, 18,700
$Co\ SO_4.(ANT)_2(DMF)_2$	8,000, 14,700, 18,800sh, 19,500
$NiCl_2.(ANT)_2$	7,300, 13,200
$NiBr_2.(ANT)_3(MeOH)$	7,300, 8,800, 12,500, 14,200
$Ni(NCS)_2.(ANT)_2(MeOH)_2$	8,500, 10,500, 14,000, 16,500
$Ni(NCS)_2.(ANT)_2(MeOH)$	9,200, 15,700
$Ni\ SO_4.(ANT)_2(DMF)_2$	8,300, 14,800
$NiCl_2.(ANT)_2(DMF)_2$	8,000, 14,000
$CuCl_2.(ANT)_2$	13,500
$Cu\ SO_4.(ANT)(DMF)$	11,000
$CuCl_2.(ANT)(DMF)$	14,200
$Cu(AcO)_2.(ANT)$	13,900
$CuCl_4.(HANT)_2$	13,000

and the steric hindrance caused by the substituents. The solvents tried included acetone, methanol, ethanol, water, and DMF.

3.5. X-ray diffraction powder photographs

The x-ray diffraction powder photographs of $NiCl_2.(ANT)_2$, $CuCl_2.(ANT)_2$, $CoCl_2.(ANT)_2$ and $CdCl_2.(ANT)_2$ were compared to find out if they are isomorphous.

The interplanar d spacings in Å were taken from tables giving interplanar spacings a function of 2θ. The intensity of the strongest peak was considered to be 100% and the intensities of

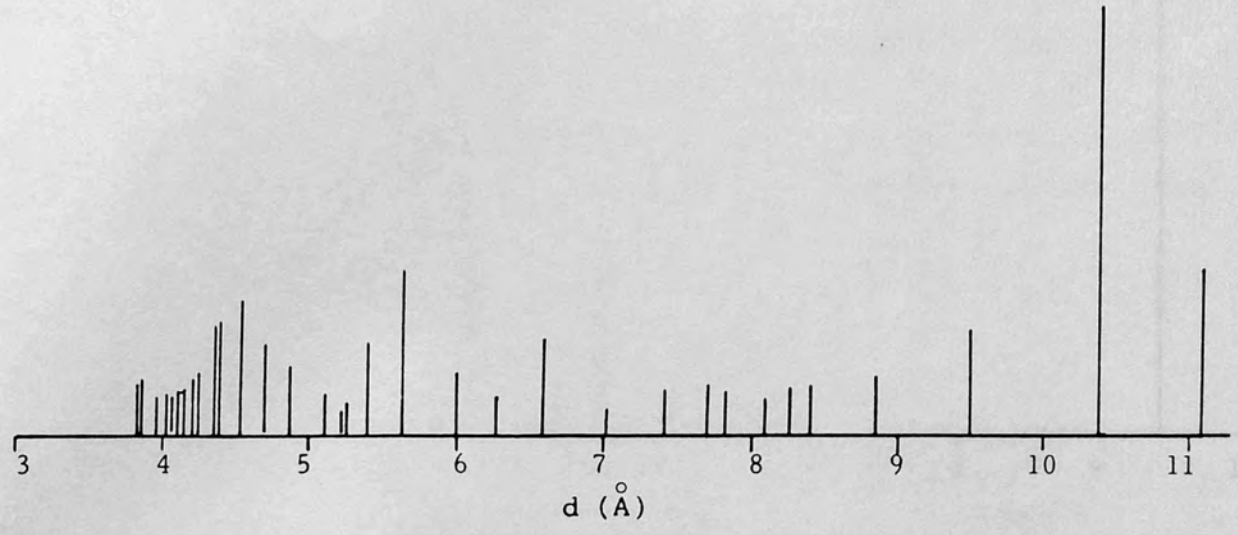

Fig. 3. X-ray powder pattern of $NiCl_2.(ANT)_2$.

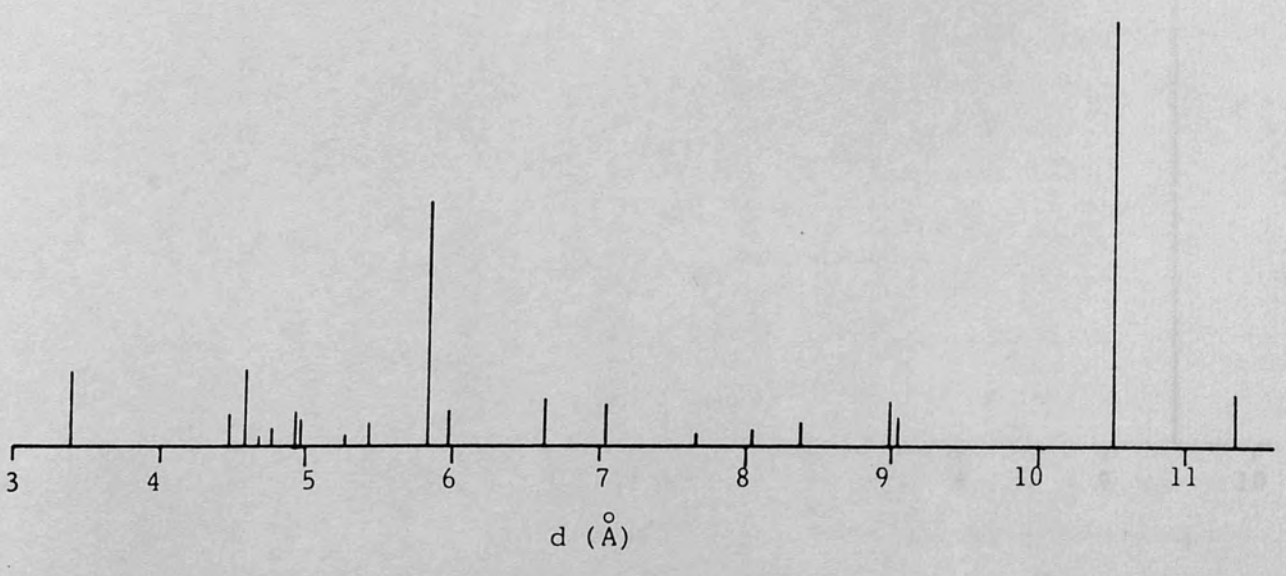

Fig. 4. X-ray powder pattern of $CdCl_2.(ANT)_2$.

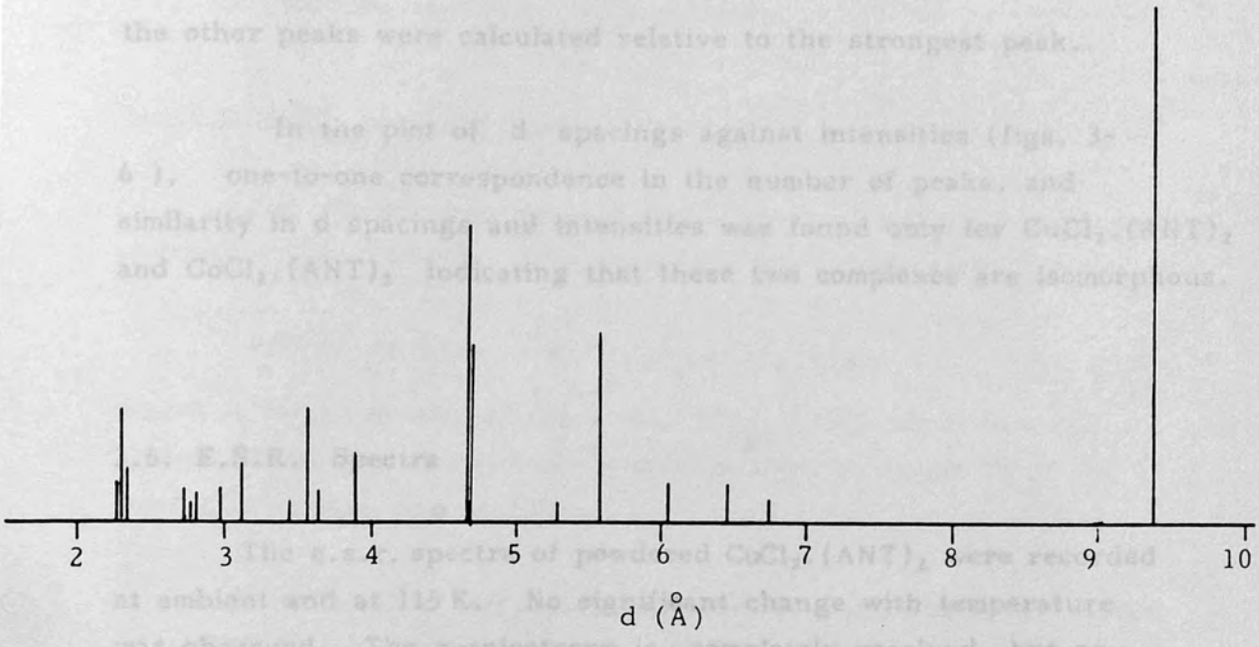

Fig. 5. X-ray powder pattern of $CoCl_2.(ANT)_2$.

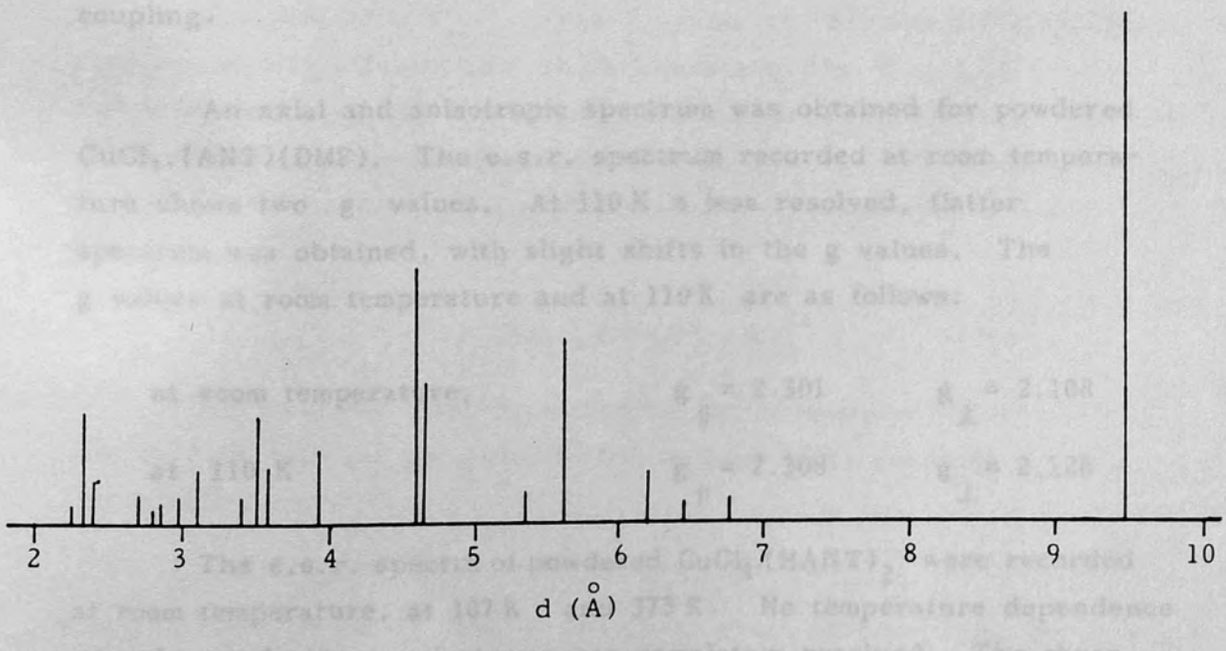

Fig. 6. X-ray powder pattern of $CuCl_2.(ANT)_2$.

the other peaks were calculated relative to the strongest peak.

In the plot of d spacings against intensities (figs. 3-6), one-to-one correspondence in the number of peaks, and similarity in d spacings and intensities was found only for $CuCl_2.(ANT)_2$ and $CoCl_2.(ANT)_2$ indicating that these two complexes are isomorphous.

3.6. E.S.R. Spectra

The e.s.r. spectra of powdered $CuCl_2.(ANT)_2$ were recorded at ambient and at 115 K. No significant change with temperature was observed. The g-anisotropy is completely resolved, but no nuclear hyperfine splitting was observed. The three rhombic g values are at $g_1 = 2.054$, $g_2 = 2.131$, $g_3 = 2.205$.

The room temperature e.s.r. spectrum of powdered $Cu\,SO_4.(ANT)$-(DMF) revealed a very broad non-symmetrical curve with a peak to peak line width of 260G indicating the presence of exchange coupling.

An axial and anisotropic spectrum was obtained for powdered $CuCl_2.(ANT)(DMF)$. The e.s.r. spectrum recorded at room temperature shows two g values. At 110 K a less resolved, flatter spectrum was obtained, with slight shifts in the g values. The g values at room temperature and at 110 K are as follows:

at room temperature,	$g_{\parallel} = 2.301$	$g_{\perp} = 2.108$
at 110 K	$g_{\parallel} = 2.308$	$g_{\perp} = 2.126$

The e.s.r. spectra of powdered $CuCl_4.(HANT)_2$ were recorded at room temperature, at 107 K and 373 K. No temperature dependence was observed, the g anisotropy was completely resolved. The three rhombic g values are at $g_1 = 2.044$, $g_2 = 2.125$ and $g_3 = 2.170$.

3.7. Magnetic Susceptibility Measurements

3.7.1. Nickel(II) Complexes

For the magnetic measurements, the temperature independent paramagnetism TIP, was calculated from the relationship.

$$TIP = 8N\beta^2/\Delta \cong 2.09/\Delta \quad \text{c.g.s.u.}$$

where Δ is the energy of the level $^3T_{2g}$ being mixed into the ground state, and amounts in these complexes to almost 7% of the room temperature susceptibility.

The values of TIP, diamagnetic correction, and θ are given in table 10.

The plots of $1/\chi_m$ (χ_m = corrected for diamagnetism) versus temperature for all the Ni(II) complexes with the exception of $NiCl_2.(ANT)_2$, gave straight lines passing through the origin.

The plot of $1/\chi_m$ versus temperature for the $NiCl_2.(ANT)_2$ complex gave a straight line which intersected the T axis at $\theta = 24K$ indicating ferromagnetic interaction between the Ni(II) ions(fig. 7). The value of the magnetic moment for this compound was calculated from the relationship corresponding to ferromagnetic interaction between metal ions.

$$\mu = 2.84[\chi_m(T - \theta)]^{\frac{1}{2}}$$

The magnetic moment, corrected for ferromagnetism in this way, was used to calculate the value of the spin-coupling constant $-\lambda'$ from the relationship

$$\mu = 2.83(1 - 4\lambda'/\Delta)$$

and was found to be 297 cm^{-1}. Whilst no great accuracy may be claimed for this value, it seems to be reasonable to account for the magnetic moment of this complex.

Table 10. Some Spectral and Magnetic Parameters

Compound	Δ cm^{-1}	$\times 10^6$ Diamagnetic Correction	$\times 10^6$ TIP c.g.s.u.	θ K	μ B.M.
$NiCl_2.(ANT)_2$	7,300	176.36	286.3	24±1	3.29
$NiBr_2.(ANT)_3(MeOH)$	8,300	231.07	251.8	0	3.14
$Ni(NCS)_2.(ANT)_2(MeOH)_2$	9,040	258.18	231.2*	0	3.20
$Ni(NCS)_2.(ANT)_2(MeOH)$	9,200		227.2	0	3.18
$NiCl_2.(ANT)_2(DMF)_2$	8,000	265.6	261.2	0	3.20

* The value of TIP was calculated by using the weighed mean of the two components of the split band as a measure of the energy of the unsplit band, Δ, in the relationship:
$TIP = 8N\beta^2/\Delta \cong 2.09/\Delta$ c.g.s.u.

Table 11.

Experimental values of the field independent susceptibility of $NiCl_2.(ANT)_2$*

T K	$\chi_g \times 10^6$	$\chi_m \times 10^6$	$1/\chi_m$	μ_{eff} B.M.
363.16	8.50	4207.25	237.68	3.39
343.16	8.98	4410.23	226.74	3.38
323.16	9.63	4680.87	213.64	3.38
299.16	10.63	5104.48	195.91	3.41
283.16	11.35	5405.11	185.01	3.42
263.16	12.48	5878.72	170.11	3.45
243.16	13.72	6399.99	156.25	3.46
223.16	15.07	6966.58	143.54	3.47
203.16	16.89	7731.46	129.34	3.49
183.16	19.06	8643.36	115.70	3.51
163.16	21.88	9825.90	101.77	3.54
143.16	25.75	11449.70	87.34	3.59
123.16	31.22	13750.11	72.73	3.65
103.16	39.20	17097.71	58.48	3.74

* c.g.s. units are used

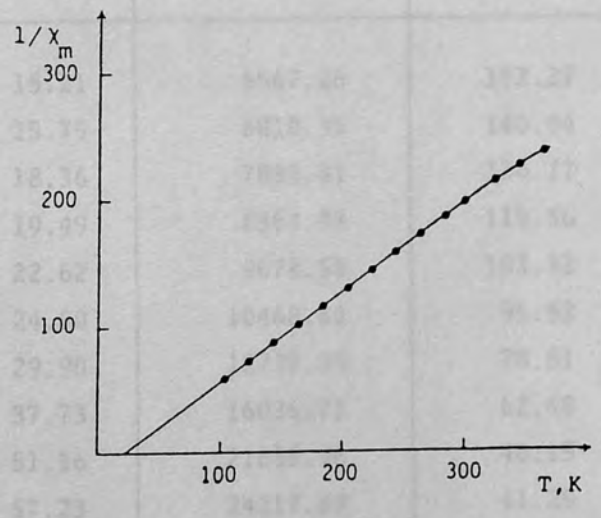

Fig. 7. Temperature dependence of the inverse magnetic susceptibility of $NiCl_2.(ANT)_2$.

3.7.2. Cobalt(II) Complexes

In octahedral cobalt(II) the ground state is $^4T_{1g}$ and a large orbital contribution to the moment is expected. Mixing of a singlet excited state lowers the moment but a value in excess of 5BM is expected. The ground state for tetrahedral cobalt (II) is $^4A_2$ and a low moment is usually obtained. An excited triplet state is comparatively low in energy and can be mixed with the ground state. Moments in the range of 4 - 5 BM have been predicted and are found experimentally.[92,93]

The term TIP is not included in the calculations of effective magnetic moments of these complexes due to the uncertainty involved in the reflectance spectral bands at high energies. However, the effect of TIP is hardly felt in complexes with three unpaired electrons and could be safely neglected.

Table 12.

Experimental values of the field independent susceptibility of $CoCl_2.(ANT)_2$*

T K	$\chi_g \times 10^6$	$\chi_m \times 10^6$	$1/\chi_m$	μ_{eff} B.M.
363.16	15.21	6567.26	152.27	4.38
343.16	15.79	6810.35	146.84	4.34
299.16	18.36	7888.41	126.77	4.36
283.16	19.49	8364.03	119.56	4.37
243.16	22.62	9678.58	103.32	4.36
223.16	24.50	10468.63	95.52	4.34
183.16	29.90	12737.05	78.51	4.34
143.16	37.73	16026.73	62.40	4.30
103.16	51.16	21668.06	46.15	4.25
91.16	57.23	24217.89	41.29	4.22

* Diamagnetic correction = 176.36×10^{-6} c.g.s.u.

$\theta = -10$ K

Table 13

Experimental values of the field-independent susceptibility of $Co\ SO_4.(ANT)_2(DMF)_2$*

Diamagnetic correction = 253.84×10^{-6} c.g.s.u.

T K	$\chi_g \times 10^6$	$\chi_m \times 10^6$	$1/\chi_m$	μ_{eff} B.M.
363.16	15.24	9261.56	107.97	5.21
343.16	16.11	9778.02	102.27	5.20
323.16	17.06	10339.22	96.72	5.19
299.16	18.37	11111.89	90.00	5.17
283.16	19.33	11681.23	85.61	5.16
263.16	20.88	12596.23	79.39	5.17
243.16	22.49	13551.90	73.79	5.15
223.16	24.45	14710.91	67.98	5.14
203.16	26.35	15829.24	63.17	5.09
183.16	28.89	17333.24	57.69	5.06
163.16	31.62	18948.39	52.77	4.99
143.16	35.70	21359.94	46.82	4.97
123.16	40.55	24226.95	41.28	4.90
103.16	45.98	27439.63	36.44	4.78
91.16	50.32	30001.16	33.33	4.70

* c.g.s. units are used.

3.7.3. Copper(II) Complexes

The effective magnetic moments of these complexes were calculated using the expression $\mu_{eff} = 2.84(\chi_{m'} \times T)^{\frac{1}{2}}$, where $\chi_{m'}$ is the molar susceptibility corrected for diamagnetic effects and Nα, where Nα is the TIP associated with the copper ion. In the present work, a value $N\alpha = 60 \times 10^{-6}$ has been used.

The results of magnetic measurements for the Cu(II) complexes indicated antiferromagnetic interaction in all complexes with the exception of $CuCl_4.(HANT)_2$, while the complex $Cu(AcO)_2.(ANT)$ exhibited a subnormal magnetic moment (Tables 14-18). The diamagnetic correction and the measured Weiss constant are given with each table.

Table 14. Experimental values of the field independent susceptibility of $CuCl_2.(ANT)_2$ *

Diamagnetic correction = 174.36×10^{-6} c.g.s.u.

θ = -13 K

T K	χ_g	χ_m	$1/\chi_m$	$\frac{u_{eff}}{B.M.}$
323.16	2.48	1493.32	669.65	1.93
299.16	3.06	1593.45	627.57	1.92
283.16	3.25	1674.66	597.14	1.92
263.16	3.50	1782.26	561.09	1.91
243.16	3.82	1917.31	521.56	1.91
223.16	4.18	2071.31	482.79	1.90
203.16	4.65	2271.15	440.30	1.90
183.16	5.22	2509.83	398.43	1.90
163.16	5.90	2801.33	356.97	1.90
143.16	6.66	3122.72	320.23	1.88
123.16	7.64	3541.24	282.39	1.86
103.16	9.14	4176.15	239.46	1.85
91.16	10.31	4671.91	214.05	1.84

* χ_g and χ_m are in 10^6 c.g.s.u.,

Table 15. Experimental values of the field-independent susceptibility of $CuSO_4.(ANT)(DMF)$*

Diamagnetic correction = 155.8×10^{-6} c.g.s.u.

θ = - 30K

TK	$\chi_g \times 10^6$ c.g.s.u.	χ_m	$1/\chi_m$	u_{eff} B.M.
343.16	3.15	1466.22	682.03	1.97
299.16	3.65	1652.95	604.98	1.96
283.16	3.89	1746.32	572.63	1.96
243.16	4.63	2026.42	493.48	1.96
223.16	5.00	2166.16	461.65	1.95
203.16	5.50	2353.20	424.95	1.94
163.16	9.98	2913.40	343.24	1.94
143.16	7.88	3251.86	307.52	1.93
123.16	8.96	3660.33	273.20	1.89
103.16	10.29	4162.18	240.26	1.85
91.16	11.43	4594.00	217.68	1.83

* χ_m is in 10^6 c.g.s.u.

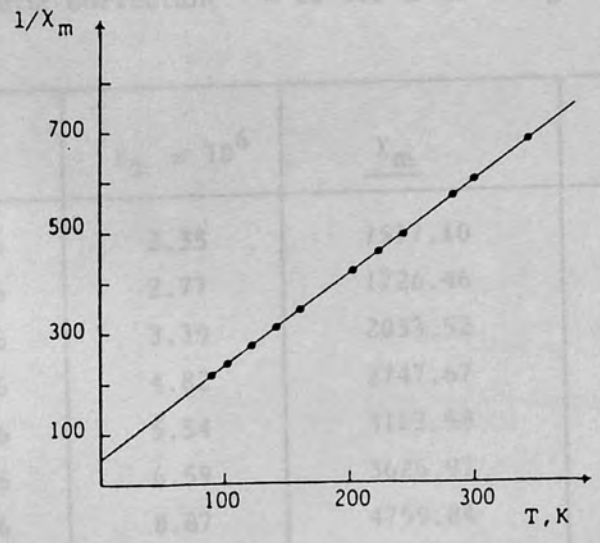

Fig. 8. Temperature dependence of the inverse magnetic susceptibility of $CuSO_4.(ANT)(DMF)$.

Table 16. Experimental values of the field-independent susceptibility of $CuCl_2.(ANT)(DMF)$ *

Diamagnetic correction = 165.8×10^{-6} c.g.s.u.

$\theta = -10$ K

T K	$\chi_g \times 10^6$	χ_m	$1/\chi_m$	μ_{eff} B.M.
299.16	3.46	1509.84	662.32	1.87
263.16	4.02	1708.08	585.45	1.87
203.16	5.39	2190.95	456.42	1.87
183.16	5.97	2397.38	417.12	1.86
163.16	6.72	2660.18	375.91	1.85
143.16	7.55	2956.65	301.67	1.83
123.16	8.89	3427.69	291.74	1.83
103.16	10.67	4056.94	246.49	1.81
91.16	11.86	4478.60	223.28	1.80

* χ_g is in c.g.s.u., χ_m is in 10^6 c.g.s.u.

Table 17. Experimental values of the field-independent susceptibility of $CuCl_4.(HANT)_2$*

Diamagnetic correction = 227.02×10^{-6} c.g.s.u.

$\theta = 0$

T K	$\chi_g \times 10^6$	χ_m	$1/\chi_m$	μ_{eff} B.M.
299.16	2.35	1517.10	659.15	1.87
263.16	2.77	1726.46	579.22	1.88
223.16	3.39	2033.52	491.76	1.88
163.16	4.82	2747.67	363.94	1.88
143.16	5.54	3103.58	322.21	1.87
123.16	6.59	3626.97	275.71	1.88
93.16	8.87	4759.84	210.09	1.88

* χ_g is in c.g.s.u., χ_m is in 10^6 c.g.s.u.

Table 18. Experimental values of the field-independent susceptibility of $[Cu(AcO)_2.(ANT)]_2$

Diamagnetic correction per copper ion = 123 x 10^{-6} cgs

T K	$\frac{\chi_m}{2} \times 10^6$ cgs	$\frac{2}{\chi_m}$ cgs	μ_{eff} B.M.
296.0	863.43	115.82	1.38
263.0	908.58	110.06	1.34
220.1	822.36	121.60	1.16
196.7	745.35	134.17	1.04
164.3	644.63	155.13	0.88
140.1	537.24	186.14	0.73
99.0	372.85	268.20	0.50
85.2	326.62	306.17	0.43

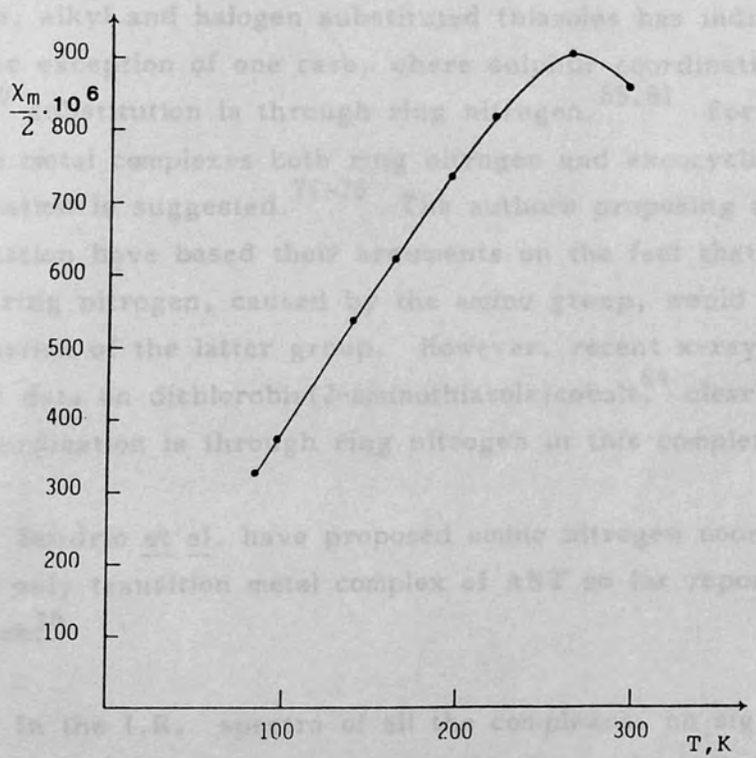

Fig. 9. Temperature dependence of the magnetic susceptibility of $[Cu(AcO)_2.(ANT)]_2$.

3.8. The donor centre in 2-amino-5-nitrothiazole

2-amino-5-nitrothiazole (ANT) has five possible centres of coordination: (1) cyclic sulphur, (2) the nitro group, (3) electrons of the ring, (4) the exocyclic nitrogen, (5) cyclic nitrogen.

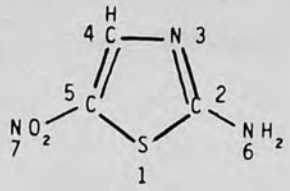

(II)

Previous work on simpler thiazoles, such as unsubstituted thiazole, alkyl and halogen substituted thiazoles has indicated that with the exception of one case, where sulphur coordination is proposed,[80] substitution is through ring nitrogen.[65,81] For the 2-amino-thiazole metal complexes both ring nitrogen and excocyclic nitrogen coordination is suggested.[71-76] The authors proposing amino nitrogen coordination have based their arguments on the fact that steric hindrance at the ring nitrogen, caused by the amino group, would favour the coordination of the latter group. However, recent x-ray crystallographic data on dichlorobis(2-aminothiazole)cobalt,[84] clearly indicates that coordination is through ring nitrogen in this complex.

Doadrio et al. have proposed amino nitrogen coordination for the only transition metal complex of ANT so far reported in the literature.[30]

In the I.R. spectra of all the complexes, no significant change was observed in the C=S vibrations, thus eliminating the possibility of sulphur coordination.

The small values of Δ. observed in the reflectance spectra

(table 9) mean that the nitro group could not be the coordinating site.[94]

The carbon-13 chemical shift differences, $\delta\Delta$, between 2-aminothiazole and 2-amino-5-nitrothiazole show a deshielding effect of 3.2ppm, 8.2ppm, and 27.7ppm at C(2), C(4), and C(5) respectively. This deshielding effect may be explained if resonance form (XIV) makes a substantial contribution to the ANT hybrid,

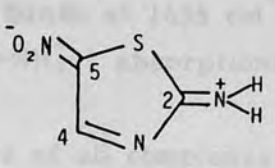

(XIV)

because, in this form, the strong electron-withdrawing resonance effect of the nitro group is capable of delocalising the electron density away from the ring, thus, making the π electrons of the ring less available for coordination than in 2-aminothiazole.

The deshielding effect at C(2) could be explained if further enhancement in the double bond character of C(2) - NH_2 , which is present in 2-aminothiazole, is considered. Accordingly, the conjugation of the nitro group with the present system will make the amino nitrogen even less basic than in 2-aminothiazole. This result is in line with previous results obtained by conformational studies by dynamic n.m.r. on 2-NN-dimethylaminothiazole, and 5-nitro-2-NN-dimethylaminothiazole,[47] that predict an enhancement in Ar-N double bond character in the latter compound.

Although the techniques mentioned above predict a reduction in the basicity of the ring nitrogen and the amino nitrogen, there is no clear indication as to which one of the two is affected most by the substitution of nitro group. The protonation of ANT in solution is studied by means of U.V. spectroscopy [95] and by measuring the

pK_a values of a number of 5-substituted 2-aminothiazoles;[44] and in both cases ring nitrogen protonation is proposed.

The I.R. spectrum of protonated ANT in solid form, which was prepared in this work, suggested the existence of a mixture of ring nitrogen and amino nitrogen protonated ANT(fig. 10). The band at 3220cm^{-1} falls in the range associated with primary amine stretching frequency, while the band at 1595 cm-1 is typical for $-NH_3^+$ absorption, because $=\overset{+}{N}H$ does not absorb in this region. The two closely located bands at 1635 cm^{-1} and 1648 cm^{-1} could be assigned to δNH_2 and $-NH_3^+$ absorptions respectively.

The I.R. spectra of all complexes showed a shifting to lower frequencies in $\nu_{sym}NH$ and $\nu_{asy}NH$. This may result from the coordination of the amine group. It might also be due to the electronic effects resulting from other coordination sites.

The coordination of $-NH_2$ nitrogen implies a shift to lower frequencies in $\nu_{asy}NH$ and $\nu_{sym}NH$, a shift to higher frequencies in δNH_2 and no shift or slight shift in the ring stretching vibration.[74]

The presence of four bands corresponding to $\nu_{sym}NH$ and $\nu_{sym}NH$, is evident in the I.R. spectra of all complexes with the exception of the spectra of mixed DMF complexes, which show only two bands in this region. The presence of more than the usual two bands associated with amine stretching vibration is probably due to the existence of dissimilar amine groups in these complexes resulting from either (a) hydrogen bonding of the NH_2 group with either the anions, or MeOH, or the nitro group, or (b) some kind of donor-acceptor interaction between the amino group and the nitro

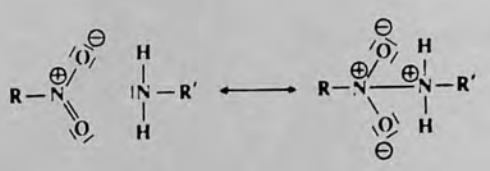

group due to charge transfer bonding,[96] or (c) due to the coordination

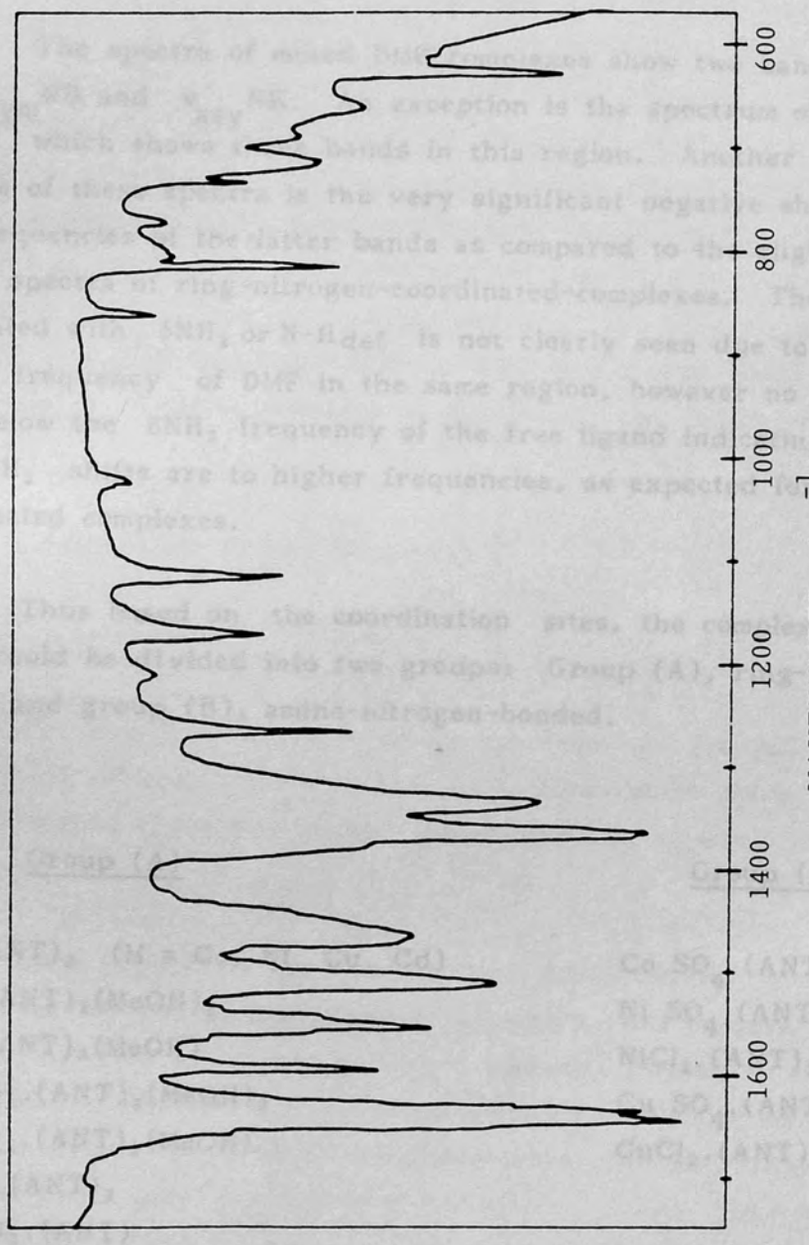

Fig. 10. Infrared spectrum of protonated 2-amino 5-nitrothiazole as nujol mull.

of the ligand to dissimilar metal ions. All these interactions, with the exception of the latter case, result in a reduction of the donor strength of the amine nitrogen, thus leaving the ring nitrogen as the potential coordinating site. The negative shift in the δNH_2 frequency further supports this proposal, because coordination of the amine nitrogen implies a positive shift in δNH_2.

The spectra of mixed DMF complexes show two bands corresponding to $\nu_{sym}NH$ and $\nu_{asy}NH$. An exception is the spectrum of $CuCl_2.(ANT)$-(DMF) which shows three bands in this region. Another important feature of these spectra is the very significant negative shift in the frequencies of the latter bands as compared to the slight shifts in the spectra of ring-nitrogen-coordinated-complexes. The band associated with δNH_2 or $N\text{-}H_{def}$ is not clearly seen due to the presence of a C=O frequency of DMF in the same region, however no band is seen below the δNH_2 frequency of the free ligand indicating that all δNH_2 shifts are to higher frequencies, as expected for amine coordinated complexes.

Thus based on the coordination sites, the complexes prepared could be divided into two groups: Group (A), ring-nitrogen-bonded and group (B), amine-nitrogen-bonded.

Group (A)	Group (B)
$MCl_2.(ANT)_2$ (M = Co, Ni, Cu, Cd)	$Co\ SO_4.(ANT)_2(DMF)_2$
$CoCl_2.(ANT)_2(MeOH)_2$	$Ni\ SO_4.(ANT)_2(DMF)_2$
$NiBr_2.(ANT)_3(MeOH)$	$NiCl_2.(ANT)_2(DMF)_2$
$Ni(NCS)_2.(ANT)_2(MeOH)_2$	$Cu\ SO_4.(ANT)(DMF)$
$Ni(NCS)_2.(ANT)_2(MeOH)$	$CuCl_2.(ANT)(DMF)$
$Ag\ NO_3.(ANT)_2$	
$Cu(AcO)_2.(ANT)$	
$CuCl.(ANT)_2$	

If the ring nitrogen can behave as the donor atom, one should wonder why 2-chloro-5-nitrothiazole(CNT) and 2-bromo-5-nitrothiazole(BNT) did not form complexes in the same manner.

Theoretical treatment [34] on 2-aminothiazole, 2-chlorothiazole, and 2-bromothiazole predicts a lower electron density at ring nitrogen for the last two molecules. In fact 2-bromothiazole forms complexes of the type $MX_2.L_2$ (M = Cu, Co; X = Cl, Br) only, whereas, 2-aminothiazole forms in addition to complexes of the type $MX_2.L_2$, complexes where four ligands are coordinated to one metal ion for the same metal salts, implying the higher basicity of the donor site in the latter. Consequently the introduction of a nitro group, as indicated by C-13 n.m.r. results, will make the ring nitrogen in CNT and BNT less basic than in ANT and would result in further reduction in σ-donor strength of the former two molecules.

3.9. Configuration of the Complexes

3.9.1. $[Cu(AcO)_2.ANT]_2$

The magnetic data, electronic spectrum and the infrared spectra are all consistent with the above formulation since, the dimeric nature of copper acetate monohydrate is retained in this complex.

Since copper(II) has a d^9 electron configuration, a monomeric complex of this metal, regardless of geometry, will possess one unpaired electron and hence exhibit a magnetic moment in the vicinity of 1.73 B.M. If, however, a normal strong metal-metal bond were to form between two of these monomers, then the two formerly unpaired electrons could pair, leading to a diamagnetic dimer. The intermediate situation should also be conceptually possible wherein the magnetic moment of the complexes could vary between zero and 1.73 B.M. as the strength of the metal-metal interaction varies. Thus, the observed magnetic moment [97] of 1.4 B.M. for copper acetate monohydrate is related to the close proximity of the two copper(II) ions. (2.64 $\mathring{A}$). [98] As the dimeric nature of copper acetate monohydrate

is retained in the ANT complex , it would be convenient to describe the structure of copper acetate monohydrate before proceeding to discuss the physical properties of the ANT complex.

Perhaps the best known and most widely studied copper(II) complex is copper(II) acetate monohydrate.[97,99,100] Direct interaction between the orbitals containing the unpaired electrons, is postulated to account for the antiferromagnetic exchange observed in this compound. Among the three possible metal-metal interactions: a σ-bond formed via overlap of d_{z^2} orbitals on each metal centre, a π-bond formed by overlap of d_{xy} or d_{yz} orbitals on each metal centre or a δ-bond formed by overlap of the d_{xy} or $d_{x^2-y^2}$ orbitals on each metal centre, the δ-bonding model has received the greatest support (fig. 11). The direct overlap between the orbitals leads

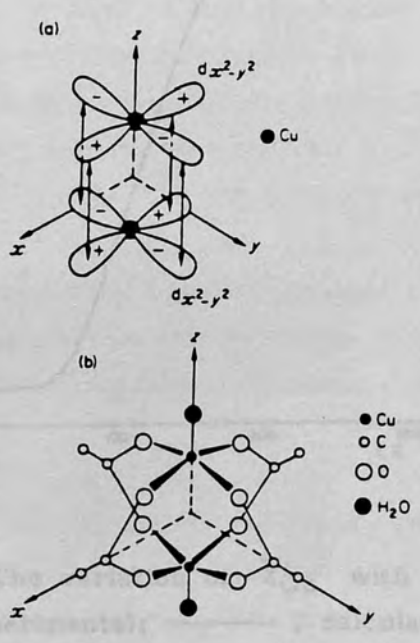

Fig. 11. (a) An illustration of the δ-bonding in, and (b) the structure of, copper(II) acetate monohydrate. (After Figgis and Martin.[97])

to a diamagnetic spin-singlet ground state for this molecule. However, the paramagnetic triplet is thermally accessible resulting in a temperature-dependent magnetic moment and antiferromagnetic interaction. The variation of the magnetic susceptibility with temperature for each copper ion in the molecule is shown in Fig. 12. and is compared with that given by the equation

$$\bar{\chi}_A = \frac{\chi_m}{2} = \frac{N\beta^2 g^2}{3kT}\left[\frac{3\exp(2x)}{3\exp(2x)+1}\right] + N\alpha \qquad (2.1)$$

where $x = J/kT$, $g = 2.16$, $J = -295\ cm^{-1}$, and a temperature independent contribution $N\alpha = 60 \times 10^{-6}$ c.g.s.u.[99]

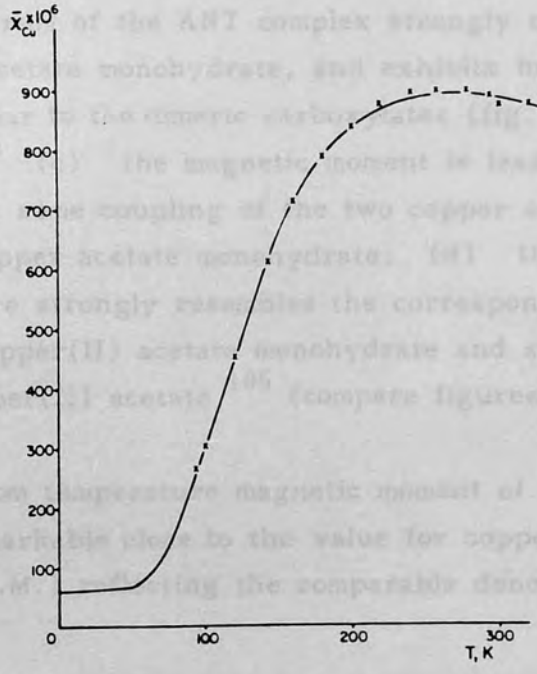

fig. 12. The variation of $\bar{\chi}_{Cu}$ with T for copper(II) acetate monohydrate. x, experimental; ——— , calculated from equation 2.1.

The influence of trans-axial ligation, (where the water molecule in copper(II) acetate monohydrate is replaced by another ligand) on metal-metal bond formation in copper(II) acetate complexes has been the subject of numerous investigations.[101-106] The differences observed in the magnetic moments and the electronic spectral bands have been

explained in terms of σ-donation and π-acceptance, and basicities of the axial ligand. It has been found that the magnetic moments of copper(II) carboxylate adduct decrease slightly as the basicity of the trans-axial ligand decreases,[105,106] the greatest decrease in moments is reported for complexes capable of π-back bonding such as triphenylphosphine, pyrazine, and 4-nitro-pyridine-N-oxide.

In $[Cu(AcO)_2.ANT]_2$ the retention of the dimeric carboxylate structure is supported by the following observations:- (a) the infrared spectrum exhibits the carboxylate stretching frequencies, ν_{COO^-} (sym) and ν_{COO^-} (assym), at 1413 cm^{-1} and 1645 cm^{-1} respectively, at quite similar energies to the corresponding bands in the spectrum of copper(II) acetate monohydrate;[107] (b) the electronic spectrum of the ANT complex strongly resembles the spectrum of copper(II) acetate monohydrate, and exhibits bands at 26,300 cm^{-1}, which are peculiar to the dimeric carboxylates (fig. 13) and their adducts;[100,105] (c) the magnetic moment is less than 1.73 B.M. suggesting that some coupling of the two copper atoms occurs as in the case for copper acetate monohydrate; (d) the variation of $\overline{\chi}_{Cu}$ with temperature strongly resembles the corresponding variation reported for copper(II) acetate monohydrate and substituted pyridine adducts of copper(II) acetate [105] (compare figures 9 and 12).

The room temperature magnetic moment of this complex, at 1.38B.M. is remarkable close to the value for copper(II) acetate monohydrate (1.4 B.M.) reflecting the comparable donor abilities of water and ANT.

Literature survey of similar complexes revealed that the room temperature magnetic moment and the positions of reflectance spectral bands are quite similar to the corresponding values for $[Cu(AcO)_2.Pyridine\ N\text{-}oxide]_2$, implying the low basicity and the high π-acceptor ability of ANT, and the coordination of ring nitrogen in ANT, because coordination of $-NH_2$ nitrogen eliminates the possibility of π back-bonding.

The complex $Cu(AcO)_2$(2-aminothiazole) has been assigned a polymeric octahedral structure.[75] However, the reported room-temperature

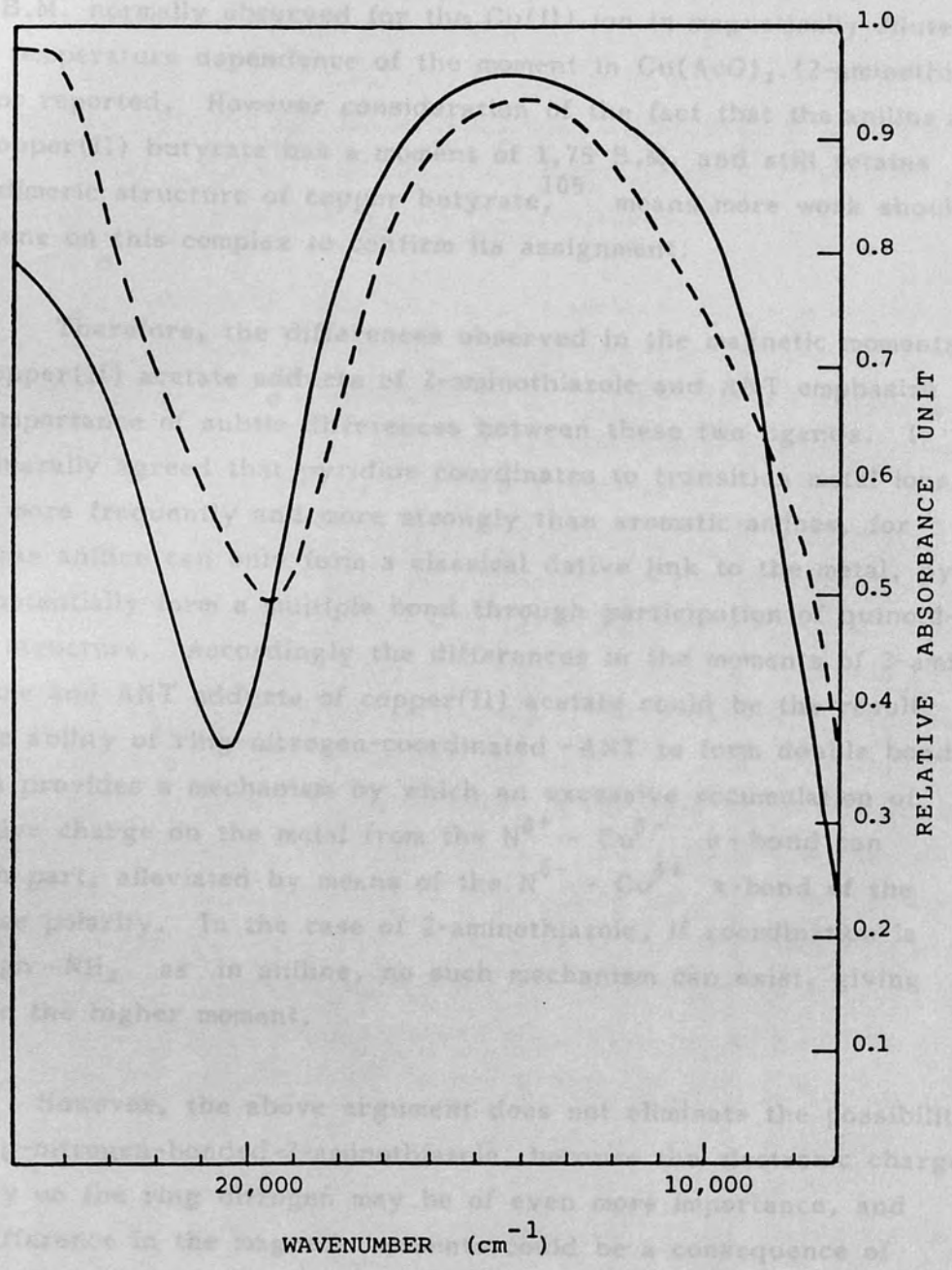

Fig. 13. Reflectance spectra of $[Cu(AcO)_2.H_2O]_2$ (——), and $[Cu(AcO)_2.(ANT)]_2$ (- - - -).

at 1.61 B.M. raises some doubts about the accuracy of this assignment, because, the magnetic moment at 1.61 B.M. is well below the value of 1.9 B.M. normally observed for the Cu(II) ion in magnetically dilute systems. The temperature dependence of the moment in $Cu(AcO)_2$.(2-aminothiazole) is not reported, However consideration of the fact that the aniline adduct of copper(II) butyrate has a moment of 1.75 B.M. and still retains the dimeric structure of copper butyrate,[105] means more work should be done on this complex to confirm its assignment.

Therefore, the differences observed in the magnetic moments of copper(II) acetate adducts of 2-aminothiazole and ANT emphasize the importance of subtle differences between these two ligands. It is generally agreed that pyridine coordinates to transition metal ions both more frequently and more strongly than aromatic amines, for whereas aniline can only form a classical dative link to the metal, pyridine can potentially form a multiple bond through participation of quinoid-type structure. Accordingly the differences in the moments of 2-amino-thiazole and ANT adducts of copper(II) acetate could be the result of the ability of ring-nitrogen-coordinated - ANT to form double bonding, which provides a mechanism by which an excessive accumulation of negative charge on the metal from the $N^{\delta+} - Cu^{\delta-}$ σ - bond can be, in part, alleviated by means of the $N^{\delta-} - Cu^{\delta+}$ π-bond of the reverse polarity. In the case of 2-aminothiazole, if coordination is through $-NH_2$ as in aniline, no such mechanism can exist, giving rise to the higher moment.

However, the above argument does not eliminate the possibility of ring-nitrogen-bonded-2-aminothiazole, because the electronic charge density on the ring nitrogen may be of even more importance, and the difference in the magnetic moments could be a consequence of the "π-deficient" character of ANT, in that the nitro group attracts electrons from the π-layer of the ring. In contrast in 2-aminothiazole the lone pair of $-NH_2$ is released to the π-layer of the ring, thereby making it "π-excessive", and lowering its capacity to form a strong coordinate link to copper. Therefore, although the coordination site in 2-aminothiazole is not clear because of insufficient data on this complex, the coordination of ANT in $[Cu(AcO)_2.ANT]_2$ is quite certainly through the ring nitrogen.

3.9.2. $MCl_2.(ANT)_2$ Complexes (M = Ni, Co, Cu, Cd)

$NiCl_2.(ANT)_2$ and $CdCl_2.(ANT)_2$ are assigned halogen-bridged polymeric octahedral stereochemistries with trans ANT molecules, while the two isomorphous complexes $CuCl_2.(ANT)_2$ and $CoCl_2.(ANT)_2$, are assigned halogen bridged, dimeric five-coordinate, approximately square pyramidal (SP) structures.

In order to explain why these complexes may assume the assigned structures, one should consider the following factors operating in these compounds. Consideration of pure steric factors resulting from the presence of $-NH_2$ and $-NO_2$ groups would imply the formation of a monomeric complex, because, $CuCl_2.(thiazole)_2$ is halogen bridged polymeric,[81] whereas, $CuBr_2.(4\text{-methylthiazole})_2$ is chloride bridged dimeric,[82] and $CuCl_2.(2,4\text{-dimethylthiazole})_2$ is square planar.[83] However ANT being a poor σ-donor and a better π-acceptor would favour the formation of halogen bridged polymeric complexes, bridging providing a means of maintaining electroneutrality at the metal ion. Moreover, donor-acceptor interaction between the nitro group and the amine group, and less likely, the π electrons of the ring would also favour such an arrangement. The result of this work showed that the last two factors are more important in determining the stereochemistries of these complexes, especially in the case of the Ni(II) complex where, where octahedral stereochemistry is much more stabilised by crystal fields for the weak field ligands and the Cd(II) complex where, steric factors are less important due to the size of the Cd(II) ion .

$NiCl_2.(ANT)_2$

The reflectance spectrum of this complex (Fig. 14) is similar to the spectra of $NiCl_2.(thiazole)_2$[68] and $NiCl_2.(quinoline)_2$.[109] It is noticeable, however that ANT produces a weaker field than thiazole, all the spectral bands appearing at lower energies for the ANT complex. This may be due either to the lower basicity of ANT or due to the steric hindrance caused by the amine and nitro groups, forcing either the nitrogen atom or the chloride ion to form longer bonds to the nickel (II) ion. The band splitting in the spectrum of this

complex is not clearly resolved like the splitting observed in the spectrum of the corresponding thiazole complex and the bands resemble more those observed in the spectrum of the sterically hindered $NiCl_2$.-(quinoline)$_2$ complex.[109] The two bands at 7,300 cm^{-1} and 13,200cm-1 could be assigned as $^3A_{2g}(F) \rightarrow {}^3T_{2g}(F)$ and $^3A_{2g}(F) \rightarrow {}^3T_{1g}(F)$. Assuming that ν_2 is 18 Dq, the calculated Dq of 733 cm^{-1} is in good agreement with that obtained from ν_1(730 cm^{-1}). Accordingly, like the $NiCl_2$.(thiazole)$_2$ the ANT complex has an essentially octahedral arrangement which could be achieved by polymeric chloride bridging, with trans ring nitrogen bonded ANT molecules, where, hydrogen bonding between the amine group and the halogen ions, and donor-acceptor interaction between the amine group and the nitro group are likely to exist (fig. 15).

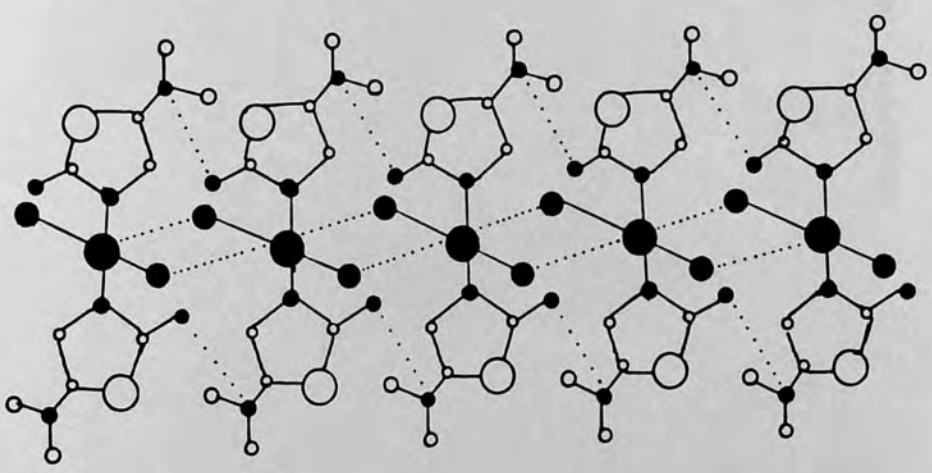

Fig. 15. Assumed structure of $NiCl_2$.(ANT)$_2$

The observed room temperature magnetic moment of 3.39 B.M. is higher than those normally found for octahedral or distorted octahedral complexes of nickel(II), and is in the range for halogen-bridged tetragonal nickel species(3.3 -4.0B.M.).[109]

However, in an octahedral complex, the nickel(II) ion has a $^3A_{2g}$ ground state, for which no orbital contribution to the magnetic moment is expected, but as the ligand field present in this complex is rather weak, the "mixing-in" of the $^3T_{2g}$ first excited state by spin-orbit

coupling may be appreciable. The value of μ_{eff} calculated by using the relationship $\mu = 2.84[\chi_m' (T - \theta)]^{\frac{1}{2}}$, corresponding to ferromagnetic interaction, is 3.29B.M., and falls in the range reported for other halogen bridged Ni(II) complexes where ferromagnetic interaction takes place.[109]

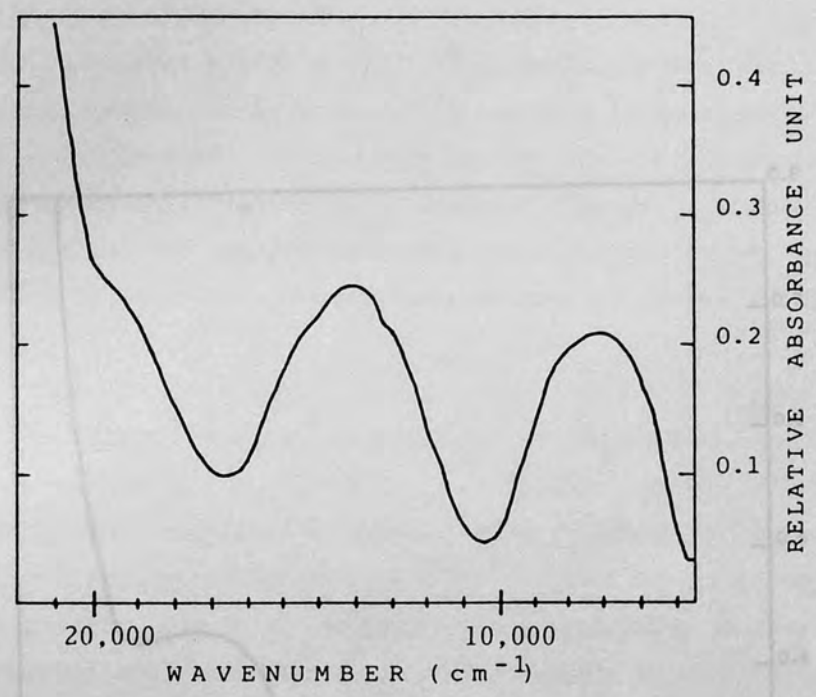

Fig. 14. Reflectance spectrum of $NiCl_2.(ANT)_2$

$\underline{CoCl_2.(ANT)_2}$

The room temperature magnetic moment of this complex, 4.36 B.M., is in the range of magnetic moments reported for high-spin, five-coordinate Co(II) complexes (4.2 - 4.4 B.M.). The reflectance spectrum of this complex (fig. 16), which shows a band at 6,300 cm^{-1} and a band at 14,700 cm^{-1} is typical for square pyramidal SP structures, because, high-spin, five-coordinate Co(II) complexes normally produce two major visible spectral bands at (5.0 - 6.5) x 10^3 and (14.0 - 16.0) x 10^3 cm^{-1}. Complexes with SP Co(II) rather than TBP, typically have their lowest energy band shifted to the high end of the low range.[110,111]

The decrease in the magnetic moment at low temperatures is probably due to antiferromagnetic interaction in this chloride bridged dimer, because orbital contribution to the magnetic moment is quenched in five coordinate cobalt(II) complexes and moments independent of temperature are expected.

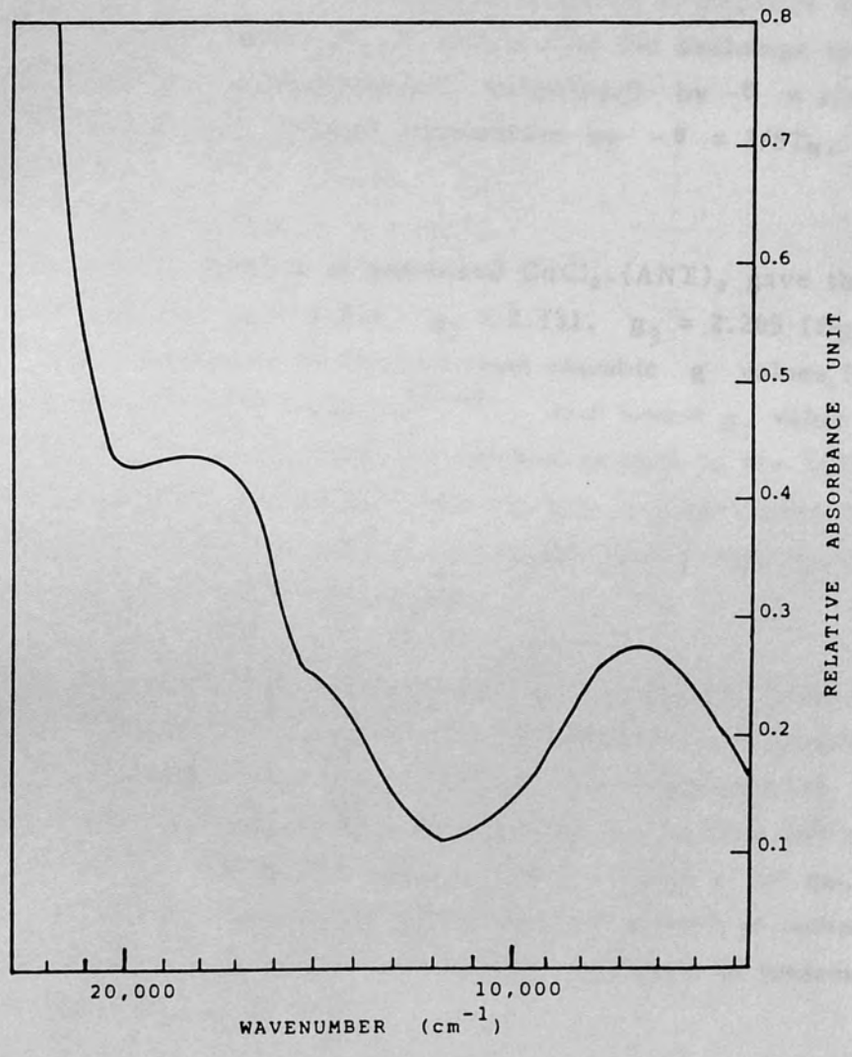

Fig. 16. Reflectance spectrum of $CoCl_2.(ANT)_2$

$CuCl_2.(ANT)_2$

The magnetic moment corrected for antiferromagnetic interaction, is 1.96 B.M. and is in the range of moments reported for five-coordinate Cu(II) ions (1.7 - 2.2B.M.). The measured Weiss constant, θ = -13 K (table. 14) is smaller than the reported values for linear chain pyridine examples which are in the range (20 - 26K); it is even smaller than the Weiss constant for the dimeric $CuCl_2.(2\text{-methyl-pyridine})_2$ complex which is -17 K.[112] Accordingly the interaction between the central metal ions in this complex is quite small, indicating a longer Cu-Cu distance. If this complex is indeed a "magnetic dimer", then the Weiss constant is related to J (where J is the exchange energy which is positive for antiferromagnetic behaviour) by $-\theta = 1/4J$, giving J = 52, and the critical temperature by $-\theta = 2/5T_N$, giving $T_N = 32.5$ [112]

The e.s.r. spectra of powdered $CuCl_2.(ANT)_2$ gave three rhombic g values at: $g_1 = 2.054$, $g_2 = 2.131$, $g_3 = 2.205$ (fig.17). The information which can be derived from rhombic g values is widely discussed by many authors.[113-116] The lowest g_1 value which is greater than 2.04 restricts the possibilities to the following:[116] (a) elongated rhombic-octahedral, (b) rhombic square-coplanar, (c) distorted-based pyramidal, (d) elongated axial symmetry, with slight misalignment of the principal axes.

The reflectance spectrum (fig. 18) shows a broad band centred at 13,500 cm^{-1}. Reflectance spectra of Cu(II) complexes are generally poor indicators of geometry; however, it has been suggested [116] that TBP Cu(II) will absorb in the range (11.8 - 12.5) x 10^3 cm^{-1}, whereas SP Cu(II) will absorb between (14.5 - 18.2) x 10^3 cm^{-1}, and complexes having intermediate geometries will absorb at intermediate in values. Therefore $CuCl_2.(ANT)_2$ can be best described as intermediate structure, resembling more SP.

The conclusion derived from the reflectance spectrum is in agreement with the e.s.r. results, that gave g_1 to be 2.054, because g_1 values for TBP are smaller than 2.04. Accordingly, like the $CoCl_2.(ANT)_2$ complex, a five-coordinate, dimeric SP structure, with bridging chloride ions could be assigned to this complex.

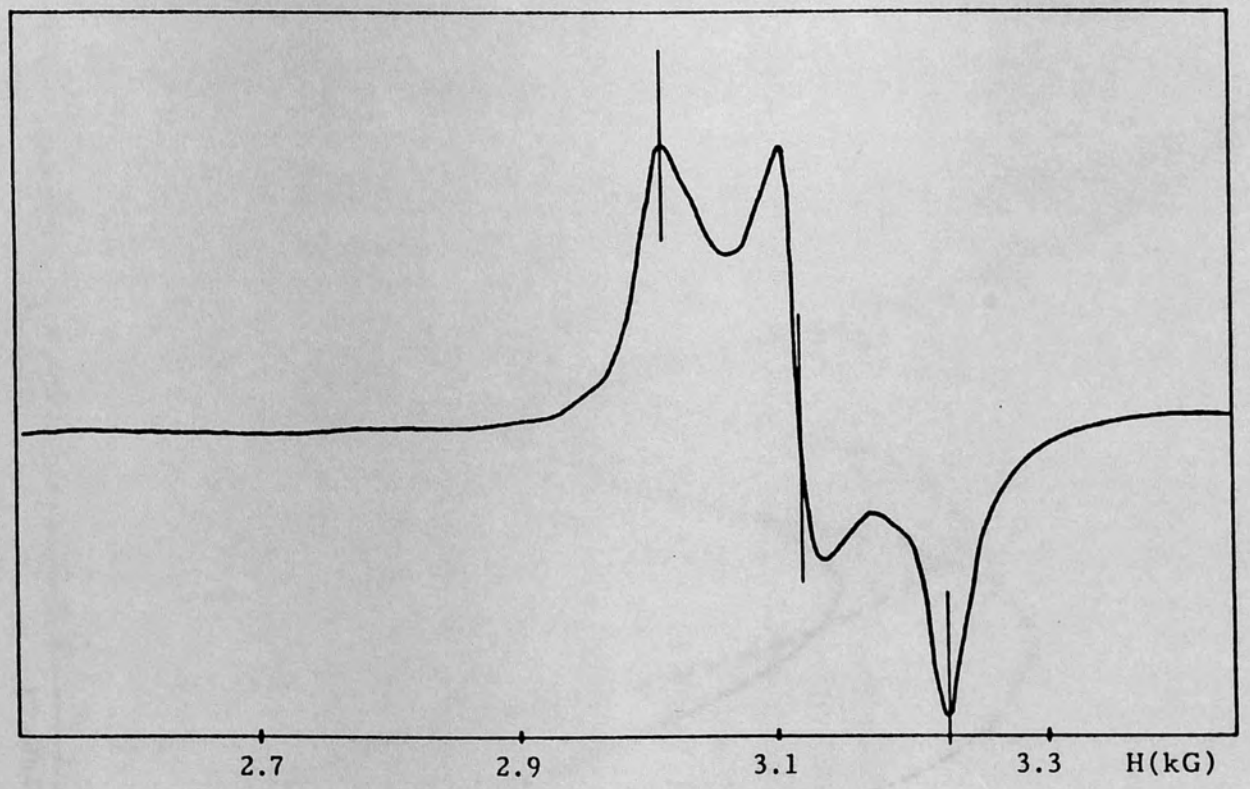

Fig. 17. Room-temperature e.s.r. spectrum (X band) of polycrystalline $CuCl_2.(ANT)_2$.

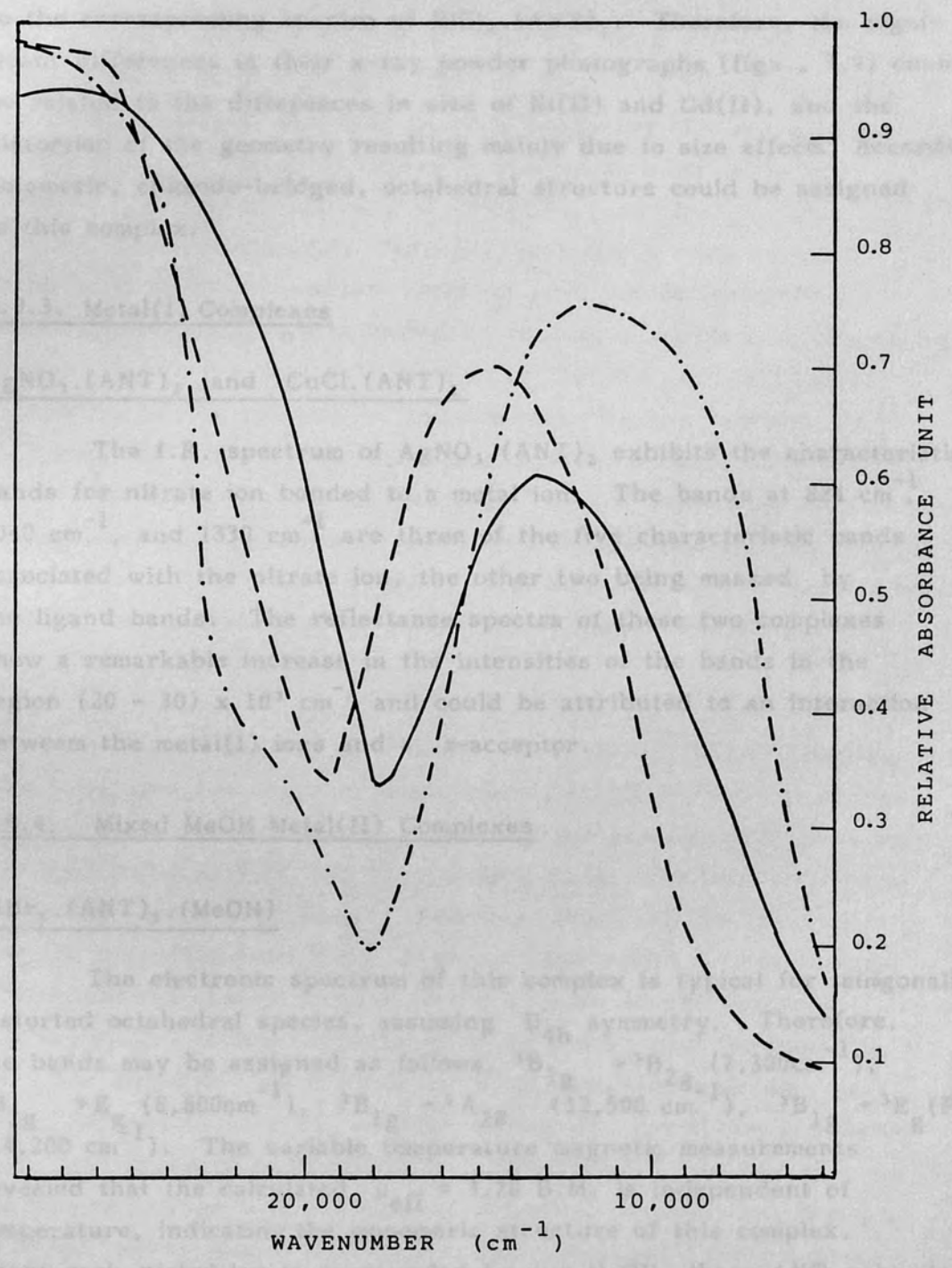

Fig. 18. Reflectance spectra of $CuSO_4.(ANT)(DMF)$ (—·—·—·—), $CuCl_2.(ANT)_2$ (————), and $CuCl_2.(ANT)(DMF)$ (- - - -).

$CdCl_2.(ANT)_2$

The I.R. and U.V. spectra of this complex are almost identical to the corresponding spectra of $NiCl_2.(ANT)_2$. Therefore, the significant differences in their x-ray powder photographs (figs., 3,4) could be related to the differences in size of Ni(II) and Cd(II), and the distortion of the geometry resulting mainly due to size effects. Accordingly, a polymeric, chloride-bridged, octahedral structure could be assigned to this complex.

3.9.3. Metal(I) Complexes

$AgNO_3.(ANT)_2$ and $CuCl.(ANT)_2$

The I.R. spectrum of $AgNO_3.(ANT)_2$ exhibits the characteristic bands for nitrate ion bonded to a metal ion. The bands at 824 cm^{-1}, 1040 cm^{-1}, and 1330 cm^{-1} are three of the five characteristic bands associated with the nitrate ion, the other two being masked by the ligand bands. The reflectance spectra of these two complexes show a remarkable increase in the intensities of the bands in the region (20 - 30) x 10^3 cm^{-1} and could be attributed to an interaction betweem the metal(I) ions and a π-acceptor.

3.9.4. Mixed MeOH Metal(II) Complexes

$NiBr_2.(ANT)_3.(MeOH)$

The electronic spectrum of this complex is typical for tetragonally distorted octahedral species, assuming D_{4h} symmetry. Therefore, the bands may be assigned as follows, $^3B_{1g} \rightarrow {}^3B_{2g}$ (7,300cm^{-1}), $^3B_{1g} \rightarrow E_g$ (8,800cm^{-1}), $^3B_{1g} \rightarrow {}^3A_{2g}$ (12,500 cm^{-1}), $^3B_{1g} \rightarrow {}^3E_g(F)$ (14,200 cm^{-1}). The variable temperature magnetic measurements revealed that the calculated μ_{eff} = 3.20 B.M. is independent of temperature, indicating the monomeric structure of this complex, where each nickel ion is surrounded by one MeOH, three ANT molecules, and two bromide ions.

$Ni(NCS)_2.(ANT)_2(MeOH)_2$ and $Ni(NCS)_2.(ANT)_2(MeOH)$

It was noticed that after the magnetic susceptibility measurement experiment following the procedure described in the experimental part, the color of $Ni(NCS)_2.(ANT)_2(MeOH)_2$ had changed from brown-yellow to bright green. The I.R.(figs. 19,20), reflectance spectra(fig. 21), and elemental analysis suggested the loss of one molecule of MeOH. Such behaviour is not unusual for $Ni(NCS)_2$ complexes. In thermal analysis of $Ni(SCN)_2(pyridine)_4$,[117] the formation of the intermediate $Ni(SCN)_2(pyridine)_2$ was detected. On the basis of the information obtained from the derivatogram, $Ni(SCN)_2.(pyridine)_2$ was prepared by heating a sample to a temperature corresponding to the horizontal section of the TG curve,[118] and by 'freezing in' the reaction by rapidly removing the furnace. It was found that $Ni(SCN)_2.(pyridine)_2$ contained thiocyanate bridges, while in $Ni(NCS)_2.(pyridine)_4$ the SCN^- was N-bonded as the isothiocyanate complex. The magnetic moment of the original complex and the decomposition product were identical (3.10 and 3.12 B.M., respectively) excluding the possibility of extensive stereochemical rearrangement during thermal decomposition.

Prolonged heating of a sample of $Ni(NCS)_2.(ANT)_2(MeOH)_2$ in the tube used for magnetic measurement, at 100°C, did not change its composition, nor did repeating the magnetic susceptibility experiment first by heating to 90°C and then cooling to liquid nitrogen temperature bring about any change; however, repeating the experiment under the described conditions, gave the same result. Consequently it seems that the change occured either because of the slow rate of cooling or due to the combined effect of cooling and the magnetic field. The magnetic moment, calculated by using the molecular mass of $Ni(NCS)_2.(ANT)_2(MeOH)_2$ and the diamagnetic correction associated with it, was found to be constant at 3.20 ± 0.05 B.M. The fact that there was no change in the weight of the tube, because the tube was sealed, makes this measurement quite reasonable. Such a case is reported for $(Cu_3Br_3.guaninium.nH_2O)_2$ [119] and is ascribed to slight changes in the lattice which change the Cu-Br-Cu angle and the delocalisation properties of the bridging ligand to just compensate for the expected decrease in the moment.

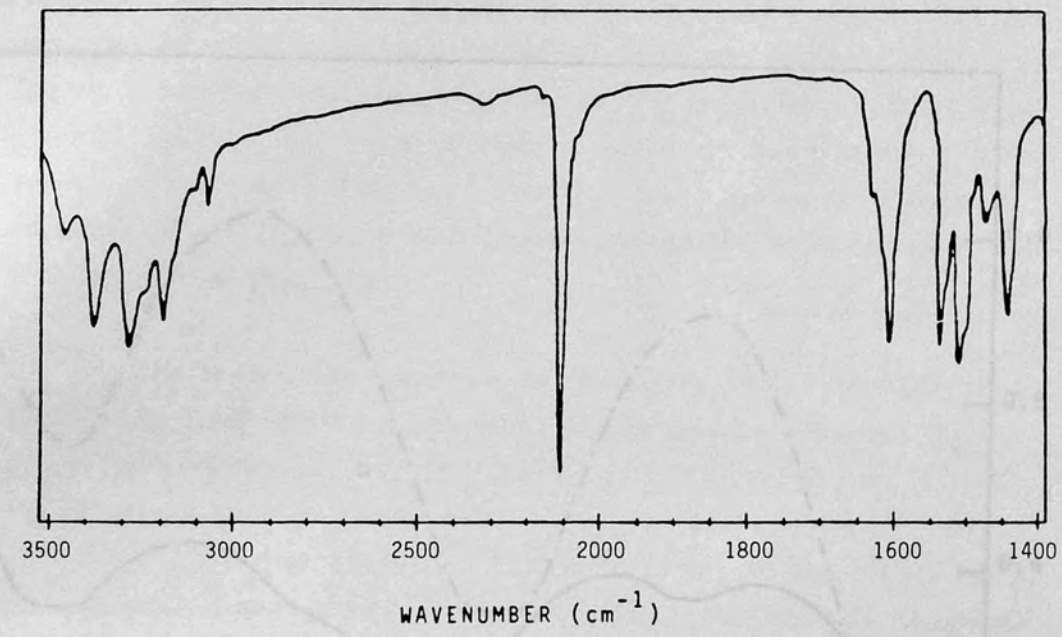

Fig. 19. Infrared spectrum of $Ni(NCS)_2.(ANT)_2(MeOH)_2$ as KBr pellet.

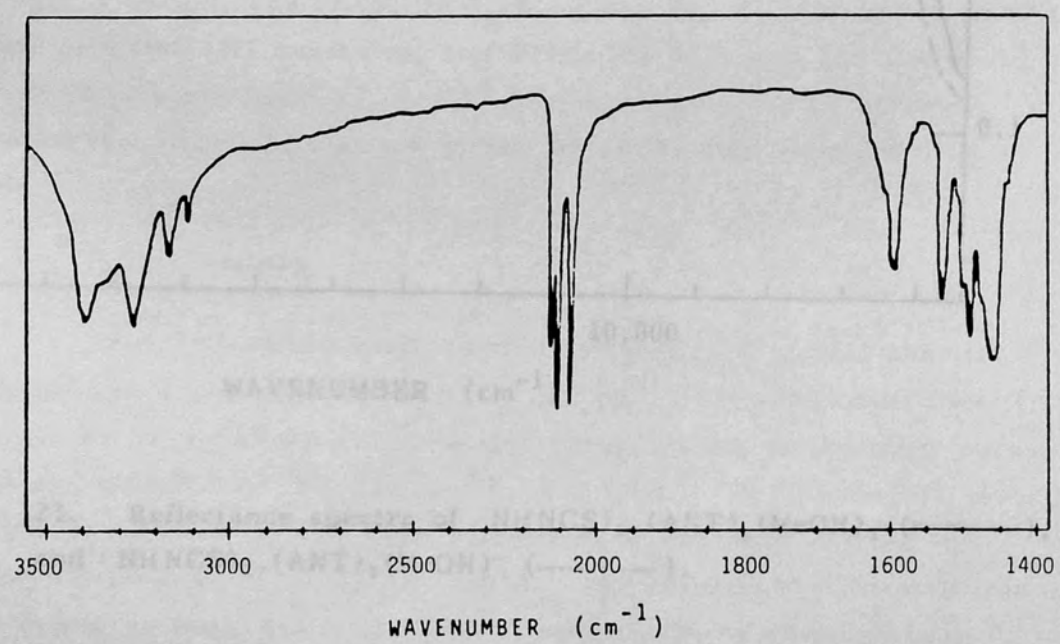

Fig. 20. Infrared spectrum of $Ni(NCS)_2.(ANT)_2(MeOH)$ as KBr pellet.

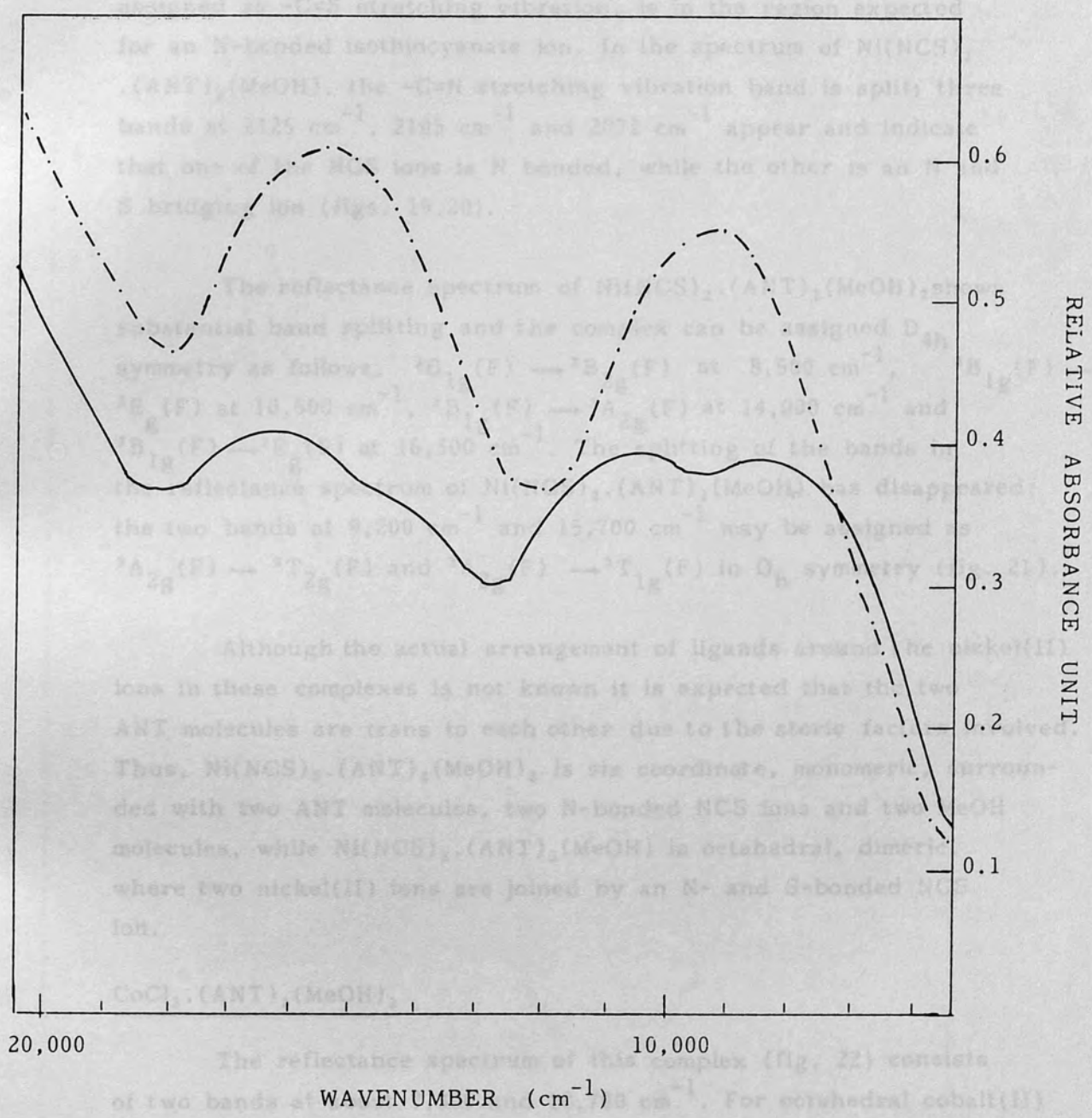

Fig. 21. Reflectance spectra of $Ni(NCS)_2.(ANT)_2(MeOH)_2$ (————), and $Ni(NCS)_2.(ANT)_2(MeOH)$ (–·–·–·–·).

The infrared spectrum shows that the -C=N stretching vibration for $Ni(NCS)_2.(ANT)_2(MeOH)_2$ is at 2107 cm^{-1}, and the band at 818 cm^{-1} assigned as -C=S stretching vibration, is in the region expected for an N-bonded isothiocyanate ion. In the spectrum of $Ni(NCS)_2.(ANT)_2(MeOH)$, the -C=N stretching vibration band is split; three bands at 2125 cm^{-1}, 2105 cm^{-1} and 2072 cm^{-1} appear and indicate that one of the NCS ions is N bonded, while the other is an N and S bridging ion (figs. 19,20).

The reflectance spectrum of $Ni(NCS)_2.(ANT)_2(MeOH)_2$ shows substantial band splitting and the complex can be assigned D_{4h} symmetry as follows, $^3B_{1g}(F) \longrightarrow {}^3B_{2g}(F)$ at 8,500 cm^{-1}, $^3B_{1g}(F) \longrightarrow {}^3E_g(F)$ at 10,500 cm^{-1}, $^3B_{1g}(F) \longrightarrow {}^3A_{2g}(F)$ at 14,000 cm^{-1} and $^3B_{1g}(F) \longrightarrow {}^3E_g(F)$ at 16,500 cm^{-1}. The splitting of the bands in the reflectance spectrum of $Ni(NCS)_2.(ANT)_2(MeOH)$ has disappeared; the two bands at 9,200 cm^{-1} and 15,700 cm^{-1} may be assigned as $^3A_{2g}(F) \longrightarrow {}^3T_{2g}(F)$ and $^3A_{2g}(F) \longrightarrow {}^3T_{1g}(F)$ in O_h symmetry (fig. 21).

Although the actual arrangement of ligands around the nickel(II) ions in these complexes is not known it is expected that the two ANT molecules are trans to each other due to the steric factors involved. Thus, $Ni(NCS)_2.(ANT)_2(MeOH)_2$ is six coordinate, monomeric, surrounded with two ANT molecules, two N-bonded NCS ions and two MeOH molecules, while $Ni(NCS)_2.(ANT)_2(MeOH)$ is octahedral, dimeric, where two nickel(II) ions are joined by an N- and S-bonded NCS ion.

$CoCl_2.(ANT)_2(MeOH)_2$

The reflectance spectrum of this complex (fig. 22) consists of two bands at about 7,300 and 18,700 cm^{-1}. For octahedral cobalt(II) complexes three bands are expected corresponding to the three spin-allowed transitions $^4T_{1g}(F) \longrightarrow {}^4T_{2g}(F)$ (ν_1), $^4T_{1g}(F) \longrightarrow {}^4A_{2g}$ (ν_2), and $^4T_{1g}(F) \longrightarrow {}^4T_{1g}(P)$ (ν_3). However, it has been pointed out that the transition $^4T_{1g}(F) \longrightarrow {}^4A_{2g}$ corresponds to a two-electron jump and as such will have a much lower oscillator strength than the other two bands and will be much weaker.[120] The band at 7,300 cm^{-1}

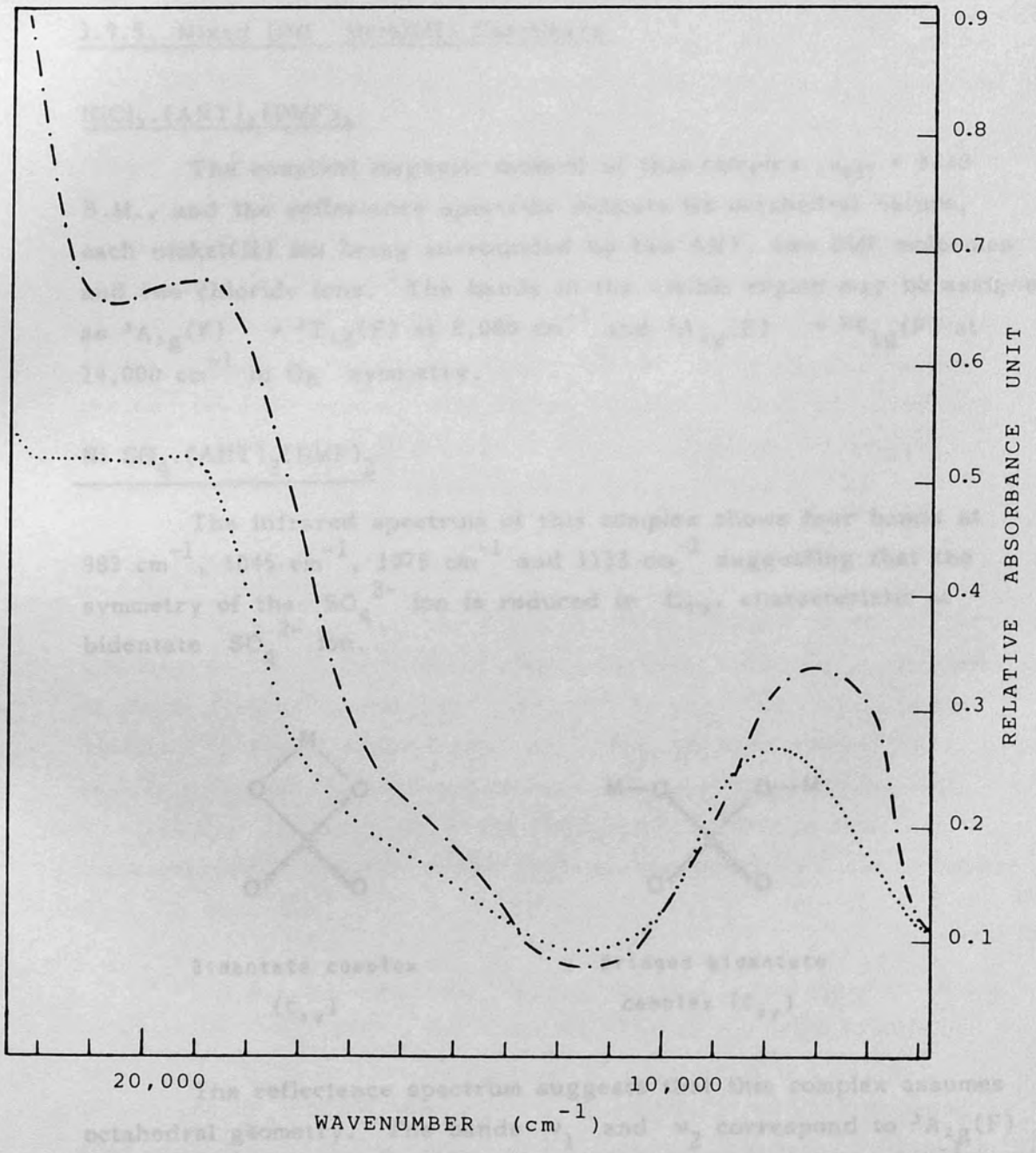

Fig. 22. Reflectance spectra of $CoCl_2.(ANT)_2(MeOH)_2$ (—·—·—·), and $Co\ SO_4.(ANT)_2(DMF)_2$ (.....).

can therefore be assigned to the ν_1 transition and the band at 18,700 cm^{-1} to the ν_3 transition, and the weak shoulder at about 14,500 cm^{-1} could be assigned to a ν_2 transition.

3.9.5. Mixed DMF Metal(II) Complexes

$NiCl_2.(ANT)_2(DMF)_2$

The constant magnetic moment of this complex μ_{eff} = 3.20 B.M., and the reflectance spectrum indicate its octahedral nature, each nickel(II) ion being surrounded by two ANT, two DMF molecules and two chloride ions. The bands in the visible region may be assigned as $^3A_{2g}(F) \rightarrow {}^3T_{2g}(F)$ at 8,000 cm^{-1} and $^3A_{2g}(F) \rightarrow {}^3T_{1g}(F)$ at 14,000 cm^{-1} in O_h symmetry.

$Ni\ SO_4.(ANT)_2(DMF)_2$

The infrared spectrum of this complex shows four bands at 983 cm^{-1}, 1045 cm^{-1}, 1075 cm^{-1} and 1153 cm^{-1} suggesting that the symmetry of the SO_4^{2-} ion is reduced to C_{2v}, characteristic of bidentate SO_4^{2-} ion.

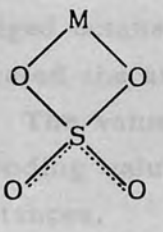

Bidentate complex (C_{2v})

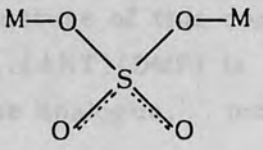

Bridged bidentate complex (C_{2v})

The reflectance spectrum suggests that this complex assumes octahedral geometry. The bands ν_1 and ν_2 correspond to $^3A_{2g}(F) \rightarrow {}^3T_{2g}(F)$ and $^3A_{2g}(F) \rightarrow {}^3T_{1g}(F)$, appearing at 8,300 cm^{-1} and 14,800 cm^{-1}. Assuming that ν_2 is 18Dq, the calculated Dq of 822 cm^{-1} is in good agreement with that obtained from ν_1 (830 cm^{-1}).

$CoSO_4.(ANT)_2(DMF)_2$

The reflectance spectrum of this complex is similar to that of the violet isomer of $Co(pyridine)_2Cl_2$ in which the cobalt is six-coordinate.[121] By analogy with the band assignments of Ferguson, the bands at about 18,800 and 19,500 cm^{-1} arise from the $^4T_{1g}(F) \rightarrow {}^4T_{1g}(P)$ transition which is split in complexes of D_{4h} symmetry or lower. That of 14,700 cm^{-1} arises from the $^4T_{1g}(F) \rightarrow {}^4A_{2g}$ transition, and the band at 8,000 cm^{-1} arising from the transition $^4T_{1g}(F) \rightarrow {}^4T_{2g}(F)$ (fig. 22). The infrared bands at 980cm^{-1}, 1,045 cm^{-1}, 1,112 cm^{-1} and 1,155 cm^{-1} indicate that the sulphate ion is bidentate assuming C_{2v} symmetry. The room temperature magnetic moment at 5.17 B.M. and the remarkable decrease in the moment with decreasing temperature (table 13) are consistent with the proposed structure. Any antiferromagnetic exchange could not be detected, because, if present, it was obscured by the magnetic propery exhibited by octahedral cobalt(II) complexes.

$CuCl_2.(ANT)(DMF)$

The position and the shape of the broad band in the reflectance spectrum at 14,500 cm^{-1} are similar to features observed in the spectrum of $CuCl_2.(thiazole)_2$ and $CuCl_2.(pyridine)_2$ (fig. 18). which have halogen bridged octahedral geometry.[68] The magnetic moment measurement results indicated the antiferromagnetic nature of this complex with $\theta = -10$ K. The value of θ for $CuCl_2.(ANT)(DMF)$ is less than the corresponding value for the pyridine analogue, indicating longer Cu - Cu distances.

The e.s.r. spectrum recorded at room temperature is shown in figure 23. At 110K a less resolved, flatter spectrum is obtained with slight shifts in the g values. The spectrum is axial with $g_\perp = 2.108$, $g_\parallel = 2.301$ with $g_\parallel > g_\perp$. Considering the data obtained from the reflectance spectrum and magnetic measurements, the e.s.r. result could be related to an elongated tetragonal-octahedral structure of this compound, because $g_\parallel > g_\perp$ is associated with tetragonally elongated octahedra, while $g_\parallel < g_\perp$ is for compressed octahedra.[122] In the axial spectrum, the g-values are related by the expression,[123]

$G = g_{\parallel} - 2/g_{\perp} - 2 \cong 40$. If $G > 40$, then the local tetragonal axes are aligned parallel or only slightly misaligned; if $G < 40$, significant exchange coupling is present[124] and the misalignment is appreciable (assuming $r_{\parallel} \cong r_{\perp}$ and the energies of the electronic transitions involved are comparable). In the case of $CuCl_2.(ANT)(DMF)$, $G = 2.79$ significantly lower than 40, indicating exchange coupling as evidenced from the magnetic measurements, and misalignment of the axes.

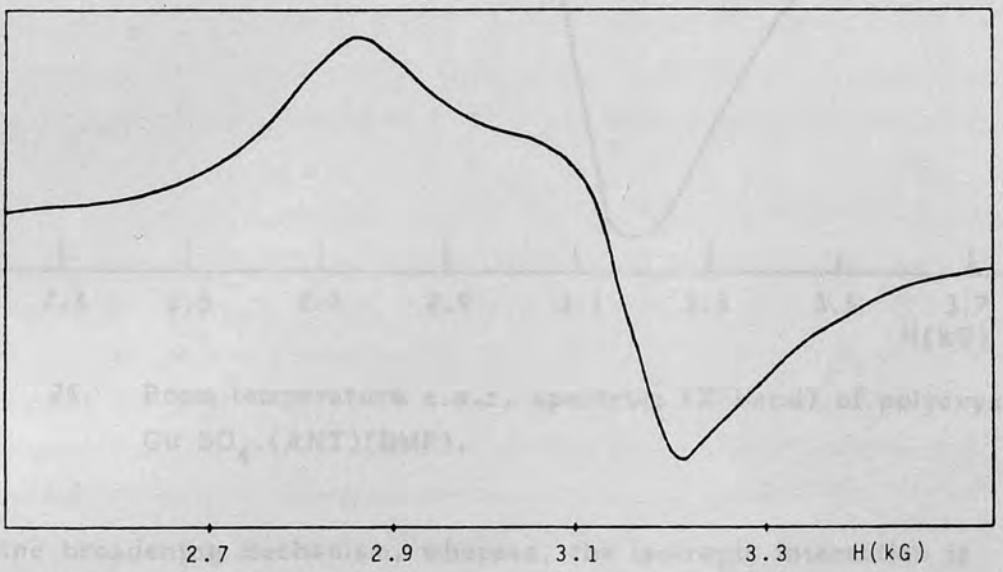

Fig. 23. E.S.R. spectrum (X band) of polycrystalline $CuCl_2.(ANT)(DMF)$

$Cu\ SO_4.(ANT)(DMF)$

Four bands in the infrared spectrum, at 995 cm^{-1}, 1065 cm^{-1}, 1133 cm^{-1} and 1170 cm^{-1} indicate a C_{2v} symmetry for the sulphate ion.

The position of the broad, featureless band at 1100 cm^{-1} in the reflectance spectrum would favour tetrahedral, rather than square planar geometry (which usually absorb at higher energies) (fig. 18).

The e.s.r. spectrum recorded at room temperature is shown in figure 24. The spectrum is not symmetrical and has a peak to peak line width at ca. 260G indicating the presence of exchange coupling. In a paramagnetic complex the anisotropic exchange is

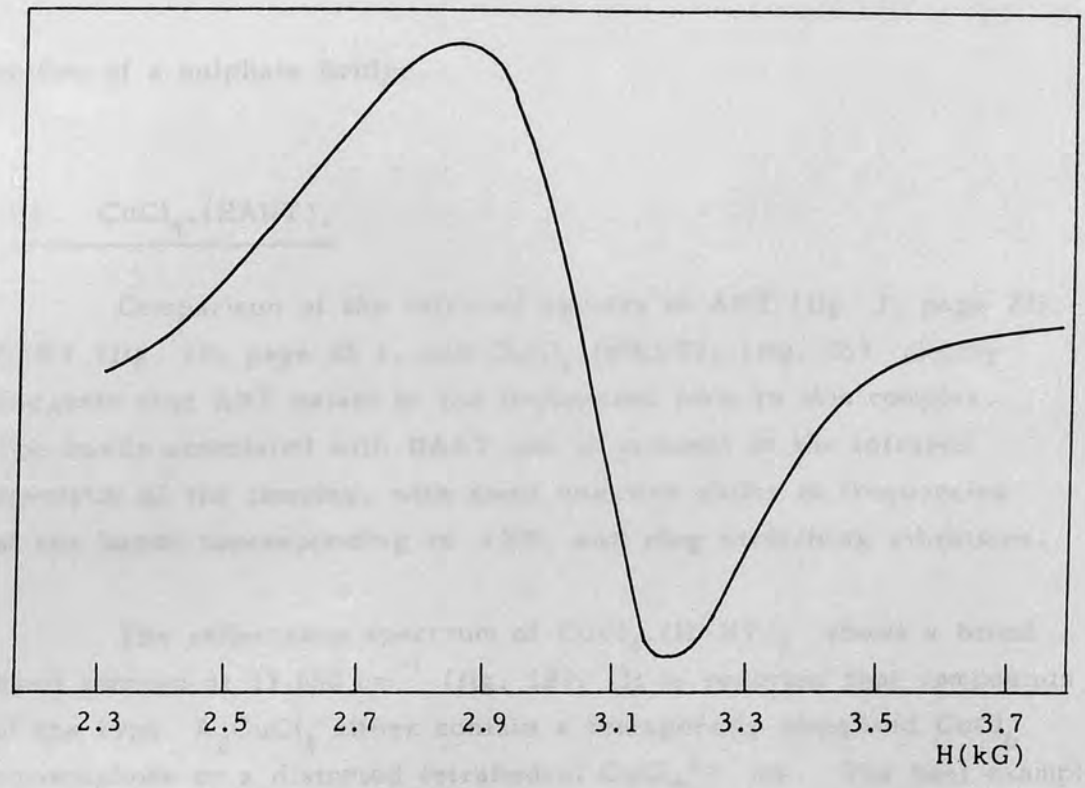

Fig. 24. Room temperature e.s.r. spectrum (X-band) of polycrystalline Cu SO_4.(ANT)(DMF).

a line broadening mechanism, whereas, the isotropic interaction is a line-narrowing term. Other line-broadening mechanisms such as dipolar and hyperfine fields would be expected to contribute at most a few guass to the line width and may be safely neglected.[125] Antisymmetrical exchange seems unlikely to provide an explanation for the line width because, it is often associated with a pronounced temperature dependence. No significant variation with temperature was observed in the spectrum recorded at 100K eliminating the possibility that antisymmetrical exchange is the cause of line broadening in this complex. Such broad line widths are observed in many bidentate ligands that provide for the possibility of an exchange pathway that may be intra or interchain in cross-linked structures. The exchange pathway in the case of Cu SO_4.(ANT)(DMF) could either be provided by the bidentate sulphate ion, or ANT could weakly interact by either of the possible donor sites with other Cu(II) ions.

The magnetic susceptibility data gives a value of θ at - 30K (table. 15), indicating an antiferromagnetic exchange which apparently is propagated through-space via O—O interactions in the 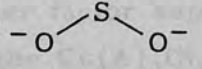

moities of a sulphate bridge.

3.9.6. $CuCl_4.(HANT)_2$

Comparison of the infrared spectra of ANT (fig. 2, page 27), HANT (fig. 10, page 45), and $CuCl_4.(HANT)_2$ (fig. 25) clearly suggests that ANT exists in the protonated form in this complex. The bands associated with HANT are all present in the infrared spectrum of the complex, with small negative shifts in frequencies of the bands corresponding to νNH_2 and ring stretching vibrations.

The reflectance spectrum of $CuCl_4.(HANT)_2$ shows a broad band centred at 13,000 cm^{-1} (fig. 18). It is reported that compounds of the type A_2CuCl_4 either contain a tetragonally elongated $CuCl_6$ chromophore or a distorted tetrahedral $CuCl_4^{2-}$ ion. The best example of square coplanar $CuCl_4^{2-}$ is $Pt(NH_3)_4CuCl_4$. Hatfield and Piper measured the reflectance spectrum of this powdered compound and observed three d-d bands in the range (10 - 15) x 10^3 cm^{-1}.[126] Furlani et al.[127] measured the crystal spectrum at 77 K of $(CH_3NH_3)_2CuCl_4$ containing the $CuCl_6$ tetragonal chromophore and observed three bands in the range (10 - 14) x 10^3 cm^{-1} which were assigned with the orbital sequence $d_{x^2-y^2} > d_{z^2} > d_{xy} > d_{xy,yz}$. Willett, Liles and Michelson reported the powder reflectance spectra of several tetrachlorocuprates(II) containing the $CuCl_6$ tetragonal chromophore, and observed a broad band at about 13,000 cm^{-1} with a shoulder at (10 - 11) x 10^3 cm^{-1}.[128] A number of compounds of the type A_2CuCl_4 containing discrete $CuCl_4^{2-}$ ions, which are flattened tetrahedra, have been studied by means of their electronic spectra,[129,130] $Cs_2CuCl_4(NMe_4)_2CuCl_4$, bis(trimethylbenzylammonium) tetrachlorocuprate(II), show bands at about 9,000 cm^{-1}, 6,000 cm^{-1}, and 4,000 cm^{-1} in their polarized crystal spectra. Accordingly, the position of the d-d transition band at 13,000 cm^{-1} is in the range associated with tetragonally elongated $CuCl_6$ chromophores. Moreover, the charge transfer band $\pi_{(n)} \rightarrow d_{x^2-y^2}$ observed in the spectra of $CuCl_6$ chromophores, as $(CH_3CHNH_3)^{2+}CuCl_4$, $(CH_3NH_3)_2Cl_4$, and $(C_2H_5NH_3)_2CuCl_4$ [126,128,131] between 24,000cm^{-1} and 25,000 cm^{-1} also appears in the spectrum of $CuCl_4(HANT)_2$. Another factor supporting this assignment is the fact that hydrogen bonding in the $Cu(A)_2Cl_4$

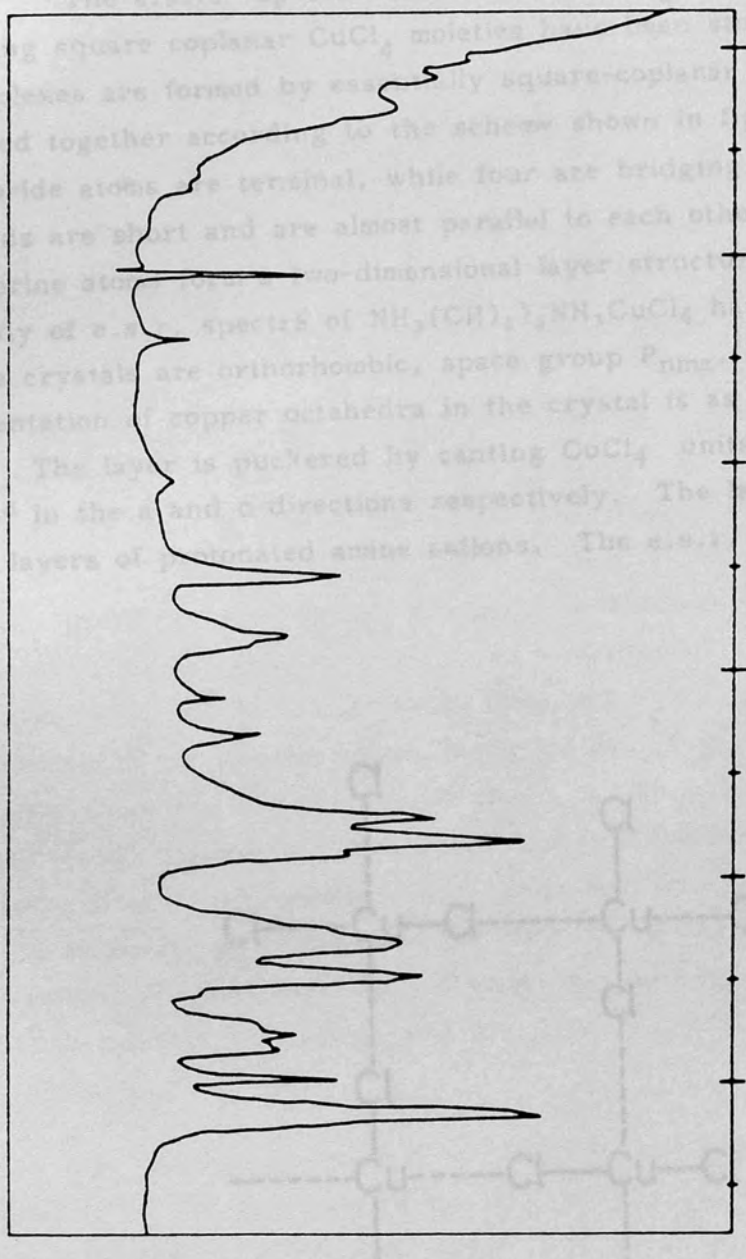

Fig. 25. Infrared spectrum of $CuCl_4.(HANT)_2$ as nujol mull.

chromophores favours the formation of square-coplanar $CuCl_4^{2-}$ rather than tetrahedral $CuCl_4^{2-}$ ion.[126,128,131]

The e.s.r. spectra of a number of A_2CuCl_4 compounds having square coplanar $CuCl_4$ moieties have been studied.[128,131] These complexes are formed by essentially square-coplanar $CuCl_4$ moities linked together according to the scheme shown in figure 26. Two chloride atoms are terminal, while four are bridging. All the terminal bonds are short and are almost parallel to each other, while the bridging chlorine atoms form a two-dimensional layer structure. A detailed study of e.s.r. spectra of $NH_3(CH)_2)_3NH_3CuCl_4$ has been performed.[131] The crystals are orthorhombic, space group P_{nma},[132] and the orientation of copper octahedra in the crystal is as shown in figure 27. The layer is puckered by canting $CuCl_4$ units by 1.6° and 9.6° in the a and c directions respectively. The layers are separated by layers of protonated amine cations. The e.s.r. spectrum of

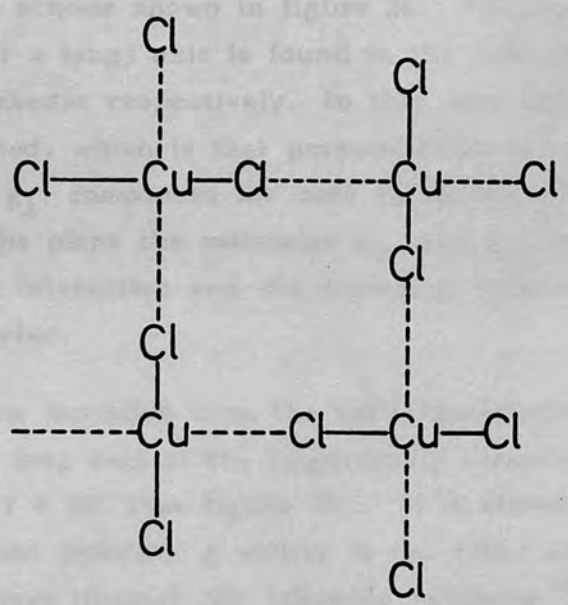

Fig. 26. A scheme of the structure of A_2CuCl_4 complexes. Two other Cu - Cl short bonds per Cu centre are orthogonal to the plane.

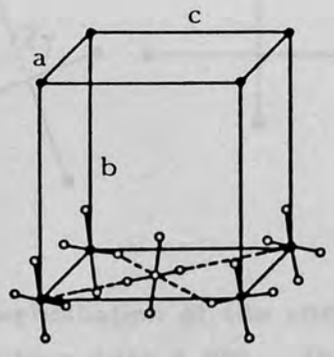

Fig. 27. Schematic representation of the structure of the $CuCl_6$ chromophore in $[NH_3(CH_2)_2NH_3]CuCl_4$ (ref. 132).

$NH_3(CH_2)_3NH_3CuCl_4$ showed that one principal g direction is parallel to b with $g_b = 2.053$, and that the principal $g_\perp$ values are isotropic (2.169), typical of $CuCl_4^{2-}$ moities.[128] Assuming that $g_b = g_\perp$ of the molecule, $g_\parallel$ is found to be 2.285, a value which compares well with those usually reported for elongated octahedral copper(II) complexes.[133] This situation is often referred to as antiferrodistortive order of octahedra, in which in one plane, long and short axes alternate according to the scheme shown in figure 26. Perpendicular to this plane a short (or a long) axis is found in the case of elongated (or compressed) octahedra respectively. In this case only one molecular g value is obtained, which is that perpendicular to the plane and is the molecular $g_\perp$ component for both elongated and compressed octahedra. In the plane the molecular $g_\parallel$ and $g_\perp$ values are averaged by the exchange interaction and the crystal g value cannot be taken as molecular g value.

A possible deviation from the antiferrodistortive limiting case occurs when the long axis of the magnetically inequivalent molecules form an angle $2\gamma \neq 90$, (see figure 28). It is shown, by standard techniques that the principal g values in the plane are related to the molecular values through the following relations.[134]

$$g_1^2 = g_\parallel^2 \cos^2\gamma + g_\perp^2 \sin^2\gamma$$

$$g_2^2 = g_\parallel^2 \sin^2\gamma + g_\perp^2 \cos^2\gamma$$

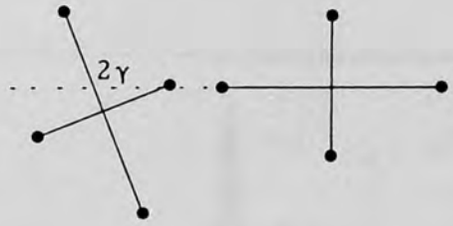

Fig. 28. A perturbation of the antiferrodistortive order with the angles between long axes ≠ 90°. The third bond direction is orthogonal to the plane.

From the above formula it is apparent that for $2\gamma = 90°$ the spectra will be isotropic in the plane, while for $2\gamma \neq 90°$ anisotropic components will show up. Angles 2γ different from 90° can originate from bond angles different from 90° in the pseudo octahedron or from a twisting of the elongation axis of two octahedra relative to each other. When long and short bonds of the octahedra do not lie exactly in a plane, crystallographic g values do not yield the molecular values directly, since no symmetry results. However, if the atomic distortions are small and the non-planarity of short and long bonds is minimal, then one may refer to the antiferrodistortive model and will find that the two principal crystallographic g values almost bisect the angles formed by the copper donor bonds.

The e.s.r. spectra of $CuCl_4.(HANT)_2$ was recorded at room temperature, at 107 K and at 373 K. No temperature dependence was observed. The g anisotropy was completely resolved. The three g values are at $g_1 = 2.044$, $g_2 = 2.125$ and $g_3 = 2.170$ (fig. 29). The value of g_1 is greater than 2.04 suggesting that this complex assumes either an elongated rhombic octahedral symmetry or elongated axial symmetry with slight misalignment of the principal axes.

It is known that powder e.s.r. techniques yield only approximate crystal g values,[135-140] and could yield only the local molecular g values if the crystal structure is known. However, for the sake of comparison with other A_2CuCl_4 chromophores, and to gain insight into the cause of anisotropy, the site g tensors and γ, half of the angle between

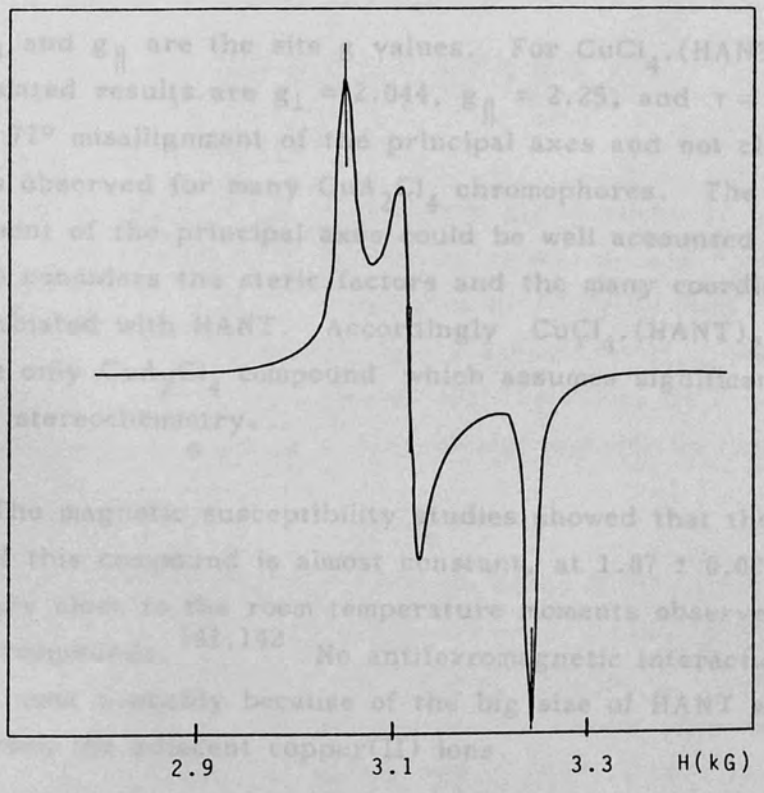

Fig. 29. Room-temperature e.s.r. spectrum (X band) of polycrystalline $CuCl_4.(HANT)_2$.

the tetragonal axes of nonequivalent sites were calculated using the g values obtained from the powder e.s.r. technique.

Following the analysis of Bertini et al.[122] and with the assumption that the copper sites are of tetragonally distorted octahedral symmetry, and using the formulation of Abe and Ono,[134] the site g tensors are related to the crystal g tensors by:

$$g_1^2 = g_\perp^2$$

$$g_2^2 = g_\perp^2 \cos^2\gamma + g_\parallel^2 \sin^2\gamma$$

$$g_3^2 = g_\perp^2 \sin^2\gamma + g_\parallel^2 \cos^2\gamma$$

where $g_{\perp}$ and $g_{\parallel}$ are the site g values. For $CuCl_4.(HANT)_2$, the calculated results are $g_{\perp} = 2.044$, $g_{\parallel} = 2.25$, and $\gamma = 38.5°$, implying 77° misallignment of the principal axes and not close to 90° as observed for many CuA_2Cl_4 chromophores. The misalignment of the principal axes could be well accounted for, when one considers the steric factors and the many coordination sites associated with HANT. Accordingly $CuCl_4.(HANT)_2$ seems to be the only CuA_2Cl_4 compound which assumes significantly distorted stereochemistry.

The magnetic susceptibility studies showed that the magnetic moment of this compound is almost constant, at 1.87 ± 0.02 B.M., and is very close to the room temperature moments observed for CuA_2Cl_4 compounds.[141,142] No antiferromagnetic interaction was detected, most probably because of the big size of HANT which would screen the adjacent copper(II) ions.

CHAPTER 4

CONCLUSIONS

The deshielding effect of the nitro group observed in the carbon-13 n.m.r. spectra of 2-chloro-5-nitrothiazole and 2-amino-5-nitrothiazole, the lack of formation of a $Ni(ANT)Cl_2$ complex where ANT is bridging like the corresponding 2-aminothiazole complex, and the failure to prepare complexes with BNT and CNT clearly indicate considerable reduction in the electron density in the donor sites of these ligands.

The formation of halogen bridged, mixed MeOH complexes and the lack of formation of complexes of higher ligand to metal ratio could be the result of ring nitrogen bonded ANT being a better π-acceptor than a σ-donor, bridging and coordination of methanol providing a means for maintaining the effective electroneutrality on the central ion.

An enhancement in the π-acceptor ability of ring nitrogen coordinated ANT, relative to 2-aminothiazole could be concluded by comparing the strucures of the complexes formed with copper(II) acetate monohydrate, and the similarity of the reflectance spectra and the magnetic moments of $[Cu(AcO)_2.(ANT)]_2$ and $[Cu(AcO)_2.$-(pyridine N-oxide)$]_2$. Therefore, the broad band observed in the near visible region in the electronic spectra of these complexes may be related to a charge transfer transition, $d \rightarrow \pi^*$, in the direction metal to ligand.

Unlike 2-aminothiazole, ANT did not form complexes in MeOH or DMF with Co(II) bromide, Ni(II) iodide or Cu(II)bromide. The lack of ring nitrogen coordinated complexes in methanol could be explained as follows. It is known that the basicities of the three anions follow the sequence $Cl^- > Br^- > I^-$, whereas the π- accepting ability of these anions is in the reverse order.[143] Accordingly electron transfer to ANT decreases along the series, $Cl^- > Br^- > I^-$, and electro-

neutrality on the metal ions prevents the formation of these complexes. To explain the lack of formation $-NH_2$ coordinated complexes with these metals, consideration of basicities and π-accepting properties alone could not be enough, because DMF is also a π-acceptor, yet $-NH_2$ coordinated complexes are formed in its presence. Therefore, two additional factors should be considered, (a) the solvating properties of DMF, (b) the hard-soft relations in ANT and the metal ions.

It is known that DMF solvates cations better than anions.[144,145] Therefore, with ligand sites being occupied by DMF molecules there will be little room for the sterically hindered ring nitrogen to form bonds with the metal centres. It is also known that DMF has a mild preference for solvating large anions which function as soft bases, e.g. Br^-, I^- and NCS^-, thus reducing their basicity needed for achieving electroneutrality at the central metal ion.[146] Further, the dipolar aprotic solvent DMF will interact with the polar ANT, by breaking the donor-acceptor interaction between the nitro group amd amine group, thus reducing the electron-withdrawing character of the nitro group thus liberating the amine group and making it more available for bonding.

In the ligand ANT, the various coordination sites present a wide range of hard and soft coordination sites. The expected order of hardness for various sites is as follows:

Nitro group > Amine Nitrogen > Ring nitrogen > Sulphur > ring electrons.

whereas, the hardness of the anions concerned is as follows:

$SO_4^{2-} > Cl^- > Br^- > NCS^-$

the sulphate ion being hard and the NCS ion soft.

Another fact is that first row transition metals are harder than second raw metals, and second row metals are harder than third row metals, and Metal(II) ions are harder than metal(I) ions.

It is also generally expected that the character of the acceptor

will vary to a certain degree with the properties of the donor. Therefore, the more polarizable the donor, the more pronounced the soft character of a certain acceptor. It is also a fact that soft acceptors prefer soft donors and hard acceptors prefer hard donors.[147]

In the complexes prepared, amine nitrogen coordination takes place with the hardest of the metal(II) ions such as Co SO_4, Ni SO_4, Cu SO_4, $NiCl_2$, $CuCl_2$, and only with the assistance of DMF.

Considerations of the above mentioned four factors, namely, (a) basicities of the anions, (b) π-accepting properties of the anions, (c) difference in solvating properties of MeOH and DMF, (d) hard-soft relationship in various acceptors and donors, could explain why the metal salts used for the preparation of the mixed methanol complexes, did not form mixed DMF complexes, and the metal salts used in the preparation of mixed DMF complexes did not give mixed MeOH complexes.

REFERENCES

1.- T. P. Singer, Methods in Enzymology, vol. 1, p. 465, Academic Press, New York (1955).

2.- A Schellonberger, Angew. Chem. Internat. Edit., 6, 1024 (1967).

3.- (a) R. Breslow, Chem . Ind. (London), 893 (1957). (b) J. Amer. Chem. Soc., 79, 1762 (1957). (c) J. Amer. Chem. Soc., 80, 3719 (1958). (d) R. Breslow, E. McNelis, J. Amer. Chem. Soc., 81, 3080 (1959).

4.- F. Kubowitz and W. Luttgens, Biochem. Z., 307, 170 (1940) .

5.- D. E. Green W. W. Westerfeld, B. Vennesland, and W. E. Knox, J. Biol. Chem., 141, 60 (1941).

6.- S. Ochoa, Nature ,144, 834, (1939).

7.- R. Nordlie and H. Lardy, The Enzymes, 6, 9 (1962).

8.- H. A. Kirst, E. F. Szymanski, D. E. Dorman, J. C. Occolowitz, N. D. Jones, M. O. Chaney, R. L. Hamil, and M. M. Hoehn, J. Antibiot., 28, 286 (1975).

9.- P. Brookes, A. T. Fuller, and J. Walker, J. Chem. Soc., 689, (1957).

10.- M. N. G. James, and K. J. Watson, J. Chem. Soc. C, 1361 (1966)

11.- J. Jadot, J. Casimir and R. Warin, Bull. Soc. Chem. Beldges, 78, 299 (1969).

12.- Y. Yamada, N. Seki, T. Kitahari, M. Takahashi and M. Matsui, Agri . Biol. Chem. Japan, 35, 780 (1970).

13.- R. Viani, J. Bricout, J. P. Marion, F. Muegglerchavan, D. Reymond, and R. H. Egli, Helv. Chim. Acta., 52, 887 (1969).

14.- O. G. Vitzthum, and P. Werkhoff, J. Food. SCI, 39, 1210 (1974).

15.- O. G. Vitzthum, and P. Werkhoff, A. Lebensm. Forsch., 156, 300 (1974).

16.- J. P. Walradt, A. O. Pittet, T. E. Kinlin, R. Muralidhara, and A. Sanderson, J. Agri. Food Chem., 19, 972 (1971).

17.- H.J. Wobben, R. Timmer, R. Ter Heide and P. J. De Valois, J. Food Sci., 36, 464 (1971).

18.- S. L. Gusinskaya, V. Y. Telly and A. Aidogdyev, Uzbek Khim. Zhur., 11, 21 (1967).

19.- M. Dymicky, C. N. Huhtanen, A. E. Wasserman, Antimicrob. Agents Chemother., 12 (3), 353, (1977).

20.- H. M. R. El-Mauaffi, Bull. Fac. Pharm. Cairo Univ., 13 (1) 111 (1974).

21.- J. Peter Islip, M. D. Closier, M. C. Neville, J. Med. Chem., 117 (2), 207 (1974).

22.- Y. Lin, B. Peter Hulbert, R. E. Bueding, J. H. Cecil, Med. Chem. , 17 (8) 835 (1974).

23.- A. Malmio, Farm. Aikak , 75 (11) 375 (1966).

24.- J. J. O'connor,, Jr. S. G. Myers, D. Maples, C. Douglas, J. W. G. Vander Noot, Anim. Sci., 30 (5) 812 (1970).

25.- E. T. Del Carmen, F. Maria, Nature Madrid, 4, 969 (1970).

26.- E. Kutter, R. H. Machleidt, Advan. Chem. Ser., 114 (1972).

27.- S. Rockwell, Z. Mroczkowski, D. W. Rupp, Radiat. Res., 90 (3) 575 (1982).

28.- D. Craciunescu, A. Doadrio and C. Ghirvu, Communication at the Fifth National Conference on Pure and Applied Physical Chemistry (1-4 September 1976), Bucharest (Roumania).

29. D. Graciunescu, A. Doadrio and C. Ghirvu, An. Quim., (1976).

30.- A. Doadrio, D. Craciunescu and C. Ghirvu, Inorg. Perspc. Biol. and Med.,1, 223 (1978).

31.- G. Vasilev, M. Genchev, K. Davarsk, G. Kimenov, G. Dokl. Bolg. Akad. Nauk, 33, 2, 261 (1980).

32.- R. Phan Tan Luu, L. Bouscasse, E.J. Vincent, and J. Metzger, Bull. Soc. Chim. France, 4,1149 (1969).

33.- E. J. Vincent, R. Phan Tan Luu, and J. Metzger, Bull. Soc. Chim. France, 11, 3530 (1966).

34.- S. Lalitha, V. Kannappan and M.J. Nanjan, Indian J. Chem., 20A, 714 (1981).

35.- M. Gelus. P. M. Vay, and G. Berthier, Theor. Chim. Acta, 9,182 (1967).

36.- G. Salmona, Y. ferre, and E. J. Vincent, J. Chim. Phys., 69,1292 (1972).

37.- C. B. Chowdhury and R. Basa, J. Indian Chem. Soc., 66, 779 (1969).

38.- E. Vincent and J. Metzger, Bull. Soc. Chim. France, 2039 (1962).

39.- R. Zahradnik and J. Koutecki, Coll. Czech. Chem. Comm., 26, 156 (1961).

40.- J. Vitry and J. Metzeger, Bull. Soc. Chim. France, 1784 (1963).

41.- D. H. McDaniel and H. C. Brown, J. Amer. Chem. Soc.,77,3756 (1953).

42.- M. Charton, J. Amer. Chem. Soc., 86,2033 (1964).

43.- M. Charton, J. Org. Chem., 30,3346 (1965).

44.- L. Forlani and G. Breviglieri, J.C.S. Perkin II, 163 (1979).

45.- M. Bosco, L. Forlani, V. Liturri, P. Riccio, and P.E. Todesco, J. Chem. Soc. (B), 1373 (1971).

46.- J. Elguero, C. Marzin, A. R. Katritzky, and P. Linda, 'The Tautomerism of Heterocycles'. Academic Press, London, 1976.

47.- L. Forlani, L. Lunazzi and A. Medici, Tetrahedron Letters, 51, 4525 (1977).

48.- O. Ceder and B. Beijer, Tetrahedron, 31, 963 (1975).

49.- L. Forlani, M. Magagni, and P.E. Todesco, Gazzetta, 109,377 (1979).

50.- L. Forlani, Gazz. Chim. Ital., 111, 159 (1981).

51.- C. Caranoni and J. P. Reboul, Acta Cryst., B38, 1255 (1982).

52.- I. T. Depeshko, V. I. Treskach, Farm. Zh.(Kiev), 5, 47 (1980).

53.- I. T. Depeshko, V. I. Treskach, N. M. Turkevich, Farmatsiya (Moscow), 28(6), 30 (1979).

54.- R. Faure, J.P. Galy, E.J. Vincent and J. Elguero, Can. J. Chem., 56, 46 (1978).

55.- L. Nygard, E. Asmussen, J. H. Hog, R.C. Maheshwari, C. H. Nelsen, I. B. Petersen, J. Rastrup-Andersen, and G. O. Sorensen, J. Mol. Struct., 8, 225 (1971).

56.- G. R. Form, E. S. Raper, T. C. Downie, Acta Cryst., B30, 342 (1974)

57.- M. Fehlmann, Acta Cryst., B26, 1736 (1970).

58.- J. D. Ekstrand, D. Van der Helm, Acta Cryst., B33, 1012 (1977).

59.- G. Pepe, M. Pierot, Acta Cryst., B28, 2118 (1972).

60.- G. Pepe, J. P. Reboul Acta Cryst., B32, 2631 (1976a).

61.- G. Pepe, J. P. Reboul, Acta Cryst., B32, 2634 (1976b).

62.- M. Sax, P. Pulsinelli, J. Pletcher, J. Amer.Chem. Soc., 96, 155 (1974).

63.- L. Power, J. Pletcher, M. Sax, Acta Cryst., B26, 143 (1970).

64.- J. Kraut, H. J. Reed, Acta Cryst., 15, 747 (1962).

65.- M. N. Hughes and K. J. Rutt, J. Chem. Soc., A 3015 (1970).

66.- W. U. Malik, K. D. Sharma, R. D. Sharma and J. S. Upadhyaya , Indian J. Chem., 15A, 152 (1977).

67.- B. S. Manhas, V. K. Bhatia and O. P. Chitkara, Indian J. Chem., 14A, 209 (1976).

68.- W. J. Eilbeck, F. Holmes and A. E. Underhill, J. Chem. Soc., A, 757 (1967).

69.- J. A. Weaver, P. Hambright, P. T. Talbert, E. Kang, N. Thorpe, Inorg. Chem. , 268 (1970).

70.- M. Goodgame and M. J. Weeks, J. Chem. Soc., A, 1156 (1966).

71.- P. P. Singh and A. K. Srivastava, Aust. J. Chem., 27, 509 (1974).

72.- P. P. Singh and A. K. Srivastava, J. Inorg. Nucl. Chem., 928 (1974).

73.- P. P. Singh and U. P. Shukla, Aust. J. Chem., 27, 1827 (1974).

74.- M. H. Sonar and A. S. R. Murty, J. Inorg. Nucl. Chem., 815 (1979).

75.- B. S. Manhas and V. K. Bhatia, Indian. J. Chem.,10, 947 (1972).

76.- E. J. Duff, M. N. Hughes, and K. J. Rutt, Inorg. Chim. Acta, 6, 408 (1972).

77.- S. R. Joshi, P. K. Srivastava and S. N. Tandon, Indian J. Chem., 11, 590 (1953).

78.- (a) M. Goodgame and F. A. Cotton, J. Amer. Chem. Soc., 84, 1953 (1962); (b) D. M. L. Goodgame, M. Goodgame and M. J. Weeks, J. Chem. Soc., A, 1125 (1976).

79.- (a) M. Goodgame and M. J. Weeks, J. Chem. Soc., A, 1156 (1966); (b) M. Goodgame and L. I. B. Haines, J. Chem. Soc.,A, 174, (1966).

80.- E. J. Duff, M. N. Hughes, and K. J. Rutt, J. Chem. Soc., A, 2354 (1968).

81.- W. E. Estes, D. P. Gavel, W. E. Hatfield, and D. J. Hodgson, Inorg. Chem., 17(6) , 1415 (1978).

82.- W. E. Marsh, T. L. Bowman, C. S. Harris, W. E. Hatfield, and D. J. Hodgson, Inorg. Chem.., 20, 3864 (1981).

83.- D. P. Gavel and D. J. Hodgson, Acta Cryst., B35, 2704 (1979).

84.- E. S. Raper, R. E. Oughtred, and I. W. Nowell and L. A. March, Acta Cryst., B37, 928 (1981).

85.- M. J. M. Campbel, D. W. Card, and R. Crzeskowiak, J. Chem. Soc., A, 672 (1970).

86.- B. Raouf (American Color and Chemical Corp.) Ger. offen 2, 714 664(Cl. CO4B45/12)08 Dec. 1971, U.S. Appl. 692, 910,04, Jun. 1976, 49pp.

87.- A. Kh. Alikhodzhaev, M. Yu. Vusupov, P. N. Pachastcharov, (Inst. Khim. Dushanbe, U.S.S.R.). Tesisy Dokl. Nauchn. Sess. Khim. Technol. Org. Soedin Sery Sernistykh Nefte, 13, 214 (1974).

88.- Inorg. Synthesis, Vol.(II), page 1.

89.- K. Ganapathi and A. Venkataraman, Proc. Indian Acad. Sci., 22A, 343 and 362 (1945).

90.- H. Babo, and B. Brijs, Helv. Chim. Acta, 33, 306 (1950).

91.- R. L. Carlin, J. Amer. Chem. Soc., 83, 3773 (1961).

92.- B. N. Figgis and J. Lewis, "The Magnetochemistry of Complex Compounds," in "Modern Coordination Chemistry," ed. J. Lewis and R. G. Wilkins, Interscience. New York (1960).

93.- N. S. Gill and R. S. Nyholm, J. Chem. Soc., 3997 (1959).

94.- D. W. Herlocker, R. S. Drago, and V. I. Meek, Inorg. Chem., 5, 2009 (1966).

95.- Tezisy Dokl.- Sim. Khim Tekhnol. Geterotsikl Soedin. Goryuch, Iskop., 2nd, 205 (1973).

96.- Mulliken, J. Amer. Chem. Soc.,74, 811 (1952).

97.- a) B. N. Figgis and R. S. Nyholm, J. Chem. Soc., 12 (1954).
b) B. N. Figgis and R. L. Martin, J. Chem. Soc., 3837 (1956).

98.- J. A. Van Nierkerk and F. R. L. Schoening, Acta Cryst., 6, 227 (1953).

99.- H. Abe and J. Shimada, Phys. Rev., 90, 316 (1953).

100.- a) E. A. Boudreaux, Inorg. Chem., 3, 506 (1964); W. Harrison, S. Rettig and J. Trotter, J. Chem, Soc., Dalton, 1852 (1972).

101.- M. Kato, H. B. Jonassen and J. C. Fanning, Chem. Rev., 64, 99 (1964).

102.- F. A. Cotton Accts. Chem. Res., 2, 240 (1969).

103.- F. A. Cotton, Quart. Rev. Chem. Soc., 20, 389 (1966).

104.- F. A. Cotton and J. G. Norman Jr., Coordin. Chem. Rev., 1, 161 (1971).

105.- E. Kokot and R. L. Martin, Inorg. Chem., 3, 1306 (1964).

106.- B. J. Edmondson and A. B. P Lever. Inorg. Chem., 4, 1608 (1965).

107.- S. Yamada, H. Nakamura and R. Tsuchida, Bull. Chem. Soc., (Japan), 31, 303 (1958).

108.- D. Hibdon and J. H. Nelson, Inorg. Chim. Acta, 7, 629 (1973).

109.- D. M. L. Goodgame and M. Goodgame, J. Chem. Soc., 207 (1963); D. M. L. Goodgame, M. Goodgame and M. J. Weeks, J. Che. Soc.(A), 5194 (1964).

110.- L. Sacconi and I. Bertini, J. Amer. Chem. Soc., 88,5180 (1966).

111.- E. M. Boge, D. P. Freyberg, E. Kokot, G. M. Mockler, and E. Sinn, Inorg. Chem., 16, 1655 (1977).

112.- K. E. Hyde, B. C. Quinn and I. P. Yang, Inorg. Nucl. Chem., 33, 2377 (1971).

113.- M. A. Hitchman, J. Chem. Soc., (A), 4 (1970).

114.- B. R. McGarvey, "Electron Spin Resonance of Transition Metal Complexes," in "Transition Metal Chemistry," ed. R. L.Garlin, M. Kekker, Inc., New York, 3, 160 (1966).

115.- J. R. Wasson, D. M. Klassan, H. W. Richardson and W. E. Hatfield, Inorg. Chem., 16, 1906 (1977).

116.- B. J. Hathaway and D. E. Billing, Coordin. Chem. Rev., 5, 143 (1970).

117.- L. Erdey, G. Liptay, Periodica Polytech., 7, 223 (1963).

118.- G. Liptay, K. Burger, E. Papp-Molnar, and Sz. Szebeni, J. Inorg. Nucl. Chem., 31, 2359 (1969).

119.- J. F. Villa, R. Doyle, H.C. Nelson and J. L. Richards, Inorg. Chim. Acta, 25, 55 (1977).

120.- S. Koide, Phil. Mag., 4, 243 (1959).

121.- J. Ferguson, J. Chem. Phys., 32, 533 (1960).

122.- I. Bertini, D. Gatteschi and A. Scozzafava, Coord. Chem. Rev., 29, 67 (1979).

123.- I. M. Procter, B. J. Hataway and P. Nicholls, J. Chem. Soc., (A), 1678 (1968).

124.- A. A. G. Tomlinson and B. J. Hathaway, J. Chem. Soc., (A), 2578 (1968).

125.- M. Lynch, K. E. Hyde, P. L. Bocko, and G. F. Kokoszka, Inorg. Chem., 563 (1977).

126.- W. E. Hatfield, T.S. Piper, Inorg. Chem., 3, 841 (1964).

127.- L. L. Furlani, A. Sgamelloti, F. Magrini, O. Cordisch, J. Mol. Spectra, 24, 270 (1967).

128.- R. D. Willett, O. L. Liles, C. Michelson, Inorg. Chem., 6, 1885 (1967).

129.- B. Morosin, K. Lawson, J. Mol. Spectroscopy, (a) 12, 98 (1964), (b) 14, 397 (1964).

130.- C. Furlani, G. Morpurgo, E. Cervone, F. Calzona, B. Baldanza, Theoret. Chim. Acta, 7, 375 (1967).

131.- Z. G. Soos, K. T. McGregor, T. T. P. Cheung and A. J. Silverstein, Phys. Rev., B, 3036 (1977).

132.- C. P. Poole, Jr., "Electron Spin Resonance, Interscience, New York, chap. 20 (1967).

133.- B. J. Hathaway and D. E. Billing, Coord. Chem. Rev., 5, 143 (1970).

134.- H. Abe and K. Ono, J. Phys. Soc. Jpn., 11, 947 (1965).

135.- R. H. Sands, Phys. Rev., 99, 1222 (1955).

136.- F. K. Kneubuhl, J. Chem. Phys., 33, 1074 (1960).

137.- R. Neiman and D. Kivelson, J. Chem. Phys., 35, 156 (1961).

138.- V. S. Korolkov and A.K. Potapovich, "Optics and Spectroscopy," 16, 251 (1964).

139.- T. S. Johnston and H. G. Hecht, J. Mol. Spec., 17, 98 (1965).

140.- J. W. Searl, R. C. Smith and S. J. Wyard, Proc. Phys. Soc., 78, 1174 (1961).

141.- L. S. De De Jongh nad A. R. Miedema, Adv. Phys., 23, 1 (1974).

142.- D. W. Phelps, D. B. Losee, W. E. Hatfield, and D. J. Hodges, Inorg. Chem., 15, 3147 (1976).

143.- W. Beck, K. Lottes, Chem. Ber., 98, 2657 (1965).

144.- For a review, see Parker, Q. Rev., Chem. Soc., 16, 163-187 (1962).

145.- Sears, Wolford, and Dawson J. Electrochem. Soc., 103, 633 (1956).

146.- Miller and Parker, J. Amer. Chem. Soc., 83, 117 (1961).

147.- C. K. Jørgensen et al. , "Structure and Bonding", 1, 207 (1966).

PART II

CHAPTER 1

THE COORDINATION CHEMISTRY OF AROMATIC AMINE N-OXIDES

1.1. Introduction

The oxygen atom in the N-oxides is more polar than in other oxo donors such as alcohols, ethers, and amides. This conclusion is supported by dipole moments[1-3] and thermodynamic studies[4]. In aromatic amine oxides the oxygen $2p\pi$ electrons are conjugated with the aromatic ring[1-3, 5-8] whereas in the aliphatic amine oxides this cannot occur. Fundamental to the chemistry of N-oxides is the fact that the dipolar N-oxide group $=N^{+}-(O)-$ is both an electron donor and an electron acceptor by the resonance effect (in addition to being an inductive electron acceptor). Taking pyridine N-oxide I as an example, this "push -pull" character is expressed by the fact that canonical forms of type II in addition to those of type III contribute to the resonance hybrid. This situation is in fundamental contrast to that appertaining to pyridine IV. In its dual role as an electron donor or acceptor, the N-oxide group resembles the nitroso group[9].

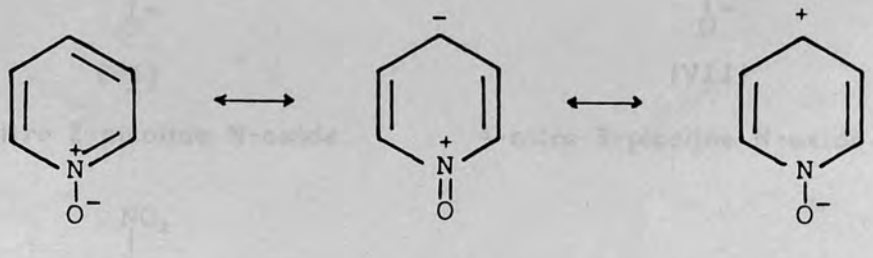

(I) (II) (III)

(IV) (V)

The basicity of aromatic N-oxides may, therefore, be systematically varied by appropriate substitution on the aromatic ring with a concomitant minimal change in steric interaction at the reaction site. These properties, plus the ready availability of an extended series of substituted pyridine N-oxides,[5] have greatly contributed to the abundance of coordination chemistry of these ligands.

In the present work the coordination chemistry of 4-nitro 2-picoline N-oxide (2-CH_3 4-NO_2 Py-NO), 4-nitro 3-picoline N-oxide (3-CH_3 4-NO_2 Py-NO), 4-nitro 2,6-lutidine N-oxide (2,6-$(CH_3)_2$ 4-NO_2 Py-NO), and 3-nitro 2,6-lutidine N-oxide (2,6,-$(CH_3)_2$ 3-NO_2 Py-NO) is studied and discussed in terms of the effect of nitro and methyl substituents.

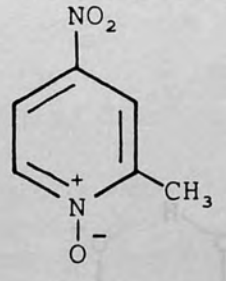

(VI)

4-nitro 2-picoline N-oxide

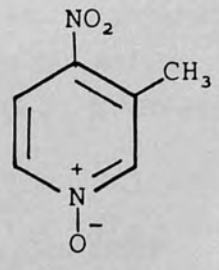

(VII)

4-nitro 3-picoline N-oxide

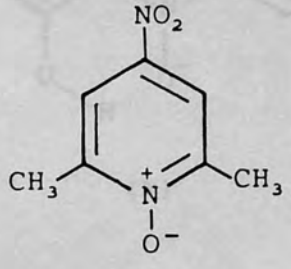

(VIII)

4-nitro 2,6-lutidine N-oxide

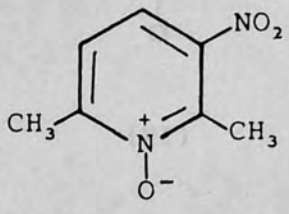

(IX)

3-nitro 2,6-lutidine N-oxide

1.2. Natural Occurrence and Biological Activity

The chemistry of heterocyclic N-oxides has gained importance due to the interesting biological activities of these compounds.[5]

In 1917 Polonovski[10] isolated from Calabar beans the first naturally occurring heterocyclic N-oxide, geneserine, which is the N-oxide of the alkaloid eserine. Relatively few aromatic heterocyclic N-oxides occur in nature, and an appreciable number of those contain a pyrazine or reduced pyrazine moiety.

The isolation of iodinin, a potent antibiotic, from Chromobacterium iodinum, in 1938[11] was followed by isolation of the antibiotic aspergillic acid from the mold Aspergillas flavus.[12] Iodinin was identified as 1,6-dihydroxyphenazine 5,10-dioxide (X)[13] and aspergillic acid as 1-hydroxy-2-pyrazinone (XI).[14,15] Other closely related compounds with antibiotic activity have since been isolated from a variety of microbial sources.

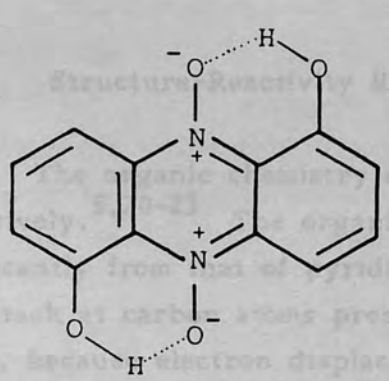

(X)

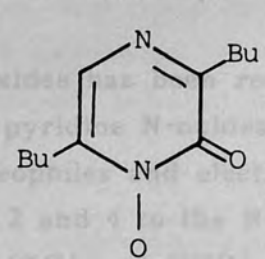

(XI)

The discovery that the antibiotics iodinin (X) and aspergillic acid (XI) are N-oxides stimulated interest in the biological activities of compounds of this type. Added interest was provided by claims that the conversion of certain alkaloids into their N-oxides led to a reduced toxicity without a parallel decrease in biological activity. A large number of heterocyclic N-oxides have been synthesized and tested for pharmacological, biological and physiological activities.[5,16,17] A few examples will serve to illustrate the variety of the N-oxides which possess biological activity and the range of this activity. 4-nitroquinoline N-oxide, which is a potent mutagen and concogen and also possesses antifungal and antibiotic activities, has been extensively studied, this compound is reduced in vivo to 4-hydroxyaminoquinoline which is the active princile. 2-Mercaptopyridine N-oxide and some of its derivatives are effective pesticides and fungicides for a broad spectrum of organisms. The antifungal activities of 4-nitropyridine N-oxide and its methyl derivatives are well known.[18] It has been suggested that the presence of the nitro group is very essential for any meaningful antifungal activity of pyridine N-oxides, and that the antifungal activity is due to the good electron accepting property of these conpounds.[18] A more general discussion of the natural occurrence and metabolism of N-oxides appears in a review by G. B. Brown.[19]

1.3. Structure-Reactivity Relations in N-oxide Chemistry

The organic chemistry of aromatic N-oxides has been reviewed extensively.[5,20-23] The organic chemistry of pyridine N-oxides differs significantly from that of pyridine. Both nucleophiles and electrophiles can attack at carbon atoms present at position 2 and 4 to the N-oxide group, because electron displacements of type (XII) and (XIII) are possible.

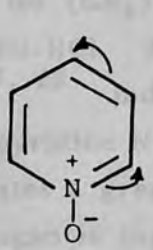

(XII)

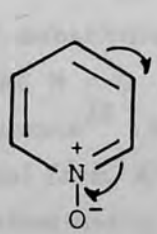

(XIII)

Electrophilic substitution which takes place only with difficulty at the 3 - position for pyridine occurs readily at the 4- and 2-positions of pyridine N-oxide.

The canonical structures XIV and XV resulting from the electron displacements of type XII and XIII for the unsubstituted pyridine N-oxides, greatly affect the reactivity of pyridine N-oxides, as well as certain other physical properties.

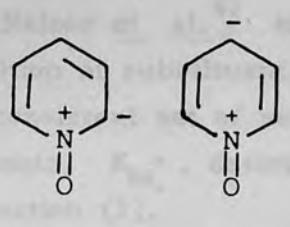

(XIV)

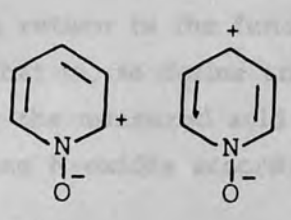

(XV)

Electron withdrawing ring substituents at the 2- and 4-positions enhance contributions from structural type XIV. Electron donating groups, on the other hand, enhance contribution of structure XV.

Much evidence has been amassed from physical measurements regarding the electron-donating and electron-accepting properties of the $N^{+}-O^{-}$ group in pyridine N-oxides, and these data are discussed under the various methods which have been applied: dipole moments, infrared stretching frequencies, infrared intensities, n.m.r. techniques, electronic absorption.

X-ray crystallographic data delineate a longer nitrogen - oxygen bond length for representative aliphatic amine N-oxides (1.424 Å for $(CH_3)_3$ - NO.HCl)[24] compared[25, 26] to 1.37 Å for Py - NO.HCl. X-ray diffraction studies of substituted pyridine N-oxides[27, 28] indicate a foreshortening of the N - O bond. In 4-nitropyridine N-oxide, for example the distance[27] is 1.260 Å. This indicates a greater contribution of canonical form XIV when para hydrogen is replaced by deactivating substituents.

1.4. Hammett Equation Treatment.

Application of the Hammett equation to heterocycles in general and N-oxides in particular was pioneered by Jaffé, who has reviewed the field.[20] Many reasonable correlations between measured physical properties of a system containing substituted pyridine N-oxides and a hybrid set of substituent parameters have been found, making comparison of the various properties of analogous systems very difficult.[20, 29, 30-40]

Nelson et al.[41] have suggested a return to the fundamental definition of substituent parameters. That is, to define an internally self-consistent set of values based upon the measured acid dissociation constants, $K_{BH_o^+}$, determined for pyridine N-oxides according to reaction (1).

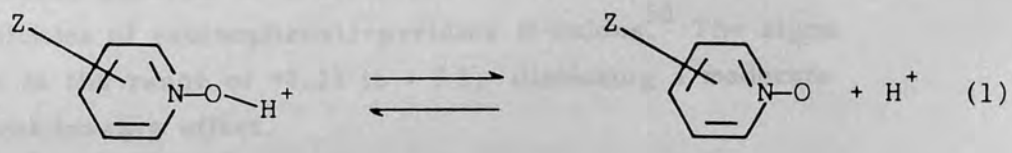

(1)

The pyridine N-oxide substituent constant, "σ_{PyNO}" is then defined according to the relationship. (2),

$$\sigma_{PyNO} = \frac{\Delta pK_{BH^+}}{\rho} \qquad (2)$$

where ΔpK_{BH^+} represents the difference between the value of the conjugate acid ionization constant for the unsubstituted pyridine N-oxide, $pK_{BH_o^+}$, and that of the substituted pyridine N-oxide, $pK_{BH_z^+}$.

$$\Delta pK_{BH^+} = pK_{BH_o^+} - pK_{BH_z^+} \qquad (3)$$

A value for ρ equal to 2.09 was chosen such that values of σ_{PyNO} most nearly conform to the existing sets of substituent constants. The σ_{PyNO} values so obtained for many 3- and 4-

substituted pyridine N-oxides were positive for electron-donating substituents and negative for electron-accepting substituents,[41] a fact which again reflects the ability of the N-oxide group to enter into strong conjugative interaction with both electron donors and strong electron acceptors.

The Hammett equation has been applied to hydrolysis of ethoxycarbonyl[42] and (4-ethoxycarbonylvinyl)-pyridine N-oxides[43] by Falkner and Harrison. The results obtained indicate that the pronounced electron-withdrawing effect of the $N^+ - O^-$ group decreases rapidly with distance. Other Hammett treatments have concerned the pK_a values of 2-substituted pyridine N-oxides[44], tautomeric equilibria,[45] infrared intensities[46,47] and frequencies,[48] and kinetics of electrophilic substitution of pyridine N-oxides.

Sigma constants for pyridine N-oxide rings considered as substituents attached to benzene have been obtained by measurement of the basicities of (aminophenyl)-pyridine N-oxides.[50] The sigma values are in the range of +0.23 to + 3.3, disclosing a moderate electron-withdrawing effect.

1.5. Physical Properties

1.5.1. Ultraviolet Absorption Spectra

A general discussion of the ultraviolet spectra of N-oxides is available in ref. 51. Papers which are principally concerned with ultraviolet spectroscopy of N-oxides are listed in ref. 52.

The effect of N-oxidation on the electronic spectrum of pyridine, is the appearance of two new bands around 330nm(and 312nm) in the spectrum of pyridine N-oxide, while the 251 and 192 and 175nm bands which appear in the spectrum of pyridine are shifted to longer wavelengths, viz. 278, 285, and 216nm respectively, in the spectrum of pyridine N-oxides. It was hence pointed out that the π electron interaction between the N-oxide group and the heterocyclic ring was responsible for the overall shifting of the bands to longer wavelengths.[18]

The electronic spectrum of pyridine N-oxide has been studied in great detail; however, the assignments of the bands have varied.[18,53,54] Substitution at the various positions on the ring usually shifts the principal bands in the electronic spectrum in varying amounts depending on the nature of substituent.

Electronic spectroscopy has been used to study the steric effects of the methyl groups substituted at the vicinal positions of a nitro group.[55] The results are interesting because of their relevance to the present work. The band which appears at 346nm in the spectrum of pyridine N-oxide is reduced in intensity in the spectra of 3-methyl-4-nitropyridine N-oxide and 3,5-dimethyl-4-nitropyridine N-oxide. From the relation $\varepsilon/\varepsilon_o = \cos^2\theta$, where ε_o is the extinction coefficint of the charge transfer band at 346nm in the spectrum of pyridine N-oxide, the angle of twist out of the molecular plane, θ, of the nitro group is calculated.[55] The values so obtained are 11° 12' and 55° 30' for 3-methyl-4-nitropyridine N-oxide and 3,5-dimethyl-4-nitropyridine N-oxide respectively, and are in very good agreement with later crystallographic results.[56] The twist angles obtained by the above mentioned two methods are smaller than those in the corresponding derivatives of 4-nitrobenzene. It was hence pointed out that the intramolecular charge transfer between the nitro group and the substituent at its para position influenced the twist angle; the twist decreases with increasing charge transfer.

1.5.2. Infrared Spectroscopy

Infrared absorption spectra of pyridine N-oxides display a prominent band between 1200-1300cm.$^{-1}$ The band often exceeds in intensity all other absorptions of the spectrum.[57,58] Shindo[57] found that the band positions were affected in a systematic manner by changing substituents on the ring. The more activating the substituent, the lower the energy of this absorption. A detailed treatment of the infrared spectra of heterocyclic compounds, including N-oxides, is given by Katritzky and Ambler.[59,60] Since then many papers dealing with the infrared spectra of substituted pyridine N-oxides

have appeared.[48,61-67] Indexes are also available which list infrared spectra by name e.g. ref. 68.

Upon coordination, ν_{NO} for pyridine N-oxides is decreased from values for the free ligand by 12 to 60cm.$^{-1}$ This shift may be regarded as arising in part from the change in the nature of the nitrogen-to-oxygen bond as a result of coordination. The formation of the O - M bond increases the electron demand of the donor oxygen atom and thereby brings about a decrease of the N=O double bond character corresponding to a diminished contribution of the resonance structure (XIV) to the overall state of the ligand molecule.[33-35, 69-72]

Garvey et al. pointed out that changes in ν_{N-O} with changing substituents for coordinated 4-substituted pyridine N-oxides often displayed a range of values similar to that for the free ligand.[32,] However, for complexes of metal ions from earlier groups of the transition series, the range is much more restricted than is the case for the uncoordinated ligands or their complexes with metal ions from later groups.

1.5.3. Nuclear Magnetic Resonance Techniques

The nuclear magnetic resonance spectrum of pyridine N-oxide itself has been completely elucidated.[73] Many papers dealing specifically with the n.m.r. spectra of N-oxides have appeared.[73-92] N.m.r. spectroscopy has been used to particular advantage in the elucidation of certain rearrangements, in the investigation of tautomerism of hydroxypyridine N-oxides and in the determination of the structures of the isomeric cinnoline 1- and 2-oxides.[79]

The carbon-13 chemical shifts of pyridine N-oxide and of a number of X-substituted pyridine N-oxides (X = 4-CH_3, 4-$N(CH_3)_2$, 4-OCH_3, 4-$COCH_3$, 4-Cl, 4-NO_2, 3-$COCH_3$, 3-CN, 3-Cl, 3-Br, 2-CH_3, 2-OCH_3, 2-$COCH_3$, 2-Cl) have been reported and discussed

in terms of the effect of the substituent on the ground state electron distribution.[80] In general, the pyridine N-oxides show a large shielding effect (~ 10ppm) at C-2, C-4, and C-6 relative to that observed in the corresponding pyridines. The only exception to the observed trend is 4-nitropyridine N-oxide in which an opposite deshielding effect at C-4 is observed. The shielding effect observed at positions 2, 4, and 6 is explained in terms of the resonance forms (XIV) making substantial contribution to the pyridine N-oxide hybrid, whereas, the deshielding effect at C-4 of 4-nitropyridine N-oxide is explained in terms of the resonance effect of the nitro group in delocalizing the electron density contributed to the 4-position and a substantial contribution of the resonance form (XV) to the pyridine N-oxide hybrid.

Nitrogen-14 n.m.r. spectra of a large set of monosubstituted pyridine N-oxides[81-88] and a number of polysubstituted N-oxides have been reported.[89 - 91] The N-14 n.m.r. spectra of mono-substituted pyridine N-oxides show a correlation between the chemical shifts and the character and the position of the substituent.[81] The substituents which exert an overall electron releasing effect (such as $-NH_2$, $-N(CH_3)_2$, $-OH$, $-OCH_3$, $-CH_2OH$ and $-CH_3$) result in a shift of the ^{14}N signal to higher fields relative to that of pyridine N-oxide. Those which exert an overall electron-withdrawing effect (such as $-NO_2$, $-COOH$, $-CHO$, $-COCH_3$ and $-CN$) give a downfield ^{14}N shift relative to pyridine N-oxide itself. A substituent in position 3 (either electron-releasing or electron-withdrawing) exerts the smallest effect on the ^{14}N chemical shift, roughly in agreement with what is expected from the inductive mechanism alone. Substitution in position 2 brings some complications arising from direct interactions between the substituent and the nitrogen atom in the ring. The spectral changes observed are fairly parallel to those found in the spectra of the parent pyridines, having resonance signals about 25ppm to higher fields than the corresponding mono-substituted pyridine derivatives (fig. 1), while, the ^{14}N resonance half-height widths for the N-oxides are much smaller as compared with the corresponding pyridine derivatives.

The Nitrogen-15 chemical shifts of alkyl substituted pyridine

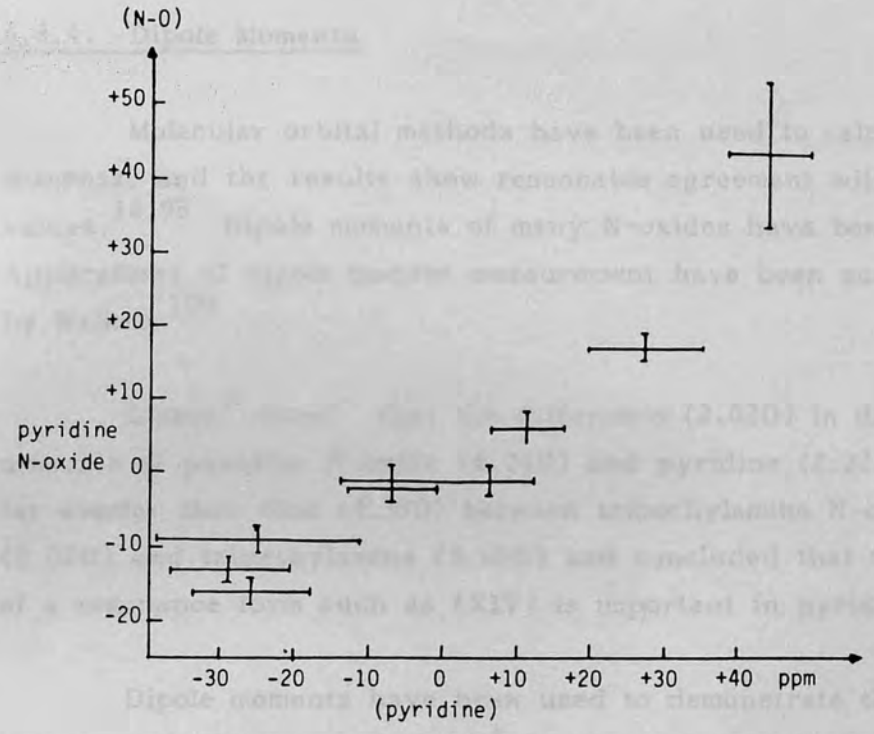

Fig. 1. Correlation of ^{14}N chemical shifts of 4-substituted pyridine N-oxides and 4-substituted pyridine derivatives.

N-oxides is reported and compared to that of corresponding pyridines.[92] The reported changes in the nitrogen resonance positions of methyl pyridine N-oxides are small except for para-substituted compounds. This is rationalized qualitatively in terms of competitive inductive vs. hyperconjugative interaction between the substituent and the nitrogen. The upfield shift in resonance position exhibited by the pyridine nitrogen nuclei upon oxide formation is explained in terms of the removal of the lone pair orbital contribution to the chemical shift.

The F-19 n.m.r. technique is employed to investigate effects due to substituents in titanium tetrafluoride-and tin tetrafluoride-substituted pyridine N-oxide adducts. While a linear correlation between chemical shifts for all chemically different fluorines and σ_{PyNO} is reported for the titanium(IV) complexes,[31,93] no such correlation is found in ^{19}F chemical shifts of tin tetrafluoride diadducts.[94]

1.5.4. Dipole Moments

Molecular orbital methods have been used to calculate dipole moments, and the results show reasonable agreement with experimental values.[18,95] Dipole moments of many N-oxides have been reported.[96-99] Applications of dipole moment measurement have been summarized by Walker.[100]

Linton[3] noted that the difference (2.02D) in dipole moments of pyridine N-oxide (4.24D) and pyridine (2.22D) is far smaller than that (4.37D) between trimethylamine N-oxide (5.02D) and trimethylamine (0.65D) and concluded that the contribution of a resonance form such as (XIV) is important in pyridine N-oxide.

Dipole moments have been used to demonstrate that interaction between substituents and the $N^{+}-O$ group decreases rapidly with distance.[101] In 4-substituted pyridine N-oxides, substitution of electron releasing groups such as -OH, $-NH_2$, $-CH_3$, leads to an increase in the dipole moment, while the substitution of electron withdrawing groups such as -CN, -NO, $-NO_2$ leads to a decrease in the dipole moment, with respect to pyridine,[18] thus demonstrating that the N-oxide group can act as a reversible electron pump capable of electron polarization into and away from the heteroaromatic ring. To illustrate this phenomenon, the dipole moment results of 4-nitropyridine N-oxide could be helpful.[18] Nitration of pyridine results in a slight decrease in the moment (from 2.22D to 1.58D), while N-oxidation of pyridine results in a large increase in dipole moment (from 2.22D to 4.24D), showing that both NO_2 and N-oxide groups in fact withdraw electrons from the pyridine ring; the N-oxide group being much more effective than the NO_2 group. However, a small value of dipole moment (0.71D) is found for 4-nitropyridine N-oxide demonstrating that N-oxide group acts as an electron releasing group in the presence of a nitro group in the 4-position of pyridine N-oxide.

Dipole moments are also important in connection with complex formation. Evidence for a weak interaction between pyridine N-oxide and carbon tetrachloride was obtained from dipole moment measurements.[102]

1.6. Metal Complexes of Aromatic N-oxides

The coordination complexes of aromatic N-oxides with various metals are discussed only as far as is necessary for an understanding and appreciation of the present work. The coordination complexes of Cu(II) and Cd(II) on the other hand, which are the main subject of the present work, are thoroughly covered. Although no complexes of Co(II) and Ni(II) could be prepared, the coordination compounds of these metals will be briefly discussed as many of their salts were tested with the aim of obtaining their complexes. Detailed discussion of the coordination compounds of amine N-oxides could be found in three excellent reviews.[103-105]

1.6.1. Generalities

One of the more notable aspects of the coordination chemistry of aromatic N-oxides is their ability to form complexes with more than forty elements of the periodic table including at least one element from each of the major groups of transition metals.

The majority of the metal complexes of aromatic N-oxides are decomposed by water. The methods employed for their preparation involve, therefore, interactions between ligand and metallic compound in non-aqueous solvents. Crystalline metal complexes with N-oxides are usually rather easily obtained, and a large number of compounds of this type are stable in the atmosphere. Special synthetic procedures or handling precautions required for certain metal complexes are mentioned in the review by Karayannis et al.[104] Perchlorate salts of the appropriate metal ions in ethanol or acetone solvents react with pyridine N-oxides generally yielding compounds having the maximum coordination number of the metal ion.[32,33,69,71,106-109] The highest possible coordination numbers are, nevertheless, not always attained in pyridine N-oxide metal complexes; for instance,

Y(III) and Ln(III) ions form $[M(\text{pyridine N-oxide})_8]^{3+}$ cationic complexes.[110] Higher coordination numbers of these metal ions are observed with other monodentate ligands e.g. certain sulphoxides yield $[YL_9]^{3+}$ and $[LnL_9]^{3+}$ complexes.[111] Anions more basic than perchlorate are often found along with the N-oxide ligands in the primary coordination sphere of the metal ion.[32,70,71,106,107,112-118]

Monodentate "oxo-ligands"[119] of the general type R_nZO (where Z is a Group VA element: N, P, As, etc.) coordinate invariably through the oxygen to metal ions.[71,72,120-125] Only in the case of metal complexes of organonitroxide free radicals has the possibility of interaction of an unoccupied orbital of the metallic compound with the three π-electron fragments N...O been advanced.[126] The nitrogen atom in tertiary amine N-oxides is devoid of a lone pair; in fact, the lone electron pair of nitrogen in tertiary amines is used for bonding to the oxygen atom during N-oxidation, i.e.

Hence, the only site available for coordination in tertiary amine N-oxides is the oxygen atom.

Upon coordination to metals the pyridine N-oxide oxygen can function as either a donor or an acceptor of π-electron density.[33,39,127] Should the metal ion possess empty d orbitals of correct symmetry donation of electron density from the highest filled π-molecular orbital of the ligand could occur. Changing substituents on the pyridine ring under these conditions increases only minimally the competition of the pyridine nitrogen atom for π-orbitals of the oxygen atom, thereby little affecting the nitrogen-oxygen bond order. On the other hand, metal ions with nearly filled d orbitals do not readily act as π-electron acceptors, and thus a metal to empty ligand π* orbital back bonding interaction becomes

preferred.[33] Nuclear magnetic resonance data[128] support a π-mechanism for spin delocalization from nickel to pyridine N-oxide donors in bis(pyridine N-oxide)bis(2,4-pentanedionato)-nickel(II). However, the data did not answer the question of whether the spin was delocalized in the highest-filled molecular orbital of the ligand or in the lowest empty antibonding orbital.

Coordination of substituted pyridine N-oxide molecules to transition metal ions evokes considerable stereochemical interest. If the metal-ligand bond has a covalent character, in addition to significant ionic character, the concepts of directed valence would predict a non-centrosymmetrical environment for the oxygen. A tetrahedral disposition (modified somewhat by multiple bonding to the pyridine nitrogen and electron pair repulsions) of oxygen lone pairs might be anticipated.[129] Trigonal planar sp^2 bonding would represent the other extreme for high nitrogen-oxygen double bond character. Thus, the M-O-N bond angle should lie somewhere between 108° and 120° as illustrated.

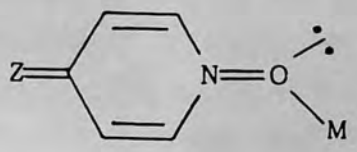

sp^2 M-O-N ⟩ ~ 120°

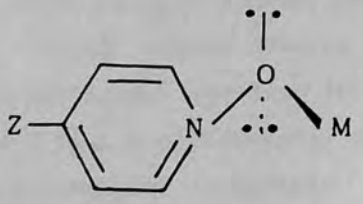

sp^3 M-O-N ⟩ ~ 108°

X-ray crystal structure determinations of various cationic and neutral aromatic N-oxide metal complexes have established[130-144] that the M-O-N bond angle lies between 108° and 134? The non-linearity of the M-O-N bond sequence is thought to be the underlying reason why the effective symmetries of cationic 3d metal complexes of the form $[ML_6]^{n+}$ and $[CuL_4]^{2+}$ are lower

than O_h and D_{4h} respectively.[123,140-143]

The aromatic rings of pyridine N-oxide(Py-NO), quinoline N-oxide (QNO) and isoquinoline N-oxide (IQNO) do not introduce severe steric hindrance during formation of cationic metal complexes.[33,69,71,110,115,120,145-155] Thus complexes of the types $[ML_6]^{n+}$ (n = 2 or 3)[33,69,71,110,114,115,146,147,151-155] and $[MOL_5]^{2+}$ (refs. 106, 145, 149) are formed during interactions of these ligands with most 3d metal perchlorates, tetrafluoroborates and, in certain cases in the presence of excess ligand, nitrates. Copper(II) generally forms $[CuL_4]^{2+}$ cationic complexes with aromatic N-oxides; and only in the cases of pyridine N-oxide and 4-methyl pyridine N-oxide were $[CuL_6]^{2+}$ complexes also isolated.[120, 157]

The presence of 3- or 4-substituents in the aromatic ring of pyridine N-oxide and 4- or 6-substituents in that of quinoline N-oxide do not introduce steric interference at the coordination site; thus $[ML_6]^{n+}$ complexes of ligands of these types with a variety of 3d metal ions have been reported.[33,69,72,146,151-153] Accordingly, the basicities of ligands of these types could be systematically varied while holding the steric factors constant. Steric effects become obvious in 2-substituted and 2,6-disubstituted pyridine N-oxides, where steric hindrance from 2-and 6-substituents tend to stabilize lower than hexacoordinated cationic complexes with 3d metal ions; however, the corresponding 6:1 complexes could also be formed under favourable reaction conditions thus indicating that steric hindrance at positions 2- and 6- does not provide a severe enough steric hindrance to impede the formation of 6:1 complexes.[157-160]

The steric effects of substituents on the aromatic ring of N-oxides are also evidenced by the influence they exert on various properties of mixed N-oxide anionic or neutral ligand metal complexes. Thus, the results of the ^{19}F n.m.r. study of diadducts of $SnF_4.2L$ and $TiF_4.2L$ with various

substituted aromatic N-oxides indicate the importance of steric factors in the formation of cis-octahedral or trans-octahedral isomers.[161-163] In $SnF_4.2L$ diadducts both the cis and the trans isomers were observed with the substituted pyridine N-oxides as long as neither the 2 nor the 6 positions were substituted. With the 2 and 6 substituted pyridine N-oxides only the trans isomer was observed and the chemical shift was related to the bulkiness of the ligand. In $TiF_4.2L$ diadducts with the same ligands one finds that with substituted pyridine N-oxides, where the substitution is in position 3, 4, and 5 or any combination thereof, only the cis isomer is observed. The titanium complexes with 2-substituted pyridine N-oxides and some 4- and 6-substituted quinoline N-oxides show both the cis and the trans isomers. Only the trans isomer is observed for $TiF_4.(2,6\text{-}(CH_3)_2\ Py\text{-}NO)_2$. Thus in $SnF_4.2L$ the trans-octahedral isomers are stabilized by steric interaction, whereas, in $TiF_4.2L$ diadducts the trans-octahedral isomers are stabilized only when there is sufficient steric interaction to overcome symmetry effects and the tendency to maximize F - to - $Ti_{p\pi} - d_\pi$ bonding.

Steric effects could also determine the mode of coordination of polyanions, as in the 3d metal nitrates. Thus the 1:2 complexes of divalent 3d metal nitrates with pyridine N-oxide and 4-substituted derivatives are hexacoordinated (the exception being the Cu(II) compound) with two chelating nitrato groups.[71,114,115,164-166] Bis(pyridine N-oxide)dinitratocobalt(II) represents possibly the first essentially octahedral nitrato complex of cobalt(II) which exhibits a magnetic moment consistent with its geometry. Similarity of optical absorption spectra for the bis- and hexakis(pyridine N-oxide) complexes $CoL_2.(NO_3)_2$ and $CoL_6.(NO_3)_2$, suggests that pyridine N-oxide and the nitrato group must be very close together in the spectrochemical series.[114] Complexes of the type $CoL_2(NO_3)_2$, where L represents 2,6-lutidine N-oxide or 2,4,6-collidine N-oxide were assigned similar structures.[117] However, later studies of M(2,6-lutidine N-oxide)$_2(NO_3)_2$ (M = Mn, Ni, Co, Zn) led to the conclusion

that these compounds are pentacoordinated, involving one mono- and one bidentate nitrato ligand.[166] Formation of complexes of this type with 2,6-lutidine N-oxide is apparently due to steric interference between the methyl ring substituents and the nitrato ligands.[166]

The effect of steric hindrance on the magnetic and electronic properties and the observed position of the (d - d) band in 1:1 complexes between N-oxides and Cu(II) halides is studied by Muto et al. in a series of papers.[167-170] Compounds of this type are binuclear, N-oxide-bridged, and exhibit subnormal and temperature-dependent paramagnetism; they have been the subject of extensive studies and will be discussed in a later section. Contrary to initial expectations that electron-withdrawing substituents would produce a comparatively small magnetic interaction by decreasing the electron density of the oxygen atoms, thus weakening the metal-oxygen covalent bonds through which the demagnetization mechanism operates, it was observed that the electron-withdrawing substituents in both inductive and resonance effects, such as COOH, $COOC_2H_5$, CH_3CO and NO_2, produce a larger demagnetization than with the parent complex with pyridine N-oxide. This indicates that substituent effects in Hammett's sense are broken down in these complexes. In a later work the same group observed that the ligand field bands at 10,000 - 14,000cm^{-1} behaved in the same way as the magnetic moments, showing the same breakdown in the relationship of Hammett's σ constants to the spectra of these compounds. However, a good linear relation was found to exist between the band positions and the magnetic moments. Thus for the same substituent group, the closer the site of substitution is to the central metal ion, the greater are the demagnetization and the shift of the d-d band to higher frequencies. In the case of the ethyl group, e.g., the effects increase in the following order of substitution 2->3->4. It can also be seen that the difference between the $\bar{\nu}_{max}$ of the d-d bands of 2- and 3-substituted complexes is fairly large, whereas the difference between those of 3-and 4-

substituted complexes is small. As for different substitutions at the same site (ethyl vs. methyl), the more bulky group has a greater demagnetization effect. This can also be observed in the greater demagnetization in the quinoline N-oxide complexes in comparison with pyridine N-oxide complexes. These trends which are illustrated in Table 1 suggest that in Cu(II)-N-oxide binuclear complexes, the steric factor is more important in determining the extent of the magnetic interaction, or the (d-d) transition energy, than the electronic effect.[167-170]

Table 1

d-d Band Maxima and Magnetic Moments of 1:1 $CuCl_2$ Substituted Pyridine N-Oxide Complexes.[169-172]

Ligand	λmax (nm)	$\bar{\nu}$max (cm^{-1})	μ_{eff} (25°C) (B.M.)
3-Cl Py-NO	820	12,200	0.46
3-HOOC Py-NO	885	11,300	0.54
3-H_5C_2OOC Py-NO	825	12,120	0.48
4-H_5C_2OOC Py-NO	830	12,050	0.50
3-CH_3CO Py-NO	900	11,110	0.57
4-NO_2 Py-NO	1100	9,090	1.20
4-CN Py-NO	805	12,420	0.96
3-HO Py-NO	795	12,580	0.37
4-HO Py-NO	*	*	0.33
2-Et Py-NO	763	13,100	0.32
3-Et Py-NO	810	12,350	0.46
4-Et Py-NO	820	12,200	0.59
2,4-$(CH_3)_2$ Py-NO	765	13,070	0.37
QNO	733	13,640	0.33
4-(CH_3) QNO	750	13,330	0.40
IQNO	810	12,350	0.51

* Not available

1.6.2. Nickel and Cobalt Complexes

There have been several detailed reports[71,108,114,171-184] concerning complexes of pyridine N-oxide with nickel(II) and cobalt(II). No coordination complexes of cobalt(III) containing a pyridine N-oxide donor has been reported.

Infrared studies[72,114,172] and other data presented in the literature have shown that pyridine N-oxide forms hexakis-coordinated nickel(II) and/or cobalt(II) species, $[M(Py\text{-}NO)_6]^{2+}$ not only in the presence of such poorly coordinating anions as perchlorate ion,[71,108,172] but also with better coordinating agents such as nitrate ion,[114] chloride ion,[71,173] bromide ion,[71,115,173] and iodide ion.[71,115] The ease of formation of hexakis-coordinated nickel(II) and cobalt(II) complexes with pyridine N-oxide is in marked contrast to the coordination tendencies of pyridine, which has been shown to form tetragonal nickel(II)[174,175] and cobalt(II)[176] complexes $[M(Py)_4]X_2$ in the solid state and to form $[M(Py)_6]^{2+}\ X_2^-$ (M = Co(II), Ni(II); X = ClO_4, BF_4) only in solution. The complex $[Ni(4\text{-}NO_2\ Py\text{-}NO)_6]Cl_2$ appears to be the only one in the literature involving a hexakis-coordinated substituted pyridine N-oxide Ni(II) halide.[103]

With sterically hindered pyridine N-oxides, complexes of the form $[ML_n]^{2+}$ $(n < 6)$ are also obtained provided the right environmental conditions exist during their preparation. A five coordinate complex of 2-picoline N-oxide with $Co(ClO_4)_2$ is reported.[177] The complex $[Co(2\text{-}(CH_3)\text{-}Py\text{-}NO)_5](ClO_4)_2$ has, according to x-ray crystallographic data, a slightly distorted bipyramidal structure.[138] Tetra-coordinated Co(II) and Ni(II) perchlorate complexes are only obtained when positions 2- and/or 6 of the pyridine N-oxide are occupied. The complexes $[Co(2,6\text{-}(CH_3)_2\ Py\text{-}NO)_4](ClO_4)_2$, $[Ni(2,6\text{-}(CH_3)_2\ Py\text{-}NO)_4](ClO_4)_2$ and $[Ni(2\text{-}CH_3\ Py\text{-}NO)_4(ClO_4)_2$ are all tetra-coordinate, having approximately square planar structures.[157,158,165]

Besides forming hexakis-coordinated Co(II) and Ni(II) complexes, the halides and nitrates of these metals form a wide variety of complexes with aromatic N-oxides. Ni(II) complexes of the form NiL_5I_2 (L = 2- or 4-picoline N-oxide) are reported.[178] The red complex $Ni(Py\text{-}NO)_4I_2$ was obtained[179] by heating the yellow $[Ni(Py\text{-}NO)_6]I_2$ at 100°C. 3:1 complexes have been reported for Co(II) halides. The bromide and the chloride 3:1 Co(II) complexes[173] are of the type $[Co(Py\text{-}NO)_6][CoX_4]$. 2:1 and 1:1 N-oxide Co(II) and Ni(II) halide aromatic N-oxide complexes are numerous and a large number of them are obtained in the form of hydrates, or alcoholates.[178,180] Magnetic (μ_{eff} = 4.50 - 4.54B.M.) and spectral properties are in favor of tetrahedral structures for CoL_2X_2 (L = Py-NO, 2-CH_3 Py-NO, 2,4-$(CH_3)_2$-Py-NO, 2,6-$(CH_3)_2$ Py-NO, 2,4,6-$(CH_3)_3$ Py-NO; X = Cl, Br, I) complexes.[117,178,181] NiL_2X_2 (L = Py-NO, X = Cl, Br; L = 2,6-$(CH_3)_2$ Py-NO, X = Br) complexes exhibit electronic spectra and magnetic moments suggestive of hexacoordinated, polynuclear structures.[178] Complexes of aromatic N-oxides with Co(II) and Ni(II) halides, involving 1:1 M to L ratio, may be obtained by utilizing triethyl orthoformate as reaction medium.[182,183] or by heating ML_2X_2 or $MLX_2.nH_2O$ complexes[178,184] and are, in general, bi- or polynuclear.[178,182,184]

A few Ni(II) and Co(II) sulphate complexes with aromatic N-oxides were reported.[104] These complexes are formulated as follows: $[Co(2,6\text{-}(CH_3)_2\ Py\text{-}NO)(OH_2)_5](SO_4)$; $[2,6\text{-}(CH_3)_2\text{-}Py\text{-}NO)(O_2SO_2)Ni(2,6\text{-}(CH_3)_2\ Py\text{-}NO)_2Ni(O_2SO_2)(2,6\text{-}(CH_3)_2\text{-}Py\text{-}NO)]$ and are binuclear pentacoordinated 2,6-lutidine N-oxide bridged, with chelating bidentate sulphate ligands.[104]

Complexes of pyridine N-oxide and quinoline N-oxide with $[M(NCS)_2]$ acceptors (M = Co, Ni) are also reported.[171] Among the structural types identified are, the octahedral monomeric $[Co(Py\text{-}NO)_4(NCS)_2]$ and octahedral pseudohalide bridged $[Co(Py\text{-}NO)_2\text{-}(NCS)_2]$ complexes. The Ni(II) pyridine N-oxide complexes contain coordinated water or ethanol, but the quinoline N-oxide complexes do not. Complexes formed by interaction of excess 2,6-lutidine N-

oxide with Ni(II) and Co(II) thiocyanates are characterized as follows: $[L_2(SCN)M(NCS)_2M(NCS)L_2]$ (M = Co, Ni; L = 2,6-lutidine N-oxide), involving pentacoordinated dimers with terminal isothiocyanato as well as bridging NCS groups.[166]

1.6.3. Copper(II) Complexes

A variety of complexes may be formed between aromatic N-oxides and copper(II) compounds. Pyridine N-oxide reacts with copper(II) perchlorate to give a yellow-green hexakis - or a blue green tetrakis (Py-NO)copper(II) salt.[107,108] Often the tetrakis compound is deposited initially from solutions of the appropriate mole ratio of ligand to metal ion, but when allowed to stand in the presence of excess ligand, the initially precipitated blue-green solid becomes more yellow in color. Copper(II) salts of anions more basic than perchlorate react with pyridine N-oxide and many of its derivatives giving rise to lower ligand to metal ratios. By far the most extensively studied are the cupric halide complexes.

Cupric halide complexes with aromatic N-oxides could be classified as (a) low and normal magnetic moment dimeric 1:1 complexes, (b) normal and low magnetic moment 1:2 dimeric complexes, (c) trans and distorted cis 1:2 monomeric complexes with normal magnetic moments, (d) polymeric complexes, (e) adducts of the above.

(a) Low and normal magnetic moment dimeric 1:1 complexes

On the basis of low magnetic moments observed at room temperature and a marked temperature dependence of the magnetic susceptibility,[107,113] the $CuLX_2$ type compounds were assigned a bi- or polynuclear structure. Complete x-ray examination of single crystals[130,134,185] confirmed the proposed structure for the complex with pyridine N-oxide. The latest refinement of the crystal structure of $[Cu(Py\text{-}NO)Cl_2]_2$ showed that the dimeric molecule consists of two distorted tetrahedra sharing an edge, with the oxygen atoms of the pyridine N-oxide ligands acting as bridging units. The

dimers are held together by weak chloride bridges,[185] the copper-copper and oxygen-oxygen intermolecular distances are 3.25Å and 2.4Å respectively (Fig. 2). However ^{35}Cl NQR studies

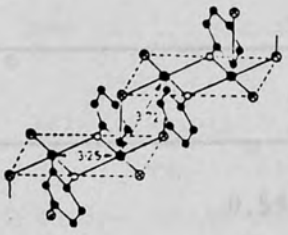

Fig. 2. The structure of $[Cu(Py\text{-}NO)Cl_2]_2$. Reported Cu-Cu distances in Å. Dotted lines define idealised planes of coordination.

and the infrared data raise some doubts on the conclusions reached above and suggest that chloride bridging between adjacent dimers does not occur.[186,187]

The magnetic data of these complexes reflect considerable spin-spin interaction between unpaired electrons on adjacent copper ions.[71,107,112-114,167-170,188,189] A superexchange mechanism operating through the bridging N-oxide oxygen atom has been suggested to account for the low magnetic moments.[37] The temperature dependence of the paramagnetism of complexes of these types was established during a number of studies;[37,112,188,190-192] μ_{eff} is generally subnormal in the 80 - 350 K region. The μ_{eff}

of a number of copper(II) halide complexes of pyridine N-oxides which are of particular relevance to the present work are given in table 2. The marked temperature dependence of the magnetic moments of these complexes indicates that below 195 K the triplet state was in most cases not appreciably populated.[37,193]

Table 2

Magnetic moments of 1:1 Cu(II) halide aromatic N-oxide complexes. (ref. 193)

Compound	μ, B.M.*
$[(Py\text{-}NO)CuCl_2]_2$	0.59, 1.06, 0.63
$[(2\text{-}CH_3\ Py\text{-}NO)CuCl_2]_2$	...
$[(3\text{-}CH_3\ Py\text{-}NO)CuCl_2]_2$	0.55, 0.97
$[(2,6\text{-}(CH_3)_2\ Py\text{-}NO)CuCl_2]_2$	0.68, 0.22
$[(2,4,6\text{-}(CH_3)_3\ Py\text{-}NO)CuCl_2]_2$	0.63
$[(4\text{-}Cl\text{-}Py\text{-}NO)CuCl_2]_2$	0.58, 0.28
$[(4\text{-}CN\text{-}Py\text{-}NO)CuCl_2]_2$	0.36
$[(4\text{-}NO_2\text{-}Py\text{-}NO)CuCl_2]_2$	1.01, 1.20. 0.95
$[(QNO)CuCl_2]_2$	0, 0.36
$[(Py\text{-}NO)CuBr_2]_2$	0.24, 0.65
$[(2\text{-}CH_3\ Py\text{-}NO)CuBr_2]_2$	...
$[3\text{-}CH_3\ Py\text{-}NO)CuBr_2]_2$	0.80
$[(2,6\text{-}(CH_3)_2\ Py\text{-}NO)CuBr_2]_2$	0.65, 0.40
$[2,4,6\text{-}(CH_3)_3\ Py\text{-}NO)CuBr_2]_2$	0.60
$[4\text{-}Cl\ PyNO)CuBr_2]_2$	0.23, 0.48
$[(4\text{-}CN\ Py\text{-}NO)CuBr_2]_2$	0.79
$[4\text{-}NO_2\ Py\text{-}NO)CuBr_2]_2$	1.77, 0.45
$[(QNO)CuBr_2]_2$	0, 0.40
$[(3\text{-}NO_2\text{-}6\text{-}CH_3\ QNO)CuBr_2]_2$	1.72

* Different values of magnetic moments are taken from different references which could be found in ref. 193

The magnetic susceptibility of Cu(II) ions in these binuclear complexes can be fitted to an equation which is derived from a simple scalar interaction of the form $-2J_{ij}S_i.S_j$. For a binuclear complex the exchange energy J is the separation between the singlet and triplet states generated by the scalar interaction. The interaction is usually antiferromagnetic and the ground state is the singlet.[190] It should be noted that Hyde et al. obtained a better fit of magnetic susceptibility and e.s.r data for the $[Cu(Py\text{-}NO)Cl_2]_2$ complex by assuming the presence of small amounts of monomeric $Cu(Py\text{-}NO)Cl_2$ species in their samples.[191]

The mechanism of superexchange in 1:1 complexes has been the subject of speculation. Watson et al. pointed out the normal length of the Cu-O bridge bonds and preferred a π-mechanism which might be influenced by the close proximity of the bridging oxygen atoms (2.5Å).[130] Muto et al. suggested the following two pathways; one which is a π-type and the other a σ-type pathway (Figs. 3a, 3b). The σ-pathway was preferred because of the

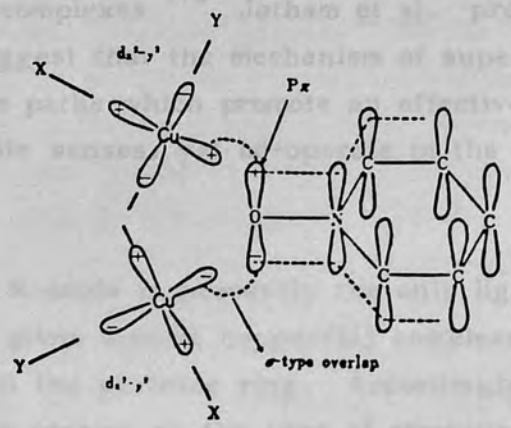

Fig. 3a. Electron exchange pathway of σ-type.

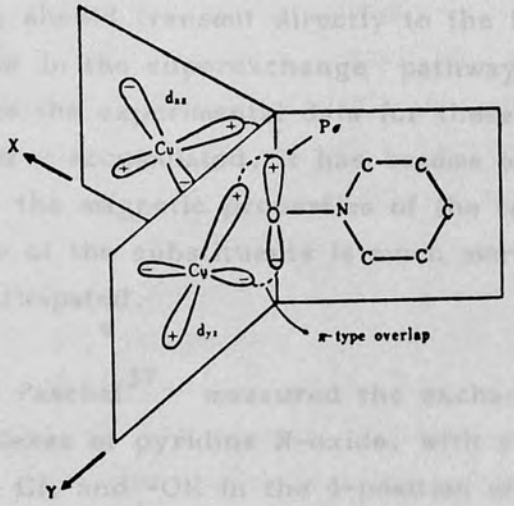

Fig. 3b. Electron exchange pathway of π-type.

intrinsically larger metal-ligand overlap integrals and because of the clear correlation between magnetic moments and d-d band maxima in these complexes.[170] Jotham et al. prefer the latter approach and suggest that the mechanism of superexchange is dominated by two paths which promote an effective metal-metal overlap in opposite senses, yet co-operate in the antiferromagnetic process.[194]

Pyridine N-oxide is presently the only ligand which is monodentate and gives dimeric copper(II) complexes with a variety of substituents on the pyridine ring. Accordingly extensive studies have been carried on the type of compounds because (1) pyridine N-oxide is a monodentate ligand, and its coordinate bond to the metal ion is not involved in any other metal ligand

bond (this eliminates the possible complexity in the demagnetization mechanism which may occur if a similar coordinate bond were part of a chelate ring); (2) the electronic effect of the substituents on the pyridine ring should transmit directly to the N-oxide oxygen atom which is in the superexchange pathway Cu - O - Cu. However as the experimental data for these pyridine N-oxide complexes have accumulated, it has become obvious that the relation between the magnetic properties of the complexes and the electronic nature of the substituents is much more complex than was initially anticipated.

Hatfield and Paschal[37] measured the exchange energies for a series of complexes of pyridine N-oxide, with substituents of $-NO_2$, -H, $-CH_3$, Cl, and -OH in the 4-position of the pyridine ring, with either copper chloride or copper bromide and reported a correlation with the substituent parameter σ_R. Kato et al. investigated a more extensive series of complexes and reported no correlation of the magnetic moments with any σ value;[167-170] however, they did report a correlation between an electronic absorption band in the region 10,000 - 14,000cm^{-1} and the room temperature magnetic moments. This correlation would imply a proportionality between the first excited singlet state and the low-lying triplet state which arises owing to the scalar coupling interaction. This would imply that the factors which affect the electronic energy levels also affect the superexchange mechanism. Changes in the geometrical distribution of ligands around the copper ion change the crystal field and shift the energy-levels. Changes in geometry may arise from the inter- and intramolecular interactions. A change in the crystal field strength of a ligand also affects the energy levels. The crystal field strength of the aromatic N-oxide ligands may be modified by the addition of substituents to the pyridine ring. This may directly change the dipolar nature of the N-O bond, or it may exert its influence through a back-π-bonding mechanism.

The influence of halide ions on the d-d band position and the demagnetization in the chloro and bromo complexes is quite

interesting because in general, it is not what would be expected from the positions of these ions in the spectrochemical series. In almost all cases, the magnetic moments of bromo complexes are smaller than those of the corresponding chloro complexes (Table 2). Hatfield and coworkers[195] suggested that this phenomenon may be due to the difference in spin-orbit coupling and temperature independent paramagnetism between chloro and bromo complexes. Kato et al.[168] suggested that the difference in nephelauxetic effects of the chloride and bromide ions produces such differences in magnetic moments. The greater cloud expanding effect of the bromide ions will produce a greater overlapping of the relevant orbitals of the metal ions and the ligand molecules. This would give greater covalency in their bonds and should give smaller magnetic moments for the bromo complexes. Figgis and Nyholm summarized the contributions of the temperature independent paramagnetism and the spin-orbit coupling in metal complexes.[196,197] With a few exceptions, the d-d bands of bromo complexes with pyridine N-oxides appear at higher wavenumbers than those of the corresponding chloro complexes. The ligand fields of these bromo complexes are larger than those of the chloro complexes suggesting smaller contribution to spin-orbit coupling. Some workers have reported the anomalous behaviour of certain dimeric copper(II) halide complexes[198-200] which could be explained by the concept of softness and hardness of metal ions and ligands.[170]

A number of chloro or nitro substituted quinoline and methyl quinoline N-oxides form magnetically normal 1:1 complexes with Cu(II) halides[113,192,201,202] (e.g. $[Cu(4\text{-}NO_2\text{-}QNO)Cl_2]_2$ with μ_{eff} = 1.98 B.M. at 4.2 K, and 2.08 B.M. at 299 K.[202] The magnetic behaviour of the latter complexes was attributed to halide-bridged dimeric structures by Hatfield and co-workers;[186] while Muto and Jonassen assumed oxygen-bridged structures for these complexes and interpreted their normal paramagnetism in terms of the electron-withdrawing effect of the nitro or chloro substituent on the bridging oxygens.[113]

(b) Normal and Low magnetic moment 1:2 dimeric complexes

1:2 N-oxide-cupric halide complexes are, in most cases, monomeric and magnetically normal. However, a few complexes of this type are binuclear and have subnormal magnetic moments. The structure of dichlorobis(pyridine N-oxide)copper(II) has been reported.[193] The complex may be considered as a pyridine N-oxide adduct of the 1:1 complex. The copper(II) ions are pentacoordinate with the extra pyridine N-oxide ligands lying trans to the plane of the joined bases. Two N-O stretching frequencies are observed in the infrared spectrum, indicative of the two types of N-oxide coordination with the lower frequency being associated with the bridged ligand. Dimeric dibromobis-(pyridine N-oxide)copper(II) was cited as probably belonging to the same structure type as the chloride analogue and as having a larger magnetic moment than the chloride analogue. This result was unexpected, for in the 1:1 series of pyridine N-oxide complexes bromides exhibit smaller room-temperature moments. The x-ray crystallographic results showed that the structures of the bromide and chloride complexes differ significantly, even though the structural unit is a penta-coordinated dimer and the copper-copper distances are about the same in both cases.[144] The principal difference between the two complexes is the orientation of the bridging plane with respect to the $Cu(halogen)_2$ groups, In the chloride dimer the chlorine, copper, and bridging oxygen atoms lie approximately in a plane, and the non-bridging oxygen atoms lie above and below this plane. The structure of the bromide complex consists of two centrosymmetric dimeric molecules crystallographically non-equivalent. In both dimers each copper atom is coordinated by two bromine atoms, and by three oxygen atoms of which two are bridging. The bromine atoms are located above and below the plane defined by the copper atoms and the bridging oxygen atoms (Figs. 4a, 4b). Therefore, for the bromide dimer to fit the structure type of the chloride dimer, the plane of the copper and bridging oxygen atoms

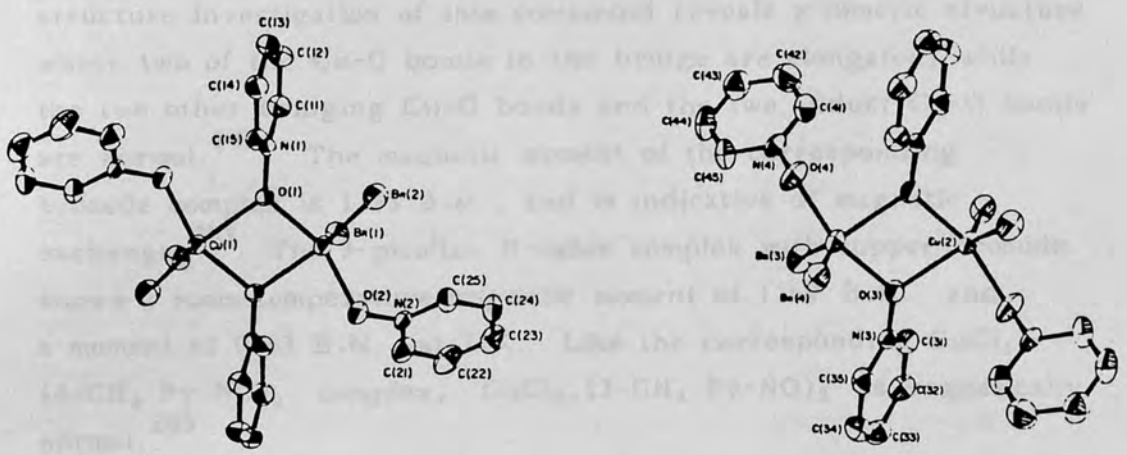

(a) (b)

Fig. 4. A view of dimer (a) and dimer (b) of dibromobis(pyridine N-oxide)-copper(II) (ref. 144).

would have to be rotated by 90° with respect to the rest of the structure.

The magnetic moment of the bromide complex (1.4 B.M.)[195] is intermediate between the value reported for the dimeric 1:2 nitrate complex (1.88 B.M.)[203] and the values reported for the chloride complex (0.46 B.M.).[195] Watson ascribed the difference in the magnetic moments of the latter two compounds to a different spacial relationship between adjacent interacting orbitals.[193] Mighell et al. gave a different explanation for the rather high magnetic moment of the bromide complex, and developed an indirect relationship between the magnetic properties of the bromide, chloride and nitrate complexes, by showing that the configuration of the bromide dimers is intermediate between two hypothetical structures postulated on the basis of two different directions of the weak bonding.[144]

Another interesting 1:2 dimeric complex is the magnetically normal dichlorobis(4-picoline N-oxide)copper(II). The crystal structure investigation of this compound reveals a dimeric structure where two of the Cu-O bonds in the bridge are elongated, while the two other bridging Cu-O bonds and the two adduct Cu-O bonds are normal.[193] The magnetic moment of the corresponding bromide complex is 1.33 B.M., and is indicative of magnetic exchange.[203] The 3-picoline N-oxide complex with copper bromide shows a room-temperature magnetic moment of 1.69 B.M. and a moment of 0.63 B.M. at 77K. Like the corresponding $CuCl_2.(4\text{-}CH_3\ Py\text{-}NO)_2$ complex, $CuCl_2.(3\text{-}CH_3\ Py\text{-}NO)_2$ is magnetically normal.[203]

(c) Trans and distorted cis 1:2 monomeric complexes with normal magnetic moments

Magnetically normal 1:2 N-oxide-copper(II) halide complexes may be obtained in two crystalline modifications (a third modification is the dimeric, N-oxide-bridged structure). Green monomeric $CuX_2.L_2$ complexes (e.g. L = 4-picoline N-oxide, X = Cl) have trans square planar geometry,[204] while yellow isomers (e.g. L = 2,6-lutidine N-oxide, X = Cl) have a distorted geometry, which is intermediate between cis square planar and tetrahedral.[193] The structure of the latter may be approximated by rotating two cis ligands by 45° about an axis bisecting them and passing through the copper atom or by rotating two tetrahedral ligands by 45° around an axis bisecting them and passing through the copper atom.[130] Watson has postulated the following mechanism for the formation of the two isomers. The 1:2 dimeric-complex is initially formed, which either crystalizes or dissociates to the cis distorted monomer. The monomer rapidly isomerizes to the thermodynamically more stable trans form.[193]

(d) Polymeric complexes

Polybis(μ-(2-picoline N-oxide)-chlorocopper(II)di-μ-chloro)-

diaquocopper, $Cu_3Cl_6(2\text{-}CH_3\ Py\text{-}NO)_2.2H_2O$, is an exceptional compound (2:3 complex). From the magnetic properties and crystallographic analysis of this compound, it was confirmed by Watson et al. that the structure of this complex consists of infinite linear chains containing both five and six-coordinateed copper(II) ions bridged by either chlorine or oxygen atoms. The structure can be regarded as an alternating linear chain consisting of $Cu_2Cl_4(2\text{-}CH_3\ Py\text{-}NO)_2$ units and $CuCl_2.2H_2O$ units joined by long Cu-Cl bonds. The same authors also proposed that the copper ions in the $Cu_2Cl_4(2\text{-}CH_3\ Py\text{-}NO)_2$ unit interact antiferromagnetically through the bridging oxygens, while the copper ions in $CuCl_2.2H_2O$ do not interact with those of the $Cu_2Cl_4(2\text{-}CH_3\ Py\text{-}NO)_2$ units through the bridging chlorine atoms (Fig. 5). Miyoshi et al. performed magnetic susceptibility and ESR measurements and confirmed the structure proposed by Watson et al. The half-field resonance near 1600 Oe in the ESR spectrum of the powder sample was assigned to the $\Delta M = \pm 2$ forbidden transition arising from the existence of the dimer species $Cu_2Cl_4(2\text{-}CH_3\ Py\text{-}NO)_2$, while the resonance at 3250 Oe was assigned to $\Delta M = \pm 1$ transition arising from magnetically isolated copper ions in the $CuCl_2.2H_2O$.[205]

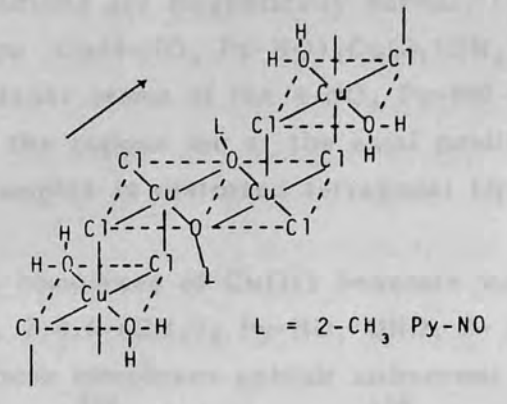

Fig. 5. Schematic crystal structure of $Cu_3Cl_6(2\text{-}CH_3\text{-}Py\text{-}NO)_2.2H_2O$. The arrow shows the c-axis direction (ref. 205).

Although the polymeric $Cu_3Cl_6(2\text{-}CH_3\ Py\text{-}NO)_2.2H_2O$ complex exhibits low magnetic moments,[132,193] several $Cu_3Cl_6L_2$ (L = 4-Cl-QNO, 4-Cl 6-CH_3-QNO) and $Cu_4Cl_8L_3$ (L = 3-NO_2-6-CH_3-QNO) complexes are magnetically normal.[192] These complexes are most probably characterised by chlorine- rather than N-oxide- bridges.

(e) Adducts of 1:1 and 1:2 complexes

Adducts are readily formed between 1:1 complexes of aromatic N-oxides and DMF, DMSO, H_2O and CH_3OH. These complexes exhibit magnetic moments similar to their parent complexes indicating that the solvent molecule does not affect significantly the orbital containing the magnetic electron. Watson has ascribed this property to the fact that magnetic electrons are localised within the plane of the bridge, and proposed a pentacoordinate trans-substituted dimeric structure, because a six coordinate structure achieved via bridging halogens would not be favoured by the steric requirements of these complexes especially if the ortho position of the ring is substituted.[193]

As in the case of with 1:1 analogues, monomeric 1:2 N-oxide-Cu(II) halide complexes may form adducts with neutral ligands; these adducts are magnetically normal.[193] A monomeric adduct of this type $Cu(4\text{-}NO_2\ Py\text{-}NO)_2CuCl_2(OH_2)_2$, consists of trans square planar atoms of the 4-NO_2 Py-NO molecules loosely bonded to the copper ion at the axial positions; the geometry of the complex is distorted tetragonal bipyramidal.

A series of 1:2 complexes of Cu(II) benzoate with N-oxides (Py-NO, 2-CH_3 Py-NO, 2,4,6-$(CH_3)_3$ Py-NO, QNO, 2- and 4-CH_3-QNO) are reported; these complexes exhibit subnormal magnetic moments (1.38 - 1.42 B.M.).[206] Cu(II) acetate[195] and salicylate analogues are also magnetically subnormal, while bis-(salicylato)-bis(Py-NO)-Cu(II) shows μ_{eff} of 1.95 B.M.[207]

Nelson et al.[208] have investigated the influence of trans-axial ligation of 4-substituted pyridine N-oxides on the metal-metal

bond formation in copper(II) acetate complexes, where they have established that the dimeric copper carboxylate structure is preserved. The results obtained are interesting because in this series of ligands, 4Z-Py-NO (Z = CH_3O, CH_3, H, Cl, NO_2), the basicities span 4 orders of magnitude while maintaining constant steric effects at the donor site. The magnetic data and the d_{xz}, $d_{yz} \longrightarrow d_{x^2-y^2}$ transition (corresponding to δ bond model in the dimer) in the visible spectra are summarised in table 3. The magnetic moment of 0.92 B.M. for the 4-nitropyridine N-oxide complex is the lowest value yet reported for copper acetates.[209] Examination of the values reported in the table clearly reveals (a) that the magnetic moments of the complexes decrease as the bacisity decreases and as the π-acceptor ability of the ligand increases (b) the energy of the band in the visible spectra increases as the magnetic susceptibility decreases and the basicity of the ligand decreases. Therefore, it is concluded that pyridine N-oxides with relatively low basicities and high π-acceptor abilities enhance copper-copper bonding and that high π-acceptor ability seems to be significantly more effective than weak σ-donation in promoting copper-copper bonding for pyridine N-oxides.

The results obtained for the copper(II) acetate complexes are in line with the results obtained by Muto et al.[167] for the 1:1 dimeric copper(II) halide complexes with 3- and 4- substituted pyridine N-oxides, because in both investigations the greatest demagnetisation of the complexes and the highest energy for the lowest band in the electronic spectra correspond to the complex containing the strongest electron-withdrawing substituent on the pyridine N-oxide, however, the approach to the problem by these two groups is different. Nelson et al. interprete their results in terms of enhanced π-back bonding in the copper(II) acetate series, while Muto et al. interprete their results for 1:1 dimeric copper(II) halides in terms of the change in spacial arrangement of the metal and ligand orbitals due to the effect of substituents on the pyridine N-oxide ring. Therefore it would be very interesting to find out if there is a link between these two approaches.

Table 3.

Electronic Spectral and Magnetic Data for the Complexes $[Cu(AcO)_2.4\text{-}Z\text{-}Py\text{-}NO]_2$

Z	$10^6\chi_{m'}$ (c.g.s.u.) *	μ_{eff} B.M.	Band I (cm^{-1})
CH_3O	950 ± 10	1.46 ± 0.02	13,590
CH_3	782 ± 40	1.37 ± 0.03	13,610
H	790 ± 50	1.37 ± 0.03	13,930
Cl	829 ± 50	1.41 ± 0.01	13,910
NO_2	360 ± 35	0.92 ± 0.02	14,690
H_2O*	891 ± 7	1.408 ± 0.007	——
H_2O**	889	1.40	——

* Data taken from reference 208, measured at 295.3 K. ** Data taken from reference 210, measured at 294.2 K

1.6.4. Cadmium(II) Complexes

Cd(II) perchlorates and tetrafluoroborates yield $[ML_6]^{2+}$ hexacoordinated cationic complexes with pyridine N-oxides.[119,211] Cd(II) halides form complexes of the following types: CdI_2L_2 (L = N-oxide), CdX_2L, $CdX_2L(OH_2)$ (X = Cl, Br, I), $Cd_3Cl_6L_2$, and $Cd_4Cl_8L_2$ (refs. 212 - 216). Based upon the observation of two metal-halogen stretching frequencies in the far infrared spectra CdI_2L_2 complexes are assigned monomeric tetrahedral structures, assuming C_{2v} symmetry.[214] Although the possibility of N-oxide bridging in the binuclear 1:1 complexes was discussed [211] the authors favour halogen bridged structures. Schmauss et al.[212] proposed tetrahedral polymeric structures of the form

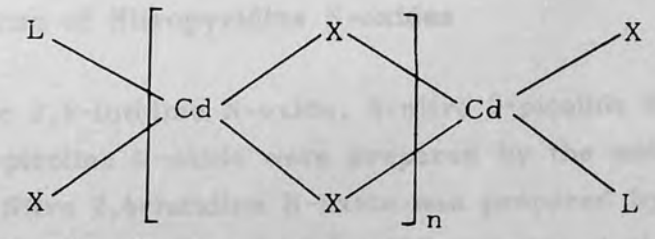

with n = 1 - 3

for CdX_2L, $Cd_3Cl_6L_2$ and $Cd_4Cl_8L_2$ complexes and found that the Cd-O bond order falls with steric hindrance near the donor site of the N-oxides. Crystal structure determination of the CdI_2Py-NO complex established that this compound is composed of infinite chains with units of Cd alternatively bridged through two iodine atoms and two oxygen atoms in an environment of pentacoordinated Cd atoms corresponding largely to a trigonal bipyramid array.[217]

Other Cd(II) complexes reported are $[Cd(NCS)_2L]_n$ (L = Py-NO, 2- 3- and 4-CH_3-Py-NO, 2,6-$(CH_3)_2$-Py-NO) involving bridging thiocyanato ligands,[166] and $Cd(ONO_2)_2$-$(2,6\text{-}(CH_3)_2\text{-Py-NO})_4$, with monodentate nitrato ligands.[218]

CHAPTER 2

EXPERIMENTAL PROCEDURES

2.1. Materials

2-Picoline N-oxide, 3-picoline N-oxide, and 2,6-lutidine-N-oxide were obtained commercially (Aldrich Chemicals). Reagent grade solvents and metal salts were used without further purification.

2.2. Preparation of Nitropyridine N-oxides

4-Nitro 2,6-lutidine N-oxide, 4-nitro 2-picoline N-oxide and 4-nitro 3-picoline N-oxide were prepared by the method of Ochiai.[22] 3-Nitro 2,6-lutidine N-oxide was prepared by first nitrating 2,6-lutidine as described by Achremowics et al.[219] and then oxidised by the method of Brown and Neil.[220] The melting points of the nitropyridine N-oxides so prepared, were consistent with the reported values. Attempts to prepare 2-nitropyridine N-oxides by the oxidation of 2-aminopyridine and its homologs were not successful as it involved the use of 40% peracetic acid[221] which was not commercially available. The 40% peracetic acid available in the department proved to be too old and did not give the expected result.

2.3. Physical Measurements

Infrared spectra in the range 600 - 180 cm^{-1} were

recorded with a Perkin-Elmer 983 spectrometer using samples as Nujol mulls supported between polyethylene discs. Raman spectra, using laser beams, were recorded on a Coderg Type PHl spectrometer attached to a Tektron IX computer. The laser beams were generated by a Coherent Radiation Model 52 Regulated DC Ion Laser Power Supply instrument. Electronic spectra in various solvents were studied on a Unicam SP8-100 recording spectrometer. The instruments used, and the methods employed for the x-ray powder photographs, reflectance, n.m.r., e.s.r., infrared spectra (in the range 4000 - 600 cm^{-1}) and magnetic susceptibility studies were the same as described in part I of the present work.

2.2. Preparation of Cu(II) Halide Complexes

2.4.1. Preparation of 1:2 Complexes

$CuCl_2.(2\text{-}CH_3\ 4\text{-}NO_2\ Py\text{-}NO)_2$

This complex was prepared by mixing warm 1-butanol solutions of anhydrous $CuCl_2$ and the ligand in a 1:4 molar ratio. On standing for a few hours brown crystals precipitated. These were filtered, washed with 1-butanol, and dried in the air.

$CuCl_2.(2,6\text{-}(CH_3)_2\ 4\text{-}NO_2\ Py\text{-}NO)_2$,

$CuBr_2.(2,6\text{-}(CH_3)_2\ 4\text{-}NO_2\ Py\text{-}NO)_2$,

$CuCl_2.(2,6\text{-}(CH_3)_2\ 3\text{-}NO_2\ Py\text{-}NO)_2$,

$CuBr_2.(2,6\text{-}(CH_3)_2\ 3\text{-}NO_2\ Py\text{-}NO)_2$,

$CuBr_2.(2\text{-}CH_3\ 4\text{-}NO_2\ Py\text{-}NO)_2$

These complexes were prepared by adding a hot ethanol solution of the ligand to a hot solution of cupric chloride or bromide in

ethanol. The products crystallised immediately or after standing in ice and were filtered, dried in air and recrystallised from ethanol or 1-butanol. The $CuBr_2.L$ analogue could not be formed even when stoichiometric ratios of $L:CuBr_2$ of 1:10 was used. $CuBr_2.L_2$ was always obtained.

$CuCl_2.(3\text{-}CH_3\ 4\text{-}NO_2\ Py\text{-}NO)_2$ (yellow)

A hot concentrated solution of the ligand in ethanol was treated with a methanol solution of anhydrous $CuCl_2$ (metal to ligand molar ratio 1:4). On standing a few hours yellow crystals precipitated. These were filtered, washed with methanol and dried in a desiccator over $CaCl_2$.

$CuCl_2.(3\text{-}CH_3\ 4\text{-}NO_2\ Py\text{-}NO)_2$ (orange)

This complex was prepared by adding a warm 1-butanol solution of anhydrous $CuCl_2$ to a warm 1-butanol solution of the ligand in a 1:3 molar ratio. The orange crystals were collected by filtration, washed with cold 1-butanol, and placed in a desiccator for drying. Attempts to recrystallise these orange crystals from warm 1-butanol gave a mixture of yellow and orange crystals. When ethanol or methanol was used for recrystallisation purposes only the yellow isomer was obtained.

$CuBr_2.(2,6\text{-}(CH_3)_2\ 4\text{-}NO_2\ Py\text{-}NO)_2$ (dark brown)

The ligand was dissolved in a 9:1 mixture of ethanol and acetone, the solution was stirred at 50°C, and an excess of $CuBr_2$ (ligand to salt molar ratio 1:7) was then added. The solution was refluxed for 2 hours, during which period, a white precipitate was formed. Further addition of $CuBr_2$ resulted in more of the white precipitate, which was identified as CuBr. The solution was cooled to ca. 35°C and the white precipitate filtered off. Upon standing a few hours, dark, wine-

red, needle-like crystals precipitated. The crystals were filtered off, washed with cold acetone and dried in a desiccator. When ground, the color of the complex was dark brown.

2.4.2. Preparation of 1:1 Complexes

$CuCl_2.(2\text{-}CH_3\ 4\text{-}NO_2$ Py-NO), $CuCl_2.(3\text{-}CH_3\ 4\text{-}NO_2$ Py-NO)

A warm, concentrated ethanol solution of the ligand was added to a warm ethanol solution containing excess anhydrous $CuCl_2$. The precipitates were collected after standing for several minutes, and dried under vacuum.

$CuBr_2.(3\text{-}CH_3\ 4\text{-}NO_2$ Py-NO)

A warm 1-butanol solution of the ligand was added to a 1-butanol solution containing $CuBr_2$ in a 1:1 molar ratio. Shining wine red, flake-like crystals precipitated after a few minutes, which were filtered off and dried in a desiccator containing anhydrous $CaCl_2$. Several attempts were made to obtain complexes of other stoichiometries by varying the ligand-$CuBr_2$ ratio and using different solvents, but no other complexes could be isolated.

2.5. Preparation of Copper(II) Acetate Complexes

$Cu(AcO)_2.(3\text{-}CH_3\ 4\text{-}NO_2$ Py-NO) and $Cu(AcO)_2.(2,6\text{-}(CH_3)_2$ Py-NO)

A hot concentrated acetic acid solution of copper(II) acetate was treated with an acetic acid solution of the ligand (ligand to salt ratio 5:1). The resultant dark green solution

was evaporated by boiling to ca. one third. On standing overnight green crystals precipitated. These were filtered off, washed with a few drops of acetic acid, and dried in a desiccator. Several attempts were made to prepare copper(II) acetate complexes with other nitropyridine N-oxides studied in the present work, but no complexes could be isolated.

2.6. Preparation of Cadmium(II) Complexes

$CdCl_2.(4\text{-}NO_2\ Py\text{-}NO)_2$,

$CdCl_2.(3\text{-}CH_3\ 4\text{-}NO_2\ Py\text{-}NO)_2$,

$CdCl_2.(2\text{-}CH_3\ 4\text{-}NO_2\ Py\text{-}NO)$,

$CdCl_2.(2,6\text{-}(CH_3)_2\ 4\text{-}NO_2\ Py\text{-}NO)$,

$CdCl_2(2,6\text{-}(CH_3)_2\ 3\text{-}NO_2\ Py\text{-}NO)$

These complexes were prepared by allowing an excess of ligand to react with a hot solution of $CdCl_2$ in ethanol. The complexes which precipitated or crystallised out on stirring the mixture were suction filtered, washed with ethanol and dried in a desiccator.

$CdCl_2.(4\text{-}NO_2\ Py\text{-}NO)$

An ethanol solution of the ligand was added to a warm solution containing $CdCl_2$ in 1:1 molar ratio. A white precipitate formed after several hours. This was collected and dried in the air. 4-Nitro 3-picoline N-oxide did not yield a 1:1 complex even when excess $CdCl_2$ was used.

CHAPTER 3

RESULTS AND DISCUSSION

3.1. Carbon-13 N.M.R. Results

Natural abundance carbon-13 n.m.r. spectra were recorded using $CDCl_3$ as solvent. More polar solvents were avoided because of the reported substantial solvent effects on carbon-13 chemical shifts and carbon-hydrogen coupling constants.[222] $CDCl_3$ also provided the signal for an internal deuterium field-frequency lock. Chemical shifts were obtained by using Me_4Si as an internal chemical shift standard. Proton coupled spectra were recorded as an aid in signal assignment. An additional assignment aid was realised by the observation that the signals from C-2 and the carbon atom containing the nitro group were slightly broadened because of ^{14}N-^{13}C coupling and nitrogen quadrupolar interaction. The spectra were recorded at room temperature.

The chemical shifts for the pyridine N-oxides are given in Table 4. In order to gain more insight into the effects of the $-NO_2$ group, the carbon-13 chemical shifts of the 3- and 4-nitro substituted pyridine N-oxides were compared to those of the corresponding substituted pyridine N-oxides. The carbon chemical shift differences, $\Delta\delta$, so obtained are given in Table 5.

The carbon-13 n.m.r. spectra of 4-nitropyridine N-oxide is previously reported.[80] The observed deshielding at the 4-position of the ring is interpreted by considering the substantial contribution from resonance form (XVI) to the hybrid which characterises 4-nitropyridine N-oxide The proposed quinoidal nature of this molecule is consistent with the x-ray crystallographic

Table 4. Carbon-13 Chemical Shifts for Substituted Pyridine N-oxides*

Substituents X	No.	δC^{13}					
		C-2	C-3	C-4	C-5	C-6	Me
H**	1	138.2	125.3	124.8	125.3	138.2	
4-NO_2**	1'	140.1	120.7	142.0	120.7	140.1	
2-CH_3**	2	148.5	125.0	126.1	123.1	138.8	17.2
2-CH_3 4-NO_2	2'	150.87	120.83	142.22	118.29	140.27	18.01
3-CH_3	3	138.92	136.74	127.22	125.37	136.26	18.19
3-CH_3 4-NO_2	3'	141.77	133.05	143.52	122.06	137.93	18.08
2,6-$(CH_3)_2$	4	147.02	122.701	122.51	122.701	147.02	16.64
2,6-$(CH_3)_2$ 4-NO_2	4'	150.35	117.97	140.92	117.97	150.35	18.53
2,6-$(CH_3)_2$ 3-NO_2	4''	149.25	156.20	122.78	120.18	148.19	6-Me = 18.92 2-Me = 14.57

* Chemical shifts are in ppm and were obtained by using Me_4Si as an internal chemical shift standard.
** Data taken from ref. 80.

Table 5. Effect of Nitro Substituent on the Carbon-13 Chemical Shifts

Compound	$\Delta\delta$*					
	C-2	C-3	C-4	C-5	C-6	Me
$\delta 1 - \delta 1'$	+1.9	-4.6	+17.2	-4.6	+1.9	
$\delta 2 - \delta 2'$	+2.37	-4.17	+16.12	-4.81	+1.47	+0.81
$\delta 3 - \delta 3'$	+2.85	-3.69	+16.3	-3.31	+1.67	-0.11
$\delta 4 - \delta 4'$	+3.33	-4.73	+18.41	-4.73	+3.33	+1.89
$\delta 4 - \delta 4''$	-2.23	+33.50	+0.27	-2.52	+1.17	6-Me= +2.28 2-Me= -2.07

* $\Delta\delta = \delta^{13}C$ (pyridine or methyl substituted pyridine N-oxide) - $\delta^{13}C$ (corresponding nitropyridine-N-oxide). A negative value indicates greater shielding in the nitropyridine N-oxide. Carbon-13 chemical shift differences, $\Delta\delta$, are in ppm.

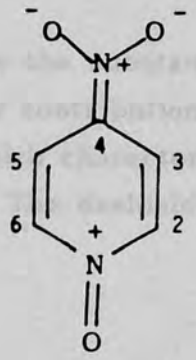

(XVI)

data,[27] which indicates that the length of the carbon-carbon bonds parallel to the molecular axis is much shorter than that of other carbon-carbon bonds.

Comparison of the Carbon-13 chemical shifts of 4-nitropyridine N-oxides with those of corresponding pyridine N-oxides revealed that, in general, the 4-nitropyridine N-oxides show a shielding effect (3.3 - 4.9ppm) at C-3 and C-5, a small deshielding effect at C-2, C-6 (1.47 - 3.33ppm), and very significant deshielding effect at C-4 (16.12 - 18.41ppm). Therefore, as in 4-nitropyridine N-oxide, the contribution of the resonance form (XVI) to the hybrid which characterises these 4-nitropyridine-N-oxides is important. Although non-bonded interaction between the N-O and C-2 - CH_3 methyl groups is reported to take place in these compounds,[223] the minor differences observed in the chemical shift difference $\Delta\delta$ could be explained if hyperconjugation of the methyl groups with the ring system is considered. Hyperconjugation of methyl groups in 4-nitropyridine N-oxides is expected to be more important than in the corresponding pyridine N-oxides, because in the former both the N-O and the NO_2 groups are electron-withdrawing in nature.

Although other factors are known to be important, increasing electron density at carbon is associated with a shielding effect and decreasing electron density with a deshielding effect.[224] The slight variation of $\delta 2 - \delta 2'$ in 4-nitro 2-picoline N-oxide relative to $\delta 1 - \delta 1'$ in 4-nitropyridine N-oxide (see Table 5)

could be explained if besides the substantial contribution of the resonance form (XVI), minor contribution from the resonance form (VIa) to the hybrid which characterises 4-nitro 2-picoline N-oxide (VI) is considered. The deshielding observed at the

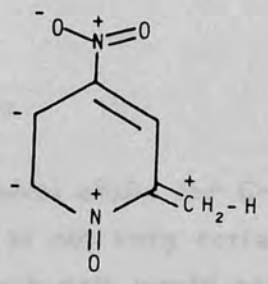

(VIa)

methyl carbon supports the above argument.

The small variation of $\delta 3 - \delta 3'$ in 4-nitro 3-picoline N-oxide (VII) relative to $\delta 1 - \delta 1'$ is probably a result of the slight twisted nature of the NO_2 group which is expected to weaken the contribution of the resonance form (XVI). The negligible shielding at the methyl carbon in 4-nitro 3-picoline N-oxide would imply that hyperconjugation is even less important in this compound than in 3-picoline N-oxide.

The increased shielding effect at C-3, C-5 and the increased deshielding effect at C-2, C-4, C-6 and the methyl carbons in 4-nitro 2,6-lutidine N-oxide (VIII) relative to 4-nitro pyridine N-oxide is probably the result of the contributions of canonical forms (VIIIa) and (VIIb).

Carbon-13 chemical shift data for 3-nitropyridine N-oxide were not available. Therefore the observed chemical shift differences $\delta 4 - 4\delta''$ in 3-nitro 2,6-lutidine N-oxide (IX) could not be included in the appropriate comparison.

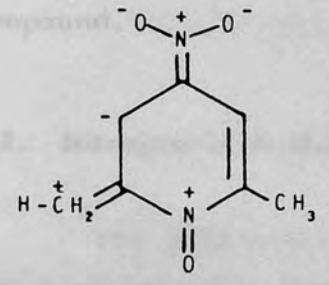

(VIIIa)

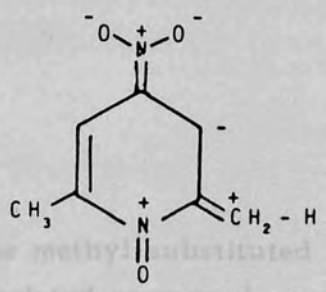

(VIIIb)

Assignment of the chemical shifts for C-4, C-5, and C-2, C-6, and the methyl carbons is not very certain; however, interchanging the chemical shifts in each pair would not result in significant difference in the chemical shift differences or the interpretation of the results. The observed chemical shift difference $\Delta\delta$ could best be explained if resonance forms (IXa and IXb) are considered to make a substantial contribution to the 3-nitro 2,6-lutidine N-oxide hybrid (IX). The observed significant deshielding, and hence, lower electron density, at the 3 position of 3-nitro-2.6-lutidine N-oxide implies that the NO_2 group is not in a twisted

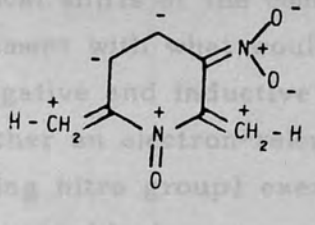

(IXa)

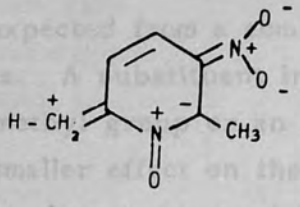

(IXb)

form in this compound as expected from consideration of steric effects imposed by the methyl group at 2 position. Therefore,

either a considerable change in bond angles, or non-bonded interaction between N-O and C-2 $-CH_3$ would be expected in this compound.

3.2. Nitrogen-14 N.M.R. Results

The N-14 n.m.r. spectra of the methyl substituted 3- and 4-nitropyridine N-oxides and the related compounds were recorded using acetone, methanol and chloroform as solvents. A trace amount of nitromethane served as internal standard. The chemical shifts obtained showed a substantial dependence on the solvent used (Tables 6a and 6b).

An investigation of the spectral data shows that the $-CH_3$ group, which exerts an overall electron releasing effect, results in a shift of N-14 signals to higher fields, and that the nitro group, which exerts an overall electron-withdrawing effect, gives a downfield N-14 shift relative to pyridine N-oxide and methyl substituted pyridine N-oxides.

Comparison of the N-14 chemical shifts of the compounds 1, 2, and 4 revealed that as the number of methyl groups in an ortho position to the ring nitrogen increases the N-14 signal shifts to higher fields. The same trend is also observed in the chemical shifts of the compounds 1', 2' and 4' and is in agreement with what would be expected from a combination of conjugative and inductive effects. A substituent in position 3 (either an electron-releasing methyl group or an electron withdrawing nitro group) exerts a smaller effect on the N-14 chemical shift, roughly in agreement with what is expected from a mainly inductive mechanism.

In order to assess the effect of the nitro group, the nitrogen-14 chemical shifts of the 3- and 4-nitro substituted pyridine N-oxides were compared to those of the corresponding parent compounds.

Table 6a. Nitrogen-14 NMR Results for 4-Nitropyridine-N-oxides and the Related Pyridine N-oxides

Substituents X	No.	Solvent	NO_2-N	N-oxide N
H**	1	Acetone satd.		+85 ± 1
		Chloroform satd.		+85 ± 1
		Methanol dil.***		+94 ± 1
4-NO_2	1'	Acetone satd.	+15.06	+70.71
		Chloroform satd.	+13.03	+70.16
		Methanol dil.***	+14.26	+71.30
2-CH_3	2	Acetone satd.		+85.52
		Chloroform satd.		+90.98
		Methanol dil.***		+98.11
2-CH_3 4-NO_2	2'	Acetone satd.	+15.19	+73.88
		Chloroform satd.	+11.77	+71.07
		Methanol satd.	+12.53	+74.10
3-CH_3	3	Acetone satd.**		+82.± 1
		Chloroform satd.		+88.01
		Methanol satd.**		+95 ± 2
3-CH_3 4- NO_2	3'	Acetone satd.	+13.01	+73.03
		Chloroform satd.	+19.78	+81.98
		Methanol satd.	+15.25	+80.43
2,6-$(CH_3)_2$	4	Chloroform satd.		+96.29
2,6-$(CH_3)_2$ 4-NO_2	4'	Acetone satd.	17.45	77.50
		Chloroform satd.	+11.32	+74.24

* Chemical shifts (ppm) referred to CH_3NO_2 as internal standard.

** Data taken from ref. 81. *** Saturated solution diluted twice.

Table 6b. Nitrogen-14 NMR Results for 3-Nitropyridine N-oxides

Substituents X	No.	Solvent	NO_2- N	N-oxide N
3-NO_2**	1''	Acetone satd.		+81 ± 1
		Chloroform satd.		+78 ± 2
		Methanol satd.		+90 ± 2
2,6-$(CH_3)_2$ 3-NO_2	4''	Acetone satd.	+9.31	+87.46
		Chloroform satd.	+6.33	+84.21
		Methanol satd.	+10.86	+94.16

** Data taken from ref. 81.

Table 7. Effect of Nitro Substituent at Positions 3- and 4- of the Pyridine N-oxides on the Nitrogen-14 Chemical Shifts

Compound	Δδ		
	Acetone	Chloroform	Methanol
1 - 1'	+14.29	+14.89	+22.70
1 - 1''	+4.00	+7.00	+4.00
2 - 2'	+11.64	+19.07	+24.01
3 - 3'	+8.97	+6.03	+14.53
4 - 4'		+22.05	
4 - 4''		+12.08	

The nitrogen chemical shift difference $\Delta\delta$, is given for each of the solvents used (Table 7). However, the most reliable results are expected in $CDCl_3$ because it is the least polar among the solvents used.

Due to the significant error inherent in the measurement of N-14 chemical shift, which sometimes can obscure substituent effects on the nitrogen resonance position, any quantitative comparison should be interpreted with caution. However, the data given in table 7 by and large can account for the gross structural changes in these compounds. In agreement with the carbon-13 n.m.r. results for the 4-nitro substituted pyridine N-oxides, the effect of the nitro group is the weakest in 4-nitro 3-picoline N-oxide confirming again the twisted nature of the nitro group. In the 3-nitro substituted pyridine N-oxides, the nitro group in 3-nitro 2,6-lutidine N-oxide is more effective in delocalising electron charge density away from the ring nitrogen than in 3-nitro-pyridine N-oxide, also in agreement with the carbon-13 n.m.r. results.

3.3. Analysis

All compounds were analyzed for C, H, N. The results of analysis are listed in tables 8a-8c. The white precipitate which formed during the preparation of $CuBr_2.(2,6\text{-}(CH_3)_2\ 4\text{-}NO_2\ Py\text{-}NO)_2$ was analysed for bromine (found: Br, 56.1; calcd. for CuBr, B, 55.7). The complex $CuCl_2(3\text{-}CH_3\ 4\text{-}NO_2\ Py\text{-}NO)_2$ (yellow) was reanalyzed after one year. The result of C, H, N analyses indicated sample decomposition (found: C,20,91; H,2.52; N,4.87, calcd. for $CuCl_2.(3\text{-}CH_3\ 4\text{-}NO_2\ Py\text{-}NO)_2$ C,32,54; H,2.7; N,12.66). Sample decomposition was later confirmed by means of infrared spectroscopy, which showed new bands in the region 3500 - 3000cm^{-1} and 1700 - 1550cm^{-1}. Similar decomposition was also detected in three other complexes, $CuCl_2.(3\text{-}CH_3\ 4\text{-}NO_2\ Py\text{-}NO)$, $CuBr_2.(3\text{-}CH_3\ 4\text{-}NO_2\ Py\text{-}NO)$ and $CuBr_2(2,6\text{-}(CH_3)_2\ 4\text{-}NO_2\ Py\text{-}NO)_2$ (Brown), however, a change in colour was observed only in the latter two

Table 8a. Analytical Data

Compound	Colour		Analysis % C	H	N
$CuCl_2.(2\text{-}CH_3\ 4\text{-}NO_2\ Py\text{-}NO)$	Orange	Found	24.9	2.1	9.4
		Calcd.	25.0	2.1	9.7
$CuCl_2.(2\text{-}CH_3\ 4\text{-}NO_2\ Py\text{-}NO)_2$	Brown	Found	32.3	2.7	12.8
		Calcd.	32.5	2.7	12.7
$CuBr_2.(2\text{-}CH_3\ 4\text{-}NO_2\ Py\text{-}NO)_2$	Wine red	Found	26.6	2.2	10.5
		Calcd.	27.1	2.3	10.5
$CuCl_2.(3\text{-}CH_3\ 4\text{-}NO_2\ Py\text{-}NO)$	Green	Found	24.8	2.1	9.6
		Calcd.	25.0	2.1	9.7
$CuCl_2.(3\text{-}CH_3\ 4\text{-}NO_2\ Py\text{-}NO)_2$	Yellow	Found	32.4	2.8	12.6
		Calcd.	32.6	2.7	12.7
$CuCl_2.(3\text{-}CH_3\ 4\text{-}NO_2\ Py\text{-}NO)_2$	Orange	Found	32.2	2.7	13.0
		Calcd.	32.6	2.7	12.7
$CuBr_2.(3\text{-}CH_3\ 4\text{-}NO_2\ Py\text{-}NO)$	Wine red	Found	19.0	1.6	7.4
		Calcd.	19.1	1.6	7.4

Table 8b. Analytical Data

Compound	Colour		Analysis % C	H	N
$CuCl_2.(2,6\text{-}(CH_3)_2\ 4\text{-}NO_2\ Py\text{-}NO)_2$	Green	Found	35.1	3.3	11.8
		Calcd.	35.7	3.4	11.9
$CuBr_2.(2,6\text{-}(CH_3)_2\ 4\text{-}NO_2\ Py\text{-}NO)_2$	Dark green	Found	29.6	2.8	10.0
		Calcd.	30.0	2.9	10.0
$CuBr_2.(2,6\text{-}(CH_3)_2\ 4\text{-}NO_2\ Py\text{-}NO)_2$	Dark brown	Found	29.7	2.9	10.0
		Calcd.	30.0	2.9	10.0
$CuCl_2.(2,6\text{-}(CH_3)_2 3\ \text{-}NO_2\ Py\text{-}NO)_2$	Green	Found	35.4	3.4	11.9
		Calcd.	35.7	3.4	11.9
$CuBr_2.(2,6\text{-}(CH_3)_2 3\text{-}\ NO_2\ Py\text{-}NO)_2$	Green	Found	29.7	2.8	10.0
		Calcd.	30.0	2.9	10.0
$CdCl_2.(2\text{-}CH_3\ 4\text{-}NO_2 Py\text{-}NO)$	White	Found	20.7	1.7	8.1
		Calcd.	21.3	1.8	8.3
$CdCl_2.(3\text{-}CH_3.\ 4\text{-}NO_2\ Py\text{-}NO)_2$	Pale Yellow	Found	29.6	2.4	11.3
		Calcd.	29.3	2.4	11.4

Table 8c. Analytical Data

Compound	Colour		Analysis %		
$CdCl_2.(2,6\text{-}(CH_3)_2\ 4\text{-}NO_2\ Py\text{-}NO)$	White	Found	23.6	2.2	7.9
		Calcd.	23.9	2.2	8.0
$CdCl_2.(2,6\text{-}(CH_3)_2\ 3\text{-}NO_2\ Py\text{-}NO)$	White	Found	23.6	2.2	7.9
		Calcd.	23.9	2.3	7.9
$CdCl_2.(4\text{-}NO_2\ Py\text{-}NO)$	White	Found	18.9	1.2	8.6
		Calcd.	18.6	1.2	8.7
$CdCl_2.(4\text{-}NO_2\ Py\text{-}NO)_2$	Yellow	Found	25.7	1.7	12.0
		Calcd.	25.9	1.7	12.1
$Cu(AcO)_2.(3\text{-}CH_3\ 4\text{-}NO_2\ Py\text{-}NO)$	Dark Green	Found	36.1	3.6	8.4
		Calcd.	35.8	3.6	8.4
$Cu(AcO)_2.(2,6\text{-}(CH_3)_2\ Py\text{-}NO)$	Green	Found	40.8	4.6	4.3
		Calcd.	40.7	4.6	4.3

complexes which had turned yellow. This decomposition is thought to be due to light rather than oxygen or moisture, because, new samples prepared after one year, were stable for a period of seven months when kept in the dark, even when not placed in a desiccator.

3.4. Copper(II) Acetate Complexes

3.4.1. Introduction

4-Nitro 3-picoline N-oxide and 2,6-lutidine N-oxide reacted with copper(II) acetate monohydrate to form the dimeric complexes $[Cu(AcO)_2.(3\text{-}CH_3\ 4\text{-}NO_2\ Py\text{-}NO)]_2$ and $[Cu(AcO)_2.(2,6\text{-}(CH_3)_2\ Py\text{-}NO)]_2$. The electronic, infrared, e.s.r. spectra and magnetic measurements supported the proposed structure. 4-Nitro 2-picoline N-oxide, 4-nitro 2,6-lutidine N-oxide and 3-nitro 2,6-lutidine N-oxide did not form complexes with the same metal salt. The results obtained are discussed in terms of steric factors, the M-O-N bond angle, the π-acceptor abilities and the basicities of the ligands.

The structure, spectral and magnetic properties of copper(II) acetate monohydrate and the related complexes are described in part I of the present work (pages 47 - 50), and pages 124, 125. The interaction of 4-substituted pyridine N-oxide with copper(II) acetate has been studied by Nelson *et al.*[208] who have reported that the magnetic moments of these complexes decrease as the basicity of the N-oxides decreases and the π-acceptor ability increases, and concluded that pyridine N-oxides with relatively low basicities and high π-acceptor abilities enhance copper-copper bonding. Therefore, based upon the results of Nelson *et al.* and the basicities of the methyl substituted nitropyridine N-oxides studied in the present work, and in the absence of other factors, all the methyl substituted nitropyridine N-oxides studied, were expected to form complexes with copper(II) acetate having magnetic moments intermediate between the values reported for pyridine N-oxide and 4-nitropyridine N-oxide Accordingly, with the aim of testing whether the steric factors.

Table 9. Infrared band assignments (cm^{-1}) for $[Cu(AcO)_2.L]_2$*

Group	2,6-Lutidine N-oxide	4-Nitro 3-Picoline N-oxide
ν_{NO}	1218	1245
$\Delta\nu_{NO}$**	32	66
ν_{COO^-}(asym)***	1619	1610 1630
ν_{COO^-}(sym)***	1428	1440
ν_{C-NO_2}		1520
δ_{NO}	892	840

* Spectra recorded as nujol mulls.

** $\Delta\nu_{NO} = \nu_{NO}$ free ligand - ν_{NO} complex.

*** The carboxylate symmetric and asymmetric stretching frequencies were taken from ref. 208.

imposed by the methyl groups at 2 and/or 6 positions of pyridine ring were the only reason why the corresponding complexes did not form, the preparation of the complex $[Cu(AcO)_2.(2,6\text{-}(CH_3)_2\ Py\text{-}NO)]_2$ was undertaken.

3.4.2. Characterisation of the Complexes

Infrared Spectra Results

The coordination of the ligands is indicated since (a) the nitrogen-oxygen stretching frequency, ν_{NO}, is shifted to lower energy upon complexation and appears at 1218 cm^{-1} and 1245 cm^{-1} in the spectra of $[Cu(AcO)_2.(2,6,\text{-}(CH_3)_2\ Py\text{-}NO)]_2$ and $[Cu(AcO)_2.(3\text{-}CH_3\ 4\text{-}NO_2\ Py\text{-}NO)]_2$ respectively, (b) in each case the N-O bending frequency δ_{NO} shifts to higher frequency, (c) $\nu_{C\text{-}NO_2}$ is shifted to higher energy by about 20 cm^{-1} in the spectrum of $[Cu(AcO)_2.(3\text{-}CH_3\ 4\text{-}NO_2\ Py\text{-}NO)]_2$ (table 9).

The retention of a dimeric carboxylate structure as opposed to a structure involving bridging N-oxides is supported by the position of the carboxylate stretching frequencies, $\nu_{COO^-(sym)}$ and $\nu_{COO^-(asym)}$, which appear at very similar energies to those reported for copper acetate monohydrate.[208] In addition, ν_{NO} for bridging amine oxide complexes is always shifted to lower energy and varies over a more limited range (ν_{NO} = 1199 - 1208 cm^{-1}) as opposed for the complexes reported herein (1218 and 1245 cm^{-1}).

Electronic Spectra Results

The reflectance spectrum of $[Cu(AcO)_2.(3\text{-}CH_3\ 4\text{-}NO_2Py\text{-}NO)]_2$ revealed three absorption bands in the regions 14,200 cm^{-1}, 26,500 cm^{-1}, and 37,500 cm^{-1}. The corresponding bands in the spectrum of $[Cu(AcO)_2.(2,6\text{-}(CH_3)_2\ Py\text{-}NO)]_2$ appear at 13,000 cm^{-1}, 31,500 cm^{-1} and 37,000 cm^{-1} (Fig. 6). The positions

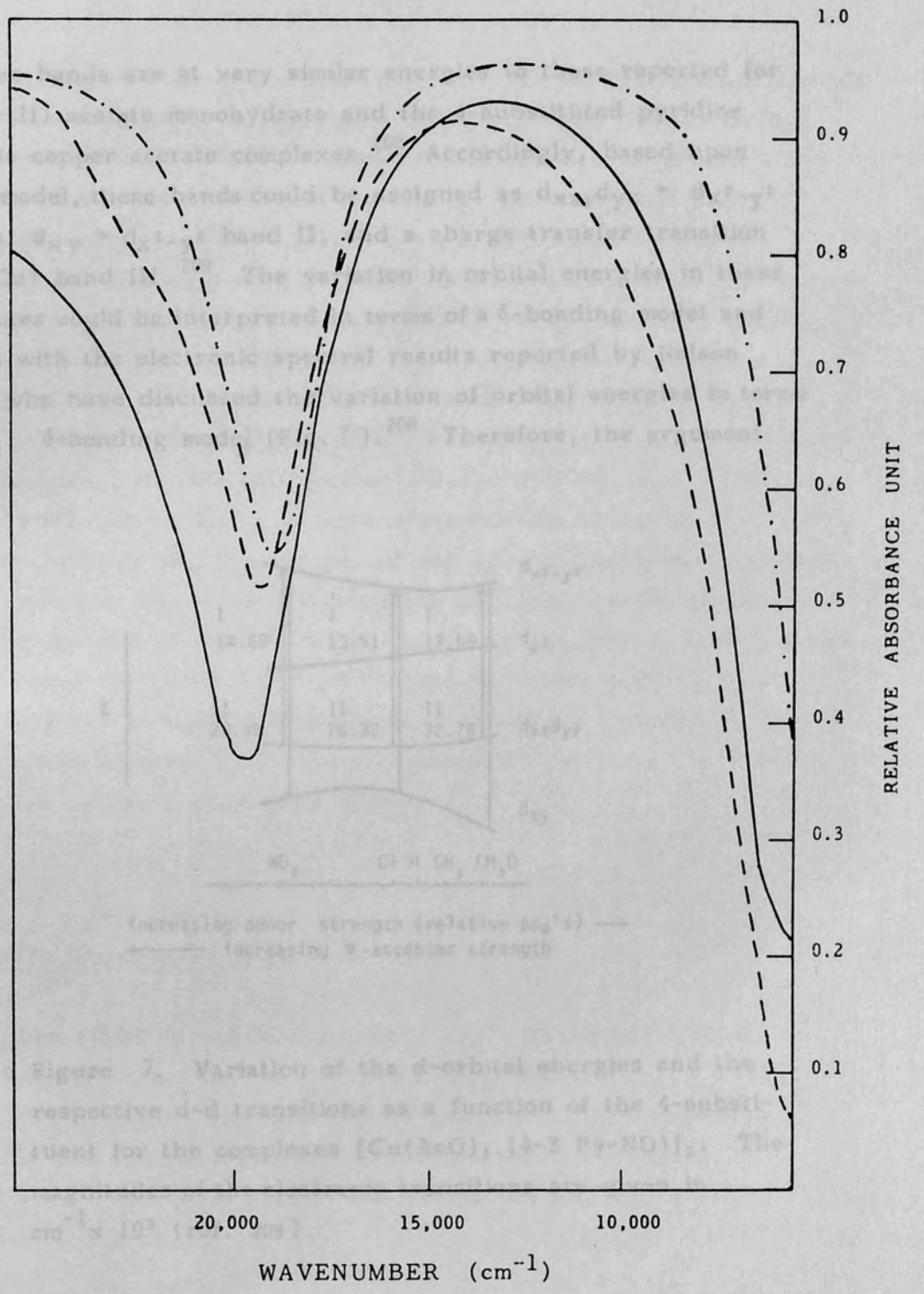

Fig. 6. Reflectance spectra of $[Cu(AcO)_2.L]_2$

——— L = H_2O

– – – – L = 3-CH_3 4-NO_2 Py-NO

—·—·—·— L = 2,6-$(CH_3)_2$ Py-NO

of these bands are at very similar energies to those reported for copper(II) acetate monohydrate and the 4-substituted pyridine N-oxide copper acetate complexes.[208] Accordingly, based upon the δ model, these bands could be assigned as $d_{xz}, d_{yz} \rightarrow d_{x^2-y^2}$ band I, $d_{xy} \rightarrow d_{x^2-y^2}$ band II, and a charge transfer transition (O → Cu) band III.[208] The variation in orbital energies in these complexes could be interpreted in terms of a δ-bonding model and agrees with the electronic spectral results reported by Nelson et al. who have discussed the variation of orbital energies in terms of a δ-bonding model (Fig. 7).[208] Therefore, the argument

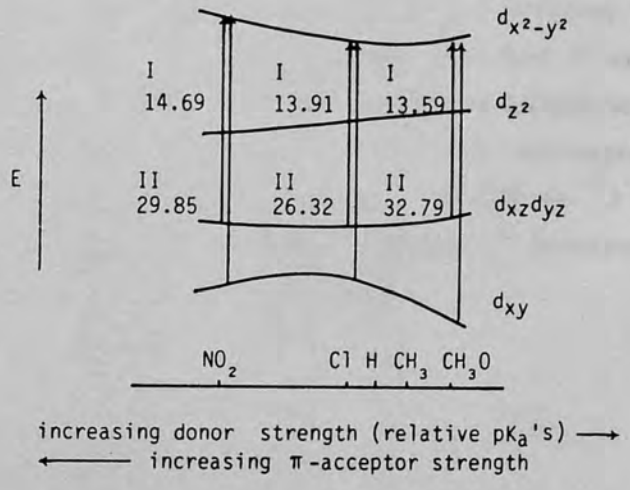

Figure 7. Variation of the d-orbital energies and the respective d-d transitions as a function of the 4-substituent for the complexes $[Cu(AcO)_2.(4\text{-}Z\ Py\text{-}NO)]_2$. The magnitudes of the electronic transitions are given in $cm^{-1} \times 10^3$ (ref. 208).

given by these authors also applies for the complexes prepared in the present work. 2,6-Lutidine N-oxide being more basic than 4-nitro 3-picoline N-oxide undergoes a stronger interaction with the d_{z^2}, d_{xz} and d_{yz} orbitals and results in an increase in these orbital energies. The $d_{x^2-y^2}$ and d_{xy} orbitals would undergo

interactions with both N-O π and π^* orbitals. In 2,6-lutidine N-oxide the π-orbital probably being higher in energy than the copper d_{xy} orbital and π^* orbital lower in energy than the $d_{x^2-y^2}$ orbital would result in destabilisation of both the $d_{x^2-y^2}$ and π-orbitals and stabilisation of d_{xy} and π^* orbitals, while in 4-nitro 3-picoline N-oxide the N-O π-orbital is probably lower in energy than the copper d_{xy} orbital and the N-O π^* orbital lower in energy than the copper $d_{x^2-y^2}$ orbital, and metal to ligand back donation will destabilise both the $d_{x^2-y^2}$ and d_{xy} orbitals while stabilising both the ligand π and π^* orbitals. The variation of band I, $d_{xz}, d_{yz} \rightarrow d_{x^2-y^2}$; and band II, $d_{xy} \rightarrow d_{x^2-y^2}$ in $[Cu(AcO)_2.(2,6\text{-}(CH_3)_2\ Py\text{-}NO)]_2$ and $[Cu(AcO)_2.(3\text{-}CH_3\ 4\text{-}NO_2\ Py\text{-}NO)]_2$ is in agreement with the above interpretation. The fact that the pK_a value reported for 2,6-lutidine N-oxide (1.442) is less than the pK_a value of 4-methoxy pyridine N-oxide (2.05),[5] while the position of band I in the 4-methoxy pyridine N-oxide complex is at a higher energy (13,590 cm^{-1}) than the corresponding band in the spectrum of 2,6-lutidine N-oxide (13,000 cm^{-1}) indicates that steric factors imposed by the methyl groups at positions 2 and 6 are responsible to bring about this change.

Magnetic Measurements

The effective magnetic moment μ_{eff} has been calculated at each temperature from the expression $\mu_{eff} = 2.84\ [(\chi_m - N\alpha)T]^{\frac{1}{2}}$, where, $N\alpha$ represents the temperature-independent paramagnetism associated with copper ion. In the present work, a value $N\alpha = 60 \times 10^{-6}$ has been used. The values obtained are given in Tables 10 and 11.

The copper(II) acetate complexes of 4-nitro 3-picoline N-oxide and 2,6-lutidine N-oxide have depressed moments of 1.28 B.M. and 1.30 B.M. respectively. These values may be compared with the subnormal magnetic moment (1.40 B.M.) which characterises the binuclear copper acetate monohydrate complex.[225] These magnetic moments, however, cannot be used to differentiate

Table 10. Magnetic Susceptibility Data for

$[Cu(AcO)_2.(3\text{-}CH_3\ 4\text{-}NO_2\ Py\text{-}NO)]_2$

Diamagnetic correction per copper ion = 137.63×10^6cgs

Temp / K	$\frac{\chi_m}{2} \times 10^6$cgs	calculated * $\frac{\chi_m}{2} \times 10^6$cgs	$\frac{\chi_{m'}}{2} \times 10^6$cgs	$\frac{\mu_{eff}}{B.M.}$
304.1	764.87	760.37	704.87	1.31
295.8	752.40	757.45	692.40	1.29
280.8	729.27	749.27	669.27	1.23
271.8	726.53	742.30	666.53	1.21
252.5	712.83	721.14	652.83	1.15
230	685.73	683.53	625.73	1.08
164.6	477.21	468.92	417.21	0.74
130	304.71	296.41	244.71	0.51
99.3	156.80	152.10	96.80	0.28
90	128.51	119.22	68.51	0.22

* Calculated from relationship (1).

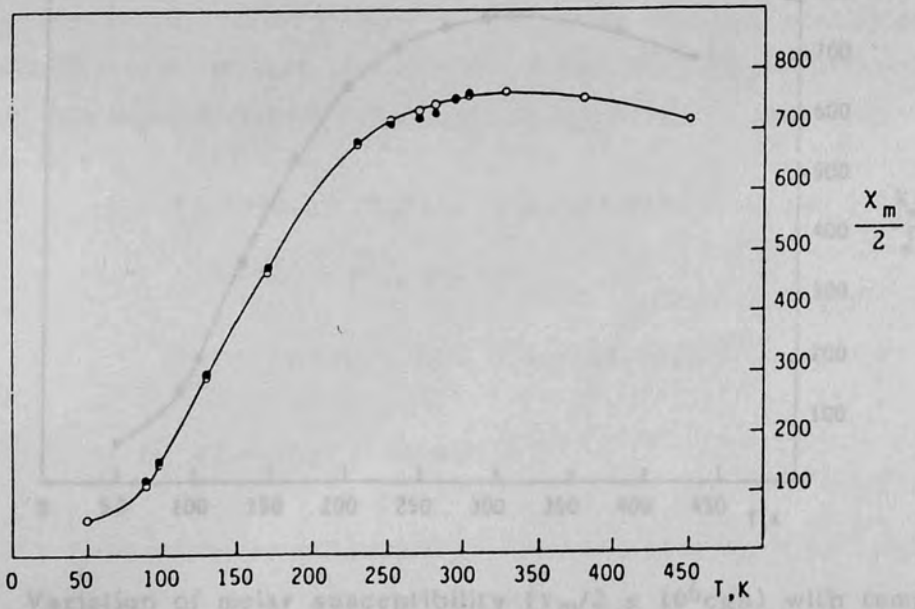

Fig. 8. Variation of molar susceptibility ($\chi_m/2 \times 10^6$ cgs) with temperature
• experimental molar suscebtibility, o calcd. from relationship (1).

Table 11. Magnetic Susceptibility Data for

$[Cu(AcO)_2.(2,6\text{-}(CH_3)_2\ Py\text{-}NO)]_2$

Diamagnetic correction per copper ion = 134.7×10^6cgs.

Temp / K	$\frac{\chi_m}{2} \times 10^6$cgs	calculated* $\frac{\chi_m}{2} \times 10^6$cgs	$\frac{\chi_{m'}}{2} \times 10^6$cgs	μ_{eff} / B.M.
295.05	773.65	771.22	713.65	1.30
263.50	751.35	758.50	691.35	1.21
231.00	713.89	721.87	653.89	1.10
199.00	658.11	651.47	598.11	0.98
166.50	535.99	533.99	475.99	0.80
131.50	369.87	356.17	309.87	0.57
104.50	195.21	208.49	135.21	0.34
91.00	151.99	146.21	91.99	0.26

* Calculated from relationship (1).

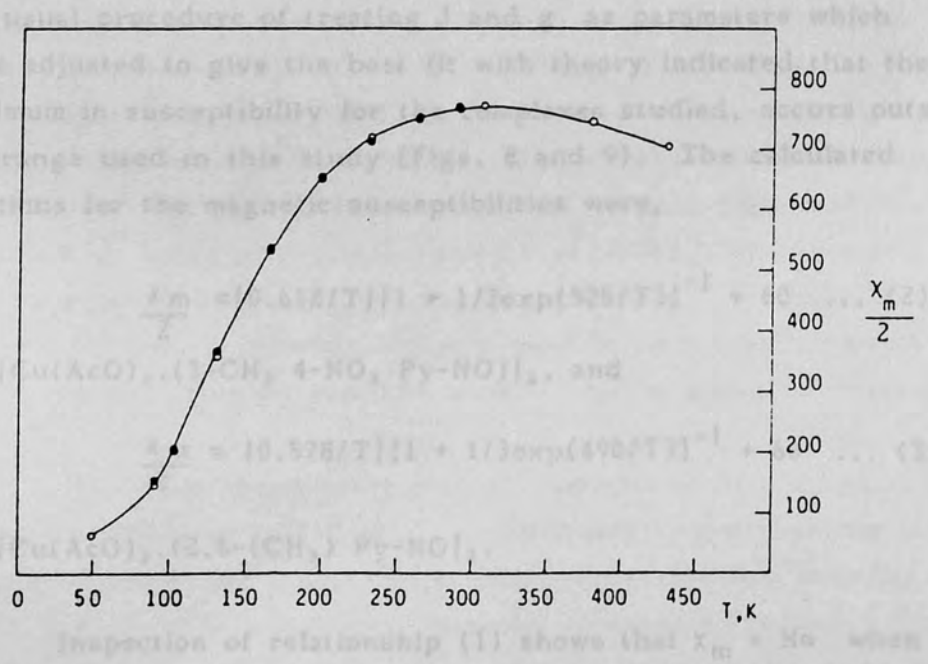

Fig. 9. Variation of molar susceptibility ($\chi_m/2 \times 10^6$cgs) with temperature • experimental molar susceptibility, o calculated from relationship (1).

between two likely structures since complexes having either bridging carboxylates or bridging pyridine N-oxides would be expected to exhibit antiferromagnetism and subnormal magnetic moments.

The anomalous temperature variation of the corrected molar magnetic susceptibility exhibited by these complexes did not reveal the maximum in susceptibility which appears in the region 255K for copper acetate monohydrate. However, the experimental data can also be fitted closely by the following relationship

$$\frac{\chi_m}{2} = \frac{g^2 N\beta^2}{3kT}\,[1 + 1/3\exp(J/kT)]^{-1} + N\alpha \quad \ldots (1)$$

previously used to describe the anomalous temperature variation of magnetic susceptibility for compounds with the molecular configuration of copper acetate.[225-227] This relationship has been calculated in terms of a spin-singlet-spin-triplet separation and J is the singlet triplet separation.[225] Application of relationship (1) by the usual procedure of treating J and g as parameters which were adjusted to give the best fit with theory indicated that the maximum in susceptibility for the complexes studied, occurs outside the range used in this study (Figs. 8 and 9). The calculated equations for the magnetic susceptibilities were,

$$\frac{\chi_m}{2} = [0.612/T][1 + 1/3\exp(525/T)]^{-1} + 60 \quad \ldots (2)$$

for $[Cu(AcO)_2.(3\text{-}CH_3\ 4\text{-}NO_2\ Py\text{-}NO)]_2$, and

$$\frac{\chi_m}{2} = [0.578/T][1 + 1/3\exp(490/T)]^{-1} + 60 \quad \ldots (3)$$

for $[Cu(AcO)_2.(2,6\text{-}(CH_3)\ Py\text{-}NO]_2$.

Inspection of relationship (1) shows that $\chi_m = N\alpha$ when $T = 0$, and rises to a maximum value at $T_N = 5J/8k$, so that the temperature of the maximum in susceptibility can be determined from the exchange energy, J.

The calculated values of χ_m at each temperature are given in tables 10 and 11, while g, J, and T_N for the complexes are:

$T_N = 328K$, $g = 2.15$, $J = 340\ cm^{-1}$

for $[Cu(AcO)_2.(3\text{-}CH_3\ 4\text{-}NO_2\ Py\text{-}NO]_2$ and

$T_N = 306.25K$, $g = 2.15$, $J = 340\ cm^{-1}$

for $[Cu(AcO)_2.(2,6\text{-}(CH_3)_2\ Py\text{-}NO)]_2$.

The g values may be compared with those obtained for copper acetate monohydrate (g = 2.13 - 2.19),[225-227] while the values of T_N obtained show that they could not have been detected in the temperature range studied. The agreement of experimental points with those calculated is remarkably good confirming the binuclear structure of these complexes. The considerable increase in J as compared to the value observed in copper acetate monohydrate, 286 cm^{-1}, is probably due to the reduction of the positive charge on the copper ions which will reduce any repulsions between them and also allow the metal orbitals to expand giving better overlap; in fact x-ray crystallographic data on copper acetate monohydrate indicate a small displacement (0.22 Å) of each copper atom out of its CuO_4 plane indicating a repulsion between neighbouring Cu atoms.[255] The decrease in Cu-Cu bond distance and the subsequent displacement of each copper atom towards the CuO_4 plane, is probably one reason why the steric factors imposed by the methyl groups in 4-nitro 2,6-lutidine N-oxide, a good π-acceptor, become more important as compared to 2,6-lutidine N-oxide which is expected to be a weaker π-acceptor.

The room temperature magnetic moment of $[Cu(AcO)_2.(3\text{-}CH_3\text{-}4\text{-}NO_2\ Py\text{-}NO)]_2$ at 1.28 B.M. is significantly larger than the moment reported for the corresponding 4-nitropyridine N-oxide (0.92 B.M.). The substantial increase in magnetic moment could not be due to the inductive effect of the methyl group at position 3 of the pyridine ring, and therefore the twisted nature of the nitro group should be responsible for the large moment.

The room temperature magnetic moment of $[Cu(AcO)_2.(2,6\text{-}(CH_3)\text{-}Py\text{-}NO)]_2$ is smaller than what would be expected from the basicity and the π-acceptor ability of 2,6-lutidine N-oxide, because the corresponding pyridine N-oxide complex is reported to have a larger magnetic moment (1.37 B.M.). This could be the result of steric factors in the 2,6-lutidine N-oxide complex. Such an effect is also described by Chatt and Shaw[228,229] in metal complexes of the types $[PR'_3\ Ni\ RX]$ and $[(PR'_3)_2\ M\ R_2]$, where M = Ni, Co, Fe, and R = substituted aryl or some other aromatic group. These authors observed that the stability of these complexes was much increased when substituents were attached in the ortho position of R. One of the causes for such additional stabilisation of the ortho-substituted aryl complexes compared to the meta- or para-substituted aryl compounds, was attributed to the shielding effect of the metal atoms by the ortho substituents.

E.S.R. Results

The final and strongest proof supporting the dimeric structure for the $[Cu(AcO)_2.(3\text{-}CH_3\ 4\text{-}NO_2\ Py\text{-}NO)]_2$ complex was afforded by the polycrystalline e.s.r. spectra of this complex. At room temperature three peaks appeared, the first peak being very close to zero magnetic field. This is quite incompatibe with a spin of 1/2, which must have Kramers's degeneracy. At 90K, the spectrum was similar but considerably weaker with narrower lines (Fig. 10). The change of intensity with temperature is thus qualitatively in agreement with the magnetic measurement results, since the intensity is simply related to the susceptibility. The main features of the e.s.r. spectra are quite similar to those reported for other polycrystalline copper(II) acetate compounds by Lewis *et al.*[230] who have recorded their spectra at a microwave frequency ν = 9.066 GHz, similar to that used in the present work (9.270301 GHz).

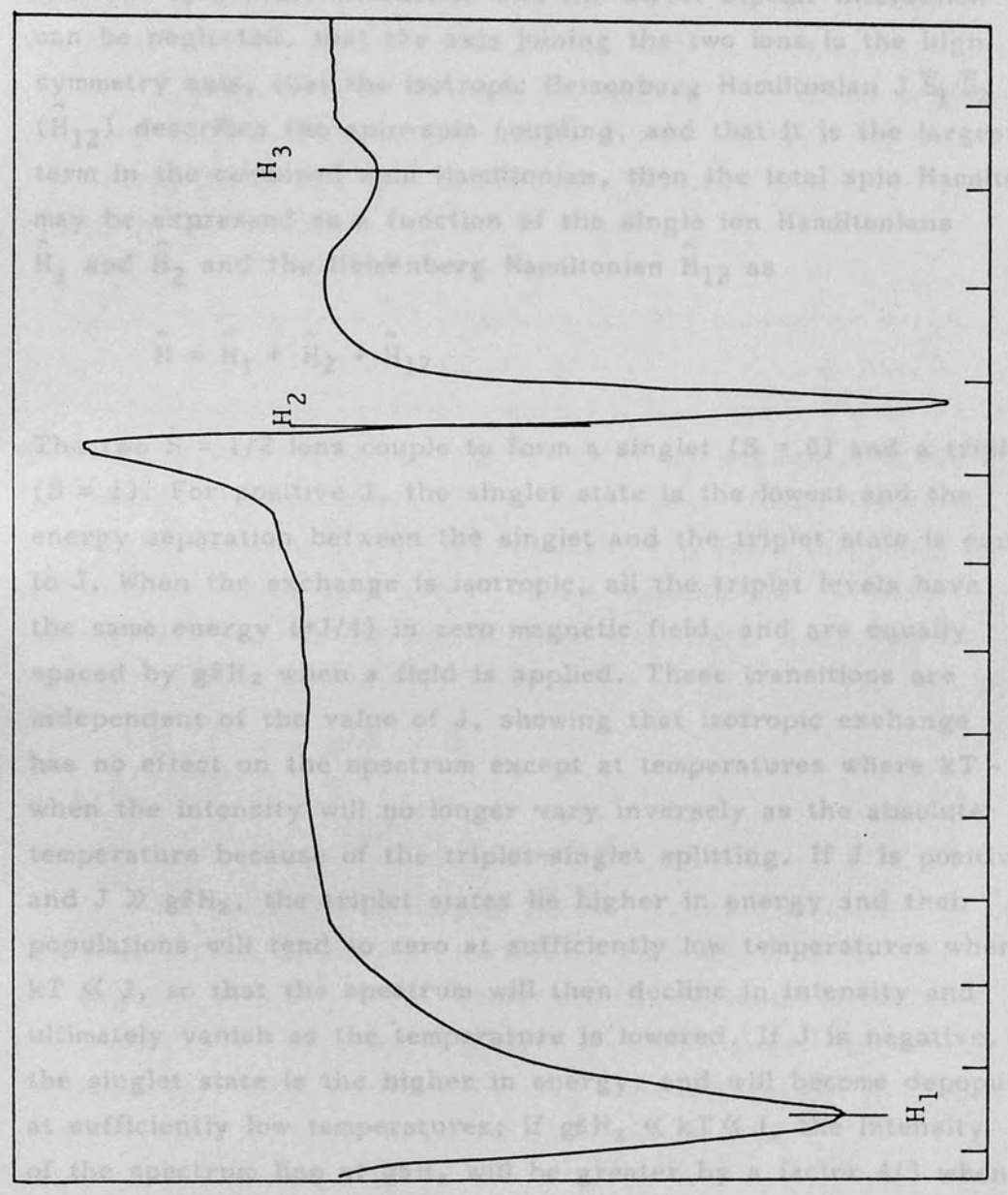

Fig. 10. E.s.r. spectrum (X band) of polycrystalline $[Cu(AcO)_2 \cdot (3\text{-}CH_3\ 4\text{-}NO_2\ Py\text{-}NO)]_2$.

The general problem of magnetic resonance in an isolated pair of identical ions, each with effective spin $S_1 = S_2 = 1/2$ and with g-tensors whose principal values and principal axes are the same is tackled by many authors.[231-233] In this system, assuming that the orbital angular momentum is completely quenched, that the spin-orbit interaction and the direct dipolar interaction can be neglected, that the axis joining the two ions is the high symmetry axis, that the isotropic Heisenberg Hamiltonian $J\,\bar{S}_1\,\bar{S}_2$ ($\hat{H}_{12}$) describes the spin-spin coupling, and that it is the largest term in the combined spin Hamiltonian, then the total spin Hamiltonian may be expressed as a function of the single ion Hamiltonians $\hat{H}_1$ and $\hat{H}_2$ and the Heisenberg Hamiltonian $\hat{H}_{12}$ as

$$\hat{H} = \hat{H}_1 + \hat{H}_2 + \hat{H}_{12}$$

The two S = 1/2 ions couple to form a singlet (S = 0) and a triplet (S = 1). For positive J, the singlet state is the lowest and the energy separation between the singlet and the triplet state is equal to J. When the exchange is isotropic, all the triplet levels have the same energy (+J/4) in zero magnetic field, and are equally spaced by $g\beta H_z$ when a field is applied. These transitions are independent of the value of J, showing that isotropic exchange has no effect on the spectrum except at temperatures where $kT \sim J$, when the intensity will no longer vary inversely as the absolute temperature because of the triplet-singlet splitting. If J is positive, and $J \gg g\beta H_z$, the triplet states lie higher in energy and their populations will tend to zero at sufficiently low temperatures when $kT \ll J$, so that the spectrum will then decline in intensity and ultimately vanish as the temperature is lowered. If J is negative, the singlet state is the higher in energy, and will become depopulated at sufficiently low temperatures; if $g\beta H_z \ll kT \ll J$, the intensity of the spectrum line at $g\beta H_z$ will be greater by a factor 4/3 when the singlet state is completely depopulated than it would have been in the absence of the exchange interaction. Thus intensity measurements in the region where $kT \sim J$ can be used to estimate the value of J.

The electron spin resonance observed in the triplet state consists of 2I + 1 lines with a hyperfine splitting of A/2, where A is the hyperfine splitting for the individual ions. Usually more than one set of 2I + 1 lines is observed in a triplet state since an anisotropic spin-spin interaction gives rise to a zero field splitting. For example, a dipole-dipole interaction will remove the three-fold degeneracy in the triplet state so that even in the absence of magnetic field, the $M_S = 0$ and $M_S = \pm 1$ levels will have different energies. The application of a magnetic field will cause the energy levels to separate and two transitions $\Delta M_S = \pm 1$ will appear in the spectrum.

In a complex which possesses an odd number of electrons, Kramer's theorem dictates that the ground state has at least a two-fold degeneracy. However, when the total number of magnetic electrons is even, then the degeneracy of the ground state may be removed in accordance with the Jahn-Teller effect. The terms in the spin Hamiltonian which analytically represent this phenomenon are usually defined as D and E. If the magnetic field is along the z-axis, then the energies of three spin states $\overline{S} = 1$, $M_S = 1$ ($|1, 1\rangle$); $\overline{S} = 1$, $M_S = 0$ ($|1,0\rangle$); and $\overline{S} = 1$, $M_S = -1$ ($|1, -1\rangle$) are

$\|1, 1\rangle$	$g\beta H_z + D$
$\|1, 0\rangle$	0
$\|1,-1\rangle$	$-g\beta H_z + D$

The two transitions from the $|1, -1\rangle$ state to the $|1, 0\rangle$ state and from the $|1, 0\rangle$ state to the $|1, 1\rangle$ state are described by the selection rule $\Delta M_S = \pm 1$. These transitions occur at energies $h\nu_1 = g\beta H_1 - D$ and $h\nu_2 = g\beta H_2 + D$ respectively. In typical experiments, the microwave frequency is held constant, $\nu_1 = \nu_2$, and the value for D is furnished by the expression[232]

$$D = \frac{g\beta(H_1 - H_2)}{2}$$

If $g\beta H_z$ is comparable with J, the spectrum is more complicated in its behaviour and is discussed in references 231 and 233.

Lewis et al. have interpreted their results by assuming that the complexes have axial symmetry and used the spin-Hamiltonian (4) [230]

$$\hat{H} = g_{\parallel} H_z \hat{S}_z + g_{\perp}(H_x \hat{S}_x + H_y \hat{S}_y) + D\hat{S}_z^2 \quad \ldots \quad (4)$$

and solving it when the applied magnetic field is along the symmetry axes of the molecule, they have obtained the energy levels (5) in the parallel direction

$$\begin{aligned} \omega_1 &= D + g_{\parallel}\beta H_{\parallel} \\ \omega_2 &= D - g_{\parallel}\beta H_{\parallel} \qquad \ldots \quad (5) \\ \omega_3 &= 0 \end{aligned}$$

and (6) in the perpendicular direction

$$\begin{aligned} \omega_1 &= -D/2 + (D^2/4 + g_{\perp}^2 \beta^2 H_{\perp}^2)^{\frac{1}{2}} \\ \omega_2 &= -D/2 - (D^2/4 + g_{\perp}^2 \beta^2 H_{\perp}^2)^{\frac{1}{2}} \qquad \ldots \quad (6) \\ \omega_3 &= 0 \end{aligned}$$

and predicted that the selection rule $\Delta Ms = \pm 1$ would allow the transitions (7) to be observed at X-band microwave frequencies.

$$\begin{aligned} h\nu &= D - g_{\parallel}\beta H_1 \\ h\nu &= -D + g_{\parallel}\beta H_2 \qquad \ldots \quad (7) \\ h\nu &= -D/2 + (D^2/4 + g_{\perp}^2 \beta^2 H_3^2)^{\frac{1}{2}} \end{aligned}$$

The above model was tested with $[Cu(AcO)_2(3\text{-}CH_3\ 4\text{-}NO_2\text{-}Py\text{-}NO)]_2$. At room temperature the three absorptions occurred at the magnetic fields expected from the above equations. The measured values of H_1, H_2 and H_3 were, 650 Gauss, 6000 Gauss, and 4675 Gauss respectively. Substitution of the H values in relationship (7) gave,

$$D = 0.3829\ cm^{-1}; \qquad g_{\parallel} = 2.47; \quad g_{\perp} = 2.10.$$

These values are in excellent agreement with the magnetic measurement results which gave g = 2.13, because

$$g = 1/3(g_{\parallel} + 2g_{\perp}) = 2.13$$

The e.s.r. spectrum of $[Cu(AcO)_2.(3\text{-}CH_3\ 4\text{-}NO_2\ Py\text{-}NO)]_2$ in methanol (10^{-2}M) was also recorded. At room temperature a single broad line appeared with g = 2.162. The frozen solution gave an axially symmetric spectrum with hyperfine splitting. (Fig. 11). The g and A values obtained are as follows:

$g_{\parallel} = 2.366 \pm 0.005$

$g_{\perp} = 2.054 \pm 0.005$

$A_{\parallel} = 134\ G \pm 5$

$A_{\perp}$ = not resolved

These values deviate quite significantly from the values obtained from the magnetic susceptibility measurements and e.s.r. spectra of pollycrystalline samples. The absence of zero-field splitting and the large value of $A_{\parallel}$ probably result from the formation of monomeric species and/or the replacement of ligand molecules by methanol.

3.4.3. Conclusions

In 2,6-lutidine N-oxide complex the presence of two methyl groups resulted in the formation of a complex having a magnetic moment smaller than the corresponding pyridine N-oxide complex, indicating the presence of a slightly shorter copper-copper distance in the former. Spectral data and magnetic measurements of 4-nitropyridine N-oxide and 4-nitro 3-picoline N-oxide complexes indicated that the presence of a nitro group at position 4 will enhance the π-acceptor properties of these ligands and would significantly increase copper-copper interaction in their corresponding

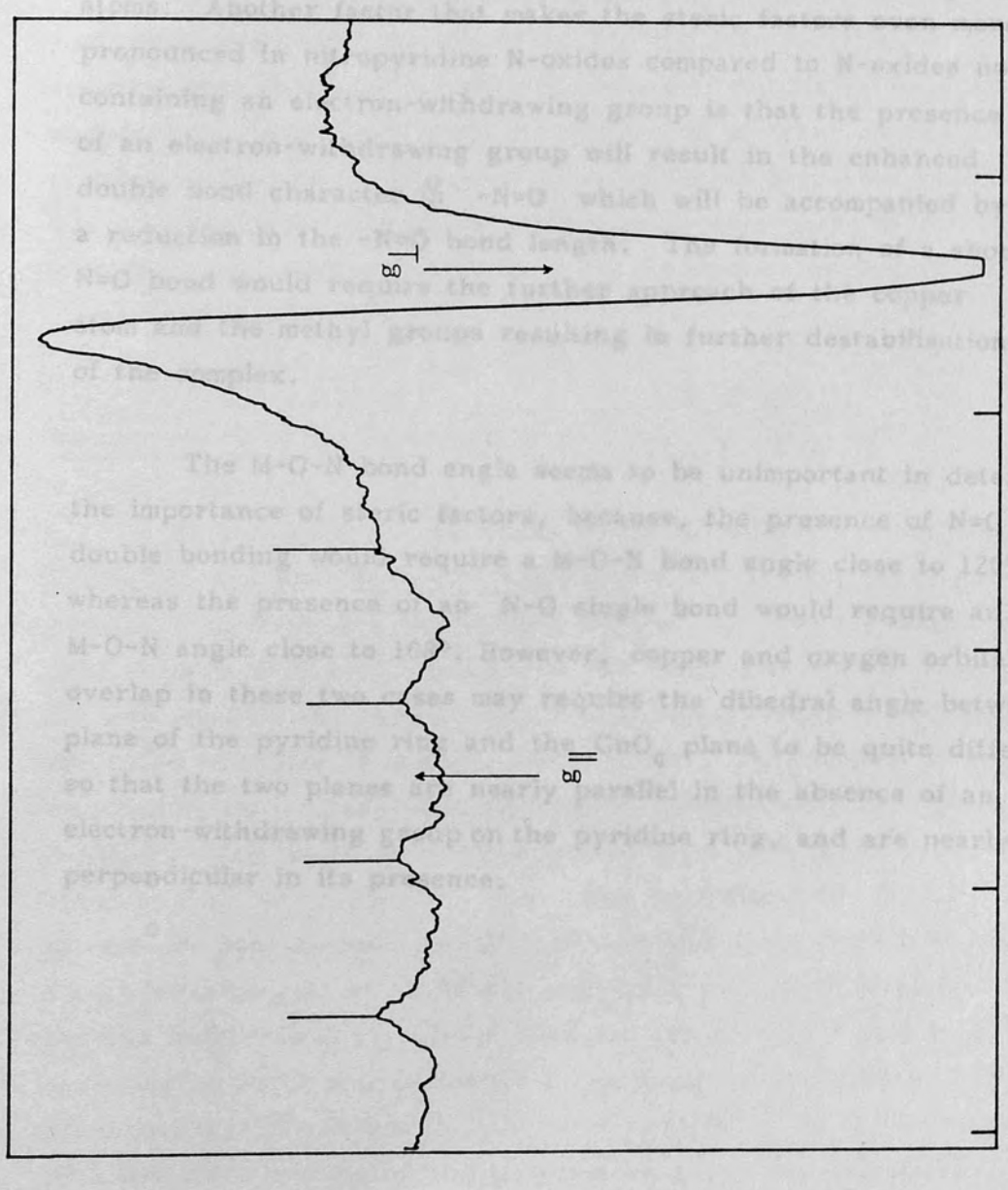

Fig. 11. E.s.r. spectrum of a solution of $[Cu(AcO)_2.(3\text{-}CH_3\ 4\text{-}NO_2\ Py\text{-}NO)]_2$ in methanol.

complexes. Therefore, the combined effect of the nitro group, and the steric factors at the 2 and 6 positions of the pyridine ring would require the formation of a complex having a relatively short copper-copper distance. This would result in the displacement of each copper atom towards the CuO_4 plane thus causing steric interaction between the methyl groups and the CuO_4 oxygen atoms. Another factor that makes the steric factors even more pronounced in nitropyridine N-oxides compared to N-oxides not containing an electron-withdrawing group is that the presence of an electron-withdrawing group will result in the enhanced double bond character in -N=O which will be accompanied by a reduction in the -N=O bond length. The formation of a shorter N=O bond would require the further approach of the copper atom and the methyl groups resulting in further destabilisation of the complex.

The M-O-N bond angle seems to be unimportant in determining the importance of steric factors, because, the presence of N=O double bonding would require a M-O-N bond angle close to 120°, whereas the presence of an N-O single bond would require an M-O-N angle close to 108°. However, copper and oxygen orbital overlap in these two cases may require the dihedral angle between the plane of the pyridine ring and the CuO_4 plane to be quite different, so that the two planes are nearly parallel in the absence of an electron-withdrawing group on the pyridine ring, and are nearly perpendicular in its presence.

3.5. Copper(II) Halide Complexes

3.5. The Crystal and Molecular Structures of $CuCl_2.(2,6\text{-}(CH_3)_2\ 3\text{-}NO_2\ Py\text{-}NO)_2$ and $CuBr_2.(2,6\text{-}(CH_3)_2\ 4\text{-}NO_2\ Py\text{-}NO)_2$ (Dark Brown)

The crystal and molecular structures of these two compounds were determined with the aim of making the interpretation of their spectroscopic data and magnetic measurement results easier, and to compare their structures with the structures of other copper(II) halide complexes of pyridine N-oxides. The molecular structure determination was also useful for comparing the molecular dimensions of the ligands with those of pyridine N-oxide and its derivatives as ligands in coordination compounds.

The structure of $CuCl_2.(2,6\text{-}(CH_3)_2\ 3\text{-}NO_2\ Py\text{-}NO)_2$

This compound crystallises in the monoclinic system with a = 7.16669 Å, b = 20.1739 Å, c = 6.813 Å and β = 104.1°, space group $P2_1/C$. The structure was refined by least squares technique to a final R value of 0.0402. A view of the complex is shown in figure 12, and some of the bonding and non-bonding distances and angles are listed in tables 12 and 13, respectively. The complex is four coordinate, trans-planar and monomeric, where $CuCl_2.(2,6\text{-}(CH_3)_2\ 3\text{-}NO_2\ Py\text{-}NO)_2$ units are well separated from each other with the shortest Cu...Cu separation >7 Å. The four atoms Cl, O, Cl', O' around the central metal ion form a rhomboid since the Cu-O and Cu-Cl bond lengths are 1.949(1) and 2.229(0) Å, respectively, and the two independent cis Cl-Cu-O angles are 85.73(4)° and 94.27(4)°, while the O-Cu-O' and Cl-Cu-Cl' trans angles are 179.98(6) and 179.97(3)° respectively. The angle that the plane containing N_1-O_1-Cu makes with the plane containing the pyridine ring was not calculated; however, as it is seen in figure 12, this angle is probably very small so that the two planes are almost coplanar. The ring planes are inclined at an angle of 117.83(7)° to the basal plane. It is apparent that this orientation places two methyl groups, one from each ligand, into positions which block the two axial positions of the copper(II) ion, and therefore, prevent any interaction between the metal ion and neighbouring ions or donor sites.

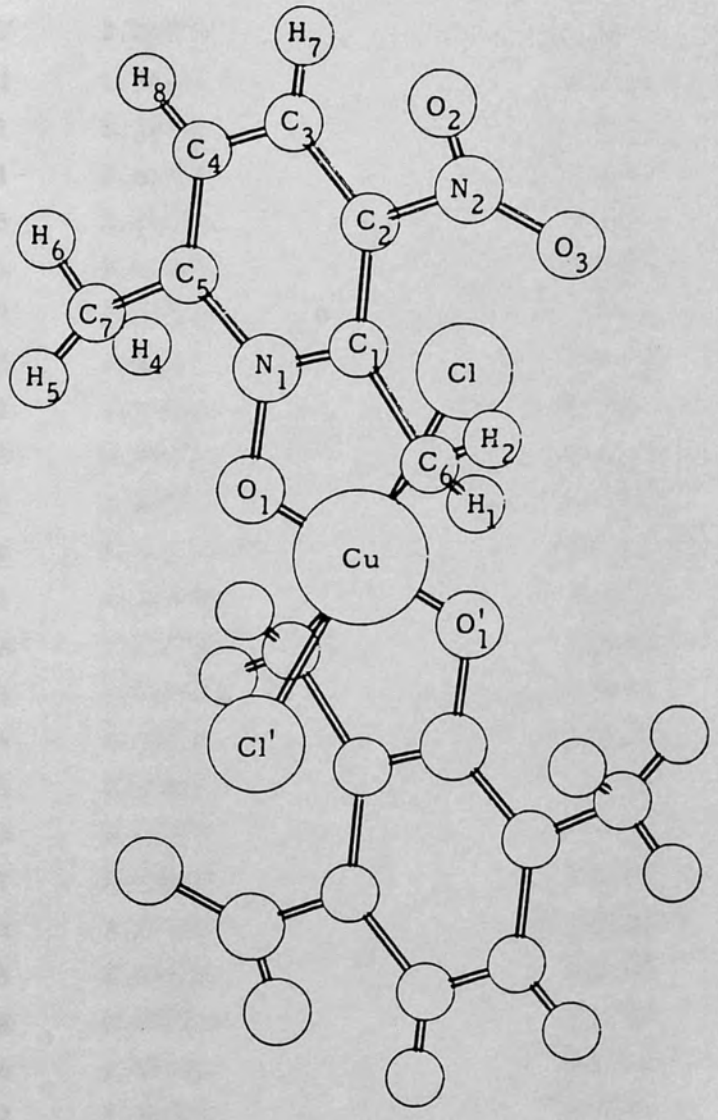

Fig. 12. A view of the complex $CuCl_2.(2,6\text{-}(CH_3)_2\ 3\text{-}NO_2\ Py\text{-}NO)_2$

(Note the crystallographers have used a different numbering system from that used elsewhere in this Thesis)

Table 12. Bonding and non-bonding distances(Å) with e.s.d.'s in parentheses for $CuCl_2.(2,6\text{-}(CH_3)_2\ 3\text{-}NO_2\ Py\text{-}NO)_2$

Cu-Cl	2.229(0)	C2-C5	2.727(2)
Cu-Cl'	2.229(0)	C2-C6	2.578(3)
Cu-O1	1.949(1)	C2-N2	1.476(2)
O1-N1	1.347(2)	C2-O2	2.324(2)
O1-C1	2.314(2)	C2-O3	2.296(2)
O1-C5	2.309(2)	C2-H1	2.672(2)
O1-C6	2.665(3)	C2-H7	2.038(2)
O1-C7	2.665(3)	C3-C4	1.372(3)
O1-H2	2.612(1)	C3-C5	2.398(3)
O1-H3	2.636(1)	C3-N2	2.429(2)
O1-H3	2.354(1)	C3-O3	2.729(2)
O1-H5	2.602(1)	C3-H8	2.038(2)
O1-H6	2.636(1)	C4-C5	1.385(3)
N1-C1	1.354(2)	C4-C7	2.537(3)
N1-C2	2.315(2)	C4-H4	2.616(2)
N1-C3	2.718(2)	C4-H7	2.044(2)
N1-C4	2.347(2)	C5-C7	1.480(3)
N1-C5	1.358(2)	C5-H4	2.027(2)
N1-C6	2.425(2)	C5-H5	2.026(2)
N1-C7	2.430(3)	C5-H6	2.023(2)
N1-H2	2.674(1)	C5-H8	2.042(2)
N1-H3	2.674(1)	N2-O2	1.213(2)
N1-H5	2.677(1)	N2-O3	1.215(2)
N1-H6	2.677(1)	N2-H1	2.611(2)
C1-C2	1.384(2)	N2-H7	2.580(2)
C1-C3	2.425(2)	O2-O3	2.143(2)
C1-C4	2.776(2)	O2-H1	2.178(2)
C1-C5	2.404(2)	O3-H4	2.720(2)
C1-C6	1.489(2)	O3-H7	2.477(2)
C1-N2	2.475(2)	O3-H8	2.752(2)
C1-H1	2.034(2)	C7-H8	2.724(2)
C1-H2	2.032(2)	H1-H2	1.551(0)
C1-H3	2.031(2)	H1-H3	1.551(0)
C2-C3	1.372(2)	H2-H3	1.551(0)
C2-C4	2.353(2)	H4-H8	2.445(0)

Table 13. Bonding and non-bonding angles(deg) with e.s.d.'s in parentheses for $CuCl_2.(2,6\text{-}(CH_3)_2\ 3\text{-}NO_2\ Py\text{-}NO)_2$

Cl -Cu-Cl'	179.97(3)	C4-C3-H7	121.27(18)
Cl-Cu-O1	85.73(4)	C3-C4-C5	120.83(16)
Cl'-Cu-O1	94.27(4)	C3-C4-H8	119.96(19)
O1-Cu-O1'	179.98(6)	C5-C4-H8	119.21(19)
Cu-O1-N1	121.24(9)	O1-C5-N1	31.25(8)
Cu-O1-C1	113.56(6)	N1-C5-C4	117.64(16)
Cu-O1-C5	119.56(7)	N1-C5-C7	117.74(17)
N1-O1-C1	31.13(8)	C4-C5-C7	124.61(18)
N1-O1-C5	31.53(8)	C1-C6-H1	110.17(17)
C1-O1-C5	62.66(6)	C1-C6-H2	110.47(17)
O1-N1-C1	117.93(14)	C1-C6-H3	110.98(16)
O1-N1-C5	117.22(14)	H1-C6-H2	107.66(18)
C1-N1-C5	124.85(14)	H1-C6-H3	108.42(20)
C2-N1-C4	60.63(7)	H2-C6-H3	109.05(20)
O1-C1-N1	30.94(8)	C2-N2-O2	119.29(15)
O1-C1-C6	86.10(12)	C2-N2-O3	116.77(16)
N1-C1-C2	115.38(14)	O2-N2-O3	123.90(17)
N1-C1-C6	117.03(15)	C2-O2-N2	33.63(9)
N1-C1-H1	143.46(12)	C2-O2-O3	61.70(7)
C2-C1-C6	127.54(16)	N2-O2-O3	28.08(10)
N1-C2-N2	151.65(13)	C2-O3-N2	35.02(10)
C1-C2-C3	123.25(16)	C2-O3-O2	63.03(7)
C1-C2-N2	119.76(15)	N2-O3-O2	28.02(10)
C1-C2-O2	96.72(12)	C2-C3-C4	118.02(16)
C1-C2-O3	141.52(13)	C2-C3-H7	120.71(18)
C3-C2-N2	116.99(15)	C5-C7-H4	110.67(21)
C3-C2-O2	137.48(14)	C5-C7-H5	110.74(21)
C3-C2-O3	92.64(12)	C5-C7-H6	110.47(20)
N2-C2-O2	27.08(8)	H4-C7-H5	108.24(22)
N2-C2-O3	28.21(8)	H4-C7-H6	108.22(23)
O2-C2-O3	55.27(7)	H5-C7-H6	108.41(25)

The Cu-Cl bond length of 2.229(0) Å is similar to other terminal Cu-Cl bond lengths in related complexes.[130,134] The Cu-O bond length of 1.949(1) Å is, as expected shorter than bridging bond lengths of 1.949(1) Åand 2.036 Å in the dimeric $CuCl_2$.(Py-NO) complex.[130] The $Cu-O_1-N_1$ bond angle is 121.24(9)° as would be required by trigonal planar sp^2 bonding (120°).[129] This angle is slightly smaller than those observed in the 1:1 dimeric complex $CuCl_2$.(Py-NO) (123.5(1.6) and 127(1.7)°).[130] The $N-O_1$ bond length is 1.347(2) Å, slightly shorter than that reported in pyridine N-oxide (1.37 Å) and is in the range reported for the N-O bond length in the dimeric copper(II) halide 1:1 complexes.[130,144,234]

Comparison of the bond lengths and bonding angles in the ligand with those observed in related ligands revealed that the C-C bond lengths in 3-nitro 2,6-lutidine N-oxide are very close to those observed in pyridine N-oxide, with C-C bonds parallel to the long molecular axis of the ligand longer than the other C-C and N-C bonds.[234] The C_1-C_6 and C_5-C_7 bond lengths at 1.480(3) and 1.489(2) Å are slightly shorter than those observed in 4-nitro 3-picoline N-oxide (1.515 Å) and 4-nitro 3,5-lutidine N-oxide (1.510 and 1.516 Å) probably due to the hyperconjugation of the methyl groups with the ring system. The nitro group is displaced from the plane of the ring with an angle of 33.7°. The reason for this displacement is not very clear and could arise either because of the steric effect of the methyl group on the carbon atom adjacent to the carbon containing the nitro group, or due to electronic and coordination requirements of the ligand. Such a twisting should occurr relatively easily because of the single bond character of C_2-N_2 at 1.476 Å.

The Structure of $CuBr_2$.(2,6-$(CH_3)_2$ 4-NO_2 Py-NO)$_2$ (Dark brown)

This compound crystallises in the orthorhombic system with a = 6.875 Å, b = 16.6511 Å, c = 17.0345 Å and β = 90.00°, space group Pbca. The complex may be described as trans-square planar since the Br-Cu-O bond angles are about 90.00° (Fig. 13); however the Cu-Br bonds are shorter (2.272 Å) than the Cu-O bonds (2.689 Å) contrary to what was expected. The angle that the plane containing N_1-O_1-Cu makes with the plane containing the pyridine ring was not

calculated; however, as it is seen in figure 13, the two planes should almost be perpendicular to each other, making the structure of this compound significantly different from that of $CuCl_2.(2,6\text{-}(CH_3)_2\ 3\text{-}NO_2\ Py\text{-}NO)_2$. The dihedral angle between the basal plane and that defined by the pyridine ring is 97.1° placing one ligand on each side of the basal plane. The long $Cu\text{-}O_1$ bond length and the orientation of the ligands with respect to the basal plane leave the two axial positions unoccupied, thus allowing some interaction to take place between a nitro-oxygen and a neighbouring copper ion (Fig. 14). This distance at 3.55 Å is very long for a Cu-O coordinated bond. Some of the bonding and nonbonding angles and distances are listed in Table 14 and 15 respectively.

It should be noted that $Cu\text{-}O_1$ and $Cu\text{-}O_3$ bond lengths are longer than what was estimated from the covalent radii of copper(II) ion and oxygen. It is suggested that in a distorted tetragonal octahedron the in-plane covalent radius of the copper(II) ion is ca. 1.30 Å and its out of plane radius is ca. 1.90 Å.[235,236] An observed bond length would then be the sum of the covalent radii of the ligand and the copper(II) ion (r_S or r_L as appropriate). For non-equivalent ligands, the observed bond-lengths will still involve the sum of the appropriate covalent radii. Using this approach, the values of short (R_S) and long (R_L) copper-oxygen bond lengths are estimated as (1.30 + 0.73 = 2.09 Å) and (1.90 + 0.73 = 2.63 Å) respectively as found in many pyridine N-oxide complexes. The observed $Cu\text{-}O_1$ and $Cu\text{-}O_3$ bond lengths at 2.689 Å and 3.55 Å are much longer than the estimated values, and therefore, could hardly be regarded as bonds. This situation is very strange since in square-coplanar complexes, the observed in-plane copper-ligand bonds are shorter than in the tetragonal-octahedral case.[237,238]

Another way of describing this complex would be to consider a linear Br-Cu-Br structure with four semi-coordinated ligands on the other axis of a grossly distorted tetragonal structure.

No indication of a quinoidal nature in the ligand in this complex was observed. The average C-C distance, 1.38 Å, and the average $C\text{-}N_1$ distance, 1.35 Å, are normal. Other indications of the absence

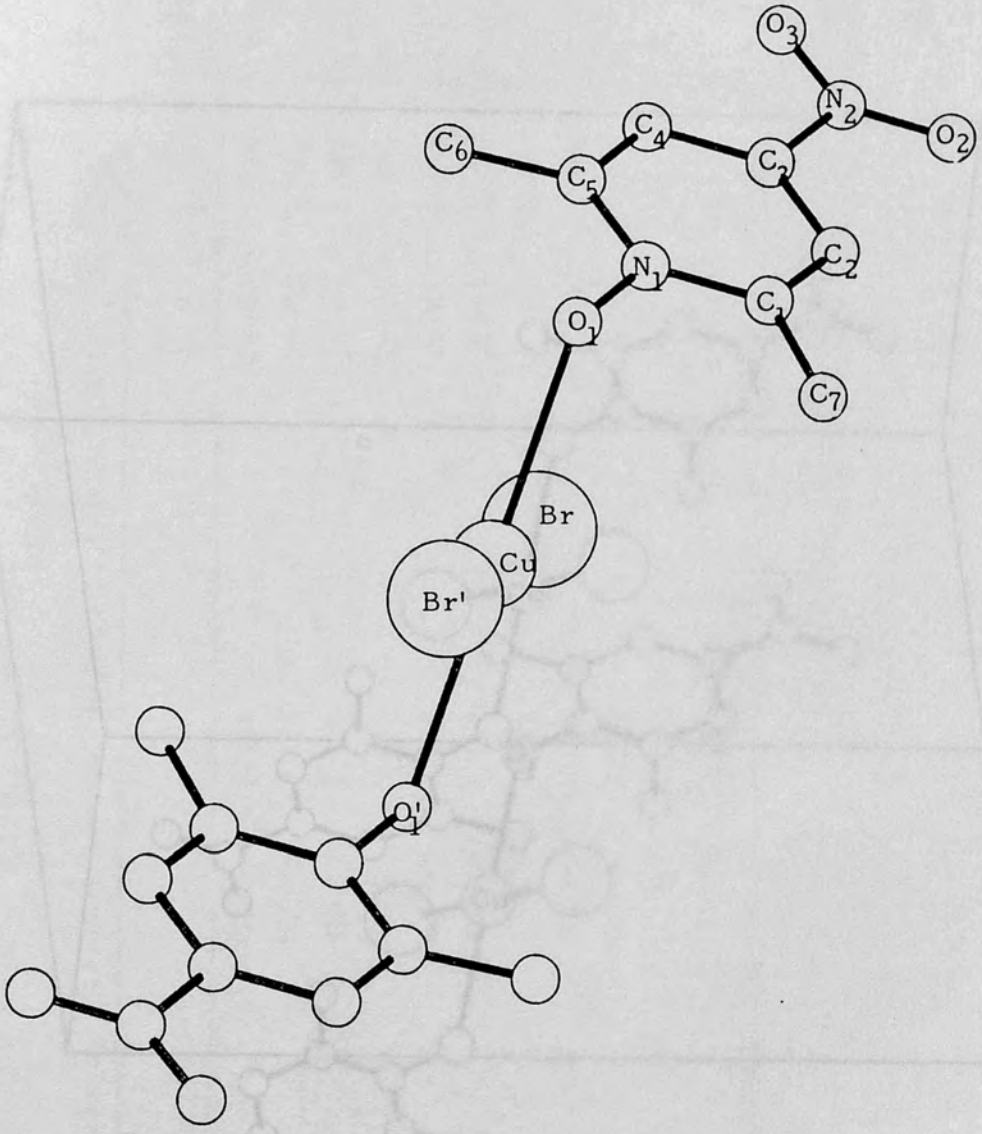

Fig. 13. A view of $CuBr_2.(2,6\text{-}(CH_3)_2\ 4\text{-}NO_2\ Py\text{-}NO)_2$ (dark brown).

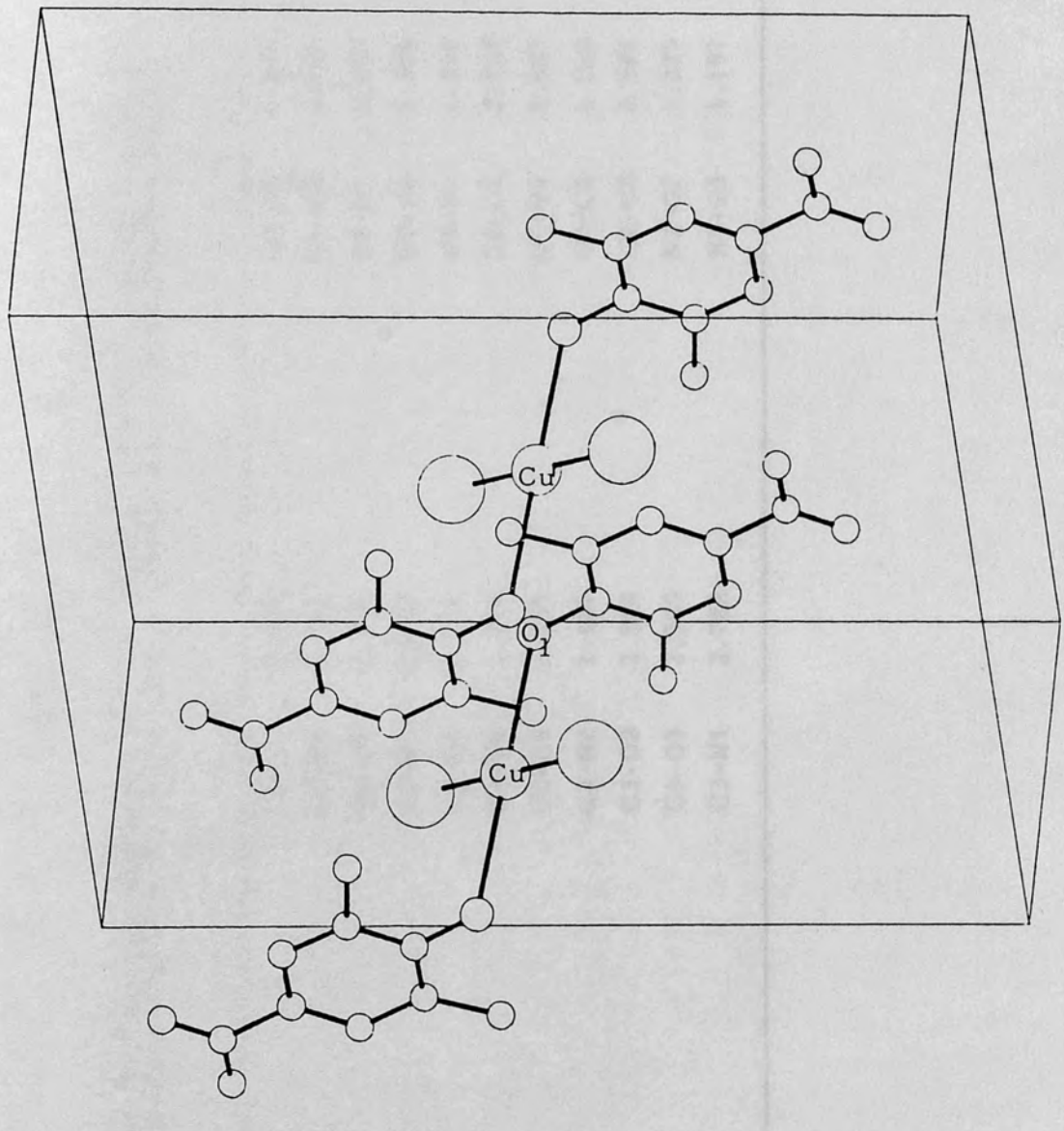

Fig. 14. A view of the complex $CuBr_2.(2,6\text{-}(CH_3)_2\ 4\text{-}NO_2\ Py\text{-}NO)_2$ (dark brown).

Table 14

Bonding and Non-bonding Distances (Å) for $CuBr_2$. $(2,6\text{-}(CH_3)_2\ 4\text{-}NO_2\ Py\text{-}NO)_2$

Cu-Br	2.272	C2-C4	2.401	C4-C5	1.374
Cu-O1	2.689	C2-C5	2.783	C4-C6	2.562
Cu-O3	3.550	C2-C7	2.527	C4-N1	2.344
Cu-Cu'	9.007	C2-N2	2.455	C5-C6	1.505
O1-N1	1.342	C2-O3	2.716	C5-N1	1.350
O1-Cu'	8.036	C3-C4	1.345	C5-O1	2.284
C1-C2	1.371	C3-C5	2.369	C6-N1	2.467
C1-C7	1.516	C3-N2	1.480	C7-C1	1.516
C1-N1	1.350	C3-O2	2.308	C7-C2	2.527
C1-O1	2.331	C3-O3	2.309	N2-O2	1.229
C2-C3	1.392	C3-N1	2.702	N2-O3	1.197

Table 15

Bonding and Non-bonding Angles (deg) for $CuBr_2.(2,6\text{-}(CH_3)_2\ 4\text{-}NO_2\ Py\text{-}NO)_2$

Cu-O1-N1	113.63	C1-C2-N1	29.21	O2-C3-O3	55.85
Cu-O1-Cu'	112.35	C3-C2-C4	28.63	O3-C3-N1	151.63
Cu-O1-C6	108.07	C3-C2-C5	58.20	C3-C4-C5	121.17
Cu-O1-C7	91.87	C3-C2-N2	32.00	C6-C5-N1	116.67
Br-Cu-Br'	180.00	C2-C3-C4	121.20	C6-C5-O1	85.73
Br-Cu-O1	89.66	C4-C3-N2	121.42	N1-C5-O1	30.94
Br-Cu-O3	90.62	C4-C3-O2	92.18	C1-C7-C2	27.39
O1-Cu-O1'	180.00	C4-C3-O3	148.02	O2-N2-O3	30.61
C2-C1-N1	121.22	C4-C5-C6	125.90	C1-N1-C5	122.02
C2-C1-C7	121.26	C4-C5-N1	117.41	C1-N1-O1	120.90
C1-C2-C3	116.97	N2-C3-O2	29.25	C1-C2-C5	58.77
C1-C2-C4	88.34	N2-C3-O3	26.60	N2-C3-N1	178.17

of quinoidal structure in the ligand is the relatively long $N_1 - O_1$ bond length at 1.34 Å, which is longer than those observed in other 4-nitropyridine N-oxides,[27,56] and the $Cu-O_1-N_1$ bond angle 113.63°, as would be required by a tetrahedral disposition of oxygen lone pairs.[129] The dihedral angle between the plane of the pyridine ring and the plane representing the NO_2 group is 139.4°. Twisted NO_2 groups were also reported in 4-nitro 3-picoline N-oxide and 4-nitro 3,5-lutidine N-oxide and the reason for the twist was ascribed to the steric effects of the methyl groups on the carbons adjacent to the carbon containing the nitro group. No such effect being present in 4-nitro 2,6-lutidine N-oxide, the probable reason for the observed twist would be the semi-coordination of a nitro group oxygen with a copper(II) ion. This twisting should be relatively easy considering the almost single bond character of C_3-N_2 at 1.480 Å.

Comment on the Structure of the Complexes

The structure of the complex $CuCl_2.(2,6-(CH_3)_2\ 3-NO_2\ Py-NO)_2$ is not novel in the series of copper(II) halide pyridine N-oxides, except for its more distorted nature, i.e. O-Cu-Cl angles not being 90°. Therefore, this complex corresponds to the green isomer of 1:2 monomeric copper(II) halide complexes of pyridine N-oxides, the distortion taking place due to the steric crowding near the donor site.

The structure of $CuBr_2.(2,6-(CH_3)_2\ 4-NO_2\ Py-NO)_2$ (dark brown) is novel in that the $Cu-O_1$ bond length is very long and the orientations of the ligands are such that each ligand can interact with two different copper(II) ions through N-oxide and nitro-oxygens. The lengthening of $Cu-O_1$ bond length is most probably due to the presence of a second competetive donor site, NO_2-oxygen, in the same ligand, so that instead of forming one strong covalent bond (as expected to be present in the green isomer of this complex), two weak bonds between the Cu(II) ion and each of the donor sites are formed. This argument also explains the strange magnetic behaviour of this complex to be discussed in a later section.

3.5.2. Reflectance Spectra

The diffuse reflectance spectra of the copper(II) halide complexes are presented in figures 14-17. These spectra may be conveniently classified into three groups by region: $\bar{\nu}_1$, 10,000 - 13650 cm^{-1}; $\bar{\nu}_2$, 15,200 - 16,500 cm^{-1}; $\bar{\nu}_3$, 18,000 - 21,300 cm^{-1}.

$\bar{\nu}_1$: All the spectra show a band of relatively low intensity in this region. From the frequency and intensity, the band in this region can undoubtedly be attributed to the so called copper band, a transition within the d shell. From the data in table 16, the following results were confirmed: 1) As expected from the spectrochemical series, the band positions of bromo complexes appear at shorter wavenumbers than those of the corresponding chloro complexes. 2) For the same substituent group, the closer the site of substitution to the central metal ion is, the greater is the energy of a d-d transition. In the case of the methyl group, e.g., these effects increase in the order 2->3-, whereas in the case of the nitro group they increase in the order 3->4-. 3) The greater the number of substituents, the higher is the energy of d-d transition, e.g., the $\bar{\nu}_1$ bands of 4-nitro 2,6-lutidine N-oxide complexes are greater than the corresponding bands of 4-nitro 2-picoline N-oxide complexes. Points 2 and 3 seem to indicate that, in these complexes, the steric factor is important in determining the position of a d-d band. This effect could be attributed to the shielding of the fifth and sixth coordination sites by chemically inert groups which increase the tetragonality of complexes and the strength of the four coordinate bonds in the plane. 4) The variation in the position of the d-d band could also be interpreted in terms of the basicities and σ-donor strengths of the ligands; 4-nitro 3-picoline N-oxide being the least basic and the weakest σ-donor among the ligands studied, will produce the smallest d-d splitting on complex formation, while 3-nitro 2,6-lutidine N-oxide being the most basic and the best σ-donor will produce the largest d-d splitting in the spectra of its complexes.

$\bar{\nu}_2$: A shoulder on the first transition $\bar{\nu}_1$ is apparent in the spectra of 1:2 complexes of 3-nitro 2,6-lutidine N-oxide, 4-nitro 2-picoline N-oxide, and 4-nitro 2,6-lutidine N-oxide. No such distinct shoulder is present in the spectrum of $CuBr_2.(2,6\text{-}(CH_3)_2\ 4\text{-}NO_2\ Py\text{-}NO)_2$ (brown),

Table 16.

Reflectance Spectra Data: Band Maxima ($cm.^{-1}$)

Ligand (L)	Complex	$\bar{\nu}_1$	$\bar{\nu}_2$	$\bar{\nu}_3$
4-Nitro 2-Picoline N-Oxide	$CuCl_2.L$	11,000		
	$CuCl_2.(L)_2$	12,600	15,200	
	$CuBr_2.(L)_2$	12,450	16,000	18,000
4-Nitro 3-Picoline N-Oxide	$CuCl_2.L$	11,000		
	$CuCl_2.(L)_2$ (orange)	11,200		
	$CuCl_2.(L)_2$ (yellow)	11,200		
	$CuBr_2.L$	10,000		18,200
4-Nitro 2,6-Lutidine N-Oxide	$CuCl_2.(L)_2$	12,800	15,500	
	$CuBr_2.(L)_2$ (green)	12,600	16,000	
	$CuBr_2.(L)_2$ (brown)	12,500		21,000
3-Nitro 2,6-Lutidine N-Oxide	$CuCl_2.(L)_2$	13,650	16,400	
	$CuBr_2.(L)_2$	13,455	16,500	21,300

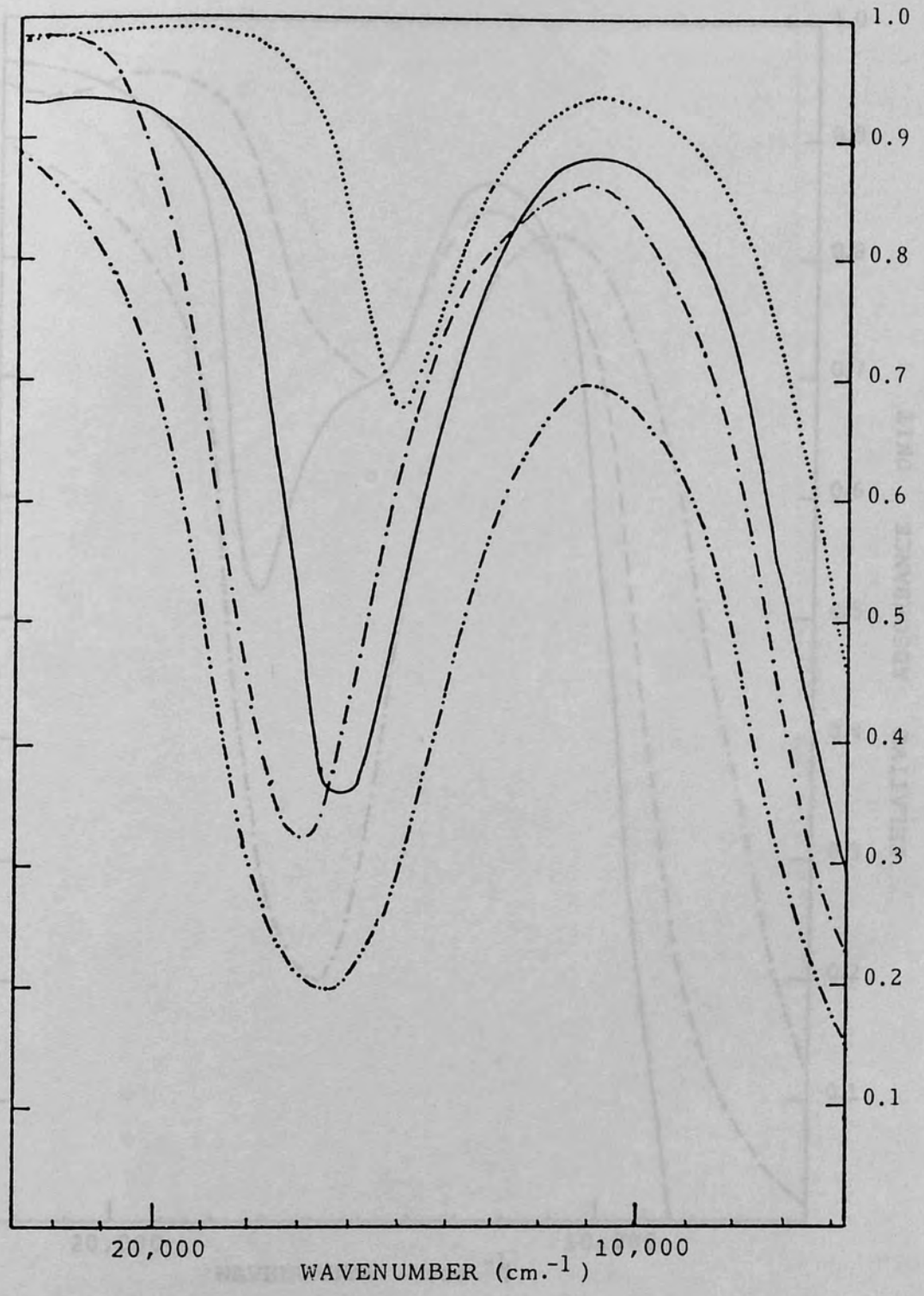

Fig. 14. Reflectance spectra of 4-nitro 3-picoline N-oxide Cu(II) halide.

—·—·—·— $CuCl_2.L$ ··—··—··— $CuCl_2.(L)_2$ (yellow)

..... $CuBr_2.L$ ———— $CuCl_2.(L)_2$ (orange)

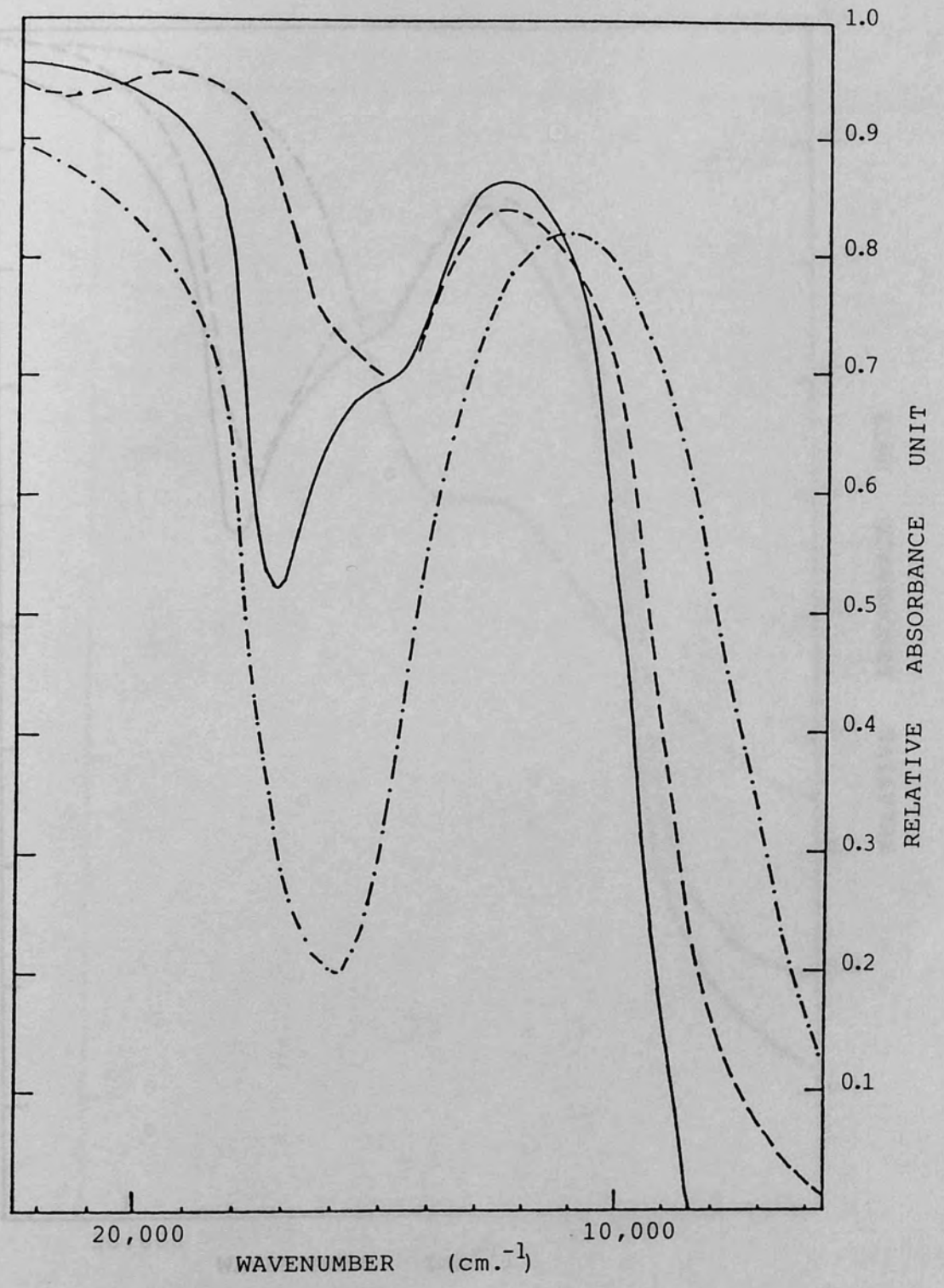

Fig. 15. Reflectance spectra of 4-nitro 2-picoline N-oxide Cu(II) halide.

—·—·—·— $CuCl_2.L$

———— $CuCl_2.(L)_2$

— — — — $CuBr_2.(L)_2$

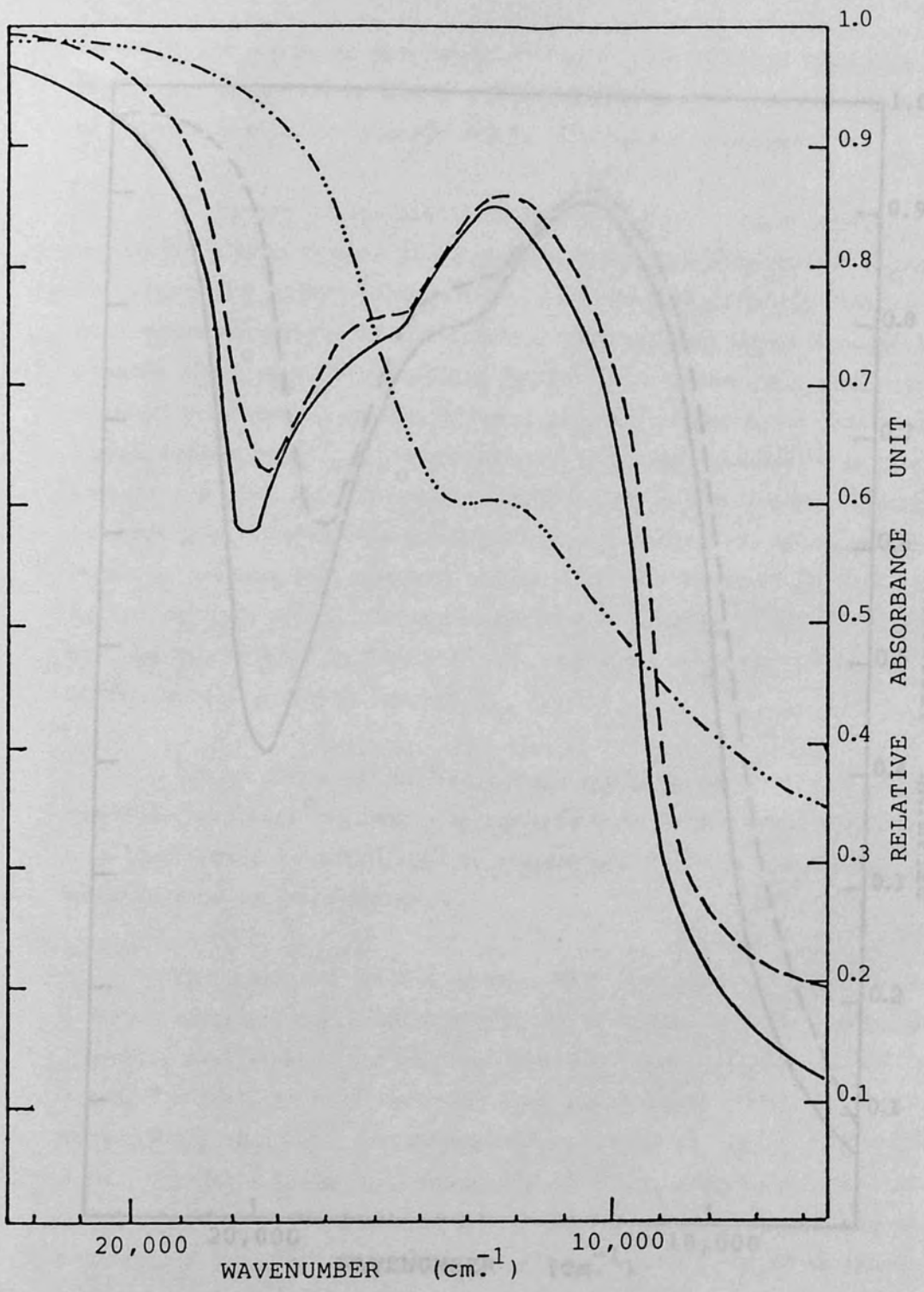

Fig. 16. Reflectance spectra of 4-nitro 2,6-lutidine N-oxide Cu(II) halide.

_ _ _ _ _ _ $CuBr_2.(L)_2$ (green) ———— $CuCl_2.(L)_2$

... _ ... _ ... _ $CuBr_2.(L)_2$ (dark brown)

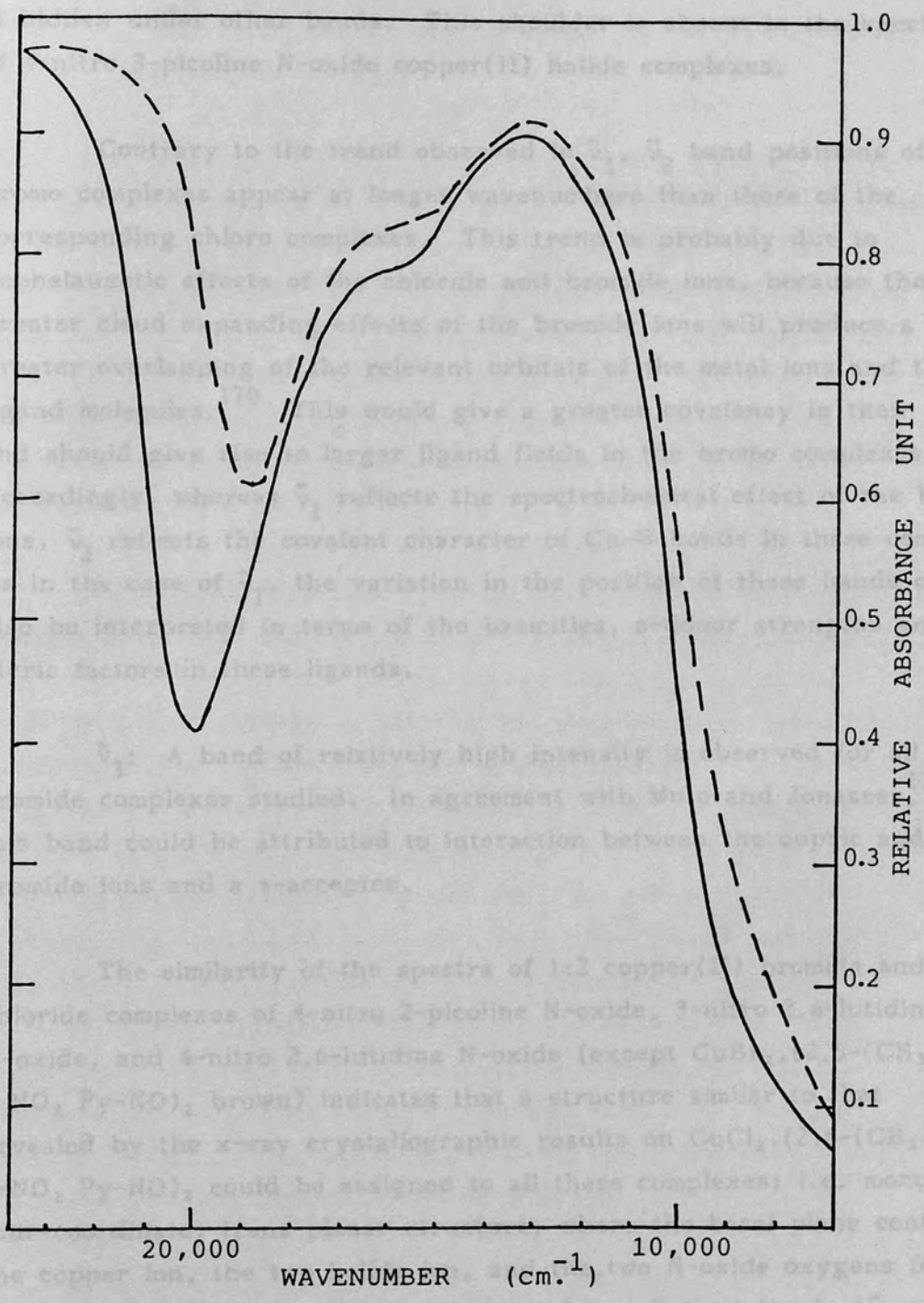

Fig. 17. Reflectance spectra of 3-nitro 2,6-lutidine N-oxide Cu(II) halide.

———— $CuCl_2.(L)_2$ — — — — — $CuBr_2(L)_2$

however the shape of the bands in the region indicate that this band is hidden under other bands. This shoulder is absent in the spectra of 4-nitro 3-picoline N-oxide copper(II) halide complexes.

Contrary to the trend observed in $\bar{\nu}_1$, $\bar{\nu}_2$ band positions of bromo complexes appear at longer wavenumbers than those of the corresponding chloro complexes. This trend is probably due to nephelauxetic effects of the chloride and bromide ions, because the greater cloud expanding effects of the bromide ions will produce a greater overlapping of the relevant orbitals of the metal ions and the ligand molecules.[170] This would give a greater covalency in their bonds and should give rise to larger ligand fields in the bromo complexes. Accordingly, whereas $\bar{\nu}_1$ reflects the spectrochemical effect of the halide ions, $\bar{\nu}_2$ reflects the covalent character of Cu-O bonds in these complexes. As in the case of $\bar{\nu}_1$, the variation in the position of these bands could also be interpreted in terms of the basicities, σ-donor strengths and the steric factors in these ligands.

$\bar{\nu}_3$: A band of relatively high intensity is observed for all the bromide complexes studied. In agreement with Muto and Jonassen,[113] this band could be attributed to interaction between the cupric and bromide ions and a π-acceptor.

The similarity of the spectra of 1:2 copper(II) bromide and chloride complexes of 4-nitro 2-picoline N-oxide, 3-nitro 2,6-lutidine N-oxide, and 4-nitro 2,6-lutidine N-oxide (except $CuBr_2.(2,6\text{-}(CH_3)_2$ $4\text{-}NO_2$ Py-NO)$_2$ brown) indicates that a structure similar to that revealed by the x-ray crystallographic results on $CuCl_2.(2,6\text{-}(CH_3)_2$ $3\text{-}NO_2$ Py-NO)$_2$ could be assigned to all these complexes; i.e. monomeric, four-coordinate, trans-planar structure, where the basal plane containing the copper ion, the two halide ion, and the two N-oxide oxygens form a rhomboid structure. The appearance of two distinct bands ($\bar{\nu}_1$ and $\bar{\nu}_2$) attributed to transitions within the d shell is probably a result of this distortion of the basal plane. Such a distortion was expected to take place because of the different ligand field strengths of the ligands and the halide ions and the steric hindrance at the donor sites in these 2- and 2,6-disubstituted nitropyridine N-oxides. The cis-tetrahedral geometry would be most stable from electrostatic and steric considerations,

since the structure of $CuBr_2.(2,6\text{-}(CH_3)_2\ Py\text{-}NO)_2$ is tetrahedral.[193] Accordingly, a back-π-bonding of the d-orbitals of the copper with the anti-bonding orbitals of the aromatic N-oxide may be responsible for stabilising the trans structure.

The spectrum of $CuBr_2.(2,6\text{-}(CH_3)_2\ 4\text{-}NO_2\ Py\text{-}NO)_2$ (brown), indicates the presence of several bands in the range 5,000 to 30,000 $cm.^{-1}$ This makes the assignment of some of them to certain d-d transitions rather ambiguous. The origin of the intense bands between 15,000 and 30,000 cm^{-1} is not clear. The high intensity of these bands could be due to charge tranfer transitions or a result of distortions from square-planar symmetry which would cause the mixing of 3d and 4s orbitals leading to an increase in the intensities of the optical transitions between the metal orbitals.

The reflectance spectra of $CuCl_2.(3\text{-}CH_3\ 4\text{-}NO_2\ Py\text{-}NO)_2$ (yellow and orange) are similar to the spectra of other previously reported monomeric 1:2 complexes. However, the spectral data are not enough to distinguish between two possible structures, i.e. cis-tetrahedral or chloride-bridged polymeric octahedral. In its spectrum $CuBr_2.(3\text{-}CH_2\ 4\text{-}NO_2\ Py\text{-}NO)$ is similar to other 1:1 dimeric complexes of pyridine N-oxides, therefore a dimeric, four-coordinate oxygen bridged structure could be assigned to this complex. The spectra of $CuCl_2.(2\text{-}CH_3\ 4\text{-}NO_2\ Py\text{-}NO)$ and $CuCl_2.(3\text{-}CH_3\ 4\text{-}NO_2\ Py\text{-}NO)$ are quite similar to the spectra of other 1:1 dimeric copper(II) chloride complexes, however the spectral data are not enough to distinguish between two possible structures, one involving bridging chloride ions, and the other involving bridging N-oxide groups, because the complexes having both geometries may absorb in the same region.

3.5.3. Visible Absorption Spectra in Solution

All the complexes were very insoluble in solvents with practically no coordinating tendency, such as benzene or chloroform, but they were soluble in organic solvents capable of coordination. The spectra in solutions are somewhat different from the reflectance spectra as shown in Table 17 and Figures 18-24. This shows

Table 17. Visible Spectral Data in a Variety of Solvents

Band Maxima (cm^{-1})

Solvents: A, Methanol; B, Acetone; C, N,N'-Dimethylformamide.

Complex	Solvent	$\bar{\nu}_1$	$\bar{\nu}_2$	$\bar{\nu}_3$
1. 4-Nitro 2-Picoline N-Oxide*				
$CuCl_2.(L)_2$	A	12,890		
	B	12,165		21,370
$CuBr_2.(L)_2$	A	11,360		
	B	**	15,340	21,460
	C	11,235	17,182	***
2. 4-Nitro 3-Picoline N-Oxide*				
$CuCl_2.(L)_2$	A	12,195		
	B	12,270		21,010
$CuBr_2.L$	A	12,270		
	B	**	15,385	***
3. 4-Nitro 2,6-Lutidine N-Oxide****				
$CuCl_2.(L)_2$	A	12,195		
	B	12,660		22,200
$CuBr_2.(L)_2$	A	12,200		
	B	**	15,290	19,230
	C	11,300	17,480	20,620
4. 3-Nitro 2,6-Lutidine N-oxide				
$CuCl_2.(L)_2$	A	12,315		
	B	12,315		***
$CuBr_2.(L)_2$	A	12,315		24,630
	B	12,200	15,290	19,920

* The spectra of the 1:1 and 1:2 complexes were the same in each solvent.

** Probable shift of band below 11,240 $cm.^{-1}$

*** Band hidden in the absorption band of the ligand.

**** The spectra of the two bromide complexes are identical.

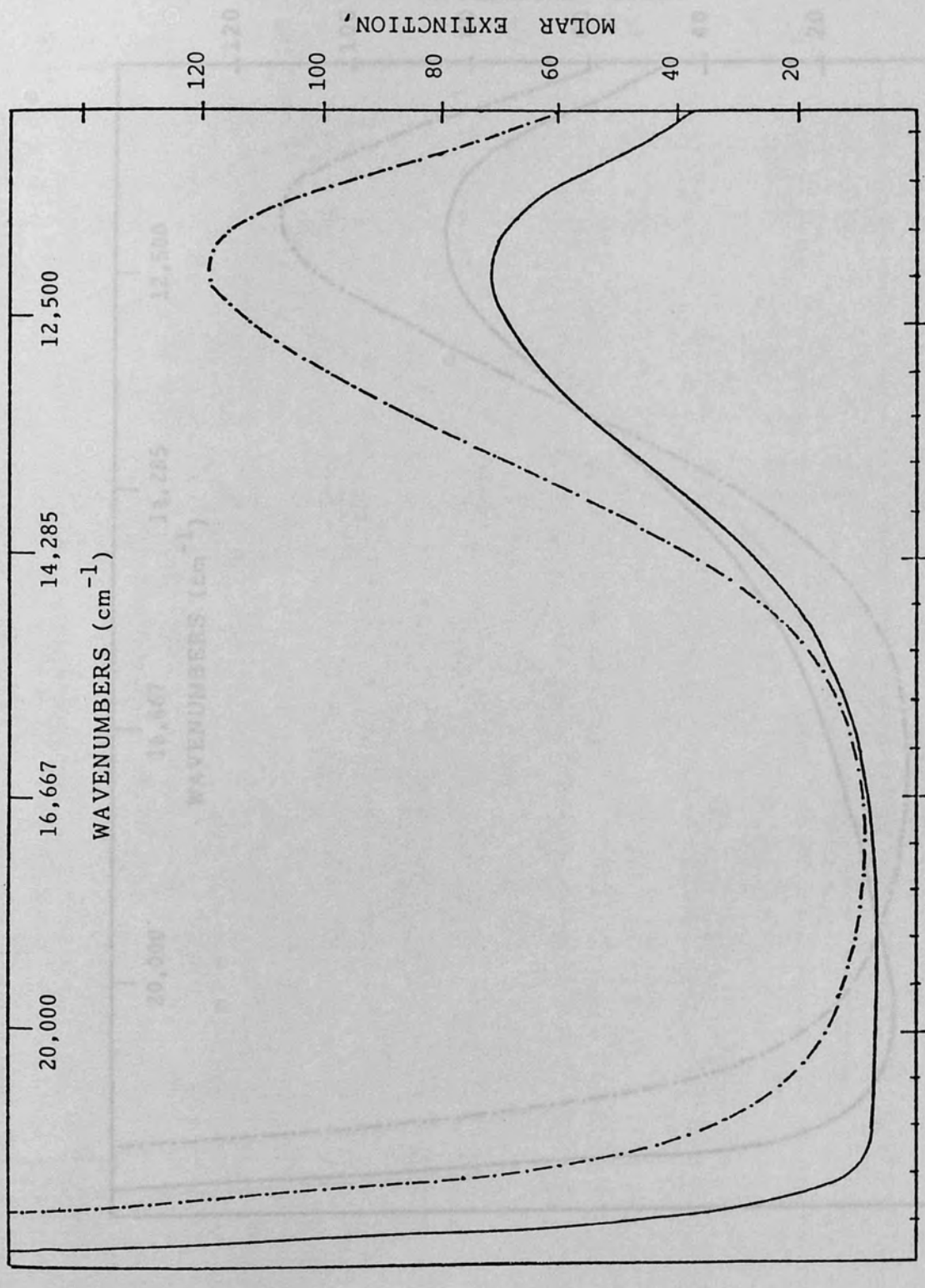

Fig. 18. Absorption spectra of 4-nitro 2-picoline N-oxide Cu(II) halides in methanol.
——— $CuCl_2.(L)_2$ —·—·—·—·— $CuBr_2.(L)_2$

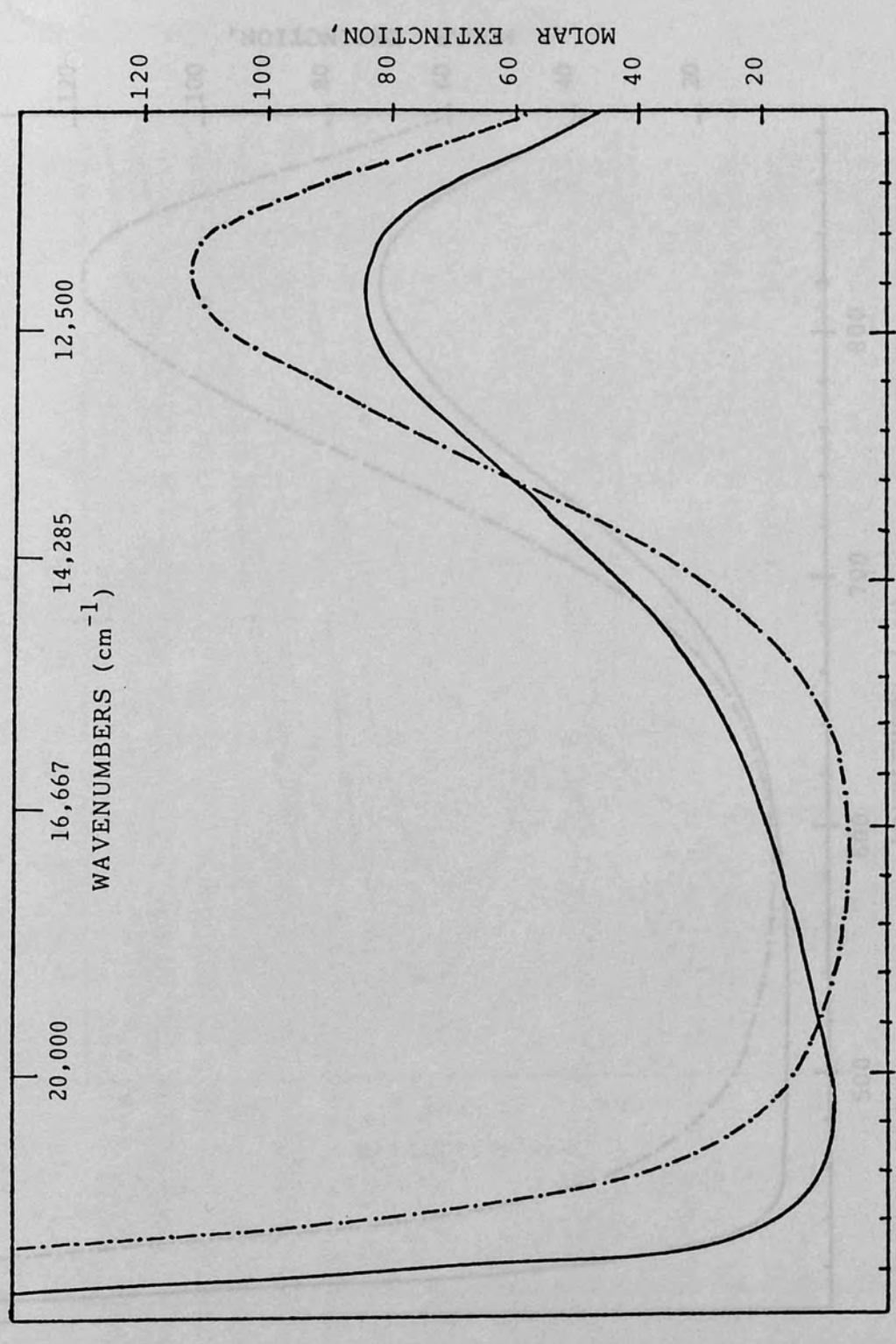

Fig. 19. Absorption spectra of 4-nitro 2,6 lutidine N-oxide Cu(II) halides in methanol.
——— $CuCl_2.(L)_2$ —·—·—·— $CuBr_2.(L)_2$

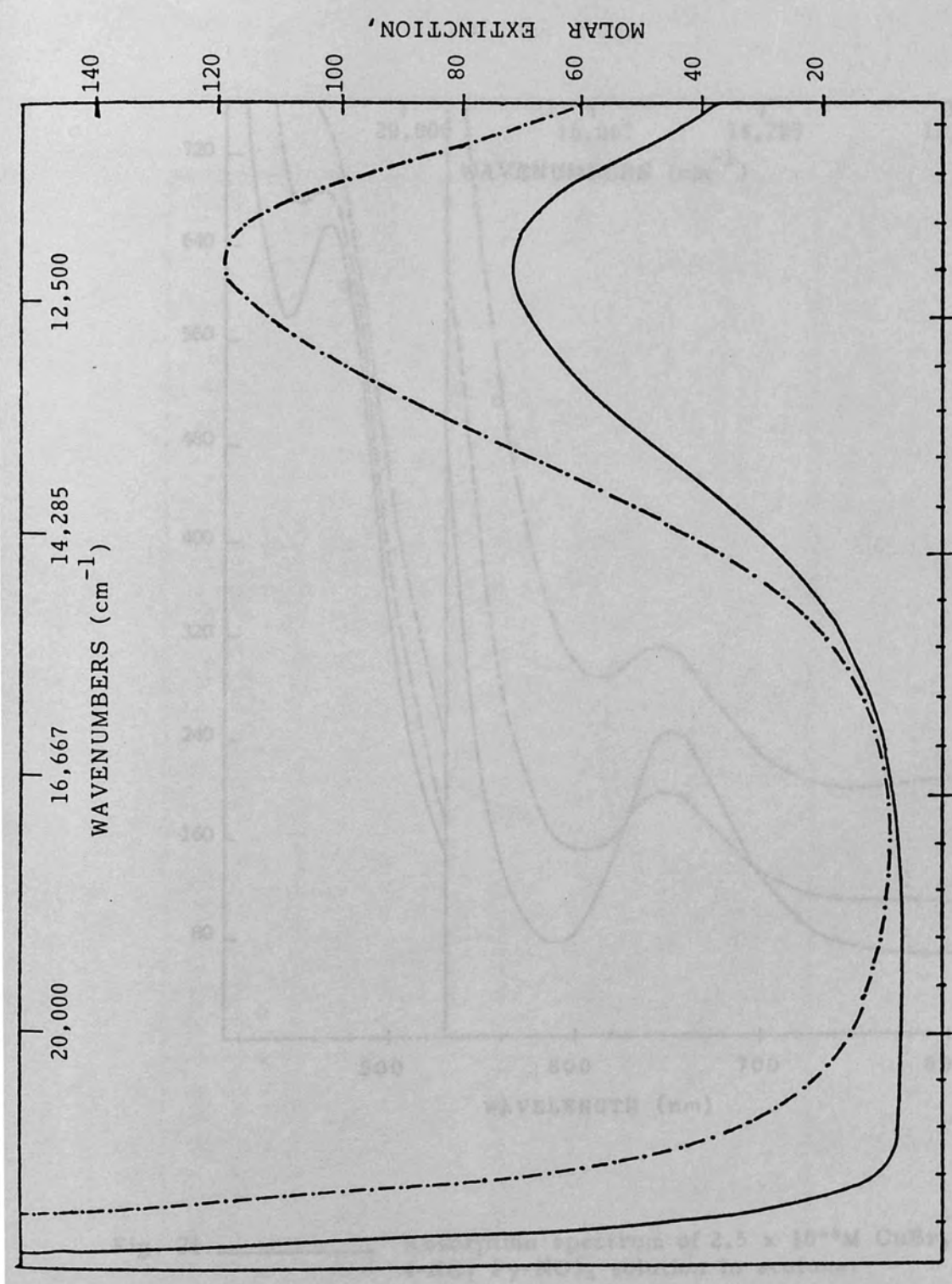

Fig. 20. Absorption spectra of 3-nitro 2,6 lutidine N-oxide Cu(II) halides in methanol.
——— $CuCl_2 .(L)_2$ —·—·—·— $CuBr_2 .(L)_2$

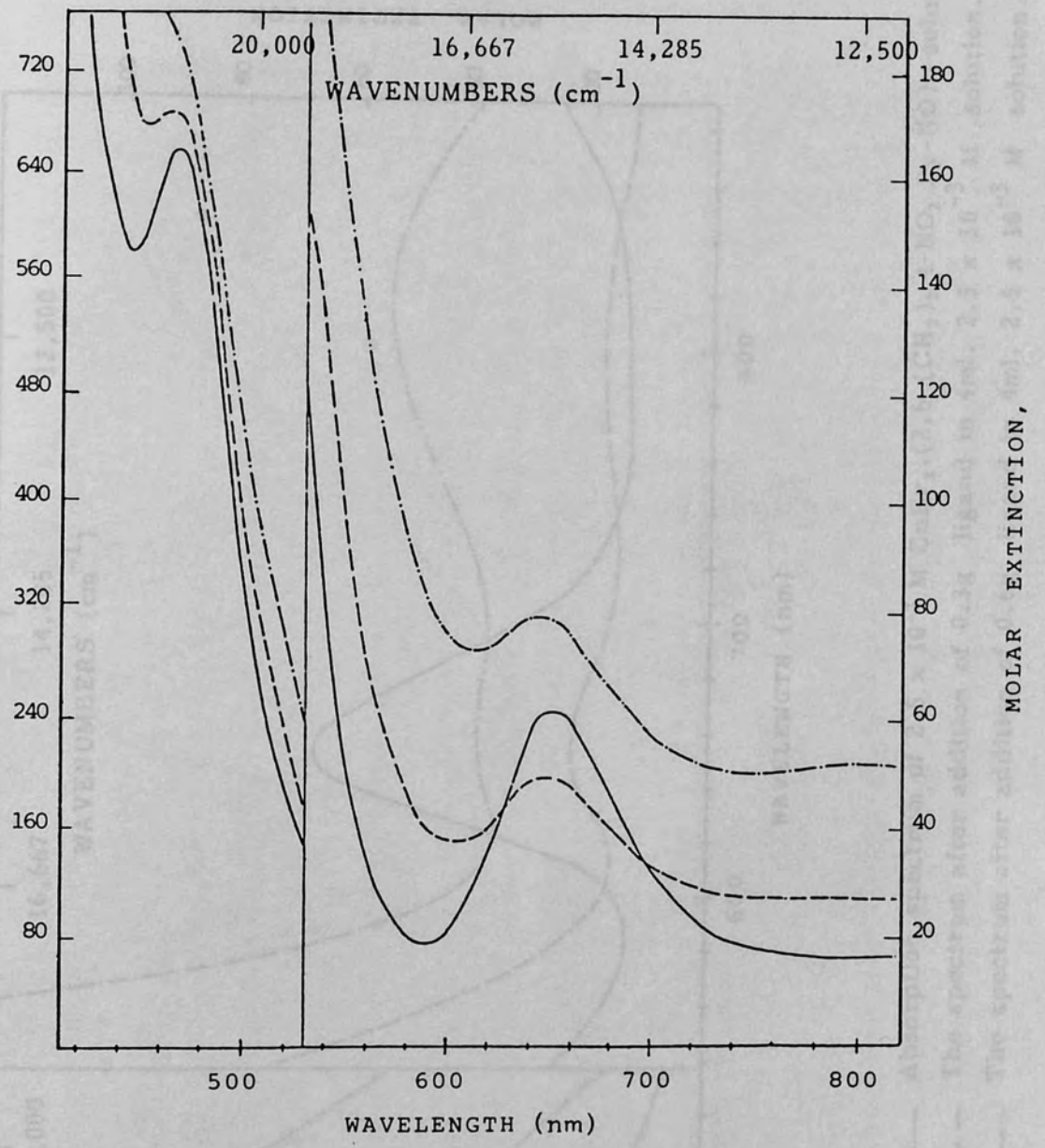

Fig. 21. ———— Absorption spectrum of 2.5×10^{-3}M $CuBr_2.(2\text{-}CH_3\ 4\text{-}NO_2\ Py\text{-}NO)_2$ solution in acetone.

– – – – – – Spectrum after addition of 0.3g ligand in 4ml of 2.5×10^{-3} M solution.

—·—·—·—·— Spectrum after addition of 0.6g ligand in 4ml of 2.5×10^{-3} M solution.

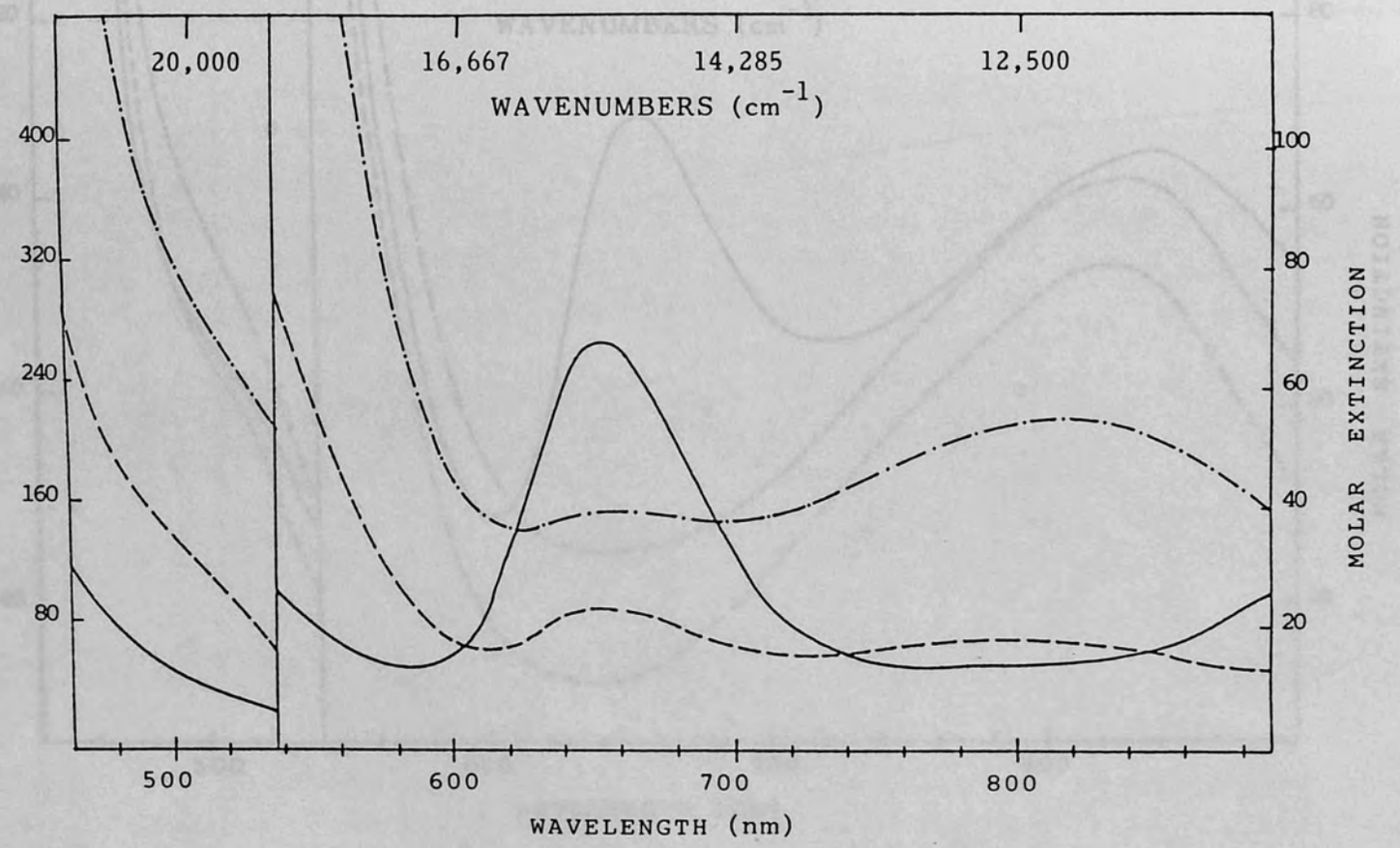

Fig. 22. ———— Absorption spectrum of 2.5×10^{-3} M $CuBr_2.(2,6\text{-}(CH_3)_2\ 4\text{-}NO_2\ Py\text{-}NO)_2$ solution in acetone.

– – – – – The spectrum after addition of 0.3g ligand in 4ml. 2.5×10^{-3} M solution.

—·—·—·— The spectrum after addition of 0.6g ligand in 4ml. 2.5×10^{-3} M solution.

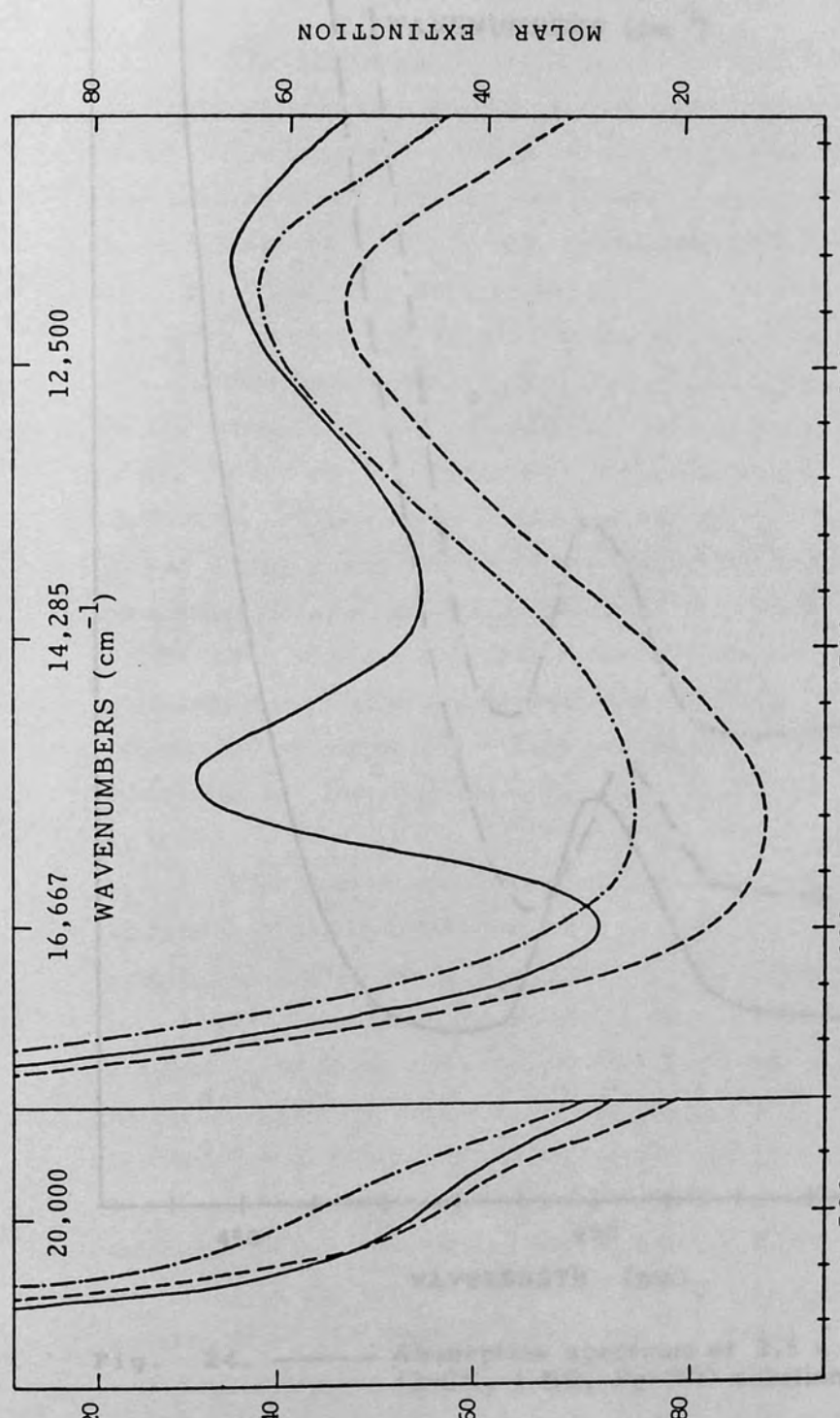

Fig. 23. ——— Absorption spectrum of 2.5×10^{-3} M $CuBr_2$.$(2,6\text{-}(CH_3)_2\ 3\text{-}NO_2\ Py\text{-}NO)_2$ solution in acetone.
– – – – The spectrum after addition of 0.3g ligand in 4ml 2.5×10^{-3} M solution.
—·—·— The spectrum after addition of 0.6g ligand in 4ml 2.5×10^{-3} M solution.

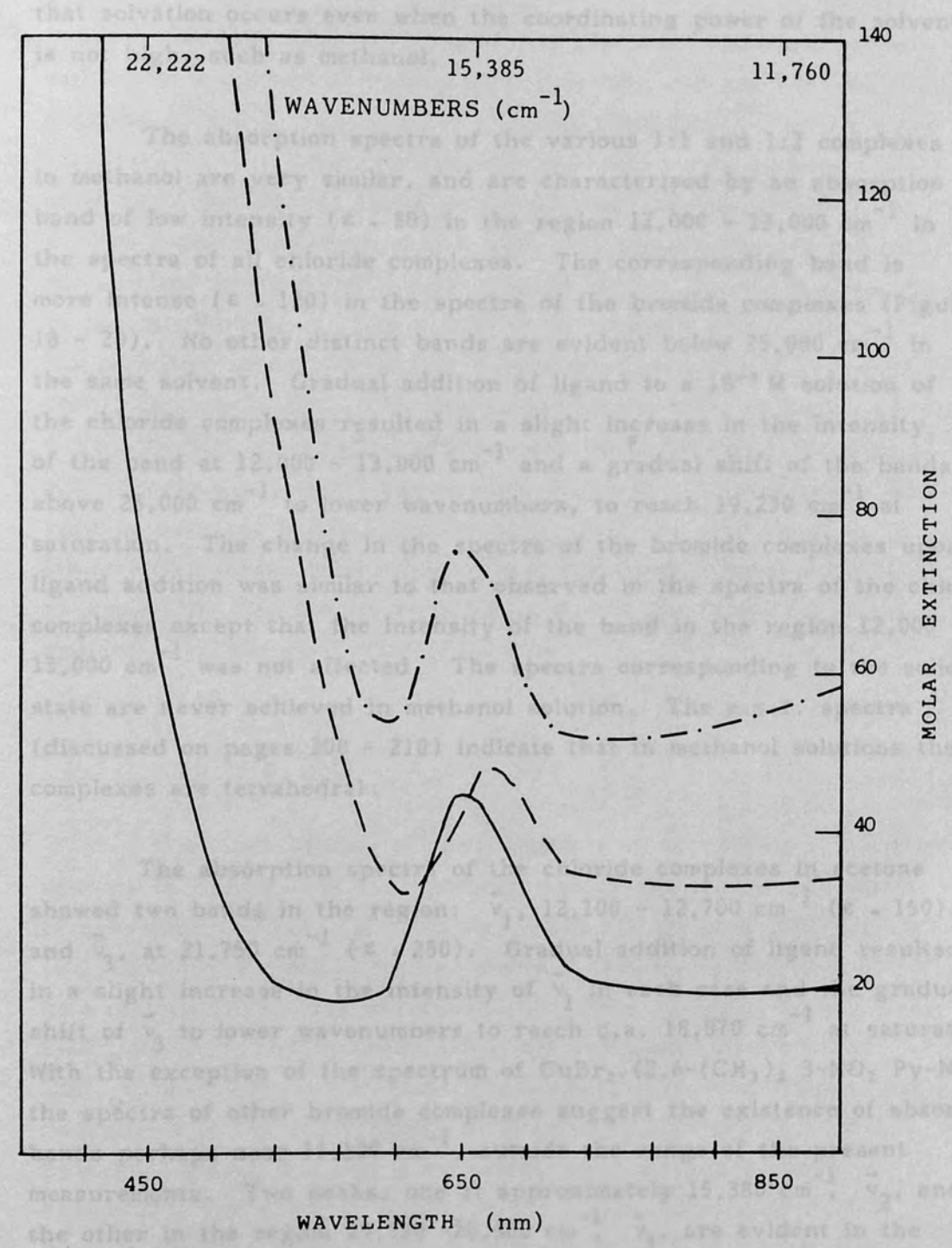

Fig. 24. ——— Absorption spectrum of 2.5×10^{-3} M $CuBr_2$. ($3\text{-}CH_3$ $4\text{-}NO_2$ Py-NO) solution in acetone.

– – – – Spectrum after addition of 0.3g ligand in 4ml of 2.5×10^{-3} solution.

–·–·– Spectrum after addition of 0.6g ligand in 4ml of 2.5×10^{-3} solution.

that solvation occurs even when the coordinating power of the solvents is not high, such as methanol.

The absorption spectra of the various 1:1 and 1:2 complexes in methanol are very similar, and are characterised by an absorption band of low intensity ($\varepsilon \sim 80$) in the region 12,000 - 13,000 cm^{-1} in the spectra of all chloride complexes. The corresponding band is more intense ($\varepsilon \sim 120$) in the spectra of the bromide complexes (Figures 18 - 20). No other distinct bands are evident below 25,000 cm^{-1} in the same solvent. Gradual addition of ligand to a 10^{-3} M solution of the chloride complexes resulted in a slight increase in the intensity of the band at 12,000 - 13,000 cm^{-1} and a gradual shift of the bands above 25,000 cm^{-1} to lower wavenumbers, to reach 19,230 cm^{-1} at saturation. The change in the spectra of the bromide complexes upon ligand addition was similar to that observed in the spectra of the chloride complexes except that the intensity of the band in the region 12,000 - 13,000 cm^{-1} was not affected. The spectra corresponding to the solid state are never achieved in methanol solution. The e.s.r. spectra (discussed on pages 208 - 210) indicate that in methanol solutions the complexes are tetrahedral.

The absorption spectra of the chloride complexes in acetone showed two bands in the region: $\bar{\nu}_1$, 12,100 - 12,700 cm^{-1} ($\varepsilon \sim 150$), and $\bar{\nu}_3$, at 21,750 cm^{-1} ($\varepsilon \sim 250$). Gradual addition of ligand resulted in a slight increase in the intensity of $\bar{\nu}_1$ in each case and the gradual shift of $\bar{\nu}_3$ to lower wavenumbers to reach c.a. 18,870 cm^{-1} at saturation. With the exception of the spectrum of $CuBr_2.(2,6\text{-}(CH_3)_2\ 3\text{-}NO_2\ Py\text{-}NO)_2$, the spectra of other bromide complexes suggest the existence of absorption bands perhaps near 11,100 cm^{-1}, outside the range of the present measurements. Two peaks, one at approximately 15,380 cm^{-1}, $\bar{\nu}_2$, and the other in the region 19,230 -25,000 cm^{-1}, $\bar{\nu}_3$, are evident in the spectra of all the bromide complexes. A band in the region of 15,380 cm^{-1} was previously reported for other pyridine N-oxide copper(II) bromide complexes in solvents which have a π-electron accepting ability, but not in solvents which do not have an appreciable π-character.[113] The band at 19,230 -25,000 cm^{-1}, $\bar{\nu}_3$, has a considerable intensity. A similar

band in the near ultraviolet region has also been observed in the spectra of a number of copper(II) complexes, and has been variously ascribed to a d-d transition,[239] a ligand transition,[240] or a charge transfer.[241] The variation of the visible absorption spectra upon addition of the ligands to the copper(II) bromide complexes of 4-nitro 2-picoline N-oxide and 4-nitro 2,6-lutidine N-oxide indicated the gradual formation of a peak near 12,350 cm^{-1}, a relative decrease in the intensity of $\bar{\nu}_2$, and a shift of $\bar{\nu}_3$ to lower wavenumbers, implying the formation of monomeric four coordinate species as in the solid state (Figures 21,22). The change in the spectrum of $CuBr_2.(3\text{-}CH_3$ $4\text{-}NO_2$ Py-NO) upon ligand addition was quite different, no sign of a band near 12,350 cm^{-1} appearing even at ligand saturation. The relative decrease in the intensity of $\bar{\nu}_2$, and the shifting of $\bar{\nu}_3$ to lower wavenumbers in the spectrum of the latter complex in a large excess of the ligand most probably is due to the formation of 1:1 dimeric species as in the solid state (Fig. 24).

3.5.4. Magnetic Data

The susceptibility of the complexes as a function of temperature appears in Tables 18 - 21. One can readily see that in the series of complexes $CuX_2.L_2$ (X = Cl, Br), only the complex $CuBr_2.(2,6\text{-}(CH_3)_2$ $4\text{-}NO_2$ $Py\text{-}NO)_2$ (brown) shows s subnormal magnetic moment. As expected from x-ray crystallographic data on $CuCl_2.(2,6\text{-}(CH_3)_2$ $3\text{-}NO_2$ $Py\text{-}NO)_2$ and the reflectance spectral data, all the other $CuX_2.L_2$ complexes are magnetically normal. The temperature dependence of the susceptibilty of the $CuBr_2.(2,6\text{-}(CH_3)_2$ $4\text{-}NO_2$ $Py\text{-}NO)_2$ (brown) complex is extraordinary. As can be seen (Table 20), the magnetic moment is low at room temperature and remains constant within ±0.05 units down to 87.7 K. Apparently, in this complex the antiferromagnetic spin coupling is affected by way of the π-system of the heterocyclic ligand, and the constant magnetic moment as the temperature decreases is due to slight changes in the lattice which changes Cu - O_1 Cu - O_3 bond distances and/or some bond angles with a consequent change in the delocalisation properties of the bridging ligand to just compensate

Table 18

Magnetic Susceptibility Data for
4-Nitro 2-Picoline N-Oxide Cu(II) Halides

Compound	Diamagnetic Correction x 10^6 cgs	Temp. K	Magnetic Susceptibility $\chi_{m'}$ x 10^6 cgs	Magnetic moment BM
$CuCl_2.L$	124.43	85.5	5835.76	2.05
		101	5068.91	2.03
		132.8	3768.62	2.01
		164.7	2985.10	1.99
		197	2451.65	1.97
		229.5	2068.22	1.96
		264.5	1778.16	1.95
		296	1588.11	1.95
$CuCl_2.L_2$	202.06	88	4422.52	1.77
		103.2	3800.34	1.78
		132.3	3011.785	1.79
		164.5	2435.69	1.80
		196.7	2029.59	1.79
		229.5	1738.63	1.79
		261.5	1529.73	1.80
		294	1380.16	1.81
$CuBr_2.L_2$	224.46	88.5	4840.34	1.86
		103	4150.73	1.86
		134	3267.89	1.88
		164	2697.73	1.89
		197.2	2254.67	1.89
		228.2	1941.92	1.89
		263.2	1702.145	1.90
		296	1535.345	1.91

Table 19

Magnetic Susceptibility Data for

4-Nitro 3-Picoline N-Oxide Cu(II) Halides

Compound	Diamagnetic Correction x 10^6 cgs	Temp. K	Magnetic Susceptibility $\chi_m \times 10^6$ cgs	Magnetic moment BM
$CuCl_2.L$	124.43	85.0	178.25	0.35
		101.5	186.16	0.39
		113.5	196.31	0.43
		165.3	235.12	0.56
		198	269.03	0.66
		230.4	312.50	0.76
		263.0	350.88	0.86
		295.3	412.66	0.99
$CuCl_2.L_2$ (orange)	202.06	87.8	4728.05	1.83
		99.5	4186.21	1.83
		132	3159.11	1.83
		164	2532.98	1.83
		228.3	1821.785	1.83
		295.7	1402.64	1.83
$CuCl_2.L_2$ (yellow)	202.6	88.3	4656.46	1.82
		99.8	4106.43	1.82
		164.3	2564.87	1.84
		230	1847.50	1.85
		296	1432.98	1.85
$CuBr_2.L$	146.83	196.7	15.69	0.16
		229.8	30.51	0.41
		262.7	89.80	0.44
		295.7	98.69	0.49

Table 20

Magnetic Susceptibility Data for

4-Nitro 2,6-Lutidine N-Oxide Cu(II) Halides

Compound	Diamagnetic Correction x 10^6 cgs	Temp. K	Magnetic Susceptibility χ_m x 10^6 cgs	Magnetic moment BM
$CuCl_2.L_2$	225.78	86.7	4400.61	1.75
		101.1	3808.64	1.76
		132.3	2960.83	1.78
		164.2	2387.09	1.78
		196.5	2002.31	1.78
		228.3	1723.35	1.78
		263.7	1490.62	1.78
		295.2	1346.22	1.79
$CuBr_2.L_2$ (Dark brown)	248.18	83.7	1503.35	1.01
		99	1276.35	1.01
		132.5	959.30	1.01
		164.2	784.26	1.02
		197	667.66	1.03
		229.5	590.30	1.045
		263	524.08	1.05
		297	469.21	1.06
$CuBr_2.L_2$ (Dark green)	248.18	87.7	4470.52	1.78
		100.5	3967.16	1.79
		131	3039.32	1.79
		163.1	2475.85	1.80
		195	2051.37	1.80
		230	1742.35	1.80
		260.4	1559.50	1.81
		292	1396.98	1.81

Table 21

Magnetic Susceptibility Data for

3-Nitro 2,6-Lutidine N-Oxide Cu(II) Halides

Compound	Diamagnetic Correction x 10^6 cgs	Temp. K	Magnetic Susceptibility $\chi_{m'}$ x 10^6 cgs	Magnetic Moment BM
$CuCl_2.L_2$	225.78	86.5	4403.58	1.75
		99	3869.64	1.76
		131.5	2981.61	1.78
		163.7	2397.09	1.78
		196.5	2014.91	1.79
		229.5	1717.02	1.78
		262	1520.30	1.79
		293.5	1340.448	1.78
$CuBr_2.L_2$	248.18	86.7	4409.26	1.76
		100.1	3871.64	1.77
		132	2975.62	1.78
		164.1	2396.11	1.78
		196.2	2003.86	1.78
		229.3	1706.86	1.78
		262.7	1503.13	1.78
		295.2	1336.45	1.78

for the expected decrease in the moment.[242] A similar superexchange mechanism operating through bridging heterocyclic ligands is also postulated in a number of heterocyclic diamine bridged copper(II) complexes such as the 1,5-naphthyridine copper(II) complex, $Cu(NO_3)_2.nap$[243] in which the Cu-Cu separation (~ 9 Å) is quite large. In the present complex the angle O_3 - Cu - Br is 90.62°, while Cu-Cu' distance is 9.007Å, very close to the value reported for 1,5-naphtyridine copper(II) complex. The $Cu-O_1$ bond distance (2.689 Å) and $Cu-O_3$ distance (3.55 Å) are larger than Cu-O semicoordination distances, therefore in this complex the spacial distribution of the coordinated atoms, and the dihedral angles formed between the plane of the coordinated atoms and that defined by the pyridine ring (97.1°) and the dihedral angle between the nitro group and the pyridine ring are more important in determining the extent of superexchange by virtue of overlap between the copper d orbitals and the N-oxide system than the Cu-O bond distances.

In the series of complexes $CuX_2.L$ (X = Cl, Br), the complexes $CuCl_2.(3\text{-}CH_3\ 4\text{-}NO_2$ Py-NO) and $CuBr_2.(3\text{-}CH_3\ 4\text{-}NO_2$ Py-NO) revealed temperature dependent subnormal magnetic moments characteristic for 1:1 dimeric pyridine N-oxide copper(II) complexes. The room temperature magnetic moments of these complexes (Table 19) are very close to the moments reported for the corresponding 4-nitropyridine N-oxide complexes (Table 2) suggesting the insignificant contribution of the methyl group at position 3 to the magnetic moment. The lower magnetic moment of the bromo complex as compared to the chloro complex is in accordance with previous results on various dimeric 1:1 complexes.[167-171] The difference in magnetic moments of chloro and bromo complexes is much bigger than what would be expected from the difference in spin-orbit coupling and temperature independent paramagnetism between these complexes. Therefore, Nephelauxetic effects of the chloride and bromide ions are at least partly responsible for the observed difference in the magnetic moments of the chloro and the bromo complexes. The greater covalency in the bonds of the bromo

complexes should give smaller magnetic moments for the bromo complex.

The magnetic properties of $CuCl_2$(2-CH_3 4-NO_2 Py-NO) are interesting, because , this is the only 1:1 $CuCl_2$.L (L = substituted pyridine N-oxide) complex, reported so far, exhibiting a normal magnetic moment. A number of nitro substituted quinoline and methyl quinoline N-oxides are also reported to form 1:1 complexes with normal magnetic moments.[113,192,201] Accordingly, as quinoline N-oxide is a ligand corresponding to a 2,3-disubstituted pyridine N-oxide, it is evident that the presence of an electron-withdrawing group and steric crowding at position 2 of the pyridine ring are responsible for this effect. Other evidences suggesting that steric factors become more important in the presence of a nitro group are: 1) the lack of formation of 1:1 complexes with 4-nitro and 3-nitro lutidine N-oxides, 2) the existence of magnetically sub-normal 1:1 lutidine N-oxide copper(II) halide complexes, 3) Our results on copper acetate substituted pyridine N-oxide complexes. Thus, the shorter N=O bond distance in the ligands containing a nitro group, would imply a further approach of the methyl group to the copper ions. This steric interaction is expected to be stronger in the dimeric 1:1 complexes than in monomeric N-oxide complexes, because the reported Cu-O-Cu bond angle is approximately 108° and the Cu-O-N bond angle is approximately 123.5° in the dimeric 1:1 copper(II) halide complexes.[130,134] Therefore a di- or polymeric structure with chloride bridges would account for the magnetic properties of $CuCl_2$.(2-CH_3 4-NO_2 Py-NO) since Willett and co-workers[244] have pointed out that bi-nuclear entities formed by bridging copper ions with chloride ions do not tend to be diamagnetic.

3.5.5. E.S.R. Results

X-band e.s.r. spectra of polycrystalline samples were recorded at room temperature (Table 22) and at temperatures in the range of 98-115K. The powder spectra of the complexes $CuCl_2.(3\text{-}CH_3\ 4\text{-}NO_2\ Py\text{-}NO)$ and $CuBr_2.(3\text{-}CH_3\ 4\text{-}NO_2\ Py\text{-}NO)$ were very informative in that they showed a transition at "half-field" confirming the antiferromagnetic dimeric nature of these complexes. The spectra of some complexes were very complicated and difficult to interpret. The spectra of the complexes in methanol were also recorded. The solid solution spectra of the complexes were all similar, showing hyperfine splitting in each case (Table 23).

Spectra of Polycrystalline 1:1 Complexes

$CuBr_2.(3\text{-}CH_3\ 4\text{-}NO_2\ Py\text{-}NO)$

The e.s.r. spectra of a powdered sample recorded at room temperature and at 98K are shown in Fig. 25 tracing A and B respectively. The room temperature spectrum exhibits an H_{MIN}, the minimum position of absorption in the spectrum of spin-coupled Cu(II) dimers. This is to be expected from a dimeric electronic system interacting simultaneously with the two copper nuclei each with a nuclear spin 3/2. This resonance at "half-field" is a formally forbidden transition corresponding to $\Delta M_S = \pm 2$ which takes place between $|1\ -1\rangle$ and $|1\ 1\rangle$ triplet levels and is expected not to show any zero-field splitting. It should be noted, however, that the intensity of the $\Delta M_S = \pm 2$ transition does depend in second order on the zero-field splitting. In the present case the intensity of this transition is approximately 0.05 times that of the $\Delta M_S = \pm 1$ transition. Finally, it should be noted that in an exchange-coupled Cu(II) dimer, the copper hyperfine spacing is half that of the analogous Cu(II) monomer.[233] At least nine copper hyperfine lines, ranging in spacing from 65 to 90G, with an average of 75G are discernible. A pattern of nine hyperfine lines results from an overlapping of two seven line patterns if the zero-field splitting in this (g) signal is equal

Table 22. Room-Temperature E.S.R. Data

Complex	g_1	g_2	g_3	$g_\perp$	$g_\parallel$	$g_{av.}$	g_{MIN}
$CuCl_2.(2\text{-}CH_3\ 4\text{-}NO_2\ Py\text{-}NO)$	..	..	..	..	..	2.110	..
$CuCl_2.(2\text{-}CH_3\ 4\text{-}NO_2\ Py\text{-}NO)_2$	2.044	2.100	2.200	..	..	..	..
$CuBr_2.(2\text{-}CH_3\ 4\text{-}NO_2\ Py\text{-}NO)_2$	2.040	2.086	2.300	..	..	..	..
$CuCl_2.(3\text{-}CH_3\ 4\text{-}NO_2\ Py\text{-}NO)$	..	..	..	2.120	..	..	4.416
$CuCl_2.(3\text{-}CH_3\ 4\text{-}NO_2\ Py\text{-}NO)_2$ (orange)	..	..	..	2.059	2.301	..	..
$CuCl_2.(3\text{-}CH_3\ 4\text{-}NO_2\ Py\text{-}NO)_2$ (yellow)	2.048	2.088	2.335	..	..	..	..
$CuBr_2.(3\text{-}CH_3\ 4\text{-}NO_2\ Py\text{-}NO)$	..	..	..	2.152	..	..	4.580
$CuCl_2.(2,6\text{-}(CH_3)_2\ 4\text{-}NO_2\ Py\text{-}NO)_2$	2.051	2.140	2.191	..	..	..	..
$CuBr_2.(2,6\text{-}(CH_3)_2\ 4\text{-}NO_2\ Py\text{-}NO)_2$	2.054	2.130	2.164	..	..	..	..
$CuCl_2.(2,6\text{-}(CH_3)_2\ 3\text{-}NO_2\ Py\text{-}NO)_2$	..	..	..	2.055	2.270	..	..
$CuBr_2.(2,6\text{-}(CH_3)_2\ 3\text{-}NO_2\ Py\text{-}NO)_2$	2.037	2.062	2.241	..	..	..	..

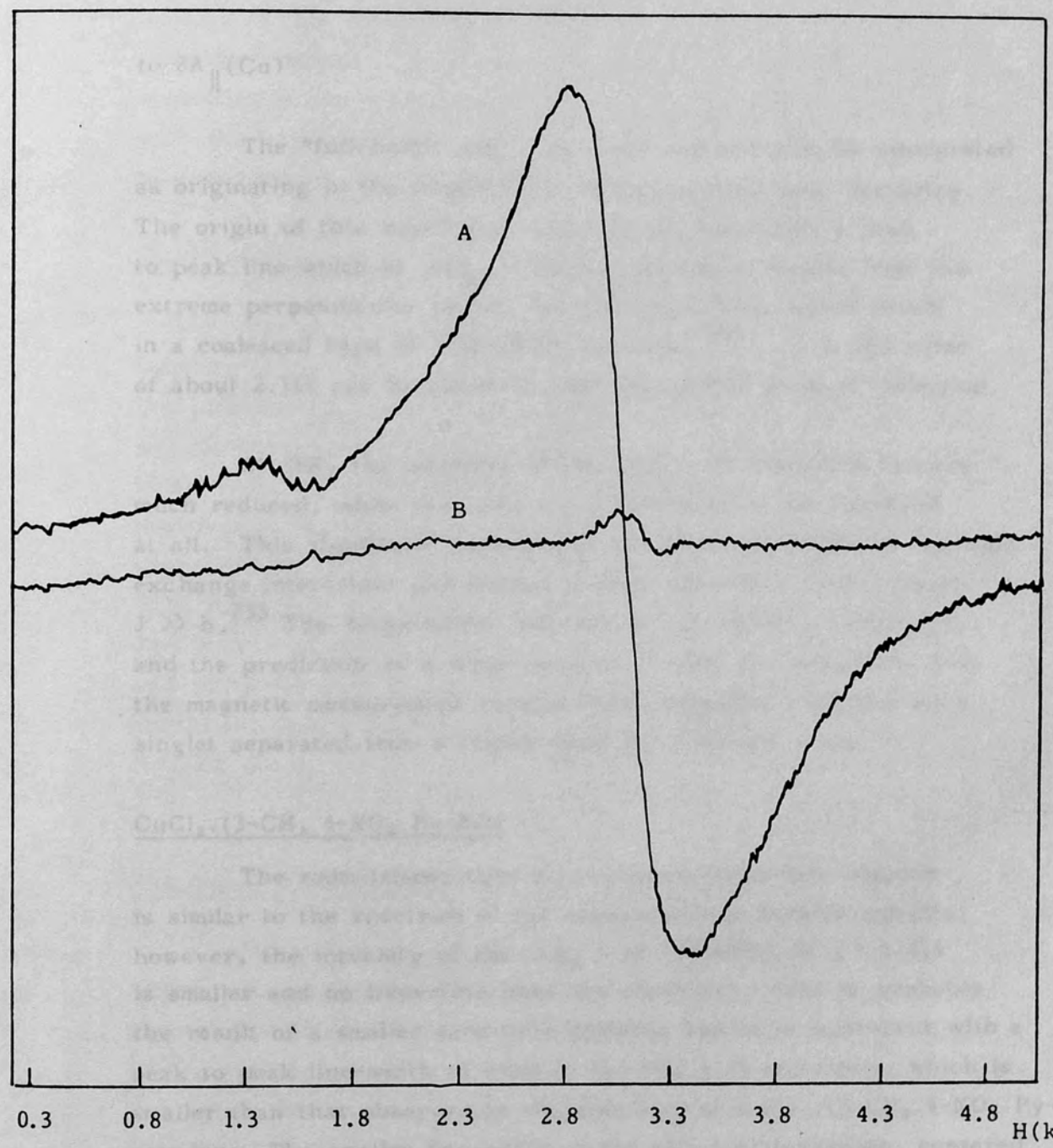

Fig. 25. E.s.r. Spectra of polycrystalline $CuBr_2.(3\text{-}CH_3\ 4\text{-}NO_2\ Py\text{-}NO)$.
Tracing A, at room-temperature.
Tracing B, at 98K.

to $2A_{\parallel}(Cu)$

The "full-field" $\Delta M_S = \pm 1$ resonance can also be interpreted as originating in the triplet state in species with axial symmetry. The origin of this broad and structureless band with a peak to peak line-width of $\Delta H_{pp} = 600G$ is probably results from two extreme perpendicular bands, low and high field, which result in a coalesced type of "full-field" spectrum.[242] A (g) value of about 2.152 can be obtained from the central point of inflection.

At 98K, the intensity of the $\Delta M_S = \pm 1$ transition is very much reduced, while the $\Delta M_S = \pm 2$ transition is not observed at all. This significant variation in the intensity is due to isotropic exchange interaction and implies a large positive J value, where $J \gg h$.[233] The temperature dependence of the e.s.r. spectrum and the prediction of a large positive J value are consistent with the magnetic measurement results which indicated a ground state singlet separated from a triplet state by J energy units.

$CuCl_2.(3\text{-}CH_3\ 4\text{-}NO_2\ Py\text{-}NO)$

The room-temperature e.s.r. spectrum of this complex is similar to the spectrum of the corresponding bromide complex; however, the intensity of the $\Delta M_S = \pm 2$ transition at $g = 4.416$ is smaller and no hyperfine lines are observed. This is probably the result of a smaller zero-field splitting and is in agreement with a peak to peak line-width of 460G in the $\Delta M_S = \pm 1$ transition, which is smaller than that observed in the spectrum of $CuBr_2.(3\text{-}CH_3\ 4\text{-}NO_2\ Py\text{-}NO)$ complex. The smaller line-width in the $\Delta M_S = \pm 1$ transition, centered at $g = 2.12$, means that the two extreme perpendicular bands in the triplet spectrum are very close to each other, thus indicating that the anisotropic components of the exchange interaction almost vanish in this complex. At 98K the intensity of the $\Delta M_S = \pm 1$ transition was weaker while the $\Delta M_S = \pm 2$ transition could not be observed.

It should be noted that the intensity of the $\Delta M_S = \pm 1$ transition at the two temperatures was much stronger in the

spectra of this complex than in the spectra of the corresponding bromide complex. The relatively stronger intensity of the $\Delta M_S = \pm 1$ transition in the spectra of the chloride complex is in agreement with the magnetic measurement results which indicated a larger magnetic moment for this complex.

$CuCl_2.(2\text{-}CH_3\ 4\text{-}NO_2\ Py\text{-}NO)$

The room-temperature e.s.r. spectrum of this complex consists of one broad resonance, with a (g) value of 2.11 at the point of inflection of the derivative spectrum. As predicted by the magnetic measurement studies, the spectrum of this complex is essentially the same at 98K, with there being no significant improvement in resolution or significant line narrowing at lower temperatures. The peak to peak line-width, ΔH_{pp} is approximately 300G indicating the presence of exchange interaction (Fig. 26). The lack of zero-field splitting, the insensitivity to temperature, and the absence of H_{MIN} in the spectra of this complex are consistent with a chloride bridged system, rather than a bridged N-oxide dimer.

Spectra of Polycrystalline 1:2 Complexes

The room-temperature e.s.r. spectra of these complexes showed either axial or rhombic spectra with lowest (g) values > 2.04. The observation of lowest (g) values greater than 2.04 is in agreement with our crystallographic and reflectance spectral results which suggested that the 1:2 complexes of 4-nitro 2-picoline N-oxide, 4-nitro 2,6-lutidine N-oxide and 3-nitro 2,6-lutidine N-oxide have approximate rhombic square-coplanar geometries.[245] The relatively higher g_3 value in the spectrum of the yellow isomer of $CuCl_2.(3\text{-}CH_3\ 4\text{-}NO_2\ Py\text{-}NO)_2$ complex suggests a tetrahedral structure for this complex.[246] No definite assignment could be made for the orange isomer.

The spectra of polycrystalline samples of $CuBr_2.(2\text{-}CH_3$

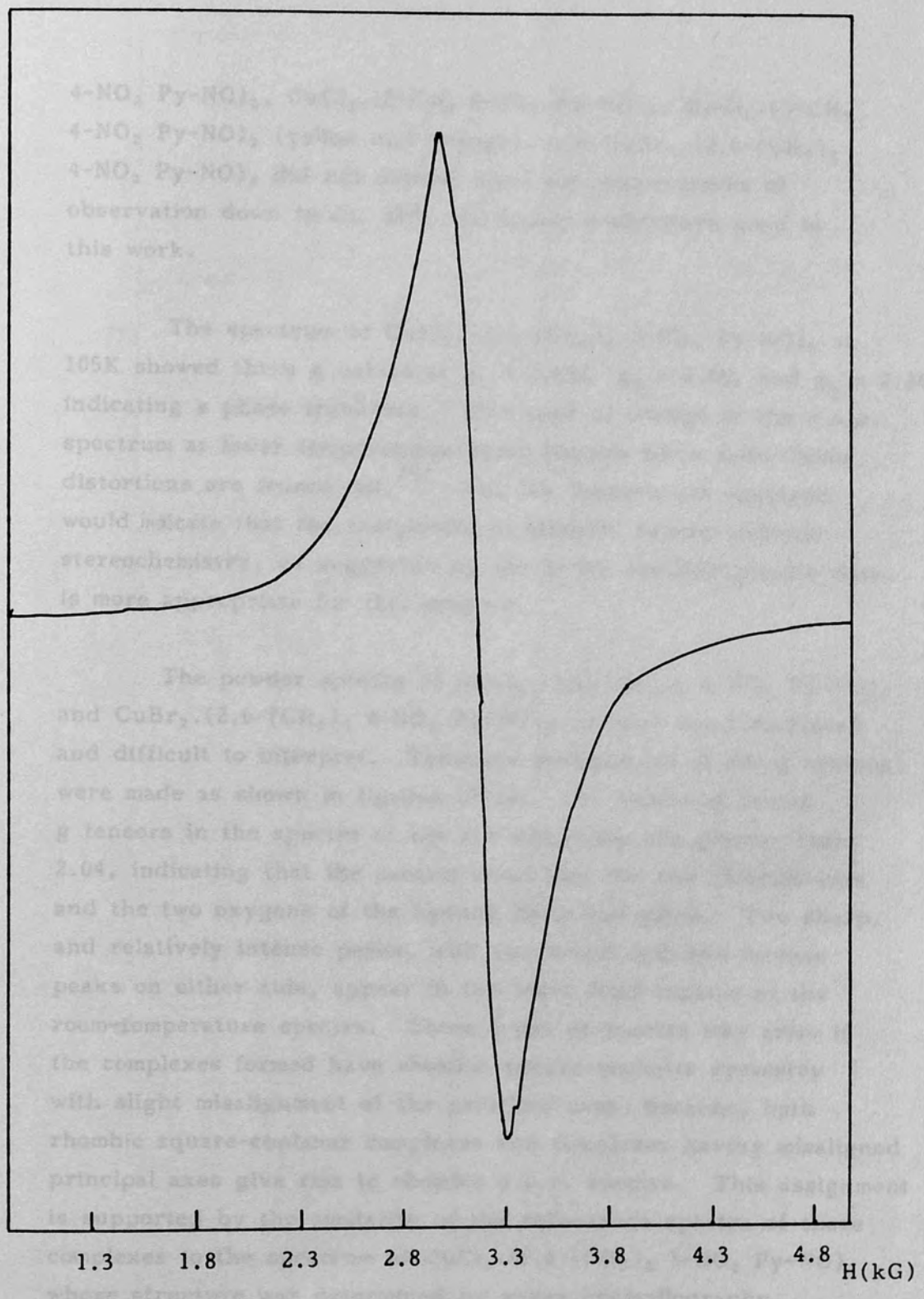

Fig. 26. X-band e.s.r. spectrum of polycrystalline sample of $CuCl_2.(2\text{-}CH_3\ 4\text{-}NO_2\ Py\text{-}NO)$.

4-NO_2 Py-NO)$_2$, $CuCl_2$.(2-CH_3 4-NO_2 Py-NO)$_2$, $CuCl_2$.(3-CH_3 4-NO_2 Py-NO)$_2$ (yellow and orange), and $CuBr_2$.(2,6-$(CH_3)_2$ 4-NO_2 Py-NO)$_2$ did not depend upon the temperatures of observation down to ca. 98K, the lowest emperature used in this work.

The spectrum of $CuCl_2$.(2,6-$(CH_3)_2$ 3-NO_2 Py-NO)$_2$ at 105K showed three g values at $g_1 = 2.035$, $g_2 = 2.06$, and $g_3 = 2.26$ indicating a phase transition. This type of change in the e.s.r. spectrum at lower temperatures could happen when Jahn-Teller distortions are frozen out.[247] The low temperature spectrum would indicate that the assignment of rhombic square-coplanar stereochemistry, as suggested by the x-ray crystallographic data, is more appropriate for this complex.

The powder spectra of $CuCl_2$.(2,6-$(CH_3)_2$ 4-NO_2 Py-NO)$_2$ and $CuBr_2$.(2,6-$(CH_3)_2$ 4-NO_2 Py-NO)$_2$ (green) are complicated and difficult to interpret. Tentative assignments of the g tensors were made as shown in figures 27,28. The values of lowest g tensors in the spectra of the two complexes are greater than 2.04, indicating that the central metal ion, the two chloride ions and the two oxygens of the ligands lie in one plane. Two sharp, and relatively intense peaks, with two broad and less intense peaks on either side, appear in the lower field regions of the room-temperature spectra. These types of spectra may arise if the complexes formed have rhombic square-coplanar symmetry with slight misalignment of the principal axes, because, both rhombic square-coplanar complexes and complexes having misaligned principal axes give rise to rhombic e.s.r. spectra. This assignment is supported by the similarity of the reflectance spectra of these complexes to the spectrum of $CuCl_2$.(2,6-$(CH_3)_2$ 3-NO_2 Py-NO)$_2$ whose structure was determined by x-ray crystallography.

At 115K the spectra of both complexes show significant

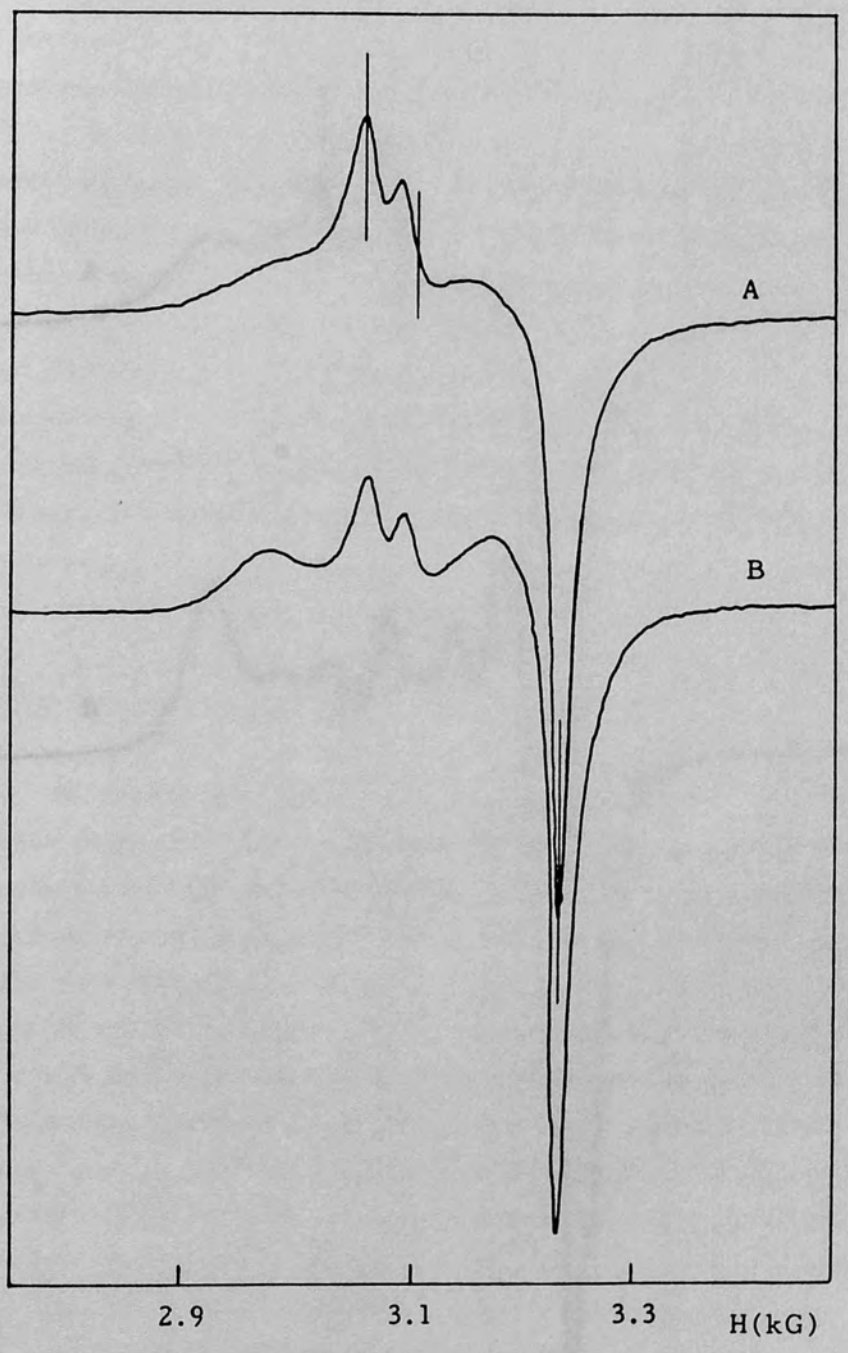

Fig. 27. E.S.R. Spectra of Polycrystalline $CuBr_2.(2,6\text{-}(CH_3)_2$ $4\text{-}NO_2$ Py-NO)$_2$ (green). Tracing A, at room-temperature. Tracing B, at 115K.

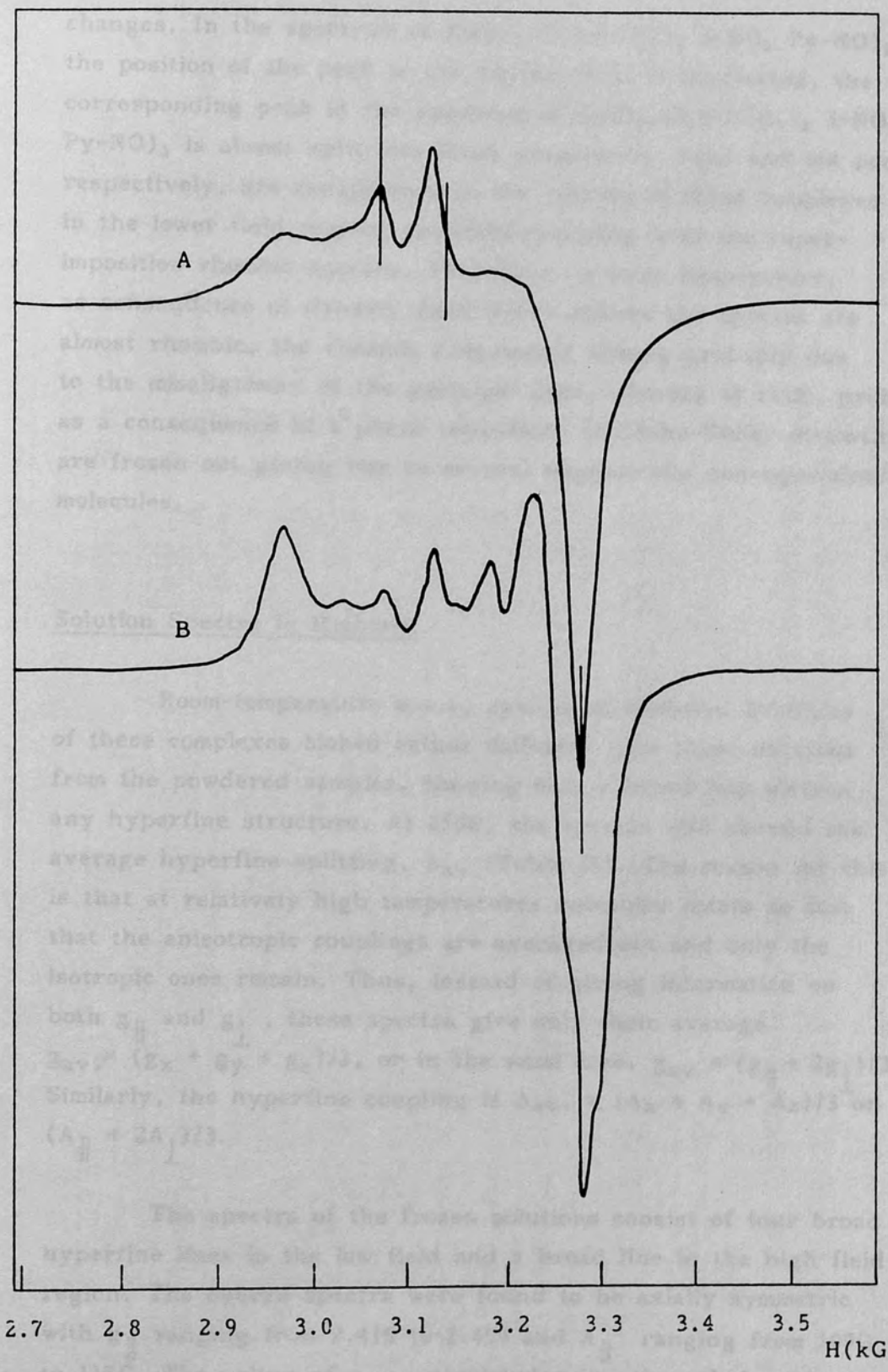

Fig. 28. E.S.R. spectra of polycrystalline $CuCl_2.(2,6\text{-}(CH_3)_2$ 4-NO_2 Py-NO). Tracing A, at room-temperature. Tracing B, at 115K.

changes. In the spectrum of $CuBr_2.(2,6\text{-}(CH_3)_2\ 4\text{-}NO_2\ Py\text{-}NO)_2$ the position of the peak at the highest field is unaffected, the corresponding peak in the spectrum of $CuCl_2.(2,6\text{-}(CH_3)_2\ 4\text{-}NO_2\ Py\text{-}NO)_2$ is almost split into three components. Four and six peaks respectively, are conspicuous in the spectra of these complexes in the lower field region, probably resulting from the superimposition rhombic spectra. Therefore, at room temperature, as consequence of dynamic Jahn-Teller effects the spectra are almost rhombic, the rhombic components arising probably due to the misalignment of the principal axes, whereas at 114K, probably as a consequence of a phase transition, the Jahn-Teller distortions are frozen out giving rise to several magnetically non-equivalent molecules.

Solution Spectra in Methanol

Room-temperature e.s.r. spectra of methanol solutions of these complexes looked rather different from those obtained from the powdered samples, showing only a broad line without any hyperfine structure. At 250K, the spectra also showed the average hyperfine splitting, $A_{av.}$(Table 23). The reason for this is that at relatively high temperatures molecules rotate so fast that the anisotropic couplings are averaged out and only the isotropic ones remain. Thus, instead of giving information on both $g_{\|}$ and $g_{\perp}$, these spectra give only their average $g_{av.} = (g_x + g_y + g_z)/3$, or in the axial case, $g_{av} = (g_{\|} + 2g_{\perp})/3$. Similarly, the hyperfine coupling is $A_{av.} = (A_x + A_y + A_z)/3$ or $(A_{\|} + 2A_{\perp})/3$.

The spectra of the frozen solutions consist of four broad hyperfine lines in the low field and a broad line in the high field region. The overall spectra were found to be axially symmetric with $g_{\|}$ ranging from 2.415 to 2.459 and $A_{\|}$ ranging from 109G to 117G. The values of $g_{av.}$ calculated using the relationship $g_{av.} = (g_{\|} + 2g_{\perp})/3$ are very close to the values obtained from the spectra recorded at 250K meaning that the configurations

Table 23. E.S.R. Data of the Complexes in Methanol Solutions

Complex	$g_{\parallel}$*	$g_{\perp}$*	$g_{av.}$*	$g_{av.}$**	$A_{\parallel}$*** *	$A_{av.}$*** **
$CuCl_2.(2\text{-}CH_3\ 4\text{-}NO_2\ Py\text{-}NO)$	2.421	2.064	2.183	2.190	115	35.8
$CuCl_2.(2\text{-}CH_3\ 4\text{-}NO_2\ Py\text{-}NO)_2$	2.459	2.064	2.196	2.192	117	38
$CuBr_2.(2\text{-}CH_3\ 4\text{-}NO_2\ Py\text{-}NO)_2$	2.423	2.063	2.183	2.186	114	33
$CuCl_2.(3\text{-}CH_3\ 4\text{-}NO_2\ Py\text{-}NO)$	2.415	2.066	2.182	2.185	115	40
$CuCl_2.(3\text{-}CH_3\ 4\text{-}NO_2\ Py\text{-}NO)_2$ (orange)	2.419	2.064	2.182	2.190	115	38
$CuCl_2.(3\text{-}CH_3\ 4\text{-}NO_2\ Py\text{-}NO)_2$ (yellow)	2.423	2.065	2.184	2.190	110	38
$CuBr_2.(3\text{-}CH_3\ 4\text{-}NO_2\ Py\text{-}NO)$	2.419	2.064	2.182	2.178	115	35
$CuCl_2.(2,6\text{-}(CH_3)_2\ 4\text{-}NO_2\ Py\text{-}NO)_2$	2.429	2.064	2.186	2.190	109	37
$CuBr_2.(2,6\text{-}(CH_3)_2\ 4\text{-}NO_2\ Py\text{-}NO)_2$	2.425	2.064	2.184	2.181	115	27
$CuCl_2.(2,6\text{-}(CH_3)_2\ 3\text{-}NO_2\ Py\text{-}NO)_2$	2.422	2.068	2.186	2.189	114	33
$CuBr_2.(2,6\text{-}(CH_3)_2\ 3\text{-}NO_2\ Py\text{-}NO)_2$	2.423	2.066	2.185	2.180	115	43

* $g_{\parallel}$, $A_{\parallel}$, $g_{\perp}$ were calculated from 10^{-3}M frozen methanol solution spectra; $g_{av.}$ was calculated from the relationship $g_{av.} = (g_{\parallel} + 2g_{\perp})/3$.

** These were calculated from the spectra of 10^{-3}M methanol solutions at 250K.

*** $A_{\parallel}$ and $A_{av.}$ are given in gauss.

of the complexes are the same at both temperatures. The $g_{\|}$ values obtained from the frozen solution spectra are rather high and the $A_{\|}$ values are rather small suggesting the presence of tetrahedral complexes, because, small values of hyperfine splitting and high values of $g_{\|}$ are related to the mixing of 3d-4p orbitals in tetrahedral symmetry.[246]

3.5.6. Infrared Spectra

The energies of the N-O stretching vibrations are detailed in Table 24. In agreement with Kida et al.[172] the N-O stretching vibration shifts to lower frequency on coordination due to a decrease in the double bond character of N-O. Splitting of the N-O frequency has been seen[112,113] for $CuBr_2.L_2$ where L = pyridine N-oxide and 4-picoline N-oxide and has been described as being due to two dissimilar copper-oxygen bonds, one involving Cu-O-Cu bridges (as in the 1:1 complex) and the other involving a less tightly bound N-O bond in the first coordination sphere. However, as can be seen from Table 24 and Figures 29, 30, in the case of nitro substitution there are multiple N-O frequencies before coordination. Even though these these frequencies are decreased on coordination, it does not necessarily follow that there are dissimilar Cu-O bonds.

The N-O double-bond character in the 1:1 complexes is expected to be smaller than that in the 1:1 complexes with a normal magnetic moment. This is because a larger electron donation from the N-O group is necessary for bridging than for forming a single coordination bond. Contrary to the expectations the absorption energies of the N-O stretching vibration of the 1:1 complexes of 4-nitro 3-picoline N-oxide were higher than the values for the 1:2 monomeric complexes. Shindo pointed out that the N-O stretching frequencies in the majority of 3-substituted pyridine N-oxides contain a fair amount of frequencies other than that of ν_{N-O}.[48] The N-O stretching frequency of pyridine N-oxides, shifts to the lower wavenumber side by 20 - 40cm^{-1} on addition of methanol, while those of 3-methyl derivatives, give a shift of ν_{N-O} to the lower wavenumber region of less than 15cm^{-1}. This fact has been ascribed to the

Table 24. Energies of the N-O Stretching Vibrations

Ligand	ν, cm^{-1}	Complex		ν, cm^{-1}
4-Nitro 2-picoline N-oxide	1285vs, 1267s		$CuCl_2.L$	1227s, 1215m
			$CuCl_2.L_2$	1250m, 1212vs
			$CuBr_2.L_2$	1222s, 1198s
4-Nitro 3-picoline N-oxide	1304s, 1256vs		$CuCl_2.L$	1258s, 1245s
		(yellow)	$CuCl_2.L_2$	1250s, 1238s
		(orange)	$CuCl_2.L_2$	1248s, 1232s
			$CuBr_2.L$	1260s, 1228m
4-Nitro 2,6-lutidine N-oxide	1282s, 1275s		$CuCl_2.L_2$	1227m, 1210s
		(green)	$CuBr_2.L_2$	1227m, 1205s
		(brown)	$CuBr_2.L_2$	1230m, 1205s
3-Nitro 2,6-lutidine N-oxide	1273s, 1260vs		$CuCl_2.L_2$	1240m, 1205s
			$CuBr_2.L$	1243vs, 1227s

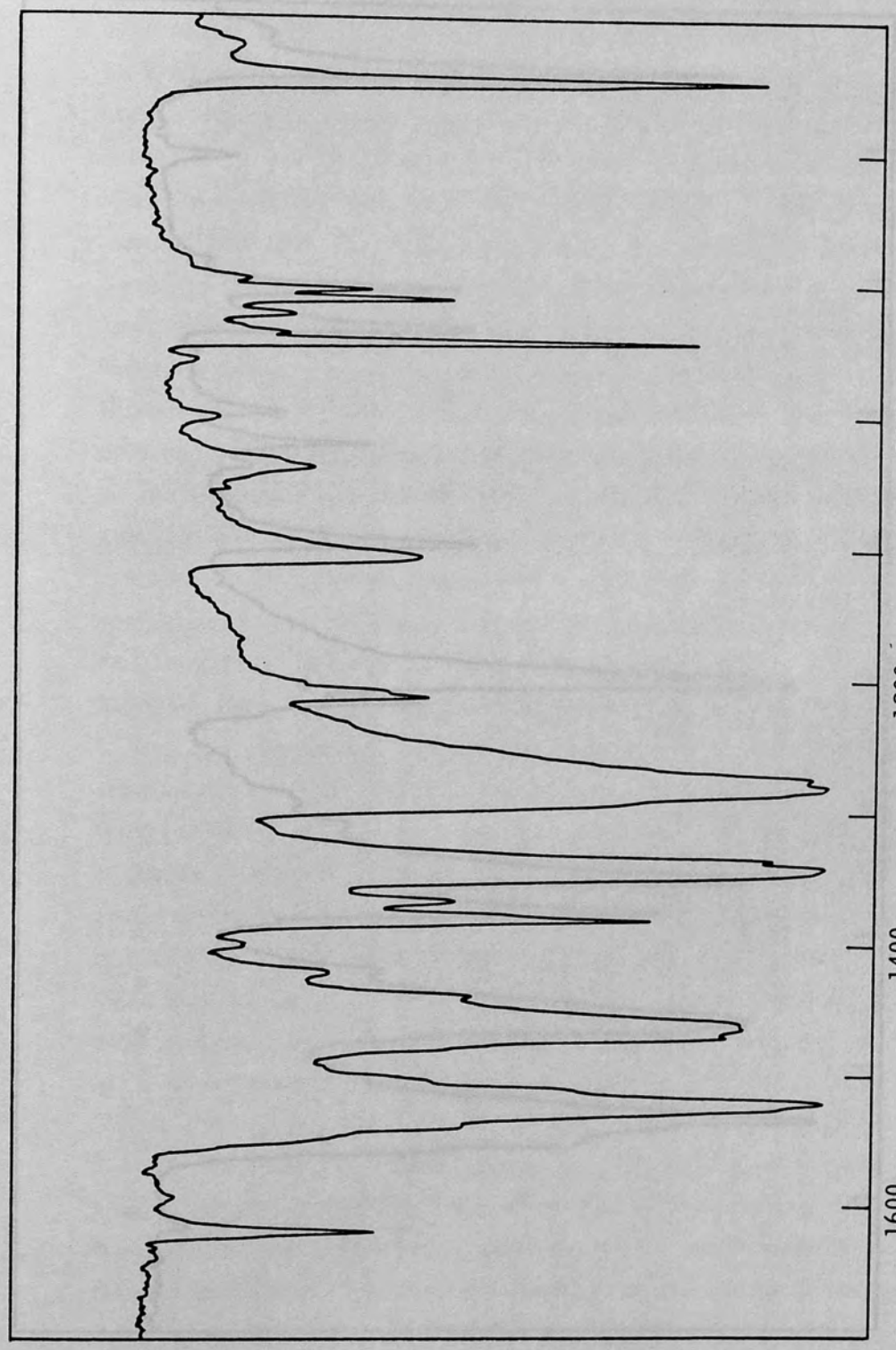

Fig. 29. Infrared spectrum of 4-nitro 2,6-lutidine N-oxide as nujol mull.

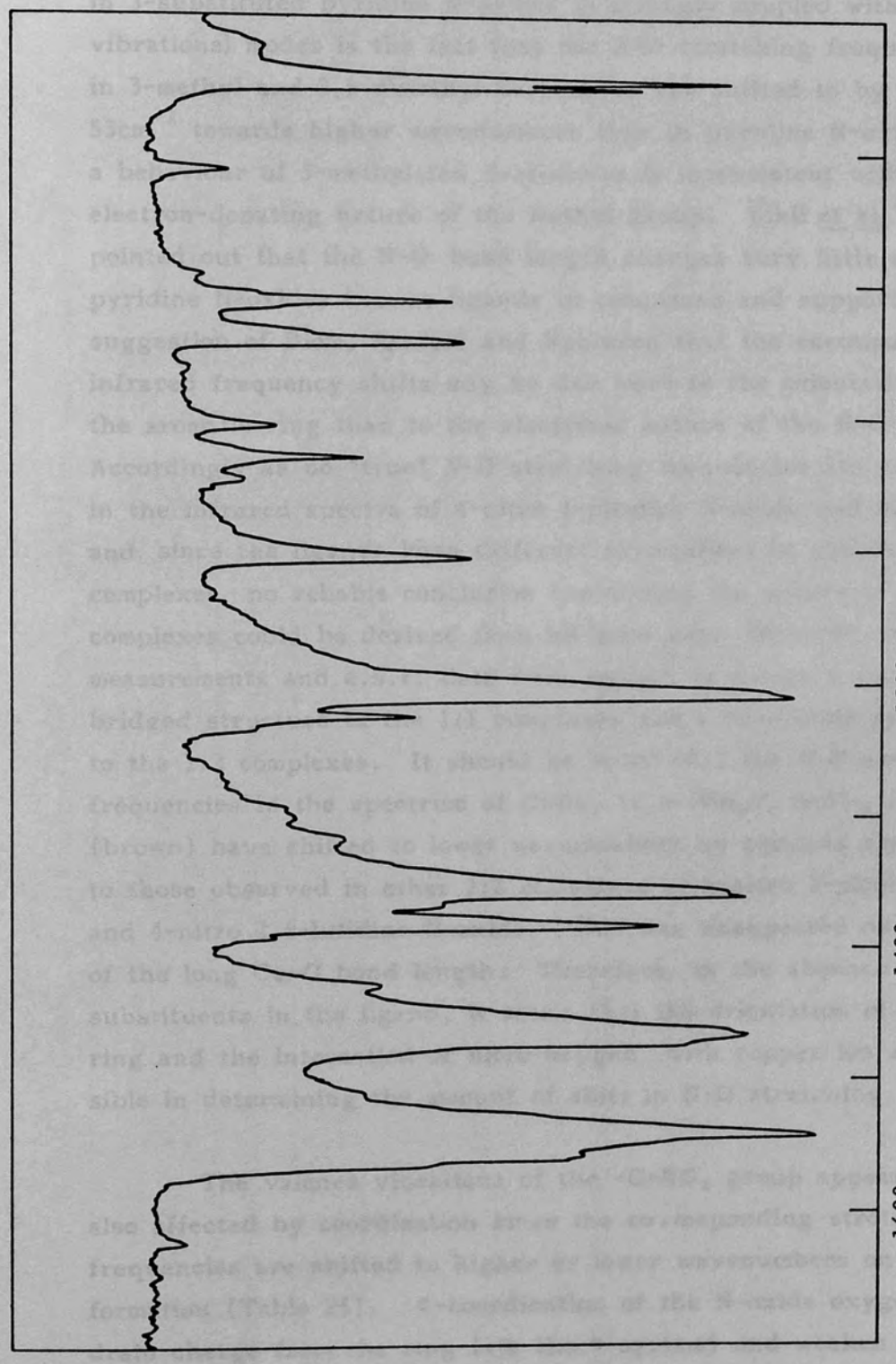

Fig. 30. Infrared spectrum of $CuCl_2.(2,6\text{-}(CH_3)_2\ 4\text{-}NO_2\ Py\text{-}NO)_2$ as nujol mull.

participation of modes other than the N-O stretching in the latter compounds. Another indication that the N-O stretching vibration in 3-substituted pyridine N-oxides is strongly coupled with other vibrational modes is the fact that the N-O stretching frequencies in 3-methyl and 3,5-dimethyl derivatives are shifted to by 20 and $53cm^{-1}$ towards higher wavenumbers than in pyridine N-oxide. Such a behaviour of 3-methylated derivatives is inconsistent with the electron-donating nature of the methyl group. Ülkü et al.[234] have pointed out that the N-O bond length changes very little when pyridine N-oxides become ligands in complexes and support the suggestion of Blom, Penfold and Robinson that the accompanying infrared frequency shifts may be due more to the orientation of the aromatic ring than to the electronic nature of the N-O bond.[248] Accordingly as no "true" N-O stretching frequencies are expected in the infrared spectra of 4-nitro 3-picoline N-oxide and its complexes, and since the ligands have different orientations in the various complexes, no reliable conclusion concerning the nature of these complexes could be derived from infrared data. However magnetic measurements and e.s.r. data were enough to assign a dimeric, oxygen bridged structure to the 1:1 complexes and a monomeric structure to the 1:2 complexes. It should be noted that the N-O stretching frequencies in the spectrum of $CuBr_2.(2,6\text{-}(CH_3)_2\ 4\text{-}NO_2\ Py\text{-}NO)_2$ (brown) have shifted to lower wavenumbers by amounts almost equal to those observed in other 1:2 complexes of 4-nitro 2-picoline N-oxide and 4-nitro 2,6-lutidine N-oxide. This was unexpected on the basis of the long Cu-O bond length. Therefore, in the absence of 3-substituents in the ligand, it seems that the orientation of the ring and the interaction of nitro-oxygen with copper ion are responsible in determining the amount of shift in N-O stretching frequencies.

The valence vibrations of the $-C-NO_2$ group appear to be also affected by coordination since the corresponding stretching frequencies are shifted to higher or lower wavenumbers on complex formation (Table 25). σ-coordination of the N-oxide oxygen would drain charge from the ring (via the π-system) and weaken the $C-NO_2$ bond, similarly metal to ligand π-back-bonding will reduce its strength. However, hydrogen bonding of nitro-oxygens or interaction of

Table 25. Energies of $-C-NO_2$ stretching vibrations in cm^{-1}

Ligand	ν-C-NO_2 (asymm.)	ν-C-NO_2 (symm.)	Complex	ν-C-NO_2 (asymm)	ν-C-NO_2 (symm.)
4-Nitro 2-picoline N-oxide	1510s	1360s	$CuCl_2.L$	1520s	1360s
			$CuCl_2.L_2$	1530s	1355s
			$CuBr_2.L_2$	1510s	1333s
4-Nitro 3-picoline N-oxide	1500s	1340m	$CuCl_2.L$	1535s	1358s
			(y) $CuCl_2.L_2$	1520s	1340m
			(o) $CuCl_2.L_2$	1522m	1360m
			$CuBr_2.L$	1533s	1355s
4-Nitro 2,6-lutidine N-oxide	1520s	1343s	$CuCl_2.L_2$	1540m	1360s
			(g) $CuBr_2.L_2$	1535s	1350m
			(b) $CuBr_2.L_2$	1530s	1350m
3-Nitro 2,6-lutidine N-oxide	1532s	1350s	$CuCl_2.L_2$	1524s	1350s
				1535s	1352m

these oxygens with a neighbouring metal ion will enhance the double bond character in $-C-NO_2$. Since only in the spectra of $CuBr_2.(2\text{-}CH_3\ 4\text{-}NO_2\ Py\text{-}NO)_2$ and the complexes of 3-nitro 2,6-lutidine N-oxide do the $-C-NO_2$ stretching vibrations appear either in their usual place or are shifted to lower wavenumbers, it seems that the nitro-oxygens in all other complexes are either hydrogen bonded to methyl groups or interact with a neighbouring copper ion.

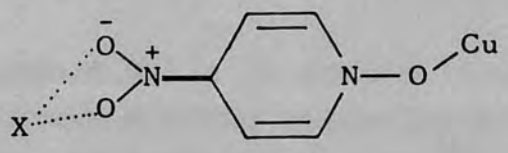

(X = Cu or H)

(XVII)

Far-Infrared Spectra

The far-infrared spectral data provided support for the suggestions made on the basis of other spectral data and revealed that the structure of $CuCl_2.(3\text{-}CH_3\ 4\text{-}NO_2\ Py\text{-}NO)_2$ (orange isomer) is trans octahedral with halide bridging. In this discussion the terms "terminal" and "bridging" are used only in a relative sense. For our purposes a terminal halogen atom is defined as one which is directly bonded in the monomeric 1:2 complexes or bonded to a copper ion when the binuclear oxygen bridged species is known to be present, and a bridging halide ion as one which is bridging two copper ions to form a dimeric or polymeric molecule. Two distinct types of bridging halogen atoms may be envisaged; firstly, those which are symmetrically disposed between the two copper atoms giving equal bond lengths and secondly, those which are unsymmetric giving to one short and one long copper-halide bond distance.

Previous far-infrared spectral studies on copper(II) chloride

complexes of pyridine N-oxides indicate that terminal metal-chlorine frequencies in the spectra of 1:1 binuclear complexes occur in the range of 344 - 302cm^{-1} and that the green 1:2 complexes exhibit metal chlorine stretching frequencies at slightly higher values whereas the yellow isomers absorb at lower frequencies.[192,203] Comparison of the spectra of the copper chloride complexes with those of the bromides and the free ligands facilitated the assignment of the infrared active copper-chlorine stretching frequencies. Although maxima were observed with all ligands in the 200 - 500cm^{-1} region, the bands which have been assigned to metal-chlorine vibrational modes are generally more intense.

It is suggested that in the presence of similar structural species the metal-bromine stretching frequencies can be estimated from the relationship ν(M-Br)/ν(M-Cl) = 0.75, [249] a metal-chlorine stretching frequency of 340cm^{-1} would correspond with a metal-halogen absorption at ca. 255cm^{-1} in the corresponding bromide complex.

Maxima assigned as metal-chlorine and metal-bromine stretching vibrations of the complexes are summarised in Table 26. The structure of the 1:1 complex of pyridine N-oxide is known to contain copper-chlorine bonds which do not interact with any neighbouring copper atoms, and thus these are terminal in character. The far-infrared spectrum of this complex shows maxima at 311(vs) and 330cm^{-1}(w,sh) which are attributed to copper-chlorine stretching frequencies. Thus for the 4-nitro 3-picoline N-oxide complex, it may be inferred that the observation of metal-chlorine stretching vibrations at 310(vs) and 335cm^{-1}(w,sh) indicates the presence of terminal metal-chlorine bonds and hence an oxygen bridged structure (Fig. 31). The copper-bromine stretching frequencies are also consistent with an oxygen bridged structure in $CuBr_2$.(3-CH_3 4-NO_2 Py-NO) (fig. 31). In the spectrum of the complex $CuCl_2$.(2-CH_3 4-NO_2 Py-NO) (with normal magnetic moment) the maxima observed at ca. 315 and 295cm^{-1} are assigned as bridging metal-chlorine stretching frequencies, because, for oxygen bridging, much higher frequencies are expected; moreover, the steric hindrance

Table 26. Summary of Metal-Halide and Metal-Oxygen Stretching Frequencies (cm^{-1})*

Compound	Colour	ν(Cu - Cl)	ν(Cu - Br)	ν(Cu -O)
$CuCl_2.(2\text{-}CH_3\ 4\text{-}NO_2\ Py\text{-}NO)$	Orange	315s 295m		402m
$CuCl_2.(2\text{-}CH_3\ 4\text{-}NO_2\ Py\text{-}NO)_2$	Brown	344vs 298s		407s
$CuBr_2.(2\text{-}CH_3\ 4\text{-}NO_2\ Py\text{-}NO)_2$	Wine red		280s 225m	415s
$CuCl_2.(3\text{-}CH_3\ 4\text{-}NO_2\ Py\text{-}NO)$	Green	335w,sh 310vs		426m
$CuCl_2.(3\text{-}CH_3\ 4\text{-}NO_2\ Py\text{-}NO)_2$	Yellow	315		**
$CuCl_2.(3\text{-}CH_3\ 4\text{-}NO_2\ Py\text{-}NO)_2$	Orange	295s 225w		390s
$CuBr_2.(3\text{-}CH_3\ 4\text{-}NO_2\ Py\text{-}NO)$	Wine red		263m 227w	418m
$CuCl_2.(2,6\text{-}(CH_3)_2\ 4\text{-}NO_2\ Py\text{-}NO)_2$	Green	340s		440m
$CuBr_2.(2,6\text{-}(CH_3)_2\ 4\text{-}NO_2\ Py\text{-}NO)_2$	Green		269s	442m
$CuBr_2.(2,6\text{-}(CH_3)_2\ 4\text{-}NO_2\ Py\text{-}NO)_2$	Brown		270s	**
$CuCl_2.(2,6\text{-}(CH_3)_2\ 3\text{-}NO_2\ Py\text{-}NO)_2$	Green	340s		410s
$CuBr_2.(2,6\text{-}(CH_3)_2\ 3\text{-}NO_2\ Py\text{-}NO)_2$	Green	270s		410s

* w=weak, m=medium, and s=strong intensity; v=very and sh=shoulder
** The intensities of the bands where ν(Cu-O) were expected were weak.

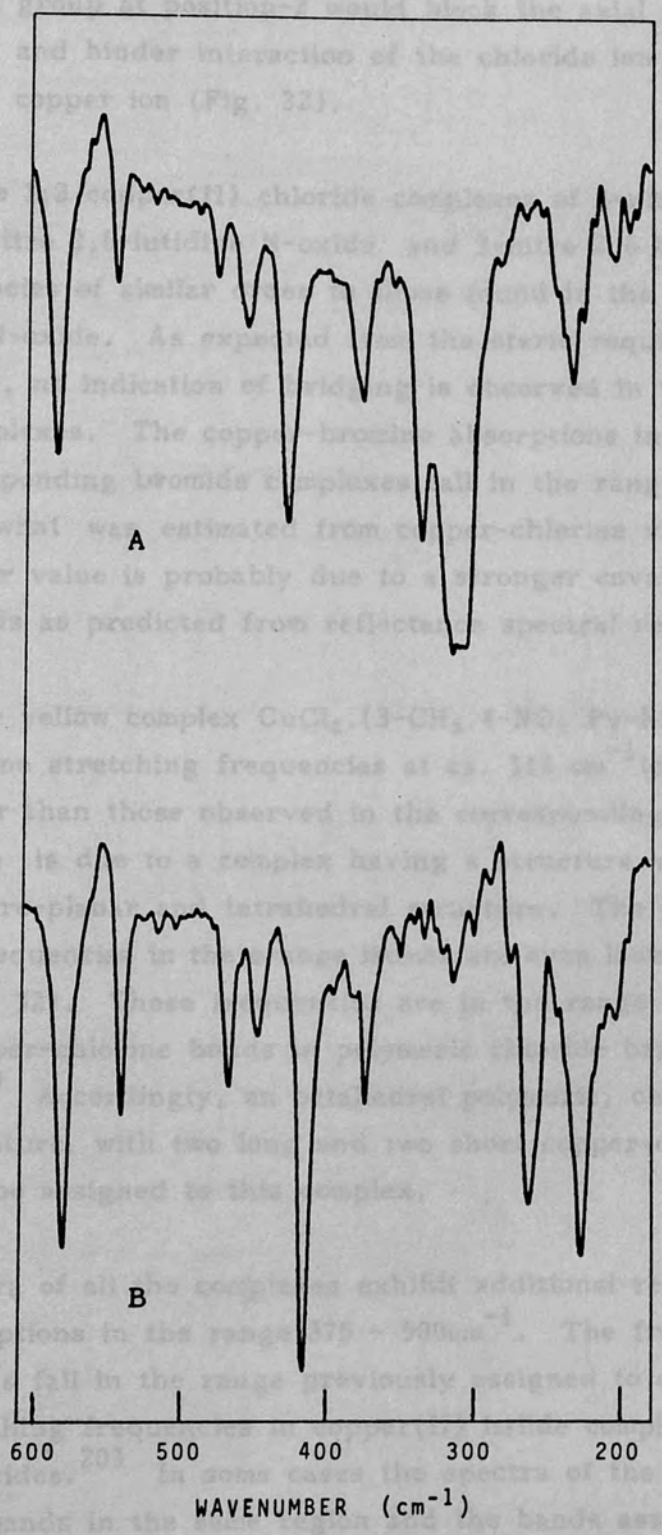

Fig. 31. Far-infrared spectra of A, $CuCl_2.(3\text{-}CH_3\ 4\text{-}NO_2\ Py\text{-}NO)$; B, $CuBr_2.(3\text{-}CH_3\ 4\text{-}NO_2\ Py\text{-}NO)$ recorded as nujol mulls.

of the methyl group at position-2 would block the axial position of the metal ion and hinder interaction of the chloride ion with a neighbouring copper ion (Fig. 32).

The 1:2 copper(II) chloride complexes of 4-nitro 2-picoline N-oxide, 4-Nitro 2,6-lutidine N-oxide and 3-nitro 2,6-lutidine N-oxide show frequencies of similar order to those found in the green complexes of pyridine N-oxide. As expected from the steric requirements of these ligands, no indication of bridging is observed in the spectra of these complexes. The copper-bromine absorptions in the spectra of the corresponding bromide complexes fall in the range 270 - 280cm^{-1} higher than what was estimated from copper-chlorine vibrations. This slighly higher value is probably due to a stronger covalent character in these bonds as predicted from reflectance spectral results.

The yellow complex $CuCl_2.(3\text{-}CH_3\ 4\text{-}NO_2\ Py\text{-}NO)_2$ shows copper-chlorine stretching frequencies at ca. 315 cm^{-1}(fig. 33). This value is lower than those observed in the corresponding 1:1 complex, and therefore is due to a complex having a structure midway between square-planar and tetrahedral structure. The copper-chlorine stretching frequencies in the orange isomer are even lower, at ca. 295 and 225cm^{-1} (Fig. 32). These frequencies are in the range associated with bridging copper-chlorine bonds in polymeric chloride bridged complexes.[250] Accordingly, an octahedral polymeric, chloride bridged structure, with two long and two short copper-chlorine bonds could be assigned to this complex.

Spectra of all the complexes exhibit additional relatively intense absorptions in the range 375 - 500cm^{-1}. The frequencies of these bands fall in the range previously assigned to copper-oxygen stretching frequencies in copper(II) halide complexes of pyridine N-oxides.[203] In some cases the spectra of the ligands also showed bands in the same region and the bands associated with copper-oxygen stetching frequencies could not be assigned. The band positions are summarized in Table 26. The numerical values of the metal-oxygen stretching frequencies clearly indicate that the 1:2 complexes having a trans planar structure absorb at higher frequencies than the yellow complex $CuCl_2.(3\text{-}CH_3\ 4\text{-}NO_2\ Py\text{-}NO)_2$. This is because,

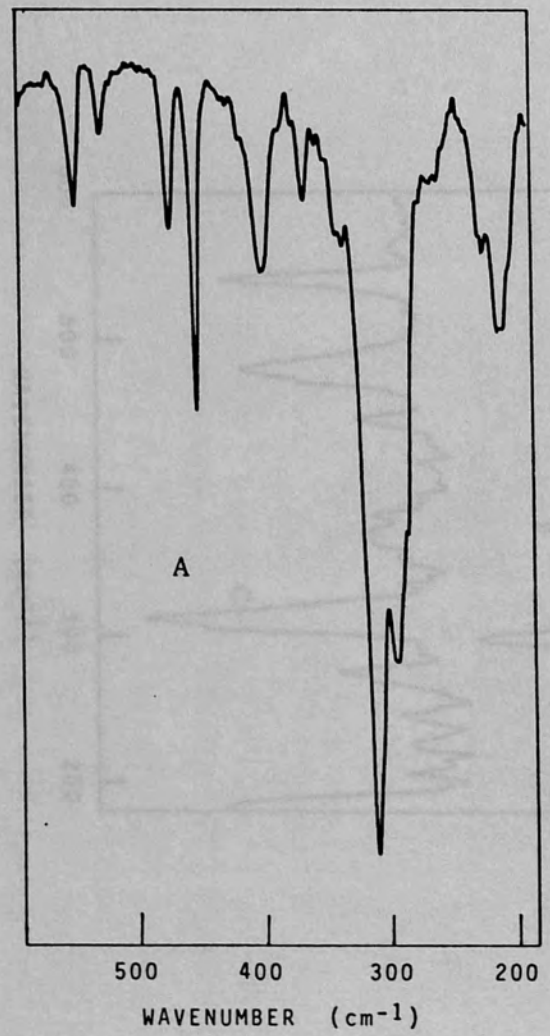

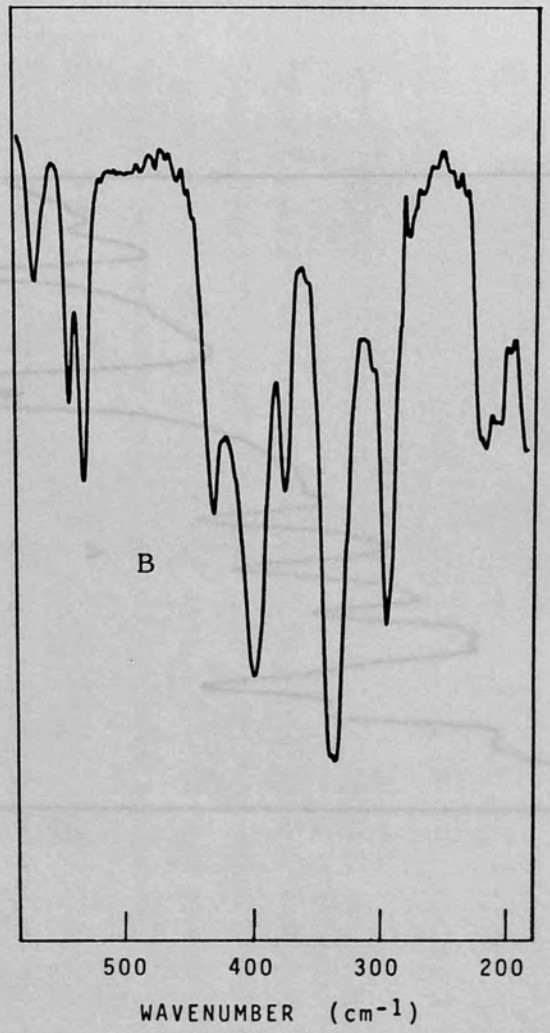

Fig. 32. Far-infrared spectra of A, $CuCl_2.(2\text{-}CH_3\ 4\text{-}NO_2\ Py\text{-}NO)$; B, $CuCl_2.(2\text{-}CH_3\ 4\text{-}NO_2\ Py\text{-}NO)_2$ recorded as nujol mulls.

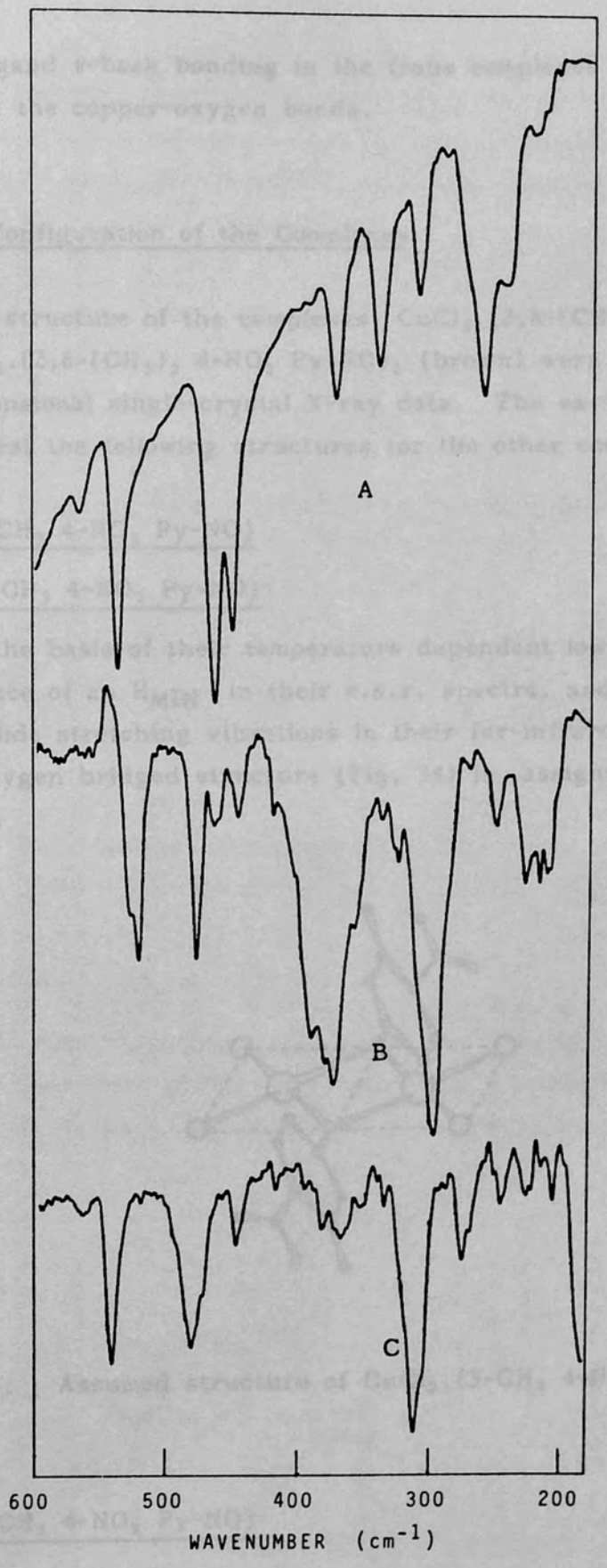

Fig. 33. Far-infrared spectra of A, 4-nitro 3-picoline N-oxide B, $CuCl_2.(3\text{-}CH_3\ 4\text{-}NO_2\ Py\text{-}NO)_2$ (orange); C, $CuCl_2.(3\text{-}CH_3\ 4\text{-}NO_2\ Py\text{-}NO)_2$ (yellow) recorded as nujol mulls.

metal to ligand π-back bonding in the trans complexes would strengthen the copper-oxygen bonds.

3.5.7. Configuration of the Complexes

The structure of the complexes $CuCl_2.(2,6\text{-}(CH_3)_2\ 3\text{-}NO_2\ Py\text{-}NO)_2$ and $CuBr_2.(2,6\text{-}(CH_3)_2\ 4\text{-}NO_2\ Py\text{-}NO)_2$ (brown) were established from three-dimensional single-crystal X-ray data. The various spectroscopic data suggest the following structures for the other complexes.

$CuCl_2.(3\text{-}CH_3\ 4\text{-}NO_2\ Py\text{-}NO)$

$CuBr_2.(3\text{-}CH_3\ 4\text{-}NO_2\ Py\text{-}NO)$

On the basis of their temperature dependent low magnetic moments, the presence of an H_{MIN} in their e.s.r. spectra, and the positions of copper-halide stretching vibrations in their far-infrared spectra, a dimeric oxygen bridged structure (Fig. 34) is assigned to these complexes.

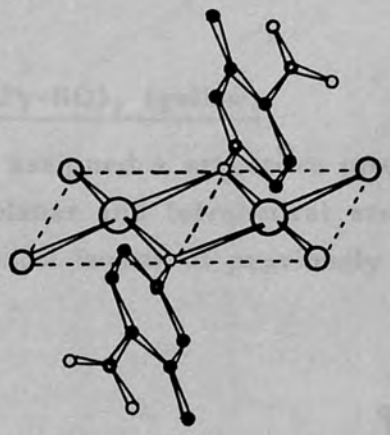

Fig. 34. Assumed structure of $CuCl_2.(3\text{-}CH_3\ 4\text{-}NO_2\ Py\text{-}NO)$.

$CuCl_2.(2\text{-}CH_3\ 4\text{-}NO_2\ Py\text{-}NO)$

This complex is assigned a halogen bridged dimeric structure

(Fig. 35). It is characterised by its normal, temperature independent magnetic moment, the absence of an H_{MIN} in its e.s.r. spectrum, and the appearance of copper-chlorine stretching vibrations in the far-infrared spectrum at wavenumbers significantly lower than what would be expected for oxygen bridged dimers.

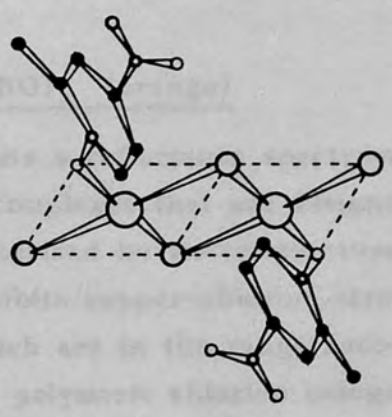

Fig. 35. Assumed structure of $CuCl_2.(2\text{-}CH_3\ 4\text{-}NO_2\ Py\text{-}NO)$.

$CuCl_2.(3\text{-}CH_3\ 4\text{-}NO_2\ Py\text{-}NO)_2$ (yellow)

This complex is assigned a structure intermediate between distorted cis-square-planar and tetrahedral structures (Fig. 36) and corresponds to the yellow isomer of previously reported 1:2 copper(II)

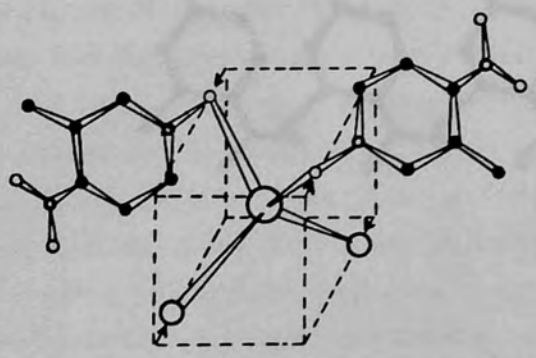

Fig. 36. Assumed structure of $CuCl_2.(3\text{-}CH_3\ 4\text{-}NO_2\ Py\text{-}NO)_2$ (yellow).

chloride complexes of pyridine N-oxides. It is characterised by its temperature independent normal magnetic moment, a reflectance spectrum which is different from the spectra of other 1:2 complexes that are assigned trans-planar geometries, the position of the copper-chlorine stretching vibration which is significantly at lower wavenumber than those revealed by the trans isomers, and the relatively high g_3 value in the e.s.r. spectrum of a powdered sample.

$CuCl_2.(3\text{-}CH_3\ 4\text{-}NO_2\ Py\text{-}NO)_2$ (orange)

This complex exhibits a reflectance spectrum which is different from the spectra of the complexes that are assigned trans-planar structures. It is characterised by its temperature independent normal magnetic moment and exhibits copper-chlorine stretching vibrations at ca. 295 and 225 cm^{-1} which are in the range associated with bridging copper-chlorine bonds in polymeric chloride bridged octahedral complexes (Fig. 37).

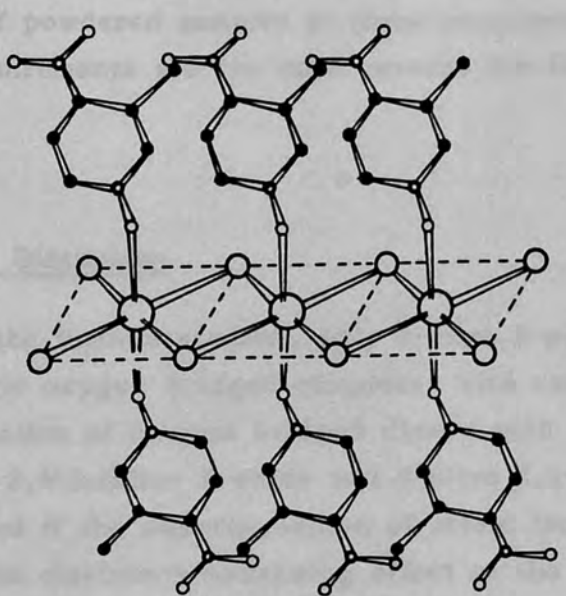

Fig. 37. Assumed structure of $CuCl_2.(3\text{-}CH_3\ 4\text{-}NO_2\ Py\text{-}NO)_2$ (orange).

$CuCl_2.(2\text{-}CH_3\ 4\text{-}NO_2\ Py\text{-}NO)_2$

$CuBr_2.(2\text{-}CH_3\ 4\text{-}NO_2\ Py\text{-}NO)_2$

$CuCl_2.(2,6\text{-}(CH_3)_2\ 4\text{-}NO_2\ Py\text{-}NO)_2$

$CuBr_2.(2,6\text{-}(CH_3)_2\ 4\text{-}NO_2\ Py\text{-}NO)_2$ (green)

$CuBr_2.(2,6\text{-}(CH_3)_2\ 3\text{-}NO_2\ Py\text{-}NO)_2$

All these complexes exhibit temperature independent normal magnetic moments, they exhibit copper-chlorine and copper-bromine stretching vibrations at wavenumbers associated with the trans square-planar isomers of previously reported copper(II) halide complexes of pyridine N-oxides. They all reveal reflectance spectra very similar to the spectrum of $CuCl_2.(2,6\text{-}(CH_3)_2\ 3\text{-}NO_2\ Py\text{-}NO)_2$ the structure of which was established from single X-ray crystallographic data, Therefore, these complexes could be assigned distorted trans-planar structures with unequal copper-halogen, copper-oxygen bond lengths and where the adjacent angles around the metal ion are not equal. Therefore, the variations in their colours could be attributed to the varying degrees of distortion of this arrangement as revealed by the e.s.r. spectra of powdered samples of these complexes. Steric effects and packing requirements are the main reasons for their distorted structures.

3.5.8. General Discussion

Among all the ligands studied, only 4-nitro 3-picoline N-oxide formed 1:1 dimeric oxygen bridged complexes with copper(II) halides. The lack of formation of oxygen bridged dimers with 4-nitro 2-picoline-N-oxide, 3-nitro 2,6-lutidine N-oxide and 4-nitro 2,6-lutidine N-oxide could be explained if the superimposition of steric factors near the donor site and the electron-withdrawing effect of the nitro group are considered. It is reported that both 2,6-lutidine N-oxide and 4-nitro pyridine N-oxide form this type of complex with copper(II) halides,[193] therefore neither the presence of methyl groups near the donor site alone, nor the electron-withdrawing effect of the nitro group alone could prevent the formation of oxygen bridged dimers. The presence of an electron-withdrawing nitro group on the pyridine ring

will result in a shorter N=O bond length, this will in turn result in the further approach of the methyl groups at 2- and 6-positions to the donor site thus preventing the formation of oxygen bridged dimers. The fact that 4-nitro 3-picoline N-oxide did not form 1:2 complexes with copper(II) bromide, and the complex $CuBr_2.(3\text{-}CH_3\ 4\text{-}NO_2\ Py\text{-}NO)$ exhibits a magnetic moment comparable with the moment of $CuBr_2.(Py\text{-}NO)$ means that, in the absence of steric factors near the donor site, nitropyridine N-oxides are electronically more suited to form oxygen bridged complexes than monomeric complexes.

In 1:2 complexes tetrahedral geometry would be most stable from strictly electrostatic and steric considerations. Trigonal planar sp^2 bonding of the N-oxide-oxygen with the copper $d_{x^2-y^2}$ orbitals implies the existence of N-oxide double bond, moreover if the orientation of the pyridine ring is as in $CuCl_2.(2,6\text{-}(CH_3)_2\ 3\text{-}NO_2\ Py\text{-}NO)_2$, back-$\pi$-bonding of d_{xz} or d_{yz} and d_{xy} orbitals of the copper ion with the empty antibonding orbitals of N-oxide can take place. In $CuBr_2.(2,6\text{-}(CH_3)_2\ 4\text{-}NO_2\ Py\text{-}NO)_2$ (dark brown), the square-planar structure is probably stabilised by the interaction of the nitro group with a neighbouring copper ion, because in this complex the tetrahedral disposition of the N-oxide-oxygen implies the absence of π^* orbitals, moreover the orientation of the ligand will not allow back-π-bonding.

The formation of halogen bridged complexes, $CuCl_2.(2\text{-}CH_3\ 4\text{-}NO_2\ Py\text{-}NO)$ and $CuCl_2.(3\text{-}CH_3\ 4\text{-}NO_2\ Py\text{-}NO)_2$ (orange), means that these ligands are better π-acceptors than σ-donors, bridging providing a means for maintaining the effective electroneutrality on the central ion. 2,6-disubstituted ligands did not form halogen bridged complexes due to the blocking of the axial positions of the metal by methyl groups.

3.6. Cadmium(II) Complexes

Cadmium(II) being a d^{10} ion does not show d-d transitions and, therefore, information regarding the stereochemistry of cadmium(II) complexes cannot be derived from their visible reflectance spectra.

In order to obtain some information on the stereochemistry of

these complexes the X-ray diffraction photographs of powdered samples of $CdCl_2.(2\text{-}CH_3\ 4\text{-}NO_2\ Py\text{-}NO)$ and $CdCl_2.(3\text{-}CH_3\ 4\text{-}NO_2\ Py\text{-}NO)_2$ complexes were recorded and compared with the diffraction photographs of $CuCl_2.(2\text{-}CH_3\ 4\text{-}NO_2\ Py\text{-}NO)$ and $CuCl_2.(3\text{-}CH_3\ 4\text{-}NO_2\ Py\text{-}NO)_2$ (yellow and orange isomers). The d-spacings and the intensities of the bands in the X-ray diffraction photographs of the cadmium(II) complexes were very different from those observed for the corresponding copper(II) complexes meaning that the cadmium(II) complexes are not strictly isomorphous with the corresponding copper(II) complexes.

3.6.1. Infrared Spectra of the Complexes

The N-O stretching vibrations of these complexes have shifted to lower wavenumbers (Table 27). Comparison of the positions of N-O stretching vibrations with those present in the spectra of copper(II) complexes of the corresponding ligands revealed that the shifts in these bands in the cadmium complexes are smaller than the shifts observed in the spectra of copper(II) chloride complexes. This eliminated the possibility of N-oxide bridging in these complexes, because bridging N-oxide oxygen implies N-O stretching vibrations occurrs at lower frequencies. The smaller shifts in these vibrations in the cadmium(II) complexes also means that Cd-O bonds are weaker than Cu-O bonds. Accordingly the stoichiometries of the cadmium(II) complexes could be associated with the strong competition of the chloride ion for a coordination site. Thus, no more than two ligands per metal ion could be realised with 4-nitro pyridine N-oxide and 4-nitro 3-picoline N-oxide, and in fact with the other ligands containing one or two methyl groups near the coordination site, only one was coordinated. These observations certainly accord with the literature on the cadmium(II) ion, which generally prefers halide ion coordination to coordination by weak monodentate oxygen donors.[215]

As in the spectra of the copper(II) complexes, the $C\text{-}NO_{2\,symm.}$ and $C\text{-}NO_{2\,asymm.}$ vibrations have shifted to higher wavenumbers, therefore as discussed previously, either some interaction between the oxygens belonging to a nito group with a neighbouring cadmium ion takes place, or the nitro group is hydrogen bonded.

Table 27. Infrared Band Assignments for Cadmium(II) Complexes *

Complex	ν_{N-O}	ν-C-NO_2 (asymm.)	ν-C-NO_2 (symm.)
$CdCl_2$.(4-NO_2 Py-NO)	1255s, 1233s	1535s	1350s
$CdCl_2$.(4-NO_2 Py-NO)$_2$	1243s, 1227s	1537s, 1515s	1320s
$CdCl_2$.(2-CH_3 4-NO_2 Py-NO)	1250s, 1230s	1527s	1360s
$CdCl_2$.(3-CH_3 4-NO_2 Py-NO)$_2$	1258s, 1230m	1520m	1340m
$CdCl_2$.(2,6-(CH_3)$_2$ 4-NO_2 Py-NO)	1247vs, 1210m	1535s	1345s
$CdCl_2$.(2,6-(CH_3)$_2$ 3-NO_2 Py-NO)	1243vs, 1227s 1220s, 1203m	1535s	1360s

* Wavenumbers are in cm^{-1}. The corresponding vibrations in the spectra of the ligands are given in Table 24, page 211 and Table 25, page 215.

The low frequency infrared spectra of all cadmium(II) chloride complexes of the ligands studied did not show any new bands in the region 260 - 600 cm^{-1}. Either a very broad band or very closely spaced bands appeared in the region 190 - 260 cm^{-1}. These bands may either be due to Cd-O stretching vibrations or due to terminal Cd-Cl stretching vibrations or a combination of both modes (Figs. 38,39). Schmauss & Specker[214] have studied a series of cadmium(II) halide complexes with a range of substituted pyridine N-oxides and observed that the frequencies of Cd-Cl stretching vibrations fall with the steric hindrance near the donor site of the ligands, and have assigned the Cd-O stretching vibration to a band at 242 cm^{-1} for the $Cd_4Cl_8.(2,6\text{-}(CH_3)_2$ Py-NO) complex. Ahuja & Rastogi[215] have also studied a series of substituted pyridine N-oxide complexes of cadmium(II) chloride and assigned the smallest Cd-O stretching frequencies at 288, 282 cm^{-1} to $CdBr_2.(4\text{-cy Py-NO})_2$, which contains the electron withdrawing CN group on the pyridine ring. Therefore, the bands in the region 190 - 260 cm^{-1} are expected to contain the Cd-O stretching frequencies, because all the ligands studied in this work contain an electron withdrawing nitro group, and three of them, namely 4-nitro 2-picoline N-oxide, 4-nitro 2,6-lutidine N-oxide, and 3-nitro 2,6-lutidine N-oxide contain one or two methyl groups near the donor site. It is very unlikely that the occurrence of Cd-O stretching vibrations at lower frequency regions is due to bridging N-oxide, because as mentioned earlier, the observed N-O stretching frequency shifts to lower wavenumbers are much smaller in the spectra of the cadmium(II) complexes than in the spectra of copper(II) complexes containing a terminal N-oxide bonded ligand.

In cadmium(II) chloride complexes, Cd-Cl stretching vibrations for terminal chloride ions are expected at ~250 - 200 cm^{-1}. The frequency of a bridging metal-halogen vibration is usually ~70 cm^{-1} lower than the corresponding terminal metal-halogen modes.[251-254] The presence of Cd-O stretching vibrations in the region 260 -190 cm^{-1} made the detection of vibrations corresponding to terminal Cd-Cl modes difficult. Accordingly, the presence of terminal chlorines in these complexes could only be inferred from the appearance of multiple bands in the region 260 - 190 cm^{-1}. Due to the lower frequency limit of the spectrometer being at ~180 cm^{-1}, the vibrations corresponding to bridging chlorines could not be detected.

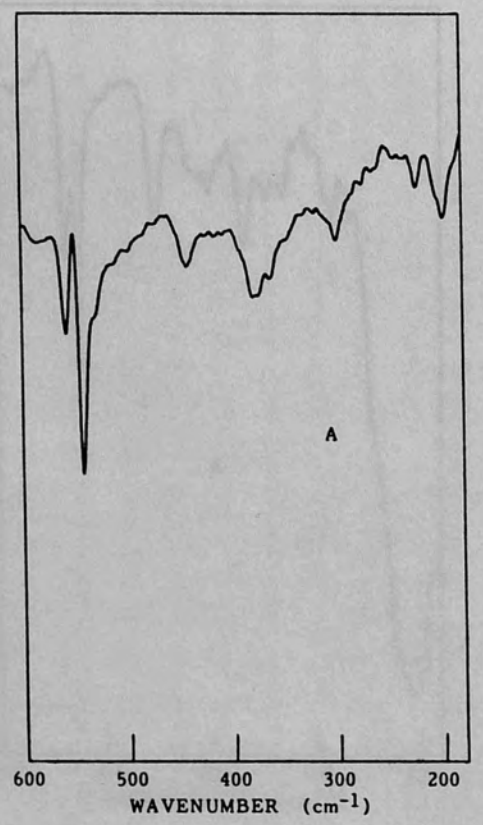

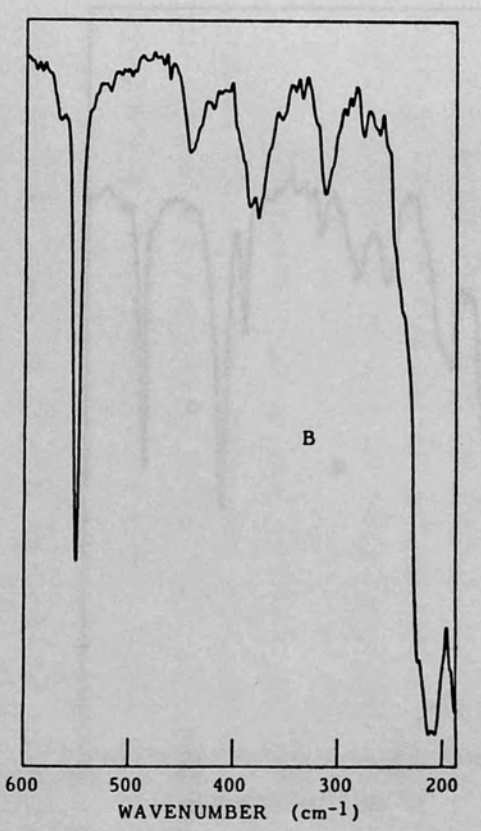

Fig. 38. Far-infrared spectra of A, 4-nitro 2,6-lutidine N-oxide; B, $CdCl_2.(2,6\text{-}(CH_3)_2\ 4\text{-}NO_2\ Py\text{-}NO)$ recorded as nujol mulls.

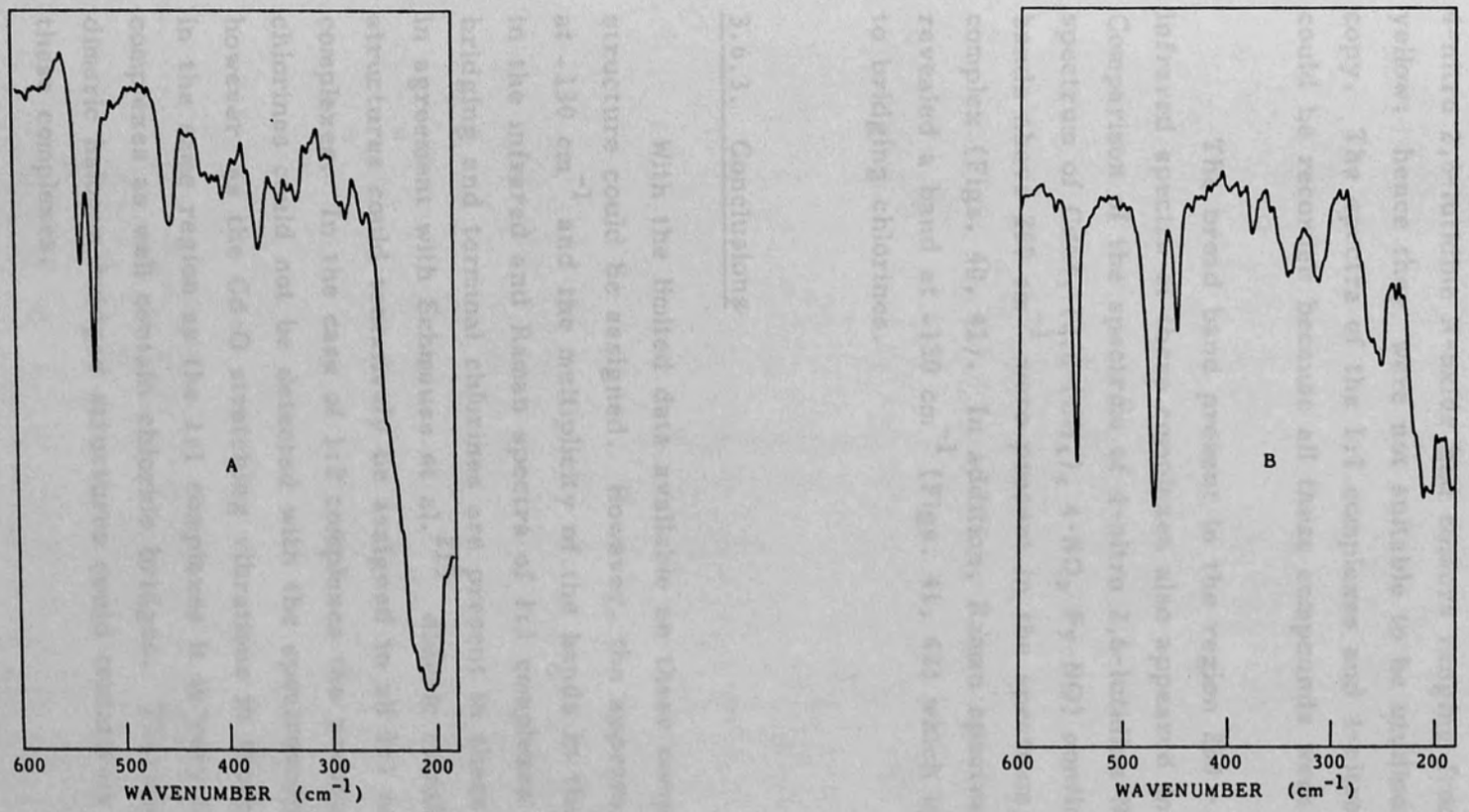

Fig. 39. Far-infrared spectra of A, $CdCl_2.(2,6\text{-}(CH_3)_2\ 3\text{-}NO_2\ Py\text{-}NO)$; B, $CdCl_2.(3\text{-}CH_3\ 4\text{-}NO_2\ Py\text{-}NO)_2$ recorded as nujol mulls.

3.6.2. Raman Spectra of the Complexes

The scope of practical application of Raman spectroscopy is limited by the fact that the spectrum of only colourless substances can be recorded. The 1:2 complexes and all the ligands studied, except 4-nitro 2,6-lutidine N-oxide had colours ranging from pale to bright yellow; hence they were not suitable to be studied by Raman spectroscopy. The spectra of the 1:1 complexes and 4-nitro 2,6-lutidine N-oxide could be recorded because all these compounds were white.

The broad band present in the region 260 - 190 cm^{-1} in the infrared spectra of these complexes also appeared in their Raman spectra. Comparison of the spectrum of 4-nitro 2,6-lutidine N-oxide with the spectrum of $CdCl_2.(2,6\text{-}(CH_3)_2\ 4\text{-}NO_2\ Py\text{-}NO)$ confirmed that no new bands above 260 cm^{-1} were present in the spectrum of the cadmium complex (Figs. 40, 41). In addition, Raman spectra of these complexes revealed a band at ~130 cm^{-1} (Figs. 41, 42) which could be assigned to bridging chlorines.

3.6.3. Conclusions

With the limited data available on these complexes no definite structure could be assigned. However, the appearance of a band at ~130 cm^{-1} and the multiplicity of the bands in the region 260 - 190 cm^{-1} in the infrared and Raman spectra of 1:1 complexes mean that both bridging and terminal chlorines are present in these complexes. Accordingly, in agreement with Schmauss et al.[215] dimeric tetrahedral chloride-bridged structures could tentatively be assigned to all 1:1 cadmium(II) halide complexes. In the case of 1:2 complexes the presence of bridging chlorines could not be detected with the spectroscopic data available; however as the Cd-O stretching vibrations in these complexes absorb in the same region as the 1:1 complexes it is very likely that these complexes as well contain chloride bridges. Therefore, pentacoordinate dimeric halogen-bridged structures could tentatively by assigned to these complexes.

The fact that only 4-nitro pyridine N-oxide and 4-nitro 3-picoline N-oxide formed 1:2 complexes and all the other ligands gave only 1:1 complexes, even in the presence of excess ligand during their preparations,

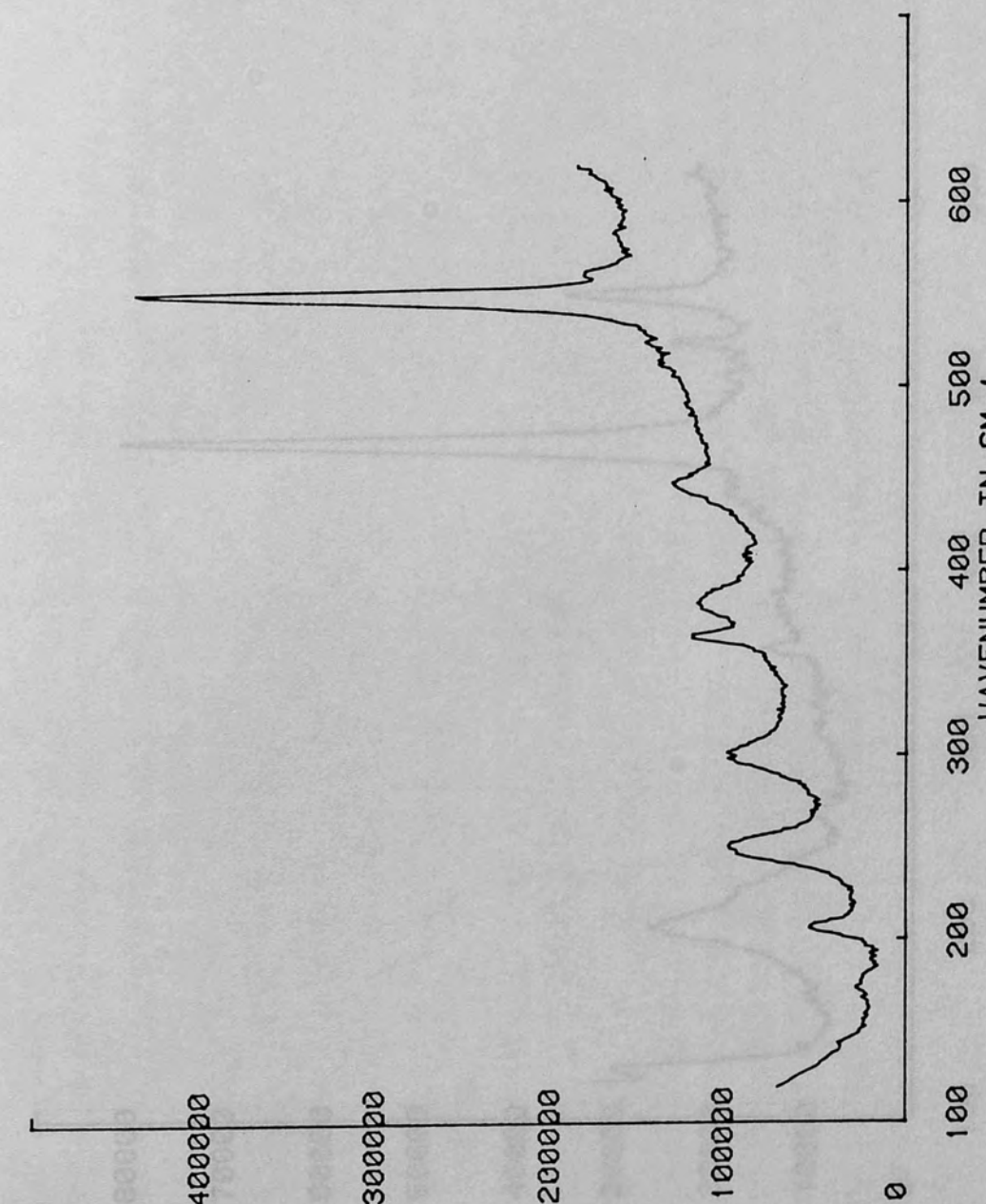

Fig. 40. Raman apectrum of 4-nitro 2,6-lutidine N-oxide.

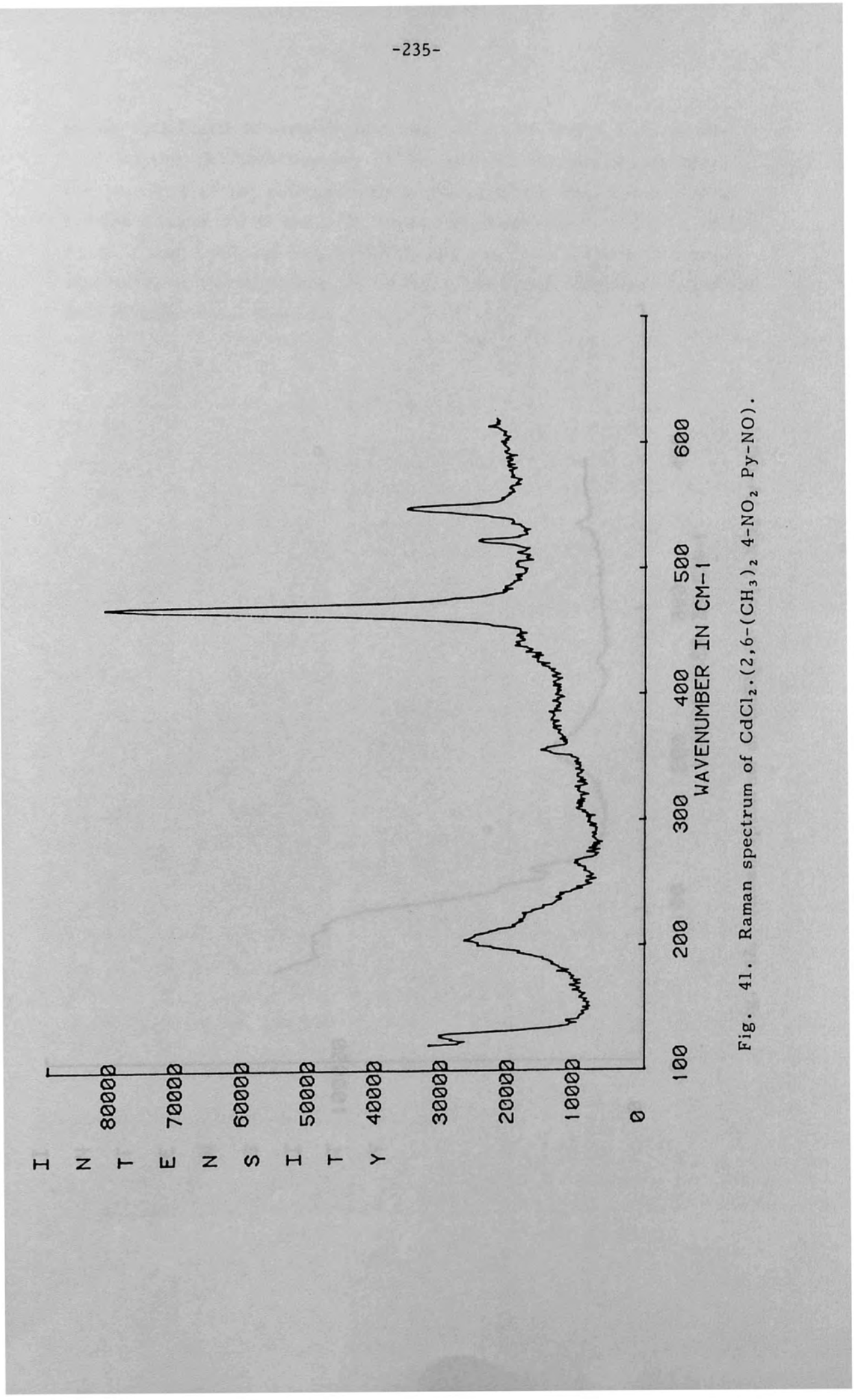

Fig. 41. Raman spectrum of $CdCl_2.(2,6\text{-}(CH_3)_2\ 4\text{-}NO_2\ Py\text{-}NO)$.

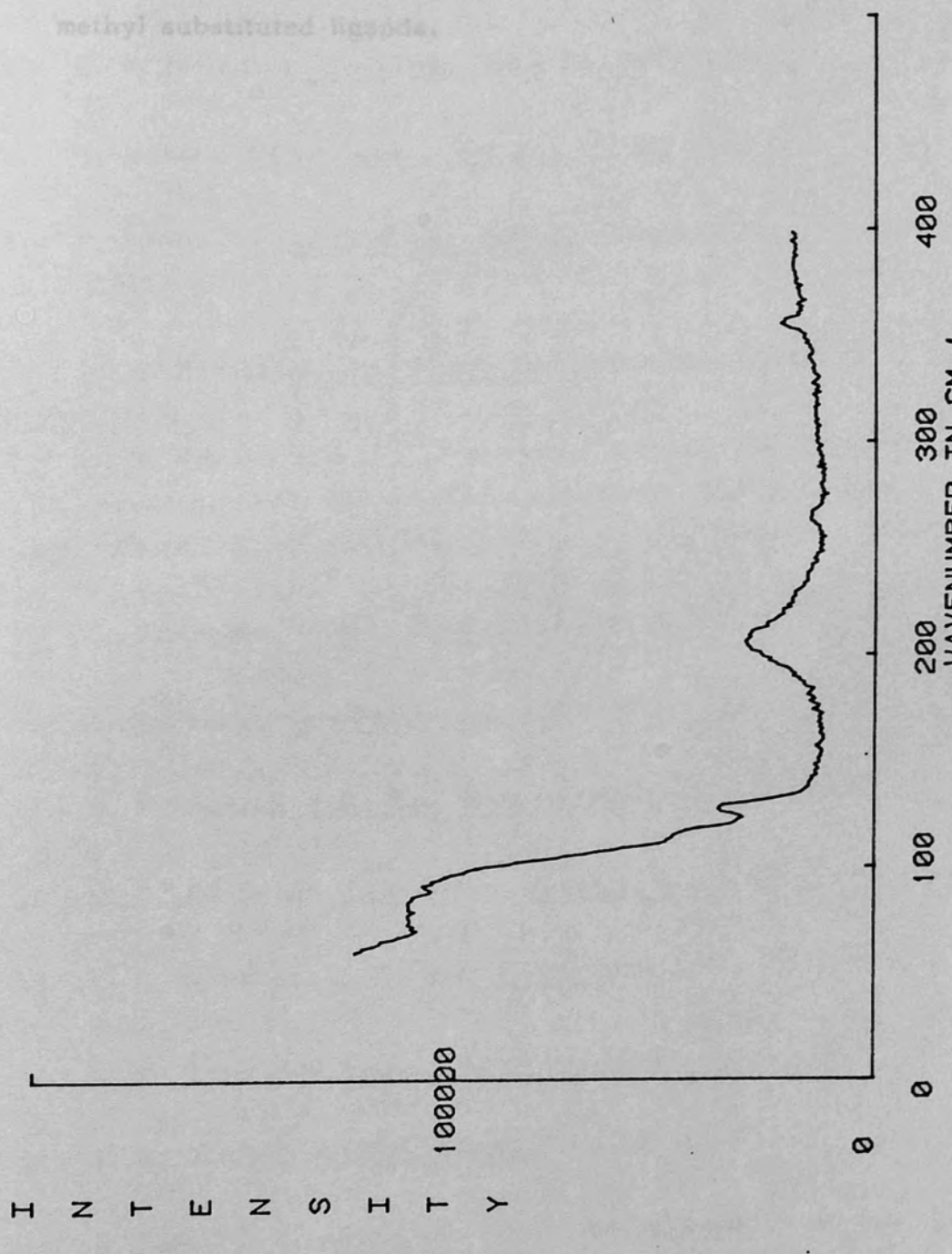

Fig. 42. Raman spectrum of $CdCl_2.(2\text{-}CH_3\ 4\text{-}NO_2\ Py\text{-}NO)$.

means that steric hindrance near the donor site is the main factor to determine the stoichiometry of the cadmium complexes, whereas, the presence of the nitro group on the pyridine ring is responsible for the weaker Cd-O bonds in these complexes, because $CdCl_2.(4\text{-}NO_2$ Py-NO) and $CdCl_2.(4\text{-}NO_2$ Py-NO)$_2$ did not show Cd-O stretching vibrations at wavenumbers higher than the other complexes containing methyl substituted ligands.

REFERENCES

1.- A. R. Katritzky, E. W. Randall and L. E. Sutton, J. Chem. Soc., 1769 (1957).

2.- N. Sharpe and S. Walker, J. Chem. Soc., 4522 (1961).

3.- E. P. Linton, J. Am.Chem. Soc., 62, 1945 (1940).

4.- T. Kubota, Coord. Chem. Review, 87, 458 (1965).

5.- E. Ochiai, Aromatic Amine Oxides, American Elsevier Publ. Co., (1967).

6.- R. A. Barnes, J. Am. Chem. Soc., 81, 1935 (1959).

7.- M. N. Adamov and I. F. Tupitsyn, Listuves fix. Rinkings, Listuvous TSR, Moskslm, Akad. Lietues TSR, Aukatvsios, Mokyhlu, 3, 277 (1963); Chem. Abstr., 60, 15165(1964).

8.- C. Valdemoro, Compt. Rend., 253, 277 (1961).

9.- R. Robinson, Tetrahedron, 1, 170 (1957).

10.- M. Polonovski, Bull. Soc. Chim. France, 21, 191 (1917).

11.- G. R. Clemo and H. McIlwain, J.Chem. Soc., 479 (1938).

12.- E. C. White and J. H. Hill, J. Bacteriol., 45, 433 (1943).

13.- G. R. Clemo and A. F. Daglish, J. Chem. Soc., 1481 (1950).

14.- J. D. Datcher, J. Biol. Chem., 171, 321 (1947).

15.- G. Dunn, J. J. Gallagher, G. T. Newbold and F. S. Spring, J. Chem. Soc.,(Supplement), 126, (1949).

16.- F. Linsker and M. T. Bogert, J. Amer. Chem. Soc.,68, 192 (1946).

17.- J. S. Paul, R. C. Reynolds, and P. O'B. Montgomery, Nature, 215, 749 (1967).

18.- G. V. Kulkarni, Arabinda Ray and C. C. Patel, J. Mol. Structure, 71, 253 (1981).

19.- G. B. Brown, Progr. Nucleic Acid Res. Mol. Biol., 8, 209 (1968).

20.- H. H. Jaffe and H. L. Jones, "Advances in Heterocyclic Chemistry", 3, 209 (1964).

21.- H. H. Jaffe, Chem. Rev., 53, 191 (1953).

22.- E. Ochiai, J. Org. Chem., 18, 534 (1953).

23.- A. R. Katritzky, Quart. Rev., (London), 10, 395 (1956).

24.- C. Rerat, Acta Cryst., 13, 63 (1960).

25.- P. G. Tsoucaris, Acta Cryst., 14, 909 (1961).

26.- Y. Namba, T. Oda, H. Ito and T. Watanabe, Bull. Chem. Soc. Japan, 33, 1618 (1960).

27.- E. L. Elchhorn, Acta Cryst., 9, 787 (1956).

28.- E. L. Eichhorn and K. Hoogsteen, Acta Cryst., 10, 382 (1957).

29.- H. H. Jaffe and G. O. Doak, J. Amer. Chem. Soc., 77, 4441 (1955).

30.- S. I. Shupack and M. Orchin, J. Amer. Chem. Soc., 85, 902 (1963).

31.- D. S. Dyer and R. O. Ragsdale, Inorg. Chem., 6, 8 (1967).

32.- R. G. Garvey and R. O. Ragsdale, J. Inorg. Nucl. Chem., 29, 745 (1967).

33.- D. W. Herlocker, R. S. Drago and V. I. Meek, Inorg. Chem., 5, 2009 (1966).

34.- C. R. Kanekar and H. V. Venkatasetty, Curr. Sci., 34, 555 (1965).

35.- C. R. Kanekar and S. V. Nipankar, Coord. Chem. Rev., 35, 361 (1966).

36.- T. Kubota and H. Miyazaki, Bull. Chem. Soc. Japan, 39, 2057 (1966).

37.- W. E. Hatfield and J. S. Paschal, J. Amer. Chem. Soc., 86, 3888 (1964).

38.- A. R. Katritzky and F. J. Swinbourne, J. Chem. Soc., 6707 (1965).

39.- F. E. Dickson, E. W. Gowling and F. F. Bentley, Inorg. Chem., 6, 1099 (1967).

40.- P. D. Kaplan and M. Orchin, Coord. Chem. Rev., 1096, (1967).

41.- J. H. Nelson, R. G. Garvey and R. O. Ragsdale, J. Heterocyclic Chem., 4, 591 (1967).

42.- P. R. Falkner and D. Harrison, J. Chem. Soc., 1171 (1960).

43.- P. R. Falkner and D. Harrison, J. Chem. Soc., 2148 (1962).

44.- M. Charton, J. Amer. Chem. Soc., 86, 2033 (1964).

45.- H. H. Jaffe, J. Amer. Chem. Soc., 77, 4445 (1955).

46.- H. Tani and K. Kukushima, J. Pharm. Soc. Japan, 81, 27 (1961).

47.- A. R. Katritzky, C. R. Palmer, F. J. Swinbourne, T.T. Tidwell, and R. D. Topsom, J. Amer. Chem. Soc., 91, 636 (1969).

48.- H. Shindo, Chem. Pharm. Bull. (Tokyo), 6, 117 (1958).

49.- G. P. Bean and A. R. Katritzky, J. Chem. Soc.,(B), 864, (1968).

50.- A. R. Katritzky and P. Simmons, J. Chem. Soc., 1511 (1960).

51.- J. W. Sidman, Chem. Rev., 58, 689 (1958).

52.- A. R. Katritzky and J. M. Lagowski, "Chemistry of the Heterocyclic N-oxides", Academic Press, London and New York (1971).

53.- J. N. Murell, "Theory of the Electronic Spectra of Organic Molecules", Methuen, London, 188 (1963).

54.- E. M. Evleth, Theor. Chim. Acta, 11, 145 (1968).

55.- M. Yamakawa, T. Kubota, K. Ezumi, and Y. Mizuno, Spectrochim. Acta, 30, 2103 (1974).

56.- M. Shiro, M. Yamakawa, and T. Kubota, Acta Cryst.B33, 1549 (1977).

57.- H. Shindo, Chem. Pharm. Bull. (Tokyo), 7, 791 (1959).

58.- G. Costa, P. Blasina, Z. Phys. Chem., 4, 24 (1955).

59.- A. R. Katritzky, and A. P. Ambler, "Physical Methods in Heterocyclic Chemistry", Vol. II, p. 161. Academic Press, London (1963).

60.- A. R. Katritzky, Quart. Rev., 13, 353 (1959).

61.- A. R. Katritzky, J. A. T. Beard and N. A. Coats, J. Chem. Soc., 3680 (1959).

62.- L. K. Dyall and K. H. Pausacker, J. Chem. Soc.,18 (1961).

63.- S. G. Bonino, Atti Acad. Naz. Lincei Rend.,Classe Sci. Fis., Nat., 35, 530 (1963).

64.- M. Szafran, Bull. Acad. Polon. Sci., Ser. Sci. Chem.,11A, 169 (1963).

65.- S. Gherstti, G. Maccagnani, A. Magnini, and F. Montanari, J. Heterocyclic Chem., 6, 859 (1969).

66.- A. R. Katritzky and J. N. Gardner, J. Chem. Soc., 2192 (1958).

67.- A. R. Katritzky and A. R. Hands. J. Chem. Soc., 2195 (1958).

68.- H. M. Hershenson, "Infrared Absorption Spectra" Indexes for 1957 and 1958-1962 (2 vols.). Academic Press, New York, (1961-1964).

69.- R. Whyman, W. E. Hatfield and J. S. Paschal, Inorg. Chim. Acta, 1, 113 (1967).

70.- P. V. Balakrishnan, S. K. Patil, and H. V. Venkatasetty, J. Inorg. Nucl. Chem., 28, 537 (1966).

71.- J. V. Quagliano, J. Fujita, G. Franz, D. J. Phillips, J. A. Walmsley, and S. Y. Tyree, J. Am. Chem. Soc., 83, 3770 (1961).

72.- Y. Kakiuti, S. Kida and J. V. Quagliano, Spectrochim. Acta, 19, 201 (1963).

73.- S. Castellano and R. Kostelnik, J. Amer. Chem. Soc., 90, 141 (1968).

74.- H. H. Perkampus and U. Kruger, Z. Phys. Chem.,(Frankfurt), 55, 202 (1967).

75.- R. A. Abramovitch and J. B. Davies, J. Chem. Soc.(B), 1137,(1966).

76.- A. R. Katritzky and J. M. Lagowski, J. Chem. Soc., 43, (1961).

77.- M. Ohtsuru, K. Tori and H. Watanabe, Chem. Pharm. Bull. (Tokyo), 15, 1015 (1967).

78.- A. G. Moritz and D. B. Paul, Aust. J. Chem., 22, 1305 (1969).

79.- H. Kano, M. Ogata and K. Tori, Chem. Pharm. Bull. (Tokyo), 10, 1123 (1962).

80.- F. J. Dinan, and R. Kolarczyk, J. Org. Chem., 44, 307 (1979).

81.- L. Stefaniak and A. Grabowska, Bulletin de L'academie Polonaise des Sciences, 4, 267 (1974).

82.- M. Witanowski, T. Saluvere, L. Stefaniak, H. Januszewski and G. A. Webb, Mol. Phys., 23, 1071 (1972).

83.- D. Herbison-Evans and R. E. Richards, Bulletin de L'academie Polonaise des Sciences, 8, 19 (1964).

84.- L. Stefaniak, Nitrogen n.m.r., Plenum Press, London-NewYork, 228 (1973).

85.- T. Wamsler, J. T. Nielsen, E. J. Pedersen and K. Schaumburg, J. Magn. Resonance, 31, 177 (1978).

86.- M. Witanowski, L. Stefaniak and G. A. Webb, Ann. Repts. NMR Spectroscopy, 7, 117 (1977).

87.- A. J. Digioia, G. T. Furst, L. Psota, and R. L. Lichter, J. Phys. Chem., 82, 1644 (1978).

88.- I. Yavari and J. D. Roberts, Org. Magn. Resonance, 12,87 (1979).

89.- M. Witanowsky, L. Stefaniak and G. A. Webb, Ann. Repts. n.m.r. Spectroscopy, IIB (1981).

90.- M. Witanowski, L. Stefaniak, B.Kamienski and G. A. Webb, Org. Magn. Resonance, 40, 305 (1980).

91.- W. Stadeli, W. Von Philipsborn, W. Wick and I. Kompis, Helv. Chim. Acta, 63, 504 (1980).

92.- A. J. DiGiola, G. T. Furst, L. Psota, and R. L. Lichter, J. Phys. Chem., 82, 1644 (1978).

93.- R. G. Garvey, J. H. Nelson and R. O. Ragsdale Coord. Chem. Rev., 3, 375 (1968).

94.- C. E. Michelson, and R. O. Ragsdale, Inorg. Chem., 9, 2718 (1970).

95.- T. Kubota and H. Watanabe, Bull. Chem. Soc. Japan, 36, 1093 (1963).

96.- Z. V. Pushkareva and O. N. Nechaeva, Zh. Obshch. Khim., 28, 2702 (1958).

97.- E. Borello and G. Lanfranco, Atti Acad. Sci. Torino, 93,1 (1959).

98.- Z. V. Pushkareva, L. V. Varyukhina and Z. Y. Kokoshko, Dokl. Acad. Nauk U.S.S.R., 108, 1098 (1956).

99.- H. Lumbroso and G. Palamibessi, Bull. Soc. Chim. France, 11, 3150 (1965).

100.- S. Walker, "Physical Methods in Heterocyclic Chemistry", Vol. I, p. 189 (A. R. Katritzky, Ed.). Academic Press, London, (1963).

101.- A. J. Boulton G. M. Glover, M. H. Hutchinson, A. R. Katritzki, D. J. Short and L. E. Sutton, J. Chem. Soc.(B), 822 (1966).

102.- A. N. Sharpe and S. Walker, J. Chem. Soc., 2974 (1961).

103.- R. G. Garvey, J. H. Nelson, and R. O. Ragsdale, Coord. Chem. Rev.,3, 375 (1968).

104.- N. M. Karayannis, L. L. Pytlewski, and C.M. Mikulski, Coord. Chem. Rev.,11, 93 (1973).

105.- M. Orchin and P. J. Schmidt, Coord. Chem. Rev., 3, 345 (1968).

106.- R. G. Garvey and R. O. Ragsdale, Inorg. Chem., 4, 1604 (1965).

107.- C. M. Harris, E. Kokot, L. Lenzer and T. N. Lockyer, Chem. Ind. (London), 651 (1962).

108.- R. L. Carlin, J. Am. Chem. Soc., 83, 3773 (1961).

109.- S. M. Horner, S. Y. Tyree and D. L. Venzky, Inorg. Chem., 1, 844 (1962).

110.- R. L. Carlin, J. Roitman, M. Dankleef and J. O. Edwards, Inorg. Chem., 1, 182 (1962).

111.- J. O. Edwards, R.J. Goetsch and J. A. Stritar, Inorg Chim. Acta, 1, 360 (1967).

112.- W. E. Hatfield, Y, Muto, H. B. Jonassen and J. S. Paschal, Inorg. Chem., 4, 97 (1965).

113.- Y. Muto and H. B. Jonassen, Bull. Chem. Soc. Japan, 39, 58 (1966).

114.- R. L. Carlin and M. J. Baker, J. Chem. Soc., 5008 (1964).

115.- K. Isslieb and A. Kreibick, Z. Anorg. Allg. Chem., 313, 338 (1961).

116.- H. N. Ramaswamy and H. B. Jonassen, J. Inorg. Nucl, Chem., 27, 740 (1965).

117.- H. N. Ramaswamy and H. B. Jonassen, Inorg. Chem., 4, 1595 (1965).

118.- L. R. Melby, N. J. Rose, E. Abramson and J. C. Caris, J. Am. Chem. Soc., 86, 5117 (1964).

119.- I. Lindqvist, Inorganic Adduct Molecules of Oxo-Compounds, Springer Verlag Berlin, 1963.

120.- R. L. Carlin, J. Am. Chem. Soc., 83, 3773 (1961).

121.- C. E. F. Rickard and D. C. Woollard, Inorg. Nucl. Chem. Letters, 14, 207 (1978).

122.- S. Kida, J. V. Quagliano, J. A. Walmsley and S. Y. Tyree, Spectrochim. Acta, 19, 201 (1963).

123.- R. S. Drago, J. T. Donoghue and D. W. Herlocker, Inorg. Chem., 4, 836 (1965).

124.- F. A. Cotton, R. D. Barnes and E. Bannister, J. Chem. Soc., London, 2199 (1960).

125.- D. J. Phillips and S. Y. Tyree, J. Am. Chem. Soc., 83, 1806 (1961).

126.- G. A. Abakumov, V. D. Tikhonov and G. A. Razuvaev, Docl. Akad. Nauk SSSR, 187, 571 (1969).

127.- R. G. Garvey and R. O. Ragsdale, J. Inorg. Nucl. Chem., 29, 1527 (1967).

128.- R. W. Kluiber and W. Dew. Horrocks, Jr., J. Am. Chem. Soc., 87, 5350 (1965).

129.- R. J. Gillespie, J. Am. Chem. Soc., 82, 5978 (1960).

130.- R. S. Sager, R. G. Williams and W. H. Watson, Inorg. Chem., 6, 951 (1967).

131.- S. Scavnicar and B. Matkovic, Chem. Commun.,297 (1967).

132.- R. S. Sager and W. H. Watson, Inorg. Chem., 7, 2035 (1968).

133.- J. D. Lee, D. S. Brown and B. G. A. Melsom, Acta Crystallogr., Sect. B, 25, 1378 (1969).

134.- H. L. Schäfer, J. C. Morrow and H. M. Smith, J. Chem. Phys., 42, 504 (1965).

135.- R. S. Sager and W. H. Watson, Inorg. Chem., 7, 1358 (1968).

136.- E. A. Blom, B. R. Penfold and W. T. Robinson, J. Chem. Soc. A, 913 (1969).

137.- W. D. Horrocks, Jr., D. H. Templeton and A. Zakim, Inorg. Chem., 7, 1552 (1968).

138.- B. A. Coyle and J. A. Ibers, Inorg. Chem., 9, 767 (1970).

139.- R. J. Williams, D. T. Croner and W. H. Watson, Acta Crystallogr. Sect. B, 27, 1619 (1971).

140.- D. Taylor, Aust. J. Chem., 31, 713 (1978).

141.- T. J. Bergendahl, J. S. Wood, Inorg. Chem., 14, 338 (1975).

142.- J. S. Wood, R. O. Day, C. P. Keijzers, E. De Boer, A. E. Yildrim, and A. A. K. Klassen, Inorg. Chem., 20, 1982 (1981).

143.- A. D. van Ingen Schenau, G. C. Verschoor, and C. Romers, Acta Crystallogr., Sect. B, 30, 1686 (1974).

144.- A. D. Mighell, C. W. Reimann and A. Santoro, Acta Cryst., Sect. B, 28, 126 (1972).

145.- S. M. Horner, S. Y. Tyree and D. L. Venezky, Inorg. Chem., 1, 844 (1962).

146.- N. M. Karayannis, M. J. Strocko, C. M. Mikulski, E. E. Bradshaw, L. L. Pytlewski and M. M. Labes, J. Inorg. Nucl. Chem., 32, 3962 (1970).

147.- J. Reedijik, Rec. Trav. Chim. Pays. Bas, 88, 499 (1969).

148.- F. Kutek and B. Dusek, Coll. Czech. Chem. Commun., 35, 13 (1970).

149.- V. Krishnan and C. C. Patel, Can. J. Chem., 43, 2685 (1965).

150.- P. R. Murthy and C. C. Patel, Can. J. Chem., 42, 856 (1964).

151.- J. H. Nelson, L. C. Nathan and R. O. Ragsdale, Inorg. Chem., 7, 1840 (1968).

152.- J. H. Nelson and R. O. Ragsdale, Inorg. Chim. Acta, 2, 230 (1968).

153.- L. C. Nathan and R. O. Ragsdale, Inorg. Chim. Acta, 3, 473 (1969).

154.- N. P. Crawform and G. A. Melson, J. Chem. Soc., A, 141 (1970).

155.- V. Krishnan and C. C. Patel, Can. J. Chem., 44, 972 (1966).

156.- D. W. Herlocker, J. Inorg. Nucl. Chem., 34, 389 (1972).

157.- N. M. Karayannis, L. L. Pytlewski and M. M. Labes, Inorg. Chim. Acta, 3, 415 (1969).

158.- G. Schmauss and H. Specker, Z. Anorg. Allg. Chem., 364, 1 (1969).

159.- P. M. Enquez, S. S. Zumdahl and L. Forshey, Chem. Commun., 1527 (1970).

160.- L. C. Nathan, J. H. Nelson, G. L. Rich and R. O. Ragsdale, Inorg. Chem., 8, 1494 (1969).

161.- C. E. Michelson and R. O. Ragsdale, Inorg. Chem., 9, 2718 (1970).

162.- C. E. Michelson, D. S. Dyer, and R. O. Ragsdale, J. Chem. Soc., (1971).

163.- D. S. Dyer and R. O. Ragsdale, Inorg. Chem., 8, 1116 (1969).

164.- N. M. Karayannis, S. D. Sonisno, C. M. Mikulski, M. J. Strocko, L. L. Pytlewski and M. M. Labes, Inorg. Chim. Acta, 4, 141 (1970).

165.- J. H. Nelson and R. O. Ragsdale, Inorg. Chim. Acta, 2, 439 (1968).

166.- N. M. Karayannis, C. M. Mikulski, L. L. Pytlewski and M. M. Labes, J. Inorg. Nucl. Chem., 34, 3139 (1972).

167.- Y. Muto, M. Kato, H. B. Jonassen and H. N. Ramaswamy, Bull. Chem. Soc. Jap., 40, 1535 (1967).

168.- M. Kato, Y. Muto, and H. B. Jonassen, Bull. Chem. Soc. Jap., 40, 1738 (1967).

169.- M. Kato, Y. Muto and H. B. Jonassen, Bull. Chem. Soc. Jap., 41, 1495 (1968).

170.- Y. Muto, M. Kato, H. B. Jonassen and L. C. Cusachs, Bull. Chem. Soc. Jap., 42, 417 (1969).

171.- G. B. Aitken and G. P. McQuillan, J. Chem. Soc., Dalton, 2637 (1973).

172.- S. Kida, J. V. Quagliano, J. A. Walmsley, and S. V. Tyree, Spectrochim. Acta, 19, 189 (1963).

173.- J. A. Bertrand and D. L. Plymale, Inorg. Chem., 3, 775 (1964).

174.- O. Bostrup and C. K. Jørgensen, Acta. Chem. Scand., 11, 1223 (1957).

175.- M. R. Rosenthal and R. S. Drago, Inorg. Chem., 4, 840 (1965).

176.- F. Mani, Inorg. Nucl. Chem. Lett., 7, 447 (1971).

177.- W. Byers, A. B. P. Lever, and R. V. Parish, Inorg. Chem., 7, 1835 (1968).

178.- D. H. Brown, D. Kenyon and D. W. A. Sharp, J. Chem. Soc. A, 1474 (1969).

179.- C. R. Kanekar and S. V. Nipankar, Curr. Sci. (India), 35, 361 (1966).

180.- O. Piovesana and J. Selbin, J. Inorg. Nucl. Chem., 31, 1671 (1969).

181.- D. A. Couch, P. S. Elmes, J. E. Ferguson, M. L. Greenfield and C. J. Wilkins, J. Chem. Soc. A, 1813 (1967).

182.- N. M. Karayannis, C. M. Paleos, L. L. Pytlewski and M. M. Labes, Inorg. Chem., 8, 2559 (1969).

183.- N. M. Karayannis, J. V. Minkiewics, L. L. Pytlewski and M M. Labes, Inorg. Chim. Acta, 3, 129 (1969).

184.- A. J. Pappas, F. A. Osterman, Jr. and H. B. Powell, Inorg. Chem., 9, 2695 (1970).

185.- R. S. Sager, J. J. Williams and W. H. Watson, Inorg. Chem., 8, 694 (1969).

186.- J. J. R. F. DaSilva and R. Wootton, Chem. Commun., 204 (1970).

187.- J. J. R. F. DaSilva, L. F. V. Boas and R. Wootton, J. Inorg. Nucl. Chem., 33, 2029 (1971).

188.- M. R. Kidd, R. S. Sager and W. H. Watson, Inorg. Chem., 6, 946 (1967).

189.- W. H. Hatfield, and J. C. Morrison, Inorg. Chem., 5, 1390 (1966).

190.- M. R. Kidd and W. H. Watson, Inorg. Chem., 8, 1886 (1969).

191.- K. E. Hyde, G. Gordon and G. F. Kokoszka, J. Inorg. Nucl. Chem., 30, 2155 (1968).

192.- R. Whyman, D. B. Copley and W. E. Hatfield, J. Amer. Chem. Soc., 89, 3135 (1967).

193.- W. H. Watson, Inorg. Chem., 8, 1879 (1969).

194.- R. W. Jotham, S. F. A. Kettle, and J. A. Marks, J. Chem Soc.,Dalton, 1133 (1972).

195.- S. J. Gruber, C. M. Harris, E. Kokot, S. L. Lenzer, T. N. Lockyer and E. Sinn, Aust. J. Chem., 20, 2403 (1967).

196.- B. N. Figgis, "Introduction to Ligand Fields," Interscience Publishers, New York, N. Y. 253 (1966).

197.- R. S. Nyholm, "The Plenary Lecture at Xth International Conference on Coordination Chemistry," Tokyo September 12, 1967; The Japanese Translation By Y. Saito, Kagaku to Kogyo (Chem & Chem. Ind., Tokyo), 21, 338 (1968).

198.- I. S. Ahuja, D. H. Brown, R. H. Nutall and D. W. A. Sharp, J. Inorg. Nucl. Chem., 27, 1105 (1965).

199.- A. E. Underhill, J. Chem. Soc., 4336 (1965).

200.- E. E. Billing, A. E. Underhill, D. M. Adams and D. M. Morris, J. Chem. Soc., (A), 902 (1966).

201.- E. Sinn, Inorg. Nucl. Chem., Lett., 5, 193 (1969).

202.- J. A. Barnes, W. C. Barnes and W. E. Hatfield, Inorg Chim. Acta, 5, 276 (1971).

203.- R. Whymann and W. E. Hatfield, Inorg. Chem., 6, 1859 (1967).

204.- D. R. Johnson and W. H. Watson, Inorg. Chem., 10, 1069 (1971).

205.- H. Miyoshi, H. Ohya-Nishiguchi, and Y. Deguchi, Bull. Chem. Soc. Japan, 45, 682 (1972).

206.- J. Kratsmar-Smogrovic and M. Melnik, Z. Naturforsch. B, 24, 1479 (1969).

207.- J. Kohout and J. Kratsmar-Smogrovic, Chem. Zvesti, 22, 481 (1968).

208.- J. H. Nelson and D. Hibdon, Inorg. Chim. Acta, 7, 629 (1973).

209.- M. Kato, H. B. Jonassen and J. C. Fanning, Chem. Rev., 64, 99 (1964).

210.- B. N. Figgis and R. L. Martin, J. Chem. Soc., 3837 (1956).

211.- A. J. Pappas, J. F. Villa and H. B. Powell, Inorg. Chem., 8, 550 (1969).

212.- G. Schmauss and H. Specker, Z. Anorg. Allg. Chem., 383, 113 (1968).

213.- O. Piovesana and J. Selbin, J. Inorg. Nucl. Chem., 31, 1671 (1969).

214.- G. Schmauss and H. Specker, Naturwissenschaften, 54, 248 (1967).

215.- I. S. Ahuja and P. Rastogi, J. Inorg. Nucl. Chem., 32, 2665 (1970).

216.- B. K. Mohanty, P. Satyanarayana, B. K. Mohapatra, J. Indian Chem. Soc., 56, 526 (1979).

217.- G. Sawitzki and H. G. von Schnering, Naturwissenschaften, 107, 3266 (1974).

218.- I. S. Ahuja and P. Rastogi, J. Inorg. Nucl. Chem.,32, 1381 (1970).

219.- L. Achremowics, T. Batkowski, Z. Skrowaczewska, Rocznili Chem., 38, 1317 (1964).

220.- E. V. Brown, R. H. Neil, J. Org. Chem., 26, 3546 (1961).

221.- E. V. Brown, J. Amer. Chem. Soc., 79, 3565 (1957).

222.- F. A. L. Anet and I. Yavari, J. Org. Chem., 41, 3589 (1976).

223.- R. J. Cushley, D. Naugler, and C. Ortiz, Can. J. Chem, 54, 3419 (1975).

224.- G. J. Martin, M. L. Martin, and S. Odiot, Org. Magn. Reson., 7, 2 (1975).

225.- B.N. Figgis and R. L. Martin, J. Chem. Soc., 3837 (1956).

226.- E. Kokot and R. L. Martin, Inorg. Chem., 3, 1306 (1964).

227.- R. W. Jotham and S. F. A. Kettle, J. Chem. Soc. (A), 2822 (1969).

228.- J. Chatt and B. L. Shaw, J. Chem. Soc., 1718 (1960).

229.- J. Chatt and B. L. Shaw, J. Chem. Soc., 285 (1961).

230.- J. Lewis, F. E. Mabbs, L. K. Royston, and W. R. Smail, J. Chem. Soc. (A), 291 (1969).

231.- P. D. W. Boyd, A. D. Toy, and T. D. Smith, J. Chem. Soc. Dalton, 1549 (1973).

232.- G. F. Kokoska, and R. W. Duerst, Coord. Chem. Rev., 5, 209 (1970).

233.- A. Abragam and B. Bleaney "Electron Paramagnetic Resonance of Transition Ions", Clarendon Press, Oxford (1970).

234.- D. Ülkü, B.P. Huddle and J. C. Morrow, Acta Cryst., B27, 432 (1971).

235.- A. A. G. Tomlinaon, B. J. Hathaway, D. E. Billing and P. Nicholls, J. Chem. Soc. (A), 65 (1969).

236.- L. Sutton, Ed., "Tables of Interatomic Distances and Configuration in Molecules and Ions," Spec. Publ. No. 11 and 18, The Chemical Society, London, 1958, 1965.

237.- I. Robertson and M. R. Turner, J. Chem. Soc. (A), 309 (1967).

238.- B. J. Hathaway, D. E. Billing and R. J. Dudley, J. Chem. Soc. (A), 1420 (1970).

239.- D. P. Graddon, J. Inorg. Nuclear Chem., 14, 161 (1960).

240.- T. S. Piper and R. L. Belford, Mol. Phys., 5, 169 (1962).

241.- D. W. Barnum, J. Inorg. Nuclear Chem., 21, 221 (1961).

242.- J. F. Villa, R. Doyle, H. C. Nelson and J. L. Richards, Inorg. Chim. Acta, 25, 49 (1977).

243.- H. W. Richardson, J. R. Wasson, and William E. Hatfield, Inorg. Chem., 16, 484 (1977).

244.- R. D. Willett, C. Dwiggens, Jr., R. Kruth, and R. F. Rundle, J. Chem. Phys., 38, 2429 (1963).

245.- B. J. Hathaway and D. E. Billing, Coord. Chem. Rev., 5, 143 (1970).

246.- M. Massacesi and G. Pointicelli, J. Mol. Structure, 51, 27 (1979).

247.- I. Bertini, D. Gattesch and A. Scozzafava, Coord. Chem. Rev. 29, 67 (1979).

248.- E. A. Blom, B. R. Penfold, W. T. Robinson, J. Chem. Soc., (A), 913 (1969).

249.- R. J. H. Clark, Spectrochim. Acta, 21, 955 (1965).

250.- M. Goldstein, E. F. Moony, A. Anderson, and H. A. Gebbie, Spectrochim Acta, 21, 105 (1965).

251.- G. E. Coates and D. Ridley, J. Chem. Soc., 166 (1964).

252.- D. M. Adams, M. Goldstein and E. F. Mooney, Trans. Faraday Soc., 1209 (1940).

253.- T. Onishi and T Shimanouchi, Spectrochim. Acta, 20, 325 (1964).

254.- I. R. Beattie, T. Gilson and P. Cocking, J. Chem. Soc. A. 702 (1967).

248.- E. A. Blom, B. R. Penfold, W. T. Robinson, J. Chem. Soc., (A), 913 (1969).

249.- R. J. H. Clark, Spectrochim. Acta, 21, 955 (1965).

250.- M. Goldstein, E. F. Moony, A. Anderson, and H. A. Gebbie, Spectrochim Acta, 21, 105 (1965).

251.- G. E. Coates and D. Ridley, J. Chem. Soc., 166 (1964).

252.- D. M. Adams, M. Goldstein and E. F. Mooney, Trans. Faraday Soc., 1209 (1940).

253.- T. Onishi and T Shimanouchi, Spectrochim. Acta, 20, 325 (1964).

254.- I. R. Beattie, T. Gilson and P. Cocking, J. Chem. Soc. A. 702 (1967).

255.- J. N. Van Niekerk and F. R. L. Schoening, Acta Cryst., 227, 6 (1953).